

**High Throughput Approaches to
Mammalian Cell Culture Process Development**

**An EngD Thesis submitted to University College
London**

by

Nicholas John Silk

Declaration

I, Nicholas John Silk, confirm that the work presented in this thesis is my own. Where information has been derived from other sources, I confirm that this has been indicated in the thesis.

Acknowledgements

I'd like to thank my supervisors at both UCL (Gary Lye and Frank Baganz) and MedImmune (Jonathan Dempsey, Marcel Kuiper, Sam Denby, Diane Hatton and Gareth Lewis) for their encouragement and support during my studies.

In addition I'd like to thank Andy Tait and the rest of the mammalian cell culture team at UCL for their ideas and enthusiasm, as well as Lucy Gardner and Richard Lugg at MedImmune for their selfless contributions of time during my time in Cambridge.

Abstract

Commercial pressures to reduce the costs and timelines involved in bringing new medicines to market are driving investment in methods for high throughput bioprocess development. The establishment of mammalian cell culture processes for therapeutic antibody production is an area of particular interest. This is an experimentally intensive procedure initially involving evaluation of a large number of clones followed by optimisation and scale-up of cell culture conditions.

In this thesis a high throughput microwell platform is established for use in early stage cell line selection and cell culture process development. It was first demonstrated that shaken 24 SRW microwells were suitable for batch suspension culture of a commercially available CHO cell line, provided that appropriate culture conditions were selected. However, a high rate of evaporation from the microwells was identified as a potential limiting factor. Further work with an industrial GS-CHO cell line led to the development of a fed-batch method. This used a combination of diluted liquid feeds and a 'sandwich lid' to counteract microwell liquid losses by water replacement and reduction of evaporation to negligible levels. This led to comparable cell growth and product formation kinetics as well as similar metabolite utilization kinetics in 24 SRW plates and conventional shake flasks.

Engineering characterisation of 24 SRW, shake flask and laboratory scale (5L) stirred tank systems was subsequently performed, encompassing the oxygen mass transfer coefficient (k_{La}), mean energy dissipation rate (P/V), and liquid phase mixing time (t_m). Mixing times in particular showed a strong

dependence on the speed and diameter of orbital shaking while in general $k_{L\alpha}$ values were sufficient ($>1h^{-1}$) for oxygen transfer not to be rate limiting. Consequently it was suggested that matched liquid phase mixing times could be a suitable scale translation parameter for the types of small scale bioreactor formats used in early stage cell culture process development.

It was subsequently demonstrated that at mixing times that promoted a homogeneous culture environment at each scale ($t_m = 5s$) similar culture performance in all three bioreactor formats could be achieved using this engineering basis for two distinct cell culture processes involving different GS-CHO cell lines and alternative feeding methodologies. Peak viable cell densities achieved in stirred tank, shake flask and 24 SRW formats were 5.9 , 6.7 and 6.4×10^6 cells mL^{-1} respectively, while antibody titres were 1.23 , 0.81 and 0.88 g L^{-1} . The higher IgG concentration in the stirred tank was attributed to tighter on-line pH control. The utilization rates for key metabolites were also closely matched.

Finally the industrial relevance of this methodology was demonstrated through the successful parallel fed-batch cultivation of more than 50 GS-CHO cell lines. The rank order of cells based on product titre agreed closely with existing development procedures using shake flasks and static microwell plates. The microwell cell culture process presented here thus offers the potential for a considerable increase in throughput during the early stages of biopharmaceutical product development.

CHAPTER 1: INTRODUCTION	17
1.1 OVERVIEW OF MAMMALIAN CELL CULTURE	17
1.2 MONOCLONAL ANTIBODIES	18
1.3 STAGES INVOLVED IN CELL CULTURE PROCESS DEVELOPMENT	20
1.4 PRODUCTION SCALE CULTURE	21
1.5 SMALL SCALE CULTURE SYSTEMS FOR CELL LINE CHARACTERISATION AND PROCESS DEVELOPMENT	25
1.5.1 <i>Miniature Stirred Tank Systems</i>	25
1.5.2 <i>Shake Flasks</i>	27
1.5.3 <i>Microwell Plates</i>	29
1.6 ALTERNATIVE CULTURE SYSTEMS	33
1.6.1 <i>SimCell</i>	33
1.6.2 <i>Micro-24</i>	34
1.6.3 <i>BioLector</i>	35
1.7 AIM AND OBJECTIVES OF THESIS	36
CHAPTER 2: MATERIALS AND METHODS	38
2.1 CELL CULTURE	38
2.1.1 <i>Cell Lines Used</i>	38
2.1.2 <i>Revival of Cells from Liquid Nitrogen Storage (applies to CHO-S line and both GS-CHO cell lines)</i>	39
2.1.3 <i>Preparation of Working Cell Bank</i>	40
2.2 SHAKE FLASK CULTURES	40
2.3 MICROWELL CULTURES	41
2.3.1 <i>24 SRW Plates:</i>	41
2.3.2 <i>24 Deep Square Well (DSW) Plates</i>	45
2.3.3 <i>96 DSW Plates</i>	45
2.4 STIRRED TANK CULTURES	46
2.5 FED BATCH PROTOCOLS	47
2.5.1 <i>CHO-S</i>	47
2.5.2 <i>GS-CHO (MedImmune)</i>	48
2.5.3 <i>GS-CHO (IMRC)</i>	49
2.6 CORRECTION OF CELL COUNTS FOR EVAPORATION	50
2.6.1 <i>Unfed Cultivations</i>	50
2.6.2 <i>Fed-Batch Cultivations</i>	50
2.7 ANALYTICAL TECHNIQUES	51
2.7.1 <i>Determination of cell viability and viable cell number</i>	51
2.7.2 <i>Determination of metabolite concentrations</i>	53
2.7.3 <i>IgG Quantification by Protein G HPLC</i>	54
2.7.4 <i>Osmolality</i>	54
2.7.5 <i>At-Line analysis of pH, Dissolved Oxygen and Carbon Dioxide</i>	55
2.7.6 <i>Cell Size</i>	56
2.7.7 <i>Cell Confluence Measurement using Cellavista</i>	56
2.7.8 <i>IgG Quantification Using the Octet</i>	57
2.8 BIOREACTOR MIXING CHARACTERISATION	57
2.8.1 <i>Observation of Liquid Phase Hydrodynamics</i>	57
2.8.2 <i>Quantification of Bioreactor Mixing Times</i>	58
2.9 DETERMINATION OF BIOREACTOR OXYGEN MASS TRANSFER COEFFICIENTS	59
2.9.1 <i>24 SRW Plates (Catechol Oxidation)</i>	59

2.9.2 24 SRW Plates (<i>PreSens System</i>)	60
2.9.3 Shake Flasks	61
2.9.4 Stirred Tank	61
2.10 DETERMINATION OF MEAN BIOREACTOR POWER INPUT	62
2.10.1 24 SRW Plates	62
2.10.2 Shake Flasks	62
2.10.3 Stirred Tank	62
2.11 DETERMINATION OF SPECIFIC OXYGEN UPTAKE RATE (OUR) IN 24 SRW PLATES	64
2.12 MEASUREMENT OF DISSOLVED OXYGEN TENSION DURING MICROWELL CULTIVATIONS	65
2.13 DERIVED GROWTH AND METABOLIC PARAMETERS	65
2.13.1 <i>Integral Viable Cell Concentration</i>	65
2.13.2 <i>Specific Antibody Production Rate</i>	66
CHAPTER 3: ESTABLISHMENT OF MICROWELL BATCH CULTURE CONDITIONS FOR A MODEL CHO-S CELL LINE	67
3.1 INTRODUCTION AND AIM	67
3.2 IMPACT OF SHAKING SPEED ON MICROWELL CHO-S CULTIVATIONS	68
3.3 IMPACT OF FILL VOLUME ON MICROWELL CHO-S CULTIVATIONS	72
3.4 COMPARISON OF DIFFERENT BREATHABLE MEMBRANES	77
3.5 BATCH CHO-S CULTIVATION IN A 5 LITRE STIRRED TANK REACTOR	80
3.5 METABOLITE PROFILES IN SHAKEN CHO-S BATCH CULTURES	86
3.6 COMPARISON OF CHO-S BATCH CULTURE KINETICS AND METABOLITE USAGE IN DIFFERENT BIOREACTOR FORMATS	92
3.8 INVESTIGATION OF CHO-S CULTIVATION IN ALTERNATIVE MICROWELL GEOMETRIES	96
3.8.1 96 DSW Plates	96
3.8.2 24 DSW Plates	100
3.9 PRELIMINARY FED-BATCH MICROWELL EXPERIMENTS	103
3.10 SUMMARY	108
CHAPTER 4: DEVELOPMENT OF A FED-BATCH CELL CULTURE METHODOLOGY IN SHAKEN 24 WELL BIOREACTORS*	109
4.1 INTRODUCTION AND AIM	109
4.2 SELECTION OF A STERILE CLOSURE	110
4.3 INITIAL PARALLEL FED BATCH EXPERIMENTS IN SHAKEN BIOREACTORS	113
4.4 FED BATCH GS-CHO CULTURE USING DILUTED BOLUS FEEDS	117
4.5 VARIATION OF CULTURE ENVIRONMENT DURING SHAKEN 24-SRW CULTURES	123
4.6 ASSESSMENT OF WELL TO WELL REPRODUCIBILITY IN PARALLEL 24 SRW CELL CULTURES	131
4.7 INVESTIGATING THE IMPACT OF A FURTHER REDUCTION IN MICROWELL EVAPORATION ON CULTURE PERFORMANCE	138
4.8 SUMMARY	144
CHAPTER 5: BIOREACTOR ENGINEERING CHARACTERISATION AND SCALE TRANSLATION	146
5.1 INTRODUCTION AND AIM	146
5.2 OXYGEN MASS TRANSFER COEFFICIENT (K _{LA})	147
5.2.1 <i>k_{la} determination in microwells</i>	147
5.2.2 <i>k_{la} determination in stirred tank bioreactors</i>	154
5.2.3 <i>Determination of Cell Specific Oxygen Uptake Rate (OUR)</i>	157
5.2.4 <i>Comparison of OUR with OTR in Shaken Microwells</i>	159
5.3 MEAN ENERGY DISSIPATION RATE	161
5.3.1 <i>Determination of mean energy dissipation</i>	161

5.3.2 <i>Experimental Results for Determination of Stirred Tank Power Number Using an Air Bearing</i>	162
5.3.3 <i>Shake Flask Predictions</i>	163
5.4 LIQUID PHASE MIXING TIME, T_M	163
5.4.1 <i>Visualisation of Bioreactor Fluid Flow and Mixing</i>	163
5.4.2 <i>Quantification of Liquid Phase Mixing Times</i>	166
5.5 SELECTION OF A SCALE TRANSLATION PARAMETER FOR MAMMALIAN CELL CULTURE	171
5.6 SUMMARY	175
CHAPTER 6: MIXING TIME AS A BASIS FOR CELL CULTURE SCALE TRANSLATION	177
6.1 INTRODUCTION AND AIM	177
6.2 FED-BATCH GS-CHO CULTIVATION AT MATCHED MIXING TIME	178
6.3 EVALUATION OF SCALE TRANSLATION BASIS WITH DIFFERENT CELL CULTURE PROCESSES	185
6.4 OPTIMISATION OF THE METHOD FOR SHAKEN 24 SRW PLATES	192
6.5 CONFIRMATION OF ADEQUATE OXYGEN SUPPLY IN MICROWELLS DURING GS-CHO CULTIVATION	197
6.6 SUMMARY	200
CHAPTER 7: CONCLUSIONS AND FUTURE WORK	201
7.1 CONCLUSIONS	201
7.2 FUTURE WORK	204
APPENDIX I: INDUSTRIAL APPLICATION AND EVALUATION OF A MICROWELL-BASED APPROACH TO CELL CULTURE PROCESS DEVELOPMENT*	210
I.1 INTRODUCTION AND AIM	210
I.2 METHODOLOGY FOR CELL LINE CHARACTERISATION	211
I.3 PARALLEL CELL CULTURE AND CELL LINE SELECTION	214
I.4 EVALUATION OF COMMERCIAL POTENTIAL	215
APPENDIX II: SUPPLEMENTARY CALCULATIONS	220
II.1 MICROSCALE OF TURBULENCE	220
II.2 EVAPORATION CORRECTION FOR FED-BATCH CULTURES IN 24 SRW PLATES	221
II.3 DETERMINATION OF CELL SPECIFIC OXYGEN UPTAKE RATE (OUR)	224
II.4 PAIRED T-TEST FOR PEAK CHO-S VIABLE CELL DENSITIES OBTAINED IN SHAKEN 24 SRW MICROWELLS AND SHAKE FLASKS	225
REFERENCES	226

List of Tables

Chapter 2: Materials and Methods

- 2.1 Chromatographic Method for IgG Quantification 54

Chapter 3: Establishment of Microwell Batch Culture Conditions for a Model CHO-S Cell Line

- 3.1 Summary of CHO-S batch growth kinetics and metabolite utilization data in different Bioreactor formats 95

Chapter 4: Development of a Fed-Batch Cell Culture Methodology in Shaken 24 Well Bioreactors

- 4.1 Rates of Evaporation from Shake Flasks and 24 Well Bioreactors 113
- 4.2 Comparison of fed-batch GS-CHO culture kinetics (diluted feeds) between microwell (24-SRW) and shake flask bioreactor geometries 128

Chapter 5: Bioreactor Engineering Characterisation and Scale Translation

- 5.1 Summary of measured and predicted k_{LA} values over a range of culture conditions 150
- 5.2 Measured and predicted k_{LA} values for a 5L stirred tank bioreactor 154
- 5.3 Values of the impeller power number N_p calculated at various impeller rotational speeds 162
- 5.4 Mean energy dissipation for a 250 mL Erlenmeyer flask 163
- 5.5 Comparison of previously used experimental conditions for fed-batch culture of an industrial GS-CHO cell line in microwell (24-SRW), shake flask and STR bioreactor geometries 172
- 5.6 Summary of experimental conditions and engineering characteristics for small scale bioreactor geometries operated at matched liquid phase mixing time, t_m 174

Chapter 6: Mixing Time as a Basis for Cell Culture Scale Translation

- 6.1 Comparison of fed-batch GS-CHO culture kinetics between microwell (24-SRW), shake-flask and stirred tank bioreactor geometries operated at matched mixing time, t_m of = 5s 184
- 6.2 Comparison of fed-batch GS-CHO culture kinetics between microwell (24-SRW), shake-flask and stirred tank bioreactor geometries operated at matched mixing time, $t_m = 5s$ 191

6.3	Comparison of fed-batch GS-CHO culture kinetics between microwell (24-SRW) and shake-flask operated at mixing times, t_m of 25s and 5s respectively	198
-----	---	-----

List of Figures

Chapter 1: Introduction

1.1	Basic structure of an IgG molecule	19
1.2	Typical stages involved in development of a production scale cell culture process	22
1.3	Single gas-permeable cassette from the SimCell	33

Chapter 2: Materials and Methods

2.1	Schematic drawings of single wells from microwell plates used for cell culture	42
2.2	(a) the underside of the Duetz sandwich lid designed for use with a 24 SRW plate and (b) the component layers of the sandwich	44
2.3	Stainless steel three-bladed impeller ($D = 67$ mm) with a dimensionless power number of 0.97 (measured at $Re = 16,000$) and a blade angle of 45°	47

Chapter 3: Establishment of Microwell Batch Culture Conditions for a Model CHO-S Cell Line

3.1	Influence of orbital shaking speed on CHO-S growth kinetics in 24SRW plates	70
3.2	CHO-S viability measured for 24SRW plates at various orbital shaking speeds	71
3.3	Influence of liquid fill volume on CHO-S culture kinetics in 24SRW plates	74
3.4	CHO-S viability measured for shake flask and 24SRW plates at various fill volumes	75
3.5	Change in mean liquid volume per well for 24SRW plates shaken at different speeds	77
3.6	Influence of breathable sealing membrane on CHO-S growth in 24SRW plates	79
3.7	CHO-S viability measured for 24SRW plates sealed with different breathable membranes, and shake flask agitated at 120 rpm	80
3.8	Mean cell diameter for CHO-S cultures measured using the CASY	83
3.9	Growth profiles for CHO-S in 5 L Stirred Tank Bioreactor	84

3.10	CHO-S viability in 5 L Stirred Tank Bioreactor	85
3.11	Glucose and Lactate profiles for CHO-S	88
3.12	Glutamine and Ammonia profiles for CHO-S	89
3.13	Glucose and Lactate profiles for CHO-S grown in a 5 L Stirred Tank Bioreactor	92
3.14	Change in well volume over time as a result of evaporation	97
3.15	Percentage change in fluid volume for 96DSW and 24SRW well formats during culture	98
3.16	CHO-S growth for a 1 mL fill volume in 96DSW plates	99
3.17	Comparison of CHO-S growth for 96DSW plate with a 1 mL fill and 25 mL shake flask	100
3.18	Comparison of CHO-S growth in 24 SRW, 24 DSW and Shake Flask formats	102
3.19	CHO-S viability profiles for cultivation in 24 SRW, 24 DSW and Shake Flask formats	103
3.20	Growth profiles for CHO-S in a shake flask and in fed and batch 24SRW plates	104
3.21	CHO-S viability measured for shake flask, fed and batch 24SRW plates	105
3.22	Glutamine utilization and ammonia production profiles for fed and batch 24SRW plate CHO-S cultures	106

Chapter 4: Development of a Fed-Batch Cell Culture Methodology in Shaken 24 Well Bioreactors

4.1	Typical GS-CHO batch culture kinetics: (♦) 24-SRW plate with a Breatheasy membrane; (●) 24-SRW plate with 'sandwich lid'; (▲) 250 mL shake flasks	112
4.2	Growth profiles for fed-batch cultivation of a GS-CHO cell line in a 24 SRW plate and shake flask	115
4.3	Viability profiles for fed-batch cultivation of a GS-CHO cell line in a 24 SRW plate and shake flask	116
4.4	Osmolality profiles for fed-batch cultivation of a GS-CHO cell line in a 24 SRW plate and shake flask	117
4.5	Growth profiles for fed-batch cultivation (diluted feeds) of a GS-CHO cell line in a 24 SRW plate and shake flask	119
4.6	Viability profiles for fed-batch cultivation (diluted feeds) of a GS-CHO cell line in a 24 SRW plate and shake flask	120
4.7	IgG production profiles for fed-batch cultivation (diluted feeds) of a GS-CHO cell line in a 24 SRW plate and shake flask	121
4.8	Osmolality profiles for fed-batch cultivation (diluted feeds) of a GS-CHO cell line in a 24 SRW plate and shake flask	122
4.9	Profiles for specific MAb productivity for fed-batch cultivation (diluted feeds) of a GS-CHO cell line in a 24 SRW plate and	123

	shake flask	
4.10	At-line pH profiles for fed-batch cultivation (diluted feeds) of a GS-CHO cell line in a 24 SRW plate and shake flask	125
4.11	At-line dissolved oxygen profiles for fed-batch cultivation (diluted feeds) of a GS-CHO cell line in a 24 SRW plate and shake flask	126
4.12	At-line dissolved carbon dioxide profiles for fed-batch cultivation (diluted feeds) of a GS-CHO cell line in a 24 SRW plate and shake flask	127
4.13	Glucose (Gluc) and lactate (Lac) profiles for fed-batch cultivation (diluted feeds) of a GS-CHO cell line in a 24 SRW plate and shake flask	129
4.14	Glutamine (Gln) and ammonia (NH ₄) profiles for fed-batch cultivation (diluted feeds) of a GS-CHO cell line in a 24 SRW plate and shake flask	130
4.15	Classification of wells on a 24 SRW plate by position	132
4.16	Viable cell density of a GS-CHO cell line 6, 10 and 15 days after inoculation, shown for corner, edge and internal wells	133
4.17	Viability of a GS-CHO cell line 6, 10 and 15 days after inoculation, shown for corner, edge and internal wells	134
4.18	Fluid volume per well for a GS-CHO cell line 6, 10 and 15 days after inoculation, shown for corner, edge and internal wells	135
4.19	IgG product titre for a GS-CHO cell line 6, 10 and 15 days after inoculation, shown for corner, edge and internal wells	136
4.20	Comparison of growth profiles for GS-CHO cells cultivated using standard and modified sandwich lids and standard and diluted bolus feeds. Cells were cultivated in 24 SRW plates	140
4.21	Viability profiles for GS-CHO cells cultivated using standard and modified sandwich lids and standard and diluted bolus feeds	141
4.22	Osmolality profiles for GS-CHO cells cultivated using standard and modified sandwich lids and standard and diluted bolus feeds	142
4.23	Dissolved oxygen profiles for GS-CHO cells cultivated using standard and modified sandwich lids and standard and diluted bolus feeds	143

Chapter 5: Bioreactor Engineering Characterisation and Scale Translation

5.1	Experimental and predicted microwell k_{La} values under mammalian cell culture conditions. Values obtained for a 24SRW, $V_L = 0.8$ mL, $D_o = 20$ mM at a range of shaking frequencies	149
-----	--	-----

5.2	Experimental set-up for determination of microwell k_{LA} by dynamic gassing out using the PreSens system	152
5.3	Plot of Log (P/V) against Log (k_{LA}), where P/V and k_{LA} are mean energy dissipation and the oxygen mass transfer coefficient respectively, at three difference values of superficial gas velocity (V_s)	155
5.4	Plot of Log (V_s) against Log (k_{LA}), where V_s and k_{LA} are superficial gas velocity and the oxygen mass transfer coefficient respectively, at three difference values of mean energy dissipation (P/V)	156
5.5	Change in dissolved oxygen tension over time in a sealed microwell containing 1 mL of CHO-S culture in CD-CHO medium	158
5.6	Fluid hydrodynamics in 24-SRW plates at shaking speeds of 140, 200, 250 and 300 rpm	165
5.7	Measured liquid phase mixing times for an orbitally shaken 24 SRW plate based on iodine decolourisation measurements	167
5.8	Measured liquid phase mixing times for an orbitally shaken 250 mL shake flask based on iodine decolourisation measurements	168
5.9	Measured liquid phase mixing times for a 5L stirred tank bioreactor based on iodine decolourisation measurements	169

Chapter 6: Mixing Time as a Basis for Cell Culture Scale

Translation

6.1	Viable cell density for fed-batch cultivation of a GS-CHO cell line in different small scale bioreactor geometries at a matched mixing time t_m of 5 s	180
6.2	Viability for fed-batch cultivation of a GS-CHO cell line in different small scale bioreactor geometries at a matched mixing time $t_m = 5$ s	181
6.3	IgG titre for fed-batch cultivation of a GS-CHO cell line in different small scale bioreactor geometries at a matched mixing time $t_m = 5$ s	182
6.4	Glucose and lactate profiles for fed-batch cultivation of a GS-CHO cell line in different small scale bioreactor geometries at a matched mixing time $t_m = 5$ s	183
6.5	Viable cell density for fed-batch cultivation of a GS-CHO cell line in different small scale bioreactor geometries at a matched mixing time $t_m = 5$ s	186
6.6	Viability for fed-batch cultivation of a GS-CHO cell line in different small scale bioreactor geometries at a matched mixing time $t_m = 5$ s	187

6.7	IgG titre for fed-batch cultivation of a GS-CHO cell line in different small scale bioreactor geometries at a matched mixing time $t_m = 5$ s	188
6.8	Glucose and lactate profiles for fed-batch cultivation of a GS-CHO cell line in different small scale bioreactor geometries at a matched mixing time $t_m = 5$ s	189
6.9	Viable cell density for fed-batch cultivation of a GS-CHO cell line	193
6.10	Viability for fed-batch cultivation of a GS-CHO cell line in different small scale bioreactor geometries at a matched mixing time $t_m = 5$ s	194
6.11	IgG titre for fed-batch cultivation of a GS-CHO cell line	195
6.12	Glucose and lactate profiles for fed-batch cultivation of a GS-CHO cell line in different small scale bioreactor geometries at a matched mixing time $t_m = 5$ s	196
6.13	Measurement of DO at the base of the microwells during 24 SRW plate cultivations of GS-CHO cells at variable shaking speed	199

Appendix I: Industrial Application ¹and Evaluation of a Microwell-Based Approach to Cell Culture Process Development

I.1	Schematic flowsheet showing the current (B) and new (A) procedures for cell line characterisation	213
I.2	Summary of viable cell count data for 54 transformed CHO cell lines cultured in three shaken 24 SRW microwell plates	217
I.3	Summary of IgG titre data for 54 transformed CHO cell lines cultured in three shaken 24 SRW microwell plates	218
I.4	Range of IgG concentrations (A) and viable cell densities (B) obtained for fed batch cultivation of 54 transformed GS-CHO cell lines in 24 SRW plates	219

Nomenclature

24 DSW	24 deep square well microplate
24 SRW	24 standard round well microplate
96 DSW	96 deep square well microplate
a_i	Specific static interfacial area, m^{-1}
Bo	Bond number, $\rho d^2g / W$, dimensionless
CCH	Cumulative cell hours, $\text{cells mL}^{-1} \text{ h}$
C^*	Saturation concentration of oxygen
C	Oxygen concentration
d_o	Orbital shaking diameter, m
d_f	Shake Flask inner diameter (m)
d_w	Microwell diameter (m)
D	Oxygen diffusion coefficient, $\text{m}^2 \text{ s}^{-1}$
D_i	Impeller diameter, m
DOT	Dissolved oxygen tension, percentage of air saturation
Fr	Froude number, $((2\pi N)^2 d_o) / 2g$, dimensionless
g	Acceleration due to gravity, 9.81 m s^{-2}
k_{La}	Oxygen mass transfer coefficient, h^{-1}
N_i	Impeller agitation rate, s^{-1}
N	Orbital shaking speed, min^{-1}
n_{crit}	Critical agitation rate, $\sqrt{((\sigma \cdot d) / (4 \cdot \pi \cdot V_L \cdot \rho \cdot d_o))}$, s^{-1}
N_p	Power number, dimensionless
Ne'	Modified power number, dimensionless
OTR	Oxygen transfer rate, $\text{mM L}^{-1} \text{ h}^{-1}$
P	Power, $N_p \rho N_i^3 D_i^5$, W m^{-3}
Ph	Phase number, $d_o/d \{1 + 3 \log_{10}[(\rho(2\pi N)/\mu)(d^2/4) ((1 - \sqrt{(1 - (4/\pi)(V_L^{1/3}/d)^2}))^2)]\}$ dimensionless
q_{nutrient}	Specific nutrient utilization rate, $\text{mg (10}^6 \text{ cells)}^{-1} \text{ h}^{-1}$
Re	Reynolds number, $(\rho N_i D_i^2) / \eta$, dimensionless
t_m	Liquid Phase Mixing Time (s)
Sc	Schmidt number, $\mu / \rho D$, (dimensionless)
VL	Liquid Fill volume, m^3
VCN	Viable cell number, mL^{-1}
W	Wetting tension, N m^{-1}
$Y_{\text{NH}_4^+/\text{gln}}$	Yield of ammonia on lactate, dimensionless
$Y_{\text{lac}/\text{gluc}}$	Yield of lactate on glucose, dimensionless

μ	Fluid viscosity, $\text{kg m}^{-1} \text{s}^{-1}$
ρ	Fluid density, kg m^{-3}
σ	Surface tension, N m^{-1}
ω	Angular velocity, m s^{-1}

Chapter 1: Introduction

1.1 Overview of Mammalian Cell Culture

Mammalian cells remain the expression system of choice for therapeutic proteins, largely due to their ability to ensure both correct folding and appropriate post-translational modifications such as glycosylation (Wurm 2004). While simpler proteins such as recombinant insulin may be produced in a system, such as *E.coli*, that lacks these abilities, larger molecules such as antibodies require a mammalian system to prevent the immunogenicity and reduced binding affinity that may be associated with improper folding or post-translational modifications (Tyther et al., 2011).

A number of mammalian cell types, including Hybridoma, Murine Myeloma and Chinese Hamster Ovary, are routinely used industrially (Chu et al., 2001). These cell lines have been adapted to grow in suspension, which allows processes to be far more scalable and flexible than if attached cells were used (Varley et al., 1999). In addition to suspension adaptation, a key process has been the development of growth media from undefined serum-containing formulations towards chemically defined recipes (Huang et al., 2010). Initial fears that this shift would render cells highly susceptible to physical forces, such as hydrodynamic shear, have proven unfounded (Nienow, 2006). The change to defined media has the twofold advantages of

greater batch-to-batch consistency and a reduction in the risk of introducing adventitious agents that might be present in serum (since it is an animal derived product).

Media development is one of a number of innovations that have driven higher viable cell densities and product titres in mammalian cell culture processes.

1.2 Monoclonal Antibodies

With sales of \$15.6 billion in the United States alone in 2008, monoclonal antibodies are the largest class of biologic drug and continued to exhibit double digit growth despite the global recession (Aggarwal, 2009).

Murine monoclonal antibodies (mAbs) were first produced in 1975 (Koehler & Milstein, 1975) and fully humanized forms by 1986 (Jones et al., 1986). Issues with murine mAbs, including short serum half life and the potential for an immunogenic response in the patient (Pavlou et al., 2005), were overcome with the advent of humanized forms.

The basic structure of an antibody is shown in Figure 1.1 and consists of two heavy and two light chains held together covalently by disulphide bonds:

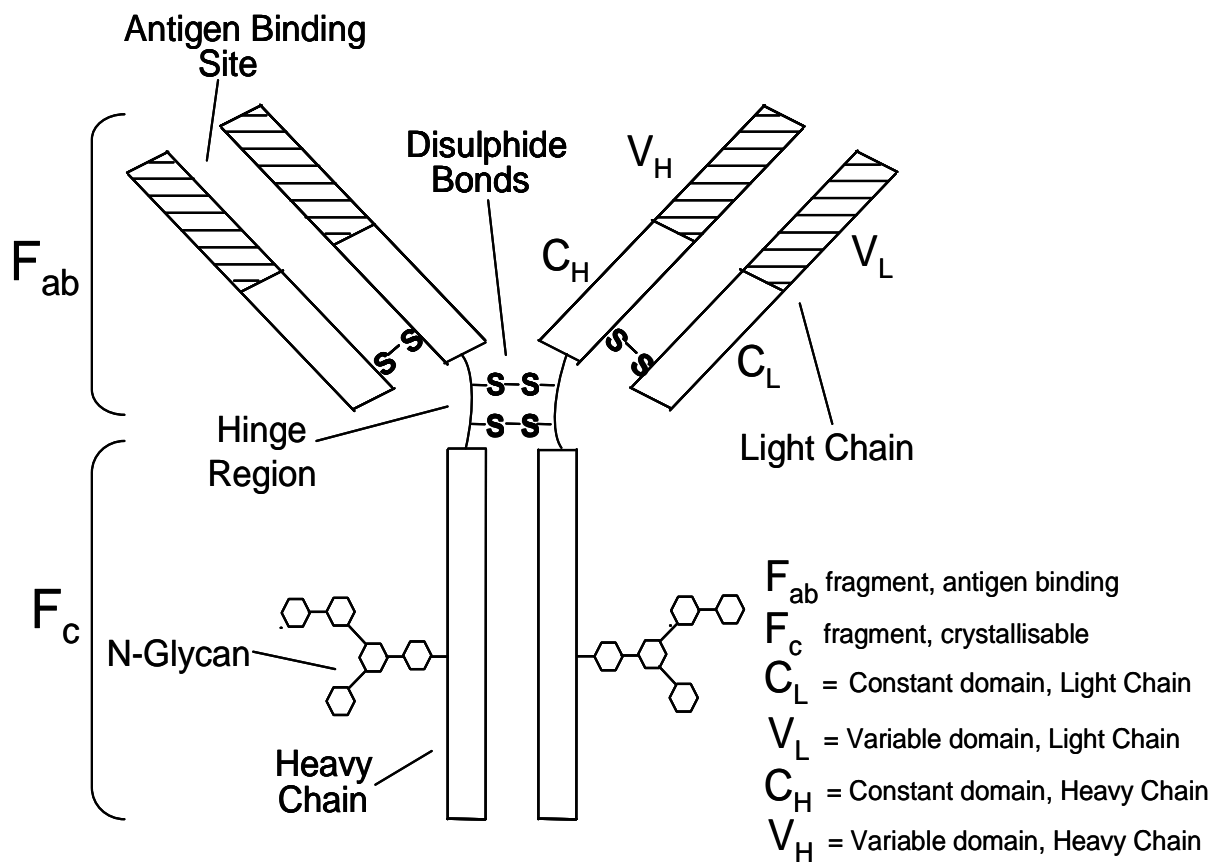


Figure 1.1: Basic structure of an IgG molecule, consisting of two heavy and two light chains with a total molecular weight of approximately 150 kDa. Disulphide bonds between the two heavy chains and between light and heavy chains are shown.

There are five isotypes of antibody molecule IgA, IgG, IgM, IgD and IgE which are distinguished by the sequence of the constant regions of their heavy chains (Woof et al., 2004). Of these antibody classes IgG molecules are the most frequently used therapeutically (Weiner et al., 2010).

The ability of the antibody to bind its target (or antigen) is conferred by the variable regions of the molecule, and it is this which makes mAbs valuable as therapeutic proteins. For example, mAbs have been extensively

used in the treatment of cancer, (Weiner et al., 2010) where it is believed that their therapeutic action is derived from a number of effects including disruption of signalling between tumour cells, and also through what is described as 'complement-dependent cytotoxicity,' which involves activation of the complement system by the mAb resulting in destruction of cancer cells.

The other significant indication for mAb products is in treatment of arthritis, for which blockbuster drugs (broadly classified as products with revenues in excess of \$1 billion annually) include Infliximab and Adalimumab ((trade names Remicade and Humira respectively) (Maggon, 2007).

The vast size of this market is what drives biopharmaceutical companies to reduce development times for new products to the minimum possible, as any delays may incur significant losses in revenue streams (Farid, 2007). The next section will begin with large scale cell culture processes and subsequently examine the options for the small scale. Specifically, to what extent these systems satisfy the simultaneous demands for high throughput and scalability that are required to reduce development times for novel products.

1.3 Stages Involved in Cell Culture Process Development

Following cell line transfection, there are a number of stages involved prior to the development of a robust manufacturing process for a

biopharmaceutical product (Figure 1.2). The first step is to select the highest producing candidates from a large pool of transfectants, typically using static microwell plates to provide the necessary throughput (Porter et al., 2010). Selected cell lines are then cultured in shake flasks and an initial culture process is developed (Betts et al., 2006), following which the culture is scaled-up to bench or pilot scale stirred-tanks (typically between 1 and 10 litre volume for bench scale and up to 80 litres for pilot vessels (Li et al., 2006). The majority of process optimisation work, in terms of feeding strategies and operating conditions, is performed at this scale (Amanullah et al., 2010). Only once a robust process has been developed can scale-up to manufacturing scale stirred tanks and process validation occur. (Xing et al., 2009)

1.4 Production Scale Culture

The majority of cell culture processes performed at commercial scale use large stirred tank bioreactors typically of 10 – 20,000 litre scale (Heath et al., 2007). This format has gradually emerged as the standard while the rival technology of the airlift has largely been superseded (Warnock et al., 2006).

The key distinction between the stirred tank (STR) and the airlift reactors is the lack of an impeller in the latter, in which liquid mixing is

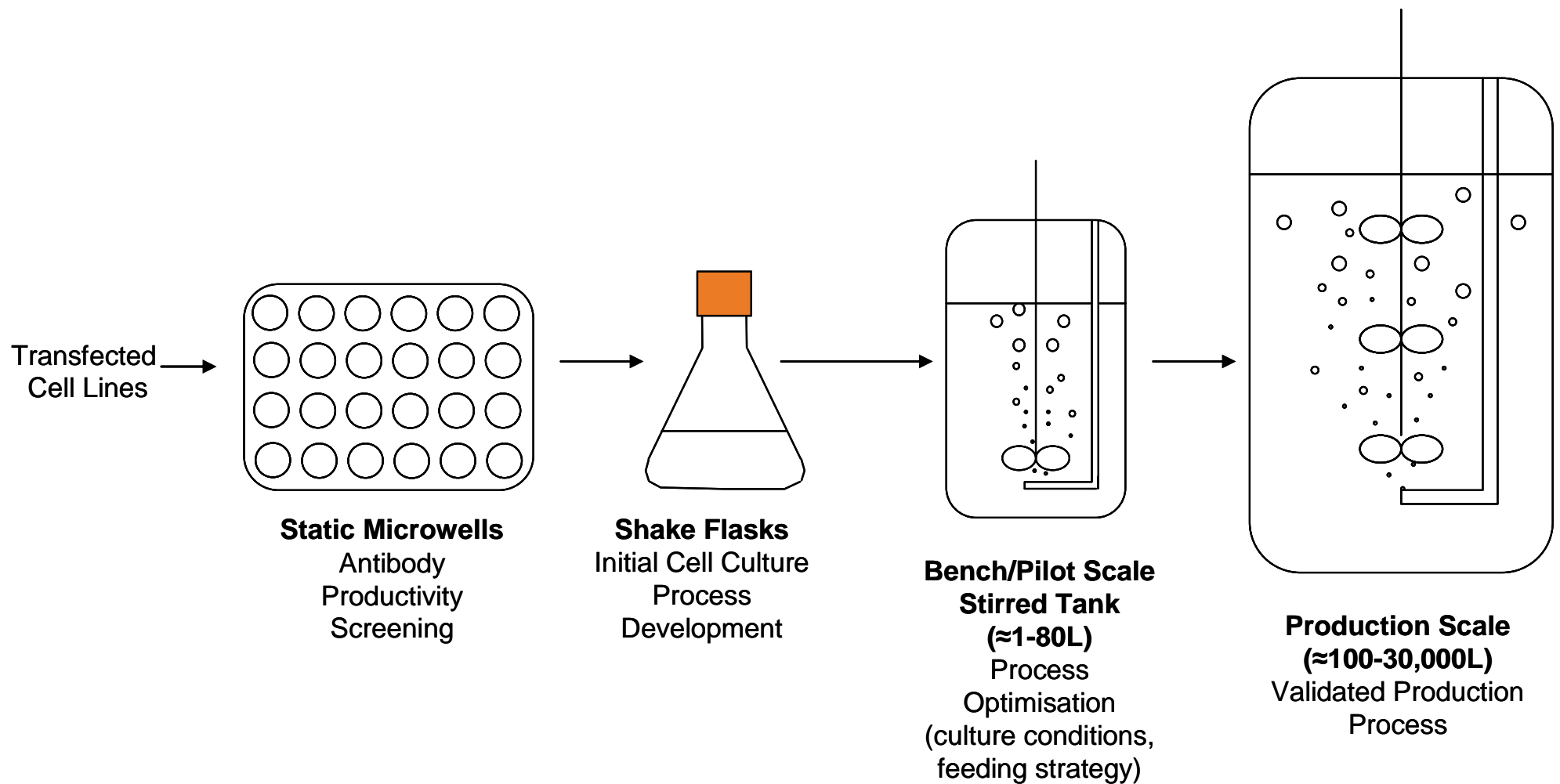


Figure 1.2: Typical stages involved in development of a production scale cell culture process.

provided entirely by the passage of air bubbles from the sparger into the 'riser' portion of the reactor. Hydrodynamic shear in the airlift is thus significantly lower than that in the STR, which was believed to be beneficial for mammalian cells due to their perceived fragility (Chisti, 2001). This was thought to be the case due to their lack of a protective cell wall when compared to bacteria (Nienow, 2006). However the notion that mammalian cells are highly shear sensitive has largely been dispelled by more recent research (Mollet et al, 2007). In addition, use of the polymer Pluronic F-68 in culture media has been demonstrated to reduce damage to mammalian cells, and the use of this agent is now widespread (Ma et al., 2004).

Process challenges in large scale cell culture are numerous, and include stripping out potentially toxic carbon dioxide from the medium, the accumulation of toxic waste products such as ammonia and lactate, provision of adequate mixing to ensure homogeneity and meeting the cellular requirement for oxygen (Zhang et al., 2010). A variety of operating strategies have been used to meet these challenges, and are often expressed in terms of the rationale by which processes are translated from the small, laboratory scale without incurring a performance loss; this is generically described as 'scale-up' (Chu et al., 2001). For example, power per unit volume (Li et al., 2006) and liquid mixing (Xing et al., 2009) are commonly used scale translation parameters.

Production scale runs for cell culture are necessarily very costly (Farid, 2009) for a number of reasons including the high price of production media used in such large volumes, and the energy costs associated with steam sterilisation, as well as the labour costs involved in setting up the reactors. As a result, significant work on process development occurs at small (generally shake flask, microwell and/or miniature stirred tank using volumes from 1 – several hundred mL of media) and bench (roughly 5 litre stirred tanks) scales prior to initial pilot runs (roughly 100 litres). The majority of biopharmaceutical companies use bench scale (1 – 10 litre) stirred tanks to validate scale-down models of their production process. Only after collection of significant quantities of process data at these stages, and the development of an appropriate feeding strategy and operating conditions, is the process scaled up for production. It is essential that the system selected for use at the small scale provides culture data that are representative of manufacturing scale, if they are to serve as acceptable ‘scale-down’ models (Li at al., 2006).

A variety of options, including use of shaken microwells as advocated by this thesis, exists for initial characterisation of cell lines and process development.

1.5 Small Scale Culture Systems for Cell Line Characterisation and Process Development

A large number of cell lines are generated by biopharmaceutical companies, all of which must undergo some limited characterisation to assess their suitability for eventual use at production scale for the market. While the shake flask has traditionally been the culture vessel used to assess cell lines at this early stage (Büchs, 2001), a number of alternative systems are now available.

1.5.1 Miniature Stirred Tank Systems: A number of manufacturers produce small scale stirred tank systems in which parallel cultivations can be performed (vendors include Infors, HEL, Das Gip and Sartorius). The principal advantage of such systems is that they retain the format used for manufacturing scale processes and as such provide a comparable engineering environment for cultured cells (Bareither et al., 2011). Consequently it is expected that data collected are likely to be representative of larger scales of operation. In addition the majority are instrumented with pH, dissolved oxygen and temperature sensors to facilitate control of these key parameters and to allow collection of process data.

The similarity of such systems to bench, pilot and manufacturing scale stirred tanks means that operators in industry will require minimal training prior to use. However, there are some disadvantages to use of these systems.

They require labour intensive set up including calibration of probes, steam sterilisation of vessels and cleaning after each run (although these considerations may be alleviated by the use of disposables containing pre-calibrated probes) which adds to energy and labour costs. Furthermore the degree of parallelisation is limited in comparison to microwell, and even shake flask, technologies with the number of stirred tank units operated simultaneously ranging from 4 to 16 (Das Gip = 16, Infors = 6, HEL = 4, Sartorius = 12 for models available in 2010), while a larger number of shake flasks can be potentially loaded into a shaken incubator and microwell plates offer as many parallel cultivations as they do wells (typically between 6 and 384 per plate).

In more recent years there has been an increasing adoption of disposable technologies for cell culture, due to a combination of convenience (units are available pre-calibrated and pre-sterilised, thus avoiding the labour-intensive requirement for set-up that is required for conventional stainless steel systems) and environmental reasons (the lack of a requirement for steam sterilisation significantly reduces the carbon footprint of these systems) (Rao et al., 2009). In addition to well-established wave bag technology (Eibl et al., 2010), a number of manufacturers have produced disposable stirred tanks, including the CellReady 3L reactor (Millipore) and the CelliGen BLU 5 and 14 L systems (New Brunswick).

1.5.2 Shake Flasks: Shake flasks have long been ubiquitous in early process development and cell line characterisation due to their ease of use and the possibility of performing large numbers of simultaneous fermentations on a single shaking platform (Betts et al., 2006). It was estimated that in 2001 90 % of cultures were performed in flasks (Büchs, 2001). In contrast to the situation described for shaken microwell plates in Section 1.5.3, widespread use of shake flasks for cell culture experiments has preceded a full understanding of the engineering environment.

This environment is entirely distinct from that in stirred tanks, as flasks lack both sparger and impeller. They therefore rely entirely on the motion of the shaking platform to generate liquid motion for mixing and gas mass transfer. They also have the disadvantage that there is no dissolved oxygen control and only limited pH control (from adjustment of the headspace carbon dioxide concentration).

A number of studies, particularly those by the group of Jochen Büchs, have characterised the engineering environment of shaken flasks though primarily for conditions suitable for microbial cell cultivation. Key parameters evaluated include power dissipation (Büchs et al., 2000) and oxygen mass transfer (Gupta et al., 2003). The concept of 'out-of-phase' conditions was also used to describe operation of shake flask culture processes under sub-optimal conditions, whereby cell growth may be limited (Büchs et al., 2001). Equation

[1.1] can be used to indicate whether operating conditions are likely to be appropriate:

$$Ph = \frac{d_s}{d_f} \left\{ 1 + 3 \log_{10} \left[\frac{\rho(2\pi N)d_f^2}{4\mu} \left(1 - \sqrt{1 - \frac{4}{\pi} \left(\frac{V_L^{1/3}}{d_f} \right)^2} \right)^2 \right] \right\} \quad [1.1]$$

It was found that when $Ph < 1.26$ conditions could be described as ‘out of phase’ such that the fluid contents of the flask do not follow the motion of the shaking platform, with the result that mixing and mass transfer may be less effective than anticipated. These studies collectively illustrate the requirement for culture conditions to be rationally and carefully selected.

With regard to mean energy dissipation, the below correlation was empirically derived to allow estimation of the power per unit volume of fluid in a shake flask (Büchs et al., 2000):

$$\frac{P}{V_L} = Ne' \rho \frac{n^3 d^4}{V_L^{2/3}} \quad [1.2]$$

These studies are valuable in ensuring that shake flask cultures are performed under optimal conditions such that oxygen mass transfer is not limiting, and fluid mixing is adequate to ensure homogeneity.

1.5.3 Microwell Plates: These are widely available in a variety of geometries and at low cost, and can allow a larger number of parallel culture experiments to be performed simultaneously, and are therefore attractive candidates for use in cell culture development (Micheletti and Lye, 2006). Strobel et al. (2001) describe cultivation of CHO cells in 96 deep square well plates, and Girard et al. (2001) use a 12 well system for microbial growth. However, there are relatively few examples in the literature of their use in this regard, and they are more traditionally associated with analytical applications such as performing ELISA assays.

As with shake flasks, characterisation of the engineering environment in shaken microwell plates is essential for the rational selection of cell culture conditions. For example, a key requirement for any cell culture system is that oxygen mass transfer is sufficient to support cell growth. Doig et al. (2005) derived a correlation that allows de novo prediction of k_{LA} values in a variety of round-well geometries, and over a range of shaking conditions, thus allowing shaking speeds to be tailored to meet cellular requirements. Complementing this work, Duetz et al. (2004) examined the impact of using square geometries on oxygen mass transfer, and it was found that the 'baffling' effect of this shape boosted both mixing and mass transfer efficiency for a given shaking speed. Direct measurement of dissolved oxygen levels within microwell plates provides another method of testing the system's mass transfer capabilities (Gernot et al., 2003). This was achieved by the use of

optical probes, a technique that can also be used to directly measure microwell k_{LA} values. However, the majority of this work was performed with reference to microbial culture, and as such is not always directly applicable to the operating conditions typical of mammalian cell culture processes.

In general, the results of these studies have indicated that oxygen limitation is unlikely to be a significant issue for microwell cultivations under the majority of conditions tested. This is due to the low oxygen demand of slow-growing mammalian cells (in marked contrast to microbial systems such as *E.Coli* for which significantly higher k_{LA} values are required). Nienow (2006) suggests that a k_{LA} value of 1 h^{-1} is sufficient to support a viable cell density of $1 \times 10^7 \text{ cells mL}^{-1}$. By comparison, (Duetz, 2007) found that the k_{LA} for a 96 standard round well geometry with a fill volume of $200 \mu\text{L}$ was approximately 25 h^{-1} under static conditions.

In addition to adequate oxygen mass transfer, it is essential that the contents of the microwells be well mixed to ensure homogeneity and thus prevent the formation of nutrient, waste product or dissolved oxygen gradients, which have been found to have a detrimental effect on cell growth (Varley et al., 1999). It has been suggested that the small liquid volumes used for microwell cultivations give a 'false sense of security' with respect to the ease of achieving good mixing Duetz (2007). On the contrary, for well geometries of less than 8 mm diameter, the surface tension of the liquid surface is an obstacle to the development of fluid turbulence and a well-mixed

environment (Duetz 2007), a phenomenon also alluded to in the work of Doig et al. (2005) on microwell oxygen transfer rates. Liquid mixing in microwell systems should therefore not be neglected.

As well as ensuring that the microwell contents are homogeneous, efficient bulk mixing is essential to ensure dispersal of oxygen throughout the culture medium once it has entered at the gas-liquid interface. Doig et al. (2005) noted that despite an apparently acceptable k_{La} , oxygen limitation at the base of a microwell could occur if bulk mixing was poor, as diffusion was then necessary for oxygen to be distributed throughout the liquid.

For mixing to occur, the surface tension of the liquid in the microwell must be broken. N_{crit} (Equation 1.3) represents the agitation speed above which the surface tension of liquid in the wells is overcome such that bulk motion of the fluid is observed (Hermann et al., 2003):

$$N_{crit} = \sqrt{\frac{\sigma \cdot d_w}{4\pi V_L \rho d_o}} \quad [1.3]$$

Where σ is the surface tension, d_w is the microwell diameter, V_L is the liquid volume in the microwell, ρ is the fluid density and d_o is the orbital shaking diameter.

Nealon et al. (2006) studied the jet mixing which occurs on liquid additions to microwell plates, which is of significance when considering that feed and alkali additions, for fed-batch operation and pH control respectively, may be required for a cell culture process. Such additions should be rapidly

mixed into the bulk fluid to avoid the development of pH or nutrient gradients that could potentially harm cells (Varley et al., 1999). An additional approach to the analysis of microwell fluid flow used computational fluid dynamics (CFD), which is also able to provide estimates of mean energy dissipation (Zhang et al., 2008). In this work it was found that CFD predictions regarding fluid flow patterns were in close agreement with those observed using a high speed camera. The results of these analyses were used as the basis for cultivation of a Hybridoma cell line at matched power per unit volume (Barrett et al., 2010).

The engineering characterisation studies described above have allowed the rational selection of conditions for cultivation of a Hybridoma cell line in a shaken 24 well system (Barrett et al., 2010) to ensure that cellular demands for oxygen and mixing are met while keeping hydrodynamic shear below potentially harmful levels. The work of the Chalmers group, who constructed a device to test the resistance of different mammalian cell types to hydrodynamic shear forces (Ma et al., 2002), enables appropriate conditions to be selected which avoid cell necrosis or apoptosis.

Using matched power input per unit volume for scale translation, comparable peak viable cell density and antibody titre were achieved for parallel Hybridoma cultures in microwell, shake flask and stirred tank reactors (Barrett et al., 2010).

1.6 Alternative Culture Systems

In addition to the widely recognised culture formats described above, a number of small scale, high-throughput systems have emerged in recent years which are less easily classified but are of significance, in particular because of their commercial availability. The following sections provide a brief overview of some of the systems available.

1.6.1 SimCell: The SimCell is a microfluidic device marketed by Seahorse Biosciences, which can be used to perform up to 1260 culture experiments simultaneously (Amanullah et al., 2010). ‘Microbioreactor Arrays’ consist of a number of gas permeable cassettes, as shown in Figure 1.3;



Figure 1.3: Single gas-permeable cassette from the SimCell (image taken from manufacturer’s information).

Rather than the orbital shaking employed for shake flask or microwell cultivations, fluid mixing is achieved through gentle rotation of the culture on

a 'carousel' in which the cassettes are mounted. Gentle movement of an air bubble within each cassette, which has a working volume of approximately 700 μL , achieves a k_{LA} value of around 7 h^{-1} and liquid mixing time of about 20 seconds (Amanullah et al., 2010). Feeding and pH control are facilitated by microfluidic devices, to which the cassettes are transported when required. Legmann et al. (2009) describe the implementation of a Design of Experiments (DOE) approach using the SimCell, and are able to demonstrate comparable performance with shake flask and 3 litre stirred tank processes. As such the SimCell may be a powerful tool for implementing Quality By Design (QBD) initiatives due to its high level of parallelisation. A key drawback is the high fixed cost of the equipment, taking it out of the price range of most companies apart from large multinationals.

1.6.2 Micro-24: Distributed by Pall, this system uses an instrumented microwell plate system to allow 24 parallel cultivations to be performed. Unlike an off-the shelf microwell plate, these units have fluorescence sensitive dissolved oxygen and pH sensors, and also a gas-permeable frit to facilitate sparging of carbon dioxide, oxygen, air and nitrogen. Each of the 24 wells in a plate offers individual control of pH, temperature and dissolved oxygen. Liquid mixing is provided by a combination of the sparged gas and an orbital shaking platform.

A recent study demonstrated that a good level of agreement between the Micro 24 and a 2 litre stirred tank was reached for culture of a CHO cell line, as assessed by comparison of cell growth, metabolite profiles, product titre and quality characteristics (Chen et al., 2008). However, this study includes limited engineering characterisation and does not attempt to define a basis for process scale-up. This system also lacks the level of parallelisation offered by the SimCell, in particular because only one plate can be operated at a time and thus does not offer a large increase in throughput considering the cost of the device.

1.6.3 BioLector: One of the most recent devices to enter the market place is the BioLector from Dasgip. Published data for use of the BioLector have so far focussed on its use in *E.coli* fermentation (Huber et al., 2009), but it has potential for application in mammalian cell culture. Its basis is a shaken microwell system using either 48 or 96 well plates which have either round or 'flower' geometry (the latter shape is intended to boost mixing and oxygen mass transfer into the culture medium). In the Huber work (2009) the BioLector is interfaced with a liquid-handling robot to form the 'RoboLector,' thus allowing automatic addition of liquids throughout the culture process.

Without evidence of industrial use in mammalian cell cultivation, the BioLector remains unproven but appears to have potential.

1.7 Aim and Objectives of Thesis

As described in Section 1.3 shake flasks currently provide the standard bioreactor format used in early stage cell culture development. However, use of shake flasks has a number of disadvantages including a lack of control over culture conditions and low throughput. Recently a number of alternative bioreactor formats have been proposed including miniature stirred bioreactors (Section 1.5.1) and a number of instrumented microwell formats (Section 1.6.2 and 1.6.3). While these provide the necessary control of culture parameters they are generally considered expensive especially for high throughput applications. Consequently the aim of this work is to establish the use of shaken microwell plates for parallel and scaleable evaluation of mammalian cell cultures.

This builds on the initial work of Barrett et al (2010) described in Section 1.5.3 who demonstrated batch cultivation of hybridoma cells in shaken 24-well plates. While illustrating the potential of suspension culture in microwells this previous work does not demonstrate the applicability of the method to fed-batch cultures or cells that reach industrially relevant cell densities and product titres. Consequently the specific objectives of this work are as follows:

- To reproduce the suspension culture methods of Barrett et al (2010) and compare optimum culture conditions for hybridoma cells with

those of a commercially available CHO cell line. This work is described in Chapter 3.

- To extend microwell culture methodology to fed-batch operation and demonstrate application of this approach to an industrial cell line. This work is covered in Chapter 4.
- To define the engineering characteristics of shaken microwells under conditions suitable for cell culture with a view to defining suitable conditions for scale translation. The measurement of key engineering parameters such as k_{La} , mixing time and power input is described in Chapter 5.
- To illustrate predictive scale translation between shaken microwell cultures and those of shake flasks and scale-down 5L STRs. This work is described in Chapter 6.

Finally, since this is an EngD project in collaboration, the microwell methodology developed here has also been evaluated in a commercial context for initial cell line selection and its performance compared to existing shake flask methods. The benefits of the microwell approach are illustrated in Appendix I.

Chapter 2: Materials and Methods

2.1 Cell Culture

2.1.1 Cell Lines Used

A total of three cell lines were used in this work. Initial batch culture experiments (Chapter 3) used a commercially available CHO-S cell line (Invitrogen, Paisley, Scotland) that did not secrete an extracellular protein product. This cell line was initially cultivated in CHO-S-SFM II media, before switching to the more industrially relevant CD-CHO (Invitrogen). The latter did not contain glutamine and so was supplemented with 8mM L-glutamine prior to use.

Subsequent work (Chapters 4 and 6) focussed on use of a proprietary GS-CHO cell line supplied by MedImmune (Cambridge, UK) which produces an IgG monoclonal antibody. This cell line was created at MedImmune using the Lonza GS (Glutamine Synthetase) system. This was cultured in CD-CHO medium without supplementation (the presence of the glutamine synthetase gene in this cell line removes the requirement for addition of L-Glutamine to the media).

Further work (Chapter 6) used a second proprietary GS-CHO cell line supplied by Lonza Biologics (Slough, UK) through the UCL IMRC Bioprocessing consortium of companies of which both MedImmune and

Lonza are members. This line also produced an IgG monoclonal antibody. (though a different one to the MedImmune supplied cell line). This was also cultured in CD-CHO medium without supplementation.

2.1.2 Revival of Cells from Liquid Nitrogen Storage (applies to CHO-S line and both GS-CHO cell lines)

A working cell bank vial containing 1mL of frozen cells was revived by initial rapid thawing in a Haake F6 water bath at 37°C, and subsequently diluted into 9 mL of CD-CHO media at 4°C (Gibco, Invitrogen). Cells were then centrifuged at 600 rpm in a Beckman GS-6 instrument (Beckman, Brea, California), following which the supernatant was discarded and the pellet resuspended in a total volume of 50 mL CD-CHO medium in a 250 mL vent cap Erlenmeyer flask, to achieve a seeding density of approximately 3.0×10^5 viable cells mL⁻¹. The flask was placed in a Galaxy R CO₂ incubator at 37°C under 5% CO₂. The GS-CHO cell lines were shaken with agitation at 140 rpm, orbital shaking diameter 25 mm on a Sartorius (Surrey, UK) Certomat MO II shaker, while the CHO-S cell line was shaken with agitation at 120 rpm, orbital shaking diameter 10 mm on an IKA (Staufen, Germany) KS 260 shaker.

Cells were subcultured at intervals of three or four days by dilution into fresh media at a seeding density of 2.0×10^5 cells mL⁻¹, using a total working volume of 50 mL in a 250 mL Erlenmeyer vent cap flask, and adding methyl sulphoxamine (MSX) at a final concentration of 25 µM (MSX was added to GS-CHO cell cultivations but not to the CHO-S cultivations).

2.1.3 Preparation of Working Cell Bank

Cells were seeded at $2.0 \times 10^5 \text{ mL}^{-1}$ in 250 mL shake flasks and cultured for 48 hours, following which the cell suspension was transferred to 50 mL centrifuge tubes and centrifuged at 200g for five minutes. Cells were then resuspended to a final concentration of $1 \times 10^7 \text{ cells mL}^{-1}$ in 1 mL of a solution consisting of 90% CD-CHO medium and 10% DMSO (Sigma, Poole, Dorset), following which cells were transferred to 1 mL sterile cryovials (Fisher, Loughborough, UK). Cryovials were then loaded into a Nalgene Mr Frosty container (Sigma) which was left in a -70°C freezer for 24 hours, following which cryovials were transferred for storage in a liquid nitrogen dewar.

2.2 Shake Flask Cultures

Shake flask cultures were performed using a variety of shaking conditions and fill volumes throughout the project. All cultures were seeded at a viable cell density of $2 \times 10^5 \text{ cells mL}^{-1}$ and incubated at 37°C and grown under a 5% CO_2 atmosphere unless otherwise stated. MSX was not added to these batch or fed-batch cultures.

CHO-S cultivations were performed using 100 mL fill volume in a 250 mL Erlenmeyer vent cap flask, using CD-CHO medium supplemented with 8

mM L-Glutamine, and shaken at 120 rpm with an orbital shaking diameter of 10 mm on an IKA KS 260 shaker.

GS-CHO cultivations (for both MedImmune and Lonza cell lines) were performed using a 50 mL fill volume in a 250 mL Erlenmeyer vent cap flask, using CD-CHO medium without L-Glutamine supplementation. These were shaken at either 140 or 220 rpm with an orbital shaking diameter of 25 mm on a Sartorius Certomat MO II shaker at a temperature of 36.5 °C (temperature specified by industrial sponsor and retained for consistency).

2.3 Microwell Cultures

2.3.1 24 SRW Plates: The majority of microwell cultivations were performed in 24 Standard Round Well (SRW) ultra low attachment plates (Corning, New York, USA). Plate Geometry is shown in Figure 2.1.

CHO-S: Batch 24 SRW cultivations were inoculated at a seeding density of 2×10^5 viable cells mL⁻¹ and a fill volume of 0.8 mL, incubated at 37°C in a humidified Galaxy R incubator under 5% CO₂ atmosphere. Plates were shaken at a range of speeds between 120 and 180 rpm at an orbital shaking diameter of 20 mm. Plates were sealed with a Breatheasy membrane (Diversified Biotech) for maintenance of sterility and minimisation of evaporation.

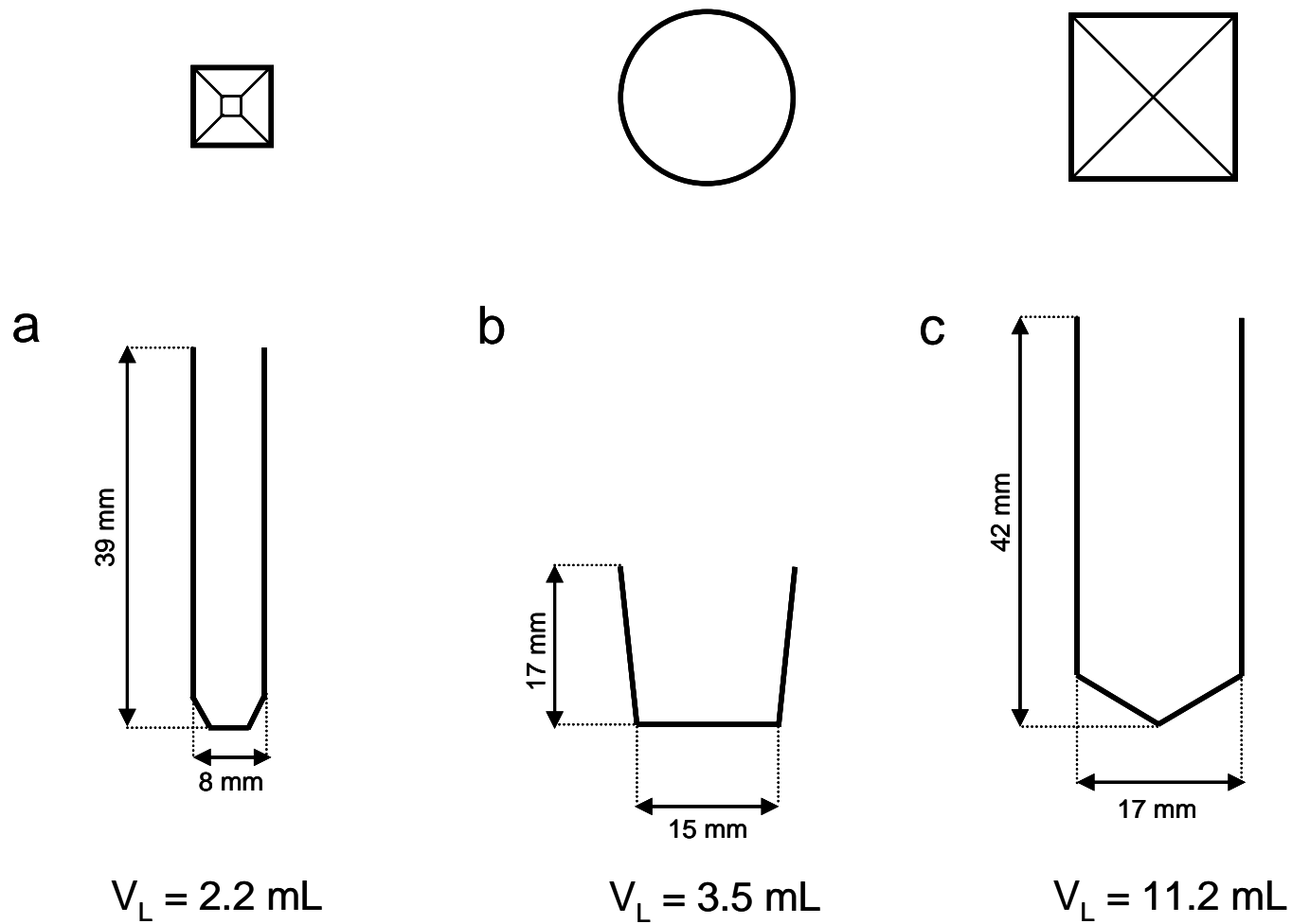


Figure 2.1: Schematic drawings of single wells from microwell plates used for cell culture, (a) 96 deep square well (DSW), (b) 24 standard round well (SRW) and (c) 24 deep square well (DSW) geometry.

GS-CHO Lines 24 SRW cultivations were inoculated at a seeding density of 2×10^5 cells mL⁻¹ and a fill volume of 0.8 mL and incubated at 36.5 °C in a Galaxy (New Brunswick Scientific, New Jersey, USA) R incubator (UCL) or Infors (Bottmingen, Switzerland) humidified incubator (MedImmune) under 5% CO₂ atmosphere. Cultures were shaken at either 140 or 220 rpm at an orbital shaking diameter of 25 mm. All plates were sealed with a 'sandwich lid' system (Duetz et al., 2000) in conjunction with a metal clamp (Enzyscreen BV, Leiden, The Netherlands) as shown in Figure 2.2. The sandwich lids were sterilised by autoclaving and subsequently oven dried before use.

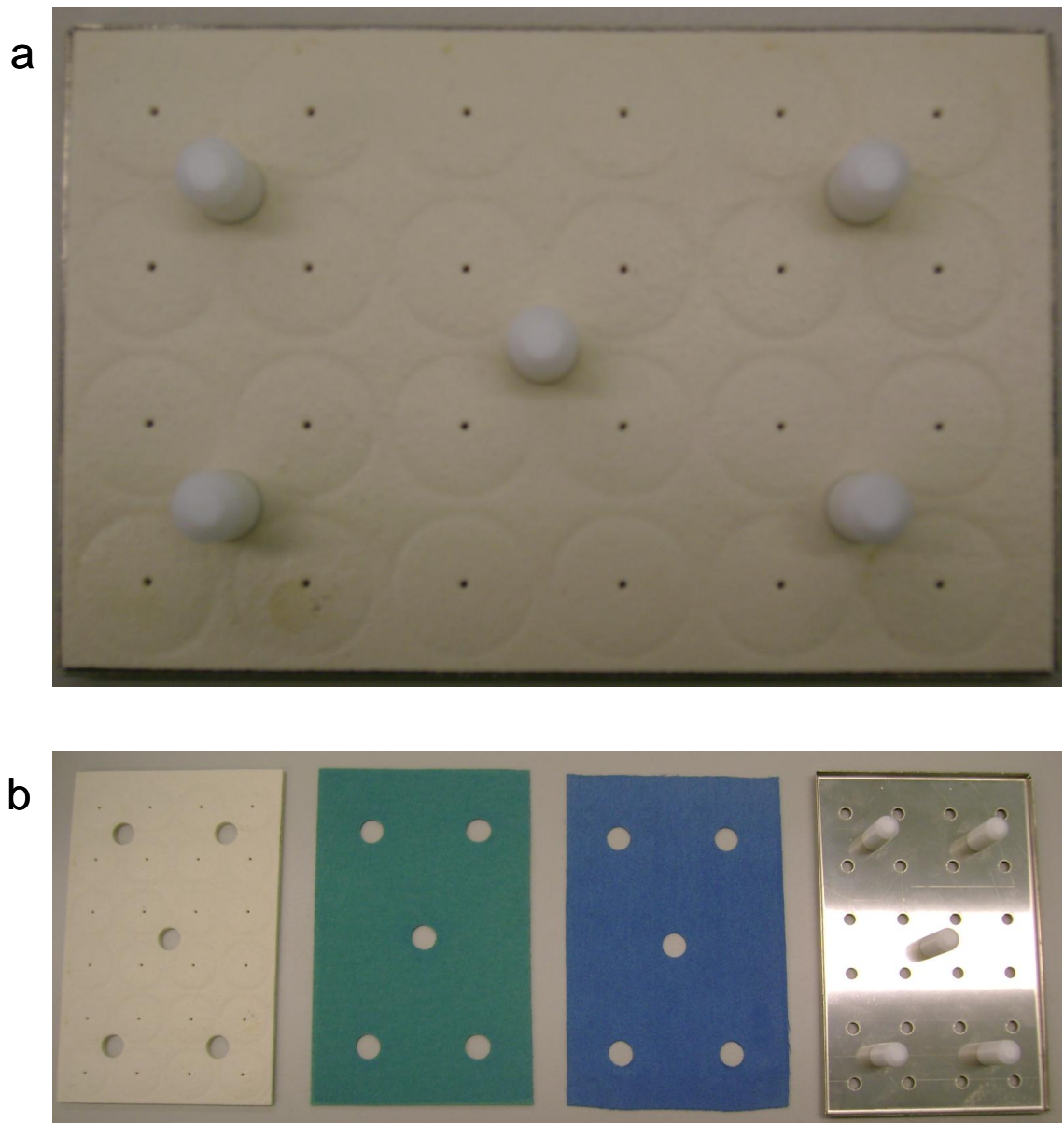


Figure 2.2: (a) the underside of the Duetz sandwich lid designed for use with a 24 SRW plate and (b) the component layers of the sandwich. From left to right, soft silicone (white), ePTFE filter (0.3 μM) laminated between two pieces of polyester/polyamide fabric (green), a microfibre filter (blue) and a stainless steel lid.

2.3.2 24 Deep Square Well (DSW) Plates: 24DSW plates from Innovative Microplate (Seahorse Bioscience, Boston, Massachusetts) were soaked in 1.0M sodium hydroxide for one hour, and then rinsed thoroughly and subsequently soaked in Milli-Q water (plate geometry shown in Figure 2.1). The plates were autoclaved (using a hold temperature of 121°C for 20 minutes) and then oven dried at 80°C prior to inoculation with CHO-S cells at a seeding density of 2×10^5 cells mL⁻¹ and a fill volume of either 0.8 mL or 2.0 mL. Plates were incubated at 37.0 °C in a Galaxy R humidified incubator under 5% CO₂ atmosphere and shaken at 180 rpm at an orbital shaking diameter of 20 mm. Plates were sealed with a Breatheasy membrane (Diversified Biotech) for maintenance of sterility.

2.3.3 96 DSW Plates: 96 DSW plates (ABgene, Surrey, UK) were sterilised and autoclaved as described in Section 2.3.2 (plate geometry shown in Figure 2.1). Once sterilised these plates were inoculated with CHO-S cells at a seeding density of 2×10^5 cells mL⁻¹ and a fill volume of 1.0 mL. Plates were incubated at 37.0 °C in a Galaxy R humidified incubator under 5% CO₂ atmosphere and shaken using an orbital shaking diameter of either 4.5 or 20 mm, using an IKA MS1 minishaker and Heidolph Rotamax 120 (Wolf Labs, York, UK) respectively. Plates were sealed with a Breatheasy membrane (Diversified Biotech) for maintenance of sterility.

2.4 Stirred Tank Cultures

Stirred tank experiments were performed using a 5 L BIOSTAT B-DCU (B.Braun Biotech, Sartorius, Surrey, UK). This had an internal diameter, T_V , of 160 mm, with a working volume of 3.5 L (liquid height $H_L \approx 2 T_V$). The vessel was unbaffled and stirred by a single three-bladed impeller ($D = 67$ mm) with a dimensionless power number of 0.97 (measured at $Re = 16,000$) operated in a down-pumping configuration with a blade angle of 45° (as shown in Figure 2.3). Temperature was controlled at 37°C and pH at 7.10, with dissolved oxygen maintained at 30% saturation by sparging a mixture of air, oxygen, carbon dioxide and nitrogen. Sodium carbonate and sodium hydrogencarbonate were used for base control at concentrations of 0.5M, and were of analytical grade (BDH Merck, Poole, Dorset, UK). Prior to cultures the pH probe (Mettler Toledo, Greifensee, Switzerland) was calibrated using standard solutions at pH 4.0 and 7.0 (Mettler Toledo).

Prior to use the tank was washed using 1.0 M sodium hydroxide (Fisher Scientific) at 50°C , and subsequently rinsed repeatedly in distilled water following which the vessel was steam sterilised, using a hold temperature of 121°C for 20 minutes. The seeding density for inoculation was 2×10^5 viable cells mL^{-1} .



Figure 2.3: Stainless steel three-bladed impeller ($D = 67$ mm) with a dimensionless power number of 0.97 (measured at $Re = 16,000$) and a blade angle of 45° .

2.5 Fed Batch Protocols

2.5.1 CHO-S: Initial fed batch cultures were performed in 24 SRW plates (Section 2.3.1) with the CHO-S cell line using a proprietary feed forward algorithm to define the feeding regime. Briefly, using metabolite and viable cell number data from the current and preceding days, the algorithm determined the quantity of liquid feed to be added to the culture in order to maintain L-

Glutamine at 2 mM. The assumption is made that the cell growth rate and specific L-Glutamine utilisation rate over the subsequent 24 hour period will match that from the previous day.

2.5.2 GS-CHO (MedImmune): The fed-batch protocol used for the MedImmune GS-CHO cell line culture in microwell plates used an existing method in place for shake flask cultivations. Feeding of the cultures commenced on day four, and involved addition of bolus feeds of a proprietary medium (containing glucose and other nutrients) immediately followed by a shot of bicarbonate solution (BDH Merck, Poole, Dorset, UK) for pH control (0.75 M sodium carbonate and 0.5 M sodium hydrogencarbonate). Addition volumes were fixed at 2% v/v and 0.25% v/v of the initial culture volume for medium and bicarbonate additions respectively and bolus feeding was continued for five consecutive days.

A second feeding strategy employing diluted feeds was also used such that liquid additions were 4% v/v and 2.5% v/v of the inoculum volume respectively. These correspond to 2x and 10x dilutions of the feed and bicarbonate solutions described in the preceding paragraph.

Fed batch operation in stirred tank cultures was performed in a number of ways. In the majority of cases feeding of the cultures commenced on day four, as with shake flasks, and involved addition of a bolus feed of a proprietary medium (containing glucose and other nutrients) fixed at 2% v/v.

However, since pH control operates as standard for the STR system, the shots of bicarbonate were not added. In a few additional experiments pH control in the STR was deactivated in order to mimic the pH profiles experienced by cultures in the microwell experiments. In this case bioreactor pH control was achieved, as with the microwells, by addition of a 0.25% (v/v) bicarbonate shot.

2.5.3 GS-CHO (IMRC): The fed batch protocol for the IMRC cell line was based on maintenance of glucose in the medium at a maximum of 2 g L⁻¹. The feed consisted of concentrated CD-CHO prepared from powder, dissolved in UHQ water, supplemented with glucose to a final concentration of approximately 120 g L⁻¹ (precise concentrations were measured post preparation as described in Section 2.7.2) and then sterile filtered using a Stericup (Millipore, Billerica, Massachusetts, USA) and a vacuum pump (Edwards, Crawley, West Sussex). Samples from cultivations were analysed for metabolite concentrations on a daily basis, and sufficient feed was then added to return the glucose concentration to 2 g L⁻¹. As with the MedImmune GS-CHO fed batch experiments, feeds for microwell cultivations were diluted further in UHQ water (by a factor of x6 compared to the feed used for the STR).

2.6 Correction of Cell Counts for Evaporation

2.6.1 Unfed Cultivations: Evaporation from 24 SRW plates may result in substantial changes in fluid volume over the course of a cultivation. To monitor the rate of evaporation, plates were weighed before and after sacrificial sampling. Gravimetric analysis was used to determine the liquid volume remaining in 24-SRW plates and shake flasks, using the assumption that the density of culture fluid was approximately equal to that of water (1 kg m^3).

The microwell volume thus determined following sacrificial sampling was then divided by the inoculated volume (at time zero) and multiplied by the cell count at each time to give the corrected figure.

2.6.2 Fed-Batch Cultivations: Despite the 0.6%(v/v) daily evaporation rate for the standard MedImmune shake flask system, which uses 50 mL of culture in a 250 mL Erlenmeyer flask, it was decided that no correction would be applied to flask cultures, primarily as this is standard industrial practise. In addition, although feed is added at 2.25%(v/v) per day for five days, no account is made for this in cell count data either.

A number of points had to be considered to allow direct comparison of the microwell and flask cell count and IgG titre data. Firstly, since no correction is made in the flasks for evaporation, the factor used for wells should not correct back to the inoculum volume, at which point no

evaporation has occurred, but rather to this volume after a 0.6%(v/v) per day has been subtracted. In effect, the correction should be made to the theoretical volume that would remain in the well if the evaporation rate were identical to that in the flask.

A further complication arises when the feed volumes for the flask and well cultures differ in terms of the % of the initial inoculum volume added. In one case, total daily additions to flasks and wells were 2.25 and 6.5 % (v/v) respectively, since the feed to wells had been diluted. This means that there is a greater addition of water to the microwells, and if this is not corrected for the cell counts cannot be directly compared as the microwell counts will be underestimates due to the dilution relative to flask cultures. Following the same principle as for the evaporation correction, the correction factor for the wells should assume that the feed addition to the wells is the same as for the flasks and then correct to this volume. Appendix II.2 gives an example calculation of how evaporation correction was applied in practise.

2.7 Analytical Techniques

2.7.1 Determination of cell viability and viable cell number

For initial CHO-S cultivations at UCL, a haemocytometer was used to perform manual cell counts on bioreactor samples. An aliquot of the cell

suspension was diluted in trypan blue (Sigma, Poole, Dorset, UK) solution to give an approximate estimated concentration of 1×10^6 viable cells mL^{-1} prior to observing cells under a light microscope.

For all subsequent GS-CHO cultivations cell counts were performed using a Vi-Cell XR automated viability analyzer (Beckman, Brea, California), with samples diluted using Dulbecco's PBS as necessary.

Within the Vi-Cell, cell suspension is mixed with trypan blue solution, before being loaded onto a haemocytometer slide for image capture. Viable cells actively export the trypan blue dye from the cytoplasm, while dead cells are unable to do this and can thus be distinguished visually by their blue appearance. The Vi-Cell captures images of the cells using a digital camera, and subsequently analyses these to determine the number of viable and dead cells. It can therefore determine both cell number and the percentage viability, distinguishing the dead cells by their blue appearance.

All analyses were performed in triplicate (where sample volume permitted). Following cell counting any remaining culture fluids were centrifuged using a Heraeus pico 21 centrifuge, and the supernatant stored frozen at $-80\text{ }^{\circ}\text{C}$ prior to further analysis of metabolite or IgG concentrations.

2.7.2 Determination of metabolite concentrations

Metabolite concentrations for culture supernatant samples were determined using a NOVA Bioprofile 400 (Nova Biomedical, Deeside, UK). Water was used for sample dilution if this was necessary to bring metabolite concentrations into the appropriate range for analysis. Unless metabolite data was necessary during cultivations to determine feeding requirements (as with the IMRC cell line fed batch experiments at UCL described in Chapter 6), supernatants were stored frozen to allow analysis of all samples from a single cultivation in a single day. This was to minimise variations that might otherwise result from recalibration of the NOVA or YSI instruments over time and/or batch to batch differences in reagent pack composition.

The Nova measures NH_4^+ using a potentiometric electrode. This has a sensing membrane specific to NH_4^+ , and develops a voltage proportional to the concentration of this ion. Glucose, lactate and glutamine are measured using amperometric electrodes, which have immobilised enzymes in their membranes. Oxidation of the substrate as it enters the enzyme layer generates hydrogen peroxide, which produces a current proportional to the concentration of the substrate concentration.

All metabolite measurements were performed in triplicate (where sample volume allowed).

2.7.3 IgG Quantification by Protein G HPLC

Quantification of IgG titre at UCL was performed by Protein G HPLC (column from Applied Biosystems, HPLC Agilent 1100 series using Chemstation version A.0901) and the method shown in Table 2.1 (loading buffer sodium phosphate buffer pH 7.0, elution buffer 20 mM glycine buffer pH 2.8). A calibration curve was used to convert the absorbance at 280 nm observed on the resultant chromatogram into an IgG concentration, with an area under the curve of 2,100 absorbance units corresponding to 1 g L⁻¹ (data not shown).

Table 2.1 Chromatographic Method for IgG Quantification

Time (minutes)	% Sodium Phosphate pH 7.0	% Glycine buffer pH 2.8	Flow rate (mL min⁻¹)
0.00	100	0	1
4.00	100	0	2
4.01	0	100	2
11.50	0	100	2
11.51	100	0	2
14.00	100	0	2

2.7.4 Osmolality

Samples were analysed for osmolality using a Gonotec Osmomat 030-D (Gonotec, Berlin, Germany).

The osmometer works on the basis that the presence of solutes in water causes a decrease in the freezing point, such that the presence of one mole of solute per kilogram of water results in a drop of 1.86 °C (Gennari, 1984). A 20 µL culture sample is rapidly frozen by the osmometer and the extent to which the freezing point has been depressed is used to determine the osmolality.

Measurements were made in triplicate (when available sample volume permitted).

2.7.5 At-Line analysis of pH, Dissolved Oxygen and Carbon Dioxide

At MedImmune pCO₂, pO₂ and pH were analysed at-line (for STR, shake flask and microwell cultures) using an ABL 800 FLEX blood gas analyzer (Roche, Basel, Switzerland).

The analyzer uses a series of electrodes to determine the pH, pCO₂ and pO₂ values. The pH electrode compares the potential developed at the electrode tip with a reference potential. The pCO₂ probe uses a semi permeable membrane over the tip of a pH electrode, through which CO₂ is able to permeate. Once CO₂ enters the space between electrode and membrane, it reacts with water to produce free hydrogen ions in direct proportion to the partial pressure of carbon dioxide in the sample. pO₂ is measured through its reaction with phosphate buffer, which produces a current in direct proportion to the partial pressure of oxygen (Hahn, 1987).

A single sample was analysed by the blood gas analyser at each sampling point. Following sampling, equilibration of the culture fluid with the atmosphere occurs and as such it is important to minimise the time between sampling and dissolved gas measurement.

2.7.6 Cell Size

Cell size analyses were performed using a Schärfe Systems CASY instrument (Sedna Scientific, Derbyshire, UK). 50 μ L culture samples were diluted by a factor of 200 in CASYton before analysing.

In the CASY, the dilute cell suspension is drawn through a capillary flow cell across which an electric current is applied. The extent to which the cells provide a resistance to the flow of current is used to generate a cell size distribution for the sample. Measurements were made in triplicate.

2.7.7 Cell Confluence Measurement using Cellavista

Culture samples were diluted by a factor of 100 in Dulbecco's PBS and subsequently 200 μ L of each diluted sample was pipetted into a 96 SRW assay plate. Plates were then centrifuged at 130g for one minute to cause cells to settle at the base of the wells, following which plates were loaded into the Cellavista (Roche, Basel, Switzerland) for analysis. The Cellavista acquires

bright field images of each individual well, subsequently analysing these to determine the cell confluence. The percentage confluency in the well can then be used to estimate the cell number.

2.7.8 IgG Quantification Using the Octet

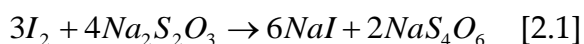
Culture samples were diluted by a factor of 10 in Dulbecco's PBS and subsequently analysed using the ForteBio (California, USA) Octet system. This system uses Protein A biosensors which interact with any IgG in the sample. The rate at which known concentrations of IgG bind to the Protein A biosensor under a set of standard conditions allows standard curves to be generated. Culture samples can then be fitted to these curves to enable the IgG concentration to be determined.

2.8 Bioreactor Mixing Characterisation

2.8.1 Observation of Liquid Phase Hydrodynamics: The fluid hydrodynamics in the shaken microwells were observed using a high speed video camera (Phantom V5.1 high-speed camera). A Perspex mimic of a single well from a 24-SRW plate was manufactured in-house and mounted on a shaker platform (Kühner AG, Basel, Switzerland) and filled with 800 μ L Milli-Q water, to which a small quantity of green food colouring (less than 0.5% of the total fluid volume) was added to aid visualisation of mixing patterns. As in our

previous work (Nealon et al., 2006), addition of the dye at this level did not alter the flow properties of the liquid. The camera was also mounted on the same platform such that the motion of the camera and microwell mimic were in unison. Images were then captured at 250 frames per second under a variety of shaking conditions.

2.8.2 Quantification of Bioreactor Mixing Times: Liquid phase mixing times in all three bioreactor geometries were determined using a method by which an iodine solution is decolourised through the addition of sodium thiosulphate (Bujalski et al., 1999) according to the following reaction:



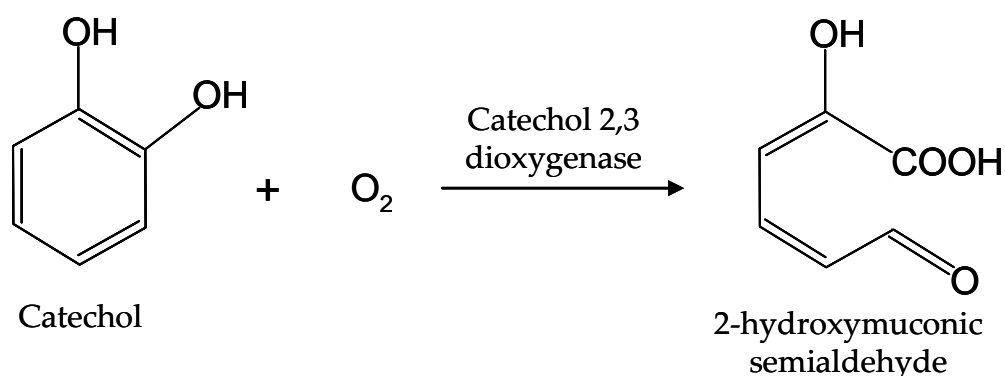
1.8 M sodium thiosulphate solution was added to 5 mM iodine solution at a volumetric ratio of 1:99. The time taken for complete decolourisation of the solution to occur under the selected mixing conditions was then determined from triplicate experiments.

For STR measurements thiosulphate additions were made as rapidly as possible using a serological pipette just under the liquid surface, with the impeller set at the required rotational speed prior to addition. For the shake flask and microwell measurements, addition was performed dropwise before

turning on the shaker, resulting in the formation of a thin liquid layer of thiosulphate at the base of the vessel. Preliminary experiments showed that this method enabled the most reproducible quantification of mixing times.

2.9 Determination of Bioreactor Oxygen Mass Transfer Coefficients

2.9.1 24 SRW Plates (Catechol Oxidation): The k_{LA} for the shaken microwells was determined experimentally using the catechol oxidation method previously developed by us. *E. coli* expressing XylE, the gene expressing catechol 2,3 dioxygenase, was first cultured and the enzyme prepared as described in Ortiz-Ochoa et al. (2005). The enzyme catalyses the reaction below:



The 2-hydroxymuconic semialdehyde (2-HS) produced absorbs light at 425 nm. Since it is known that one mole of oxygen is required to produce one mole of 2-HS, the Oxygen Transfer Rate (OTR) into the liquid can be calculated if the absorbance is measured using a suitable spectrophotometer, given that the extinction coefficient of 2-HS is $15,750 \text{ l mol}^{-1} \text{ cm}^{-1}$. Equation 2.2 then relates the measured OTR to k_{LA} :

$$\text{OTR} = k_{La} (C^* - C) \quad [2.2]$$

The saturation concentration of oxygen in the liquid (C^*) can be determined using the Henry's law constant (28.6 atm kg m⁻³ at 25°C), while it was previously demonstrated that the liquid phase oxygen concentration during the reaction (C) remains at zero throughout. Consequently calculation of the oxygen transfer rate (OTR) allows Equation 2.2 to be solved for k_{La} . Due to the limited availability of the enzyme solution, replicates were not performed.

2.9.2 24 SRW Plates (PreSens System): A 24 SRW ultra-low attachment plate (Corning) was modified by the UCL Department of Biochemical Engineering workshop through addition of oxygen-sensitive fluorophore patches (PreSens Precision Sensing GmbH, Regensburg, Germany) into two adjacent wells. The patches were positioned flush with the base of the wells, thus minimizing potential disruption to hydrodynamic conditions within the culture medium. The dynamic gassing out method (Lamping et al., 2003) in conjunction with the OXY4v2.04 software package (PreSens Precision Sensing GmbH) was used to measure the oxygen mass transfer coefficient (k_{La}) in the wells at a variety of shaking speeds and fill volumes on a shaker with a 20 mm orbital diameter.

CD-CHO media (Invitrogen) at room temperature was used for calibration of the sensor patches and for all experimental measurements. Air and nitrogen were sparged into the culture medium for calibration of 100%

and 0% points respectively. For experimental measurements, the media was gassed out using nitrogen and then the nitrogen sparge removed once 0% oxygen saturation was reached. Re-gassing of the media in air was then logged to allow determination of the oxygen transfer rate, with all measurements performed in triplicate. In order to determine the influence of the Breatheasy Sealing membrane (Diversified Biotech) on oxygen transfer, a number of measurements were taken in which a membrane was used to seal the microwell after gassing out and before re-gassing with air.

2.9.3 Shake Flasks: For the shaken flasks k_{La} was estimated based on the correlation of Gupta and co-workers (2003) as shown in Equation 2.3 below:

$$(k_{La})_{eq} = \frac{1}{V_L} \left[\frac{1}{Mk} + \frac{1}{V_L k_{La}} \right]^{-1} \quad [2.3]$$

Where $(k_{La})_{eq}$ = equivalent mass transfer coefficient, V_L = Volume of liquid in the flask, M = equilibrium constant and k = closure transfer resistance.

2.9.4 Stirred Tank: The k_{La} for the stirred tank system was determined using the dynamic gassing out method (Lamping et al., 2003) with measurements performed in CD-CHO media to ensure data were representative of oxygen transfer characteristics during cultivation. The air flow rate (100 mL min^{-1})

and impeller speed (260 rpm) were the same as used for cell cultivations. All measurements were performed in triplicate.

2.10 Determination of Mean Bioreactor Power Input

2.10.1 24 SRW Plates: All estimates of mean energy dissipation rates in 24 SRW plates were derived from computational fluid dynamics (CFD) studies (Zhang et al., 2008, Barrett et al., 2010) described previously by us.

2.10.2 Shake Flasks: The correlation of Büchs et al. (2000) allows estimation of mean energy dissipation rates for a shake flask, as shown in Equation 2.4 below:

$$\frac{P}{V_L} = Ne' \rho \frac{n^3 d^4}{V_L^{2/3}} \quad [2.4]$$

Where P = Power (W), V_L = liquid volume (m^3), ρ = liquid density ($Kg\ m^{-3}$), Ne' = modified power number, n = shaking frequency (s^{-1}), d = maximum inner diameter of shake flask.

2.10.3 Stirred Tank: A frictionless air bearing technique (Nienow et al., 1969) was used in combination with a force transducer and WinISO software from HEL (Borehamwood, Hertfordshire) to experimentally measure the power input to the STR during agitation by the pitch blade turbine (Section 2.4). All measurements used CD-CHO media, with 3.5 L present in the vessel (equal to

the working volume used in cultivations). Measurements were made in ungasged conditions at five different rotational speeds.

The force measurements obtained were converted into power using Equation 2.5:

$$P = FR\omega \quad [2.5]$$

Where P = Power (W), R = perpendicular distance from centre of rotation to force sensor (m), and ω is the angular velocity of the impeller:

$$\omega = 2\pi N_i \quad [2.6]$$

Where N_i = rotational frequency (S^{-1}).

The power values were then used to calculate the power number using 2.7:

$$N_p = \frac{P}{\rho N_i^3 D_i^5} \quad [2.7]$$

Where N_p = power number, P = power (W), ρ = liquid density ($Kg\ m^{-3}$), N_i = impeller rotational frequency (s^{-1}), D_i = impeller diameter (m).

Determination of the impeller power number allows the power dissipation to be calculated for any agitation rate in which the flow conditions are turbulent, corresponding to Reynolds numbers in excess of 10,000, where:

$$\text{Re} = \frac{\rho N_i D_i^2}{\mu} \quad [2.8]$$

Where ρ = liquid density (Kg m^{-3}), N_i = impeller rotational frequency (s^{-1}), D_i = impeller diameter (m), μ = liquid viscosity ($\text{Kg m}^{-1} \text{s}^{-1}$).

Power number was also measured for gassed conditions, using a volumetric airflow rate of 100 mL min^{-1} .

2.11 Determination of Specific Oxygen Uptake Rate (OUR) in 24 SRW plates

A batch CHO-S shake flask cultivation was performed as described in Section 2.2. Two days after inoculation, a cell count was performed following which 1mL of the cell suspension was transferred to a 24 SRW ultra-low attachment plate (Corning). This plate had been modified by the UCL Department of Biochemical Engineering workshop through addition of oxygen-sensitive fluorophore patches to the bases of the wells as described in Section 2.9.2. The well was sealed to prevent entry of air into the headspace, and the OXY4v2.04 software package (PreSens Precision Sensing GmbH) was used to measure the dissolved oxygen tension in the cell suspension. Calculation of the cell specific oxygen uptake rate (OUR) from the resulting data is described in Section 5.2.3.

2.12 Measurement of Dissolved Oxygen Tension During Microwell Cultivations

A fed-batch shake-flask cultivation was performed as described in Sections 2.2 and 2.5.2. Eleven days after inoculation, a cell count was performed on the ViCell following which the cell suspension was transferred to a PreSens 'OxoDish' in which each well has a micro-sensor attached to its base, allowing online measurement of dissolved oxygen concentration in every well. 12 wells were inoculated with a volume of 0.8 mL. The Duetz sandwich lid (described in Section 2.3.1) was used as the sterile seal, and the initial shaking conditions selected were a speed of 220 rpm with an orbital shaking diameter of 25 mm. OXY4v2.04 software package (PreSens Precision Sensing GmbH, Regensburg, Germany) was used to measure the dissolved oxygen tension in the cell suspension at 20 minute intervals, and after 24 hours, 6 sacrificial well samples were taken. These were counted on the ViCell and the OxoDish was then shaken for a further 24 hours at the lower shaking speed of 140 rpm, following which the sampling procedure was repeated.

2.13 Derived Growth and Metabolic Parameters

2.13.1 Integral Viable Cell Concentration

For each cell culture experiment performed, the mean of the viable cell density between each sampling point was taken and multiplied by the number of hours between sampling (to give units of 10^6 cells h mL⁻¹):

$$X_{ave} = \frac{X_{t_1} + X_{t_2}}{2} \quad [2.8]$$

$$IVC = \sum_t \left[\frac{X_t + X_{t+1}}{2} \right] \cdot (t_{+1} - t) \quad [2.9]$$

Where t = time (hours), X_t = viable cell concentration at time t (10^6 cells mL^{-1}).

The values for every time point were then summed to give a cumulative figure, which was then divided by 24 to give units of 10^6 cells day mL^{-1} , which can also be written as 10^9 cells day L^{-1} .

2.13.2 Specific Antibody Production Rate

The specific antibody production rate (q_{AB}) was determined by dividing the total antibody concentration by the integral viable cell density (calculated as described in Section 2.13.1) for each cultivation:

$$q_{Ab} = \left[\frac{[IgG]}{\sum_t \left[\frac{X_t + X_{t+1}}{2} \right] \cdot (t_{+1} - t)} \right] \quad [2.10]$$

Where q_{AB} = specific antibody productivity ($\text{mg } (10^9 \text{ cells.day})^{-1}$), $[IgG]$ = antibody concentration (mg L^{-1}) and X_t = viable cell concentration at time t (10^6 cells mL^{-1}).

Chapter 3: Establishment of Microwell Batch Culture Conditions for a Model CHO-S Cell Line

3.1 Introduction and Aim

Previous work has demonstrated the utility of shaken 24 SRW microtitre plates for the suspension culture of a Hybridoma cell line (Barrett et al., 2010). These culture data were underpinned by engineering characterisation studies that examined the oxygen transfer, energy dissipation and mixing characteristics in the microwells. The aim of this chapter is to explore the potential of microwell cultures for batch cultivation of a CHO-S cell line and to examine the influence of microwell culture conditions on cell growth kinetics. Specific objectives of this chapter are:

- To reproduce the suspension culture methods of Barrett et al (2010) and compare optimum culture conditions for hybridoma cells with those for a commercially available CHO cell line.
- To compare cultivation kinetics of a commercially available CHO-S cell line in shaken 24 SRW plates and standard shake flask formats
- To explore cell culture in alternative microwell geometries such as 96 DSW and 24 DSW plates.

- To investigate the challenges associated with fed batch operation in microwell plates and perform initial trial cultivations.
- To establish 5L STR cultures of CHO cell lines.

3.2 Impact of Shaking Speed on Microwell CHO-S Cultivations

The conditions initially evaluated for 24-well CHO-S culture were as previously used for hybridoma cells in the same microwell format (Micheletti et al., 2006). For hybridoma cells, it had been found that a fill volume of 0.8 mL at a shaking speed of 120 rpm (orbital diameter of 20 mm) gave comparable growth kinetics to those achieved in an Erlenmeyer Flask with a fill volume of 100 mL agitated at the same rate (orbital diameter of 10 mm). Using Computational Fluid Dynamics (CFD), the power per unit volume in the microwells was estimated at 37 W m^{-3} , which approximately matched the value of 39 W m^{-3} calculated for the shake flask (Buchs et al., 2000).

Use of these conditions for a CHO-S cell line failed to produce matched growth kinetics in the shake flask and 24-well formats, with the maximum viable cell density achieved in the microwells approximately half that attained in the flask (Figure 3.1). However, it was found that higher shaking speeds significantly increased the CHO-S culture performance in the microwells, such that the maximum cell density achieved at 180 rpm was statistically the same as that in the flask, as shown in Appendix II.4 (The cumulative cell

hours were 4.51×10^8 and 4.57×10^8 cells mL^{-1} h). As shown in Figure 3.2, cell viability profiles for CHO-S cultures in shaken 24-SRW microwells and shake flasks were also very similar.

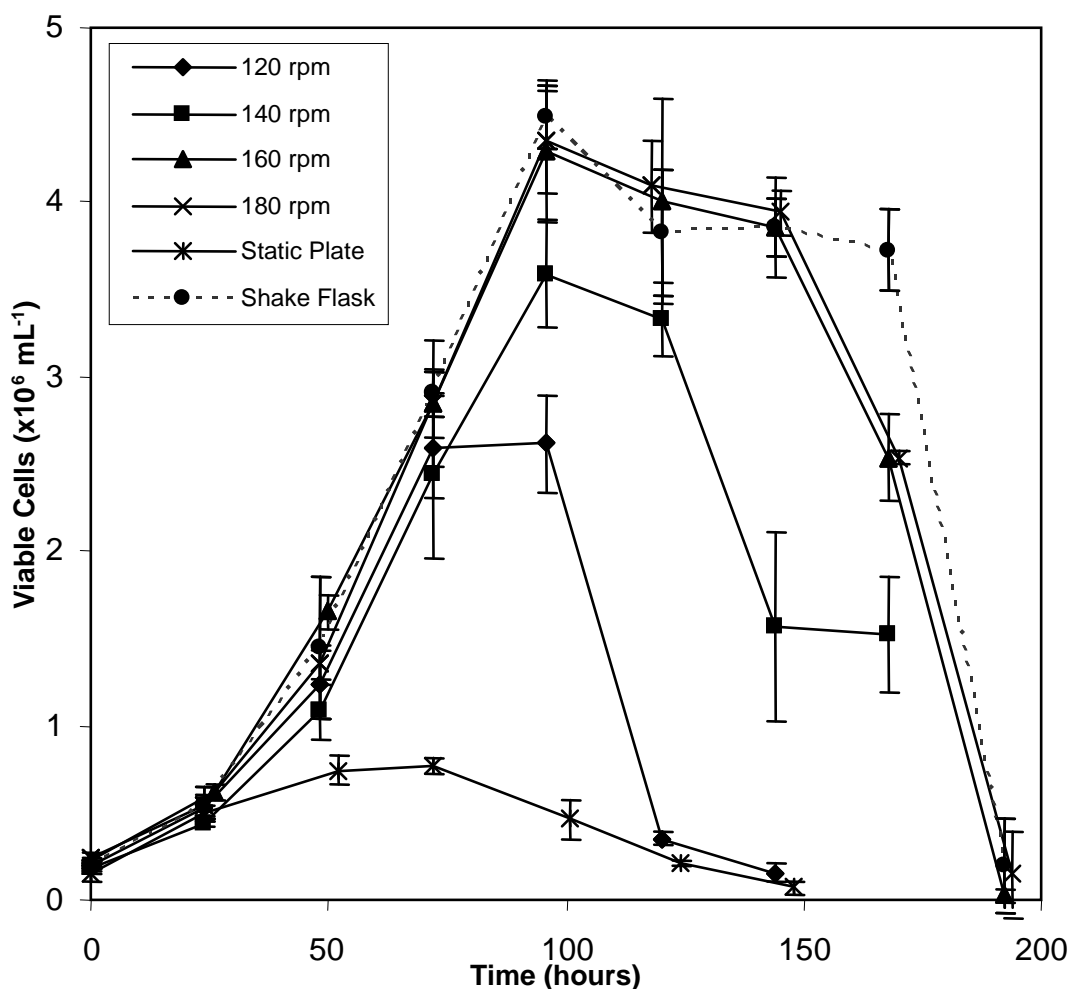


Figure 3.1: Influence of orbital shaking speed on CHO-S growth kinetics in 24SRW plates in CD-CHO medium supplemented with 8 mM L-Glutamine. Experiments performed in a humidified incubator at 37°C with 5% ambient CO₂ (as described in Section 2.3.1). Microwells and flasks were shaken on orbital shakers with diameters of 20 mm and 10 mm respectively. Control flask contained 100 mL medium and was agitated at 120rpm for approximately matched power input with microwells. Error bars represent one standard deviation about the mean (n=3).

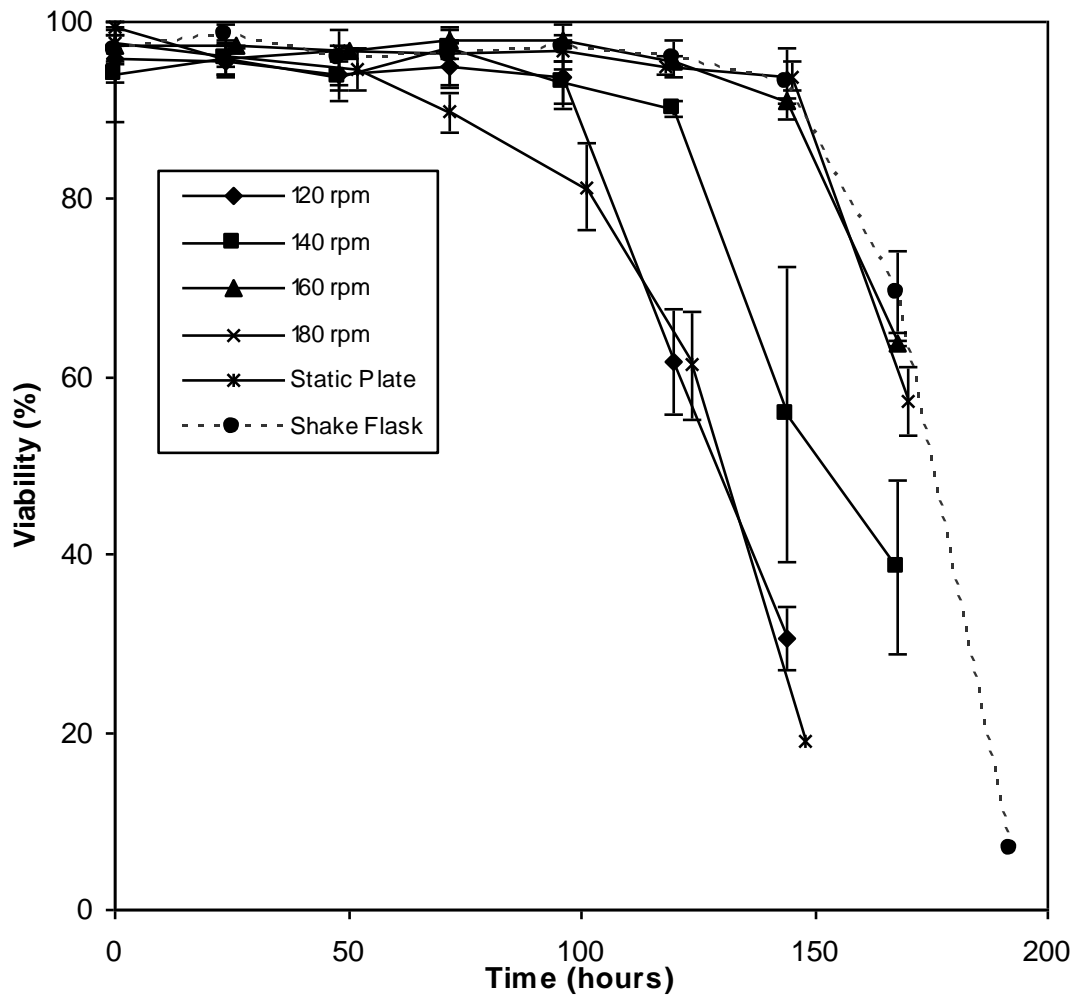


Figure 3.2: CHO-S viability measured for 24SRW plates at various orbital shaking speeds, and shake flask agitated at 120 rpm, in CD-CHO medium supplemented with 8 mM L-Glutamine. Viability was measured by trypan blue exclusion. Experiments were performed as described in Section 2.3.1. Error bars represent one standard deviation about the mean (n=3).

Initial attempts were made to use the n_{crit} correlation (Equation 1.3) to predict a minimum acceptable shaking speed for suspension cultivation in a 24SRW plate (Hermann et al, 2003). However, CHO-S cells were successfully cultivated in this format at a shaking speed of 120 rpm, and there was visible deformation of the liquid surface, despite a predicted n_{crit} of 149 rpm. Predicted n_{crit} values should therefore be used with caution. The correlation was derived for 96SRW plates, and it is likely that the greater diameter of the wells in 24SRW compared to 96SRW systems reduces the influence of adhesive forces, such that the surface tension is more easily overcome and a lower critical shaking speed is required. From direct observation, n_{crit} for the 24SRW system was approximately 56 rpm for both 1.0 and 2.0 mL fill volumes.

For the earlier hybridoma cultures described by Micheletti et al. (2006) increasing the shaking speed above 120 rpm did not improve culture performance as it did here for the CHO-S cell line. This could be explained by differences between the CHO-S and hybridoma culture performance. The peak viable cell density for hybridoma was approximately $1.2 \times 10^6 \text{ mL}^{-1}$ compared to about $4.5 \times 10^6 \text{ mL}^{-1}$ for CHO-S. This greater density for CHO-S raises the peak volumetric oxygen requirement, and increasing the shaking speed could meet this need through an increase in the interfacial area for mass transfer (Duetz et al, 2000, Büchs et al., 2001). In addition, hybridoma cells are

known to be more shear sensitive than CHO cells (Ma et al., 2002), so that improvements to mixing or mass transfer associated with increased agitation may have been negated by a corresponding increase in mechanical damage to the hybridoma cells.

3.3 Impact of Fill Volume on Microwell CHO-S Cultivations

Fill volumes of 0.4, 0.6, 0.8, 1.4 and 2.0 mL were tested for cultivation of CHO-S in the 24SRW format, under the shaking conditions used by Barrett (120 rpm with an orbital shaking diameter of 20 mm). These data were collected prior to the finding that higher rotational speeds significantly improve CHO-S culture performance, and also prior to the implementation of evaporation correction for counts (Section 2.6.1). It is likely that higher shaking speeds would have supported growth in larger fluid volumes due to enhanced mixing (Duetz, 2007).

It was found that for 1.4 and 2.0 mL liquid fill volumes shaking at 120 rpm was insufficient to maintain cells in suspension. Consequently there was poor cell growth and maximum viable cell densities of $1.3 \times 10^6 \text{ mL}^{-1}$ and $9.3 \times 10^5 \text{ mL}^{-1}$ respectively were obtained (Figures 3.3 and 3.4). Cell viability for 1.4 and 2.0 mL liquid fill volumes also declined earlier than for shake flask culture.

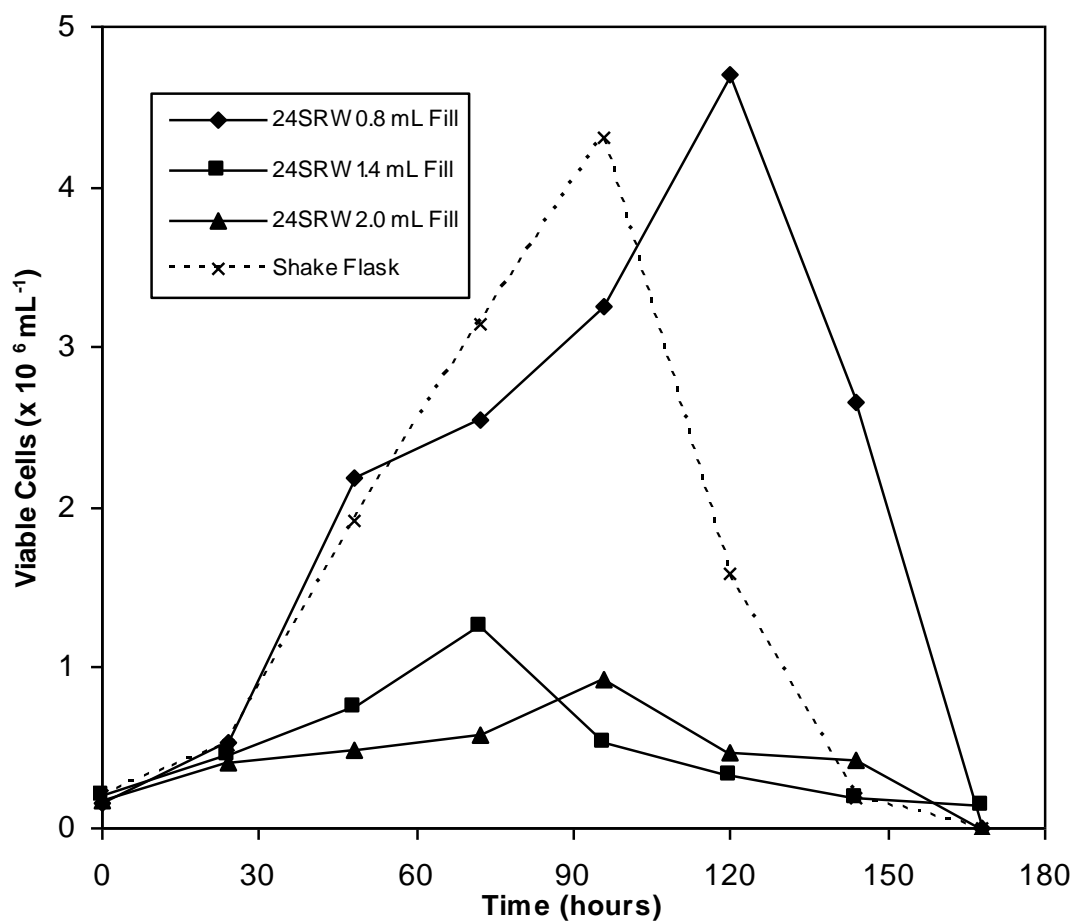


Figure 3.3: Influence of liquid fill volume on CHO-S culture kinetics in 24SRW plates in CHO-S-SFM-II medium. Experiments were performed as described in Section 2.3.1.

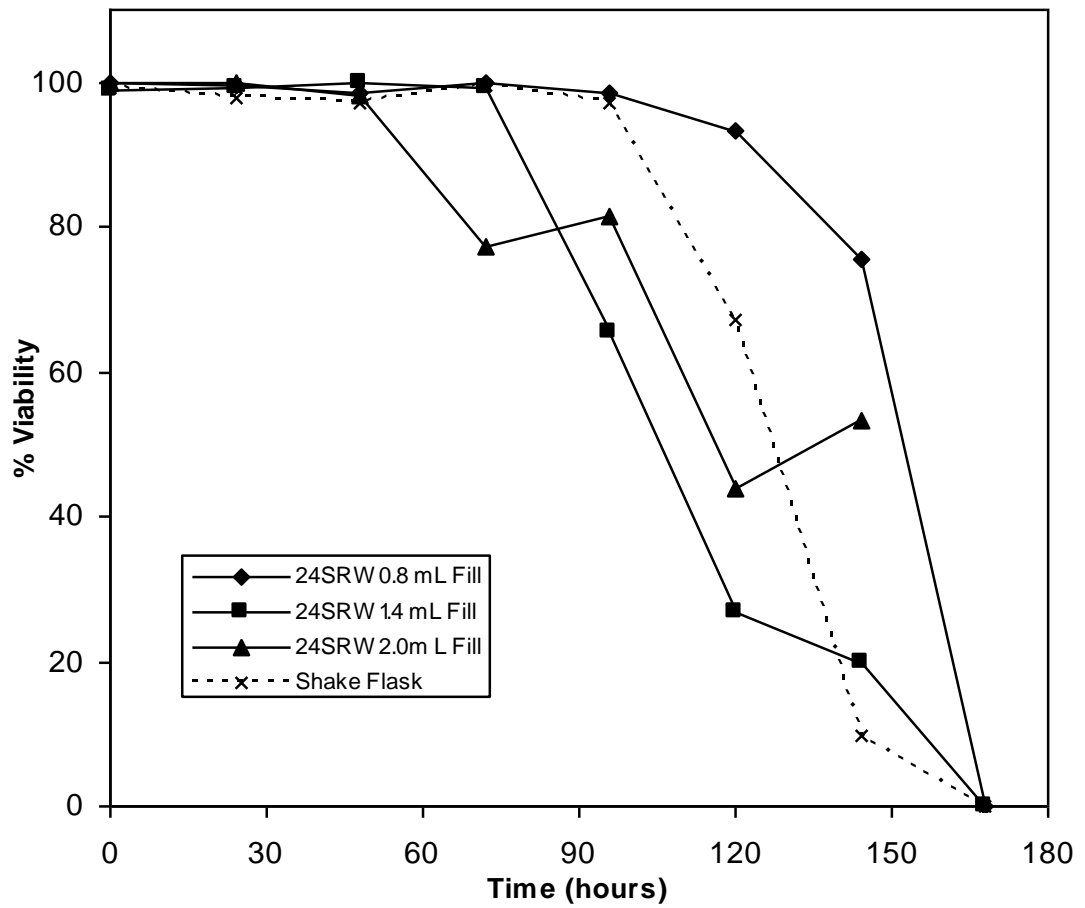


Figure 3.4: CHO-S viability measured for shake flask and 24SRW plates at various fill volumes in CHO-S-SFM-II medium. Viability was measured by trypan blue exclusion. Experiments were performed as described in Section 2.3.1.

For smaller fill volumes of 0.4 and 0.6 mL the increase in specific power input ensured cells remained suspended while an increase in surface area to volume ratio increased oxygen mass transfer into the medium. This data is not shown however, as evaporation was found to be considerable at these smaller working volumes.

The evaporation rate from the wells, even when sealed with a Breatheasy membrane, is high, despite the use of a humidified incubator. 38% and 41% of the initial liquid volume is lost after 144 hours for a 0.8 mL fill shaken at 120 and 180 rpm respectively. For cultures with initial fill volumes less than 0.8 mL the osmolality increase resulting from such evaporation will damage cells (Kimura et al., 1996). In addition the small remaining volume is insufficient for appropriate analyses to be performed, such that information from the culture is limited. Evaporation from 24SRW plates is a considerable drawback for use of this format in cell culture development, and does not occur to an appreciable extent in shake flasks or bioreactors.

Figure 3.5 shows the change in the mean well volume over time for a range of shaking speeds. It can be seen from these data that increasing the shaking speed does not appear to have a significant effect on the evaporation rate from the wells. This is surprising, as there is an increase in the interfacial area for gas-liquid mass transfer at faster speeds (Doig et al., 2005) which would be expected to lead to a higher rate of water loss. This may indicate

that it is diffusion of evaporated water vapour through the sealing membrane that limits the overall rate of evaporation.

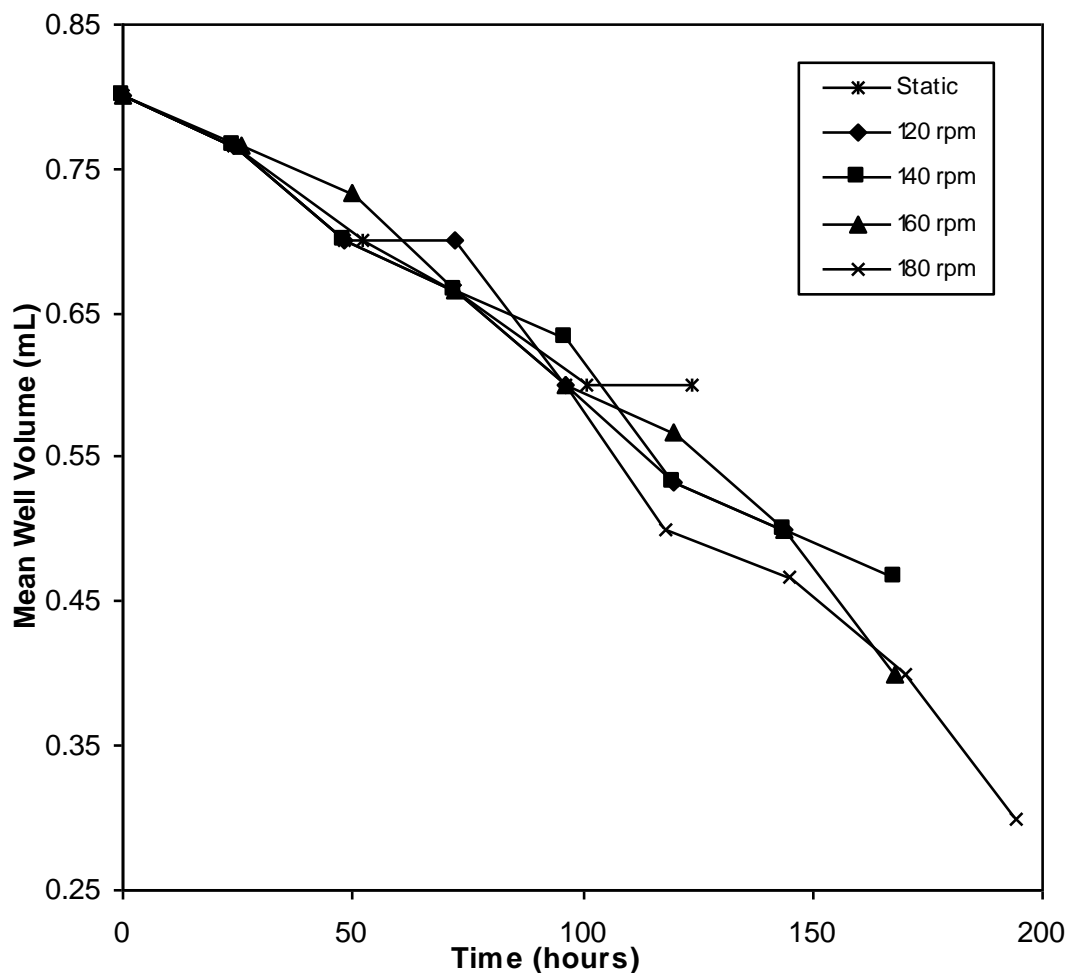


Figure 3.5: Change in mean liquid volume per well for 24SRW plates shaken at different speeds in a humidified cabinet at 37°C. Plates were shaken with an orbital diameter of 20 mm. Evaporation was quantified as described in Section 2.6.1.

3.4 Comparison of Different Breathable Membranes

The Breatheasy membrane from Diversified Biotech was used for all 24SRW experiments described previously. It was primarily selected after its successful use for hybridoma cultures in the same microwell geometry (Micheletti et al., 2006). However, in light of the evaporation problems highlighted in Figure 3.5 and the possible effects of oxygen limitation on growth kinetics, exploration of another membrane produced by Greiner was performed to assess any possible benefits.

It was found that the rate of evaporation of culture medium was even greater from 24SRW plates sealed with Greiner Sealing membrane than for those sealed with Breatheasy membrane. This loss of fluid had little impact on growth kinetics for the first 72 hours of culture, but there was a marked reduction in both cell count and viability subsequently (Figures 3.6 and 3.7). This may be a result of increased osmolality, or alternatively due to the increased concentration of a specific waste product such as lactate or ammonia. In either case, the Greiner membrane was not used in subsequent experiments since the culture performance using the Breatheasy was markedly superior. The cumulative cell hours for the Breatheasy cultivation were 3.19×10^8 compared to 1.27×10^8 cells mL⁻¹ h for microwells sealed with the Greiner membrane, and peak viable cell densities obtained were 3.59×10^6

mL⁻¹ and 2.10×10^6 mL⁻¹ respectively. It is possible that the higher rate of evaporation from this membrane correlates to a lower resistance to gas mass transfer, such that its use to seal plates in controlled humidity incubators could have positive benefits (Zimmermann et al., 2003).

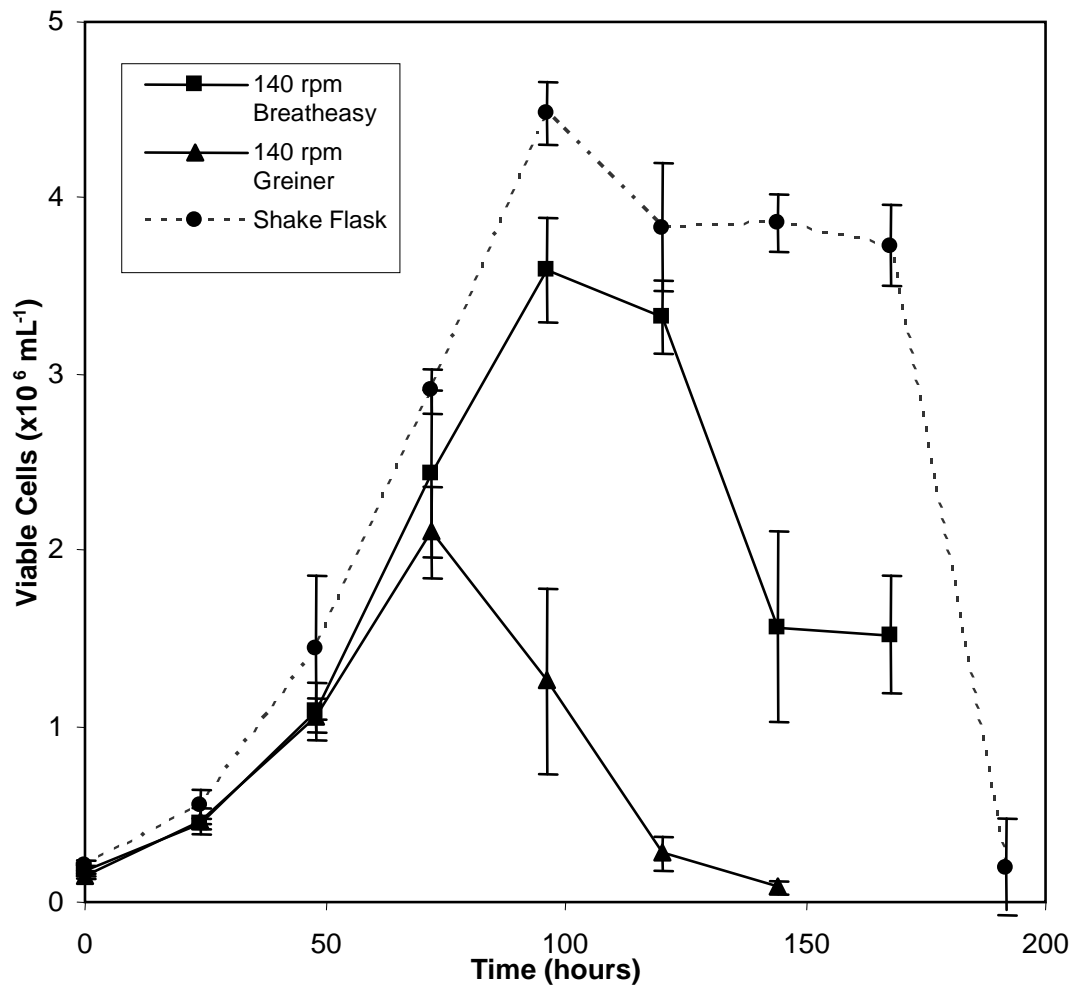


Figure 3.6: Influence of breathable sealing membrane on CHO-S growth in 24SRW plates in CD-CHO medium supplemented with 8 mM L-Glutamine. Experiments performed in a humidified incubator at 37°C with 5% ambient CO₂. Microwells and flasks were agitated at 140 rpm and 120 rpm on orbital shakers with orbital shaking diameters of 20 mm and 10 mm respectively. Control flask contained 100 mL medium for approximately matched power input with microwells. Experiments were performed as described in Section 2.3.1. Error bars represent one standard deviation about the mean (n=3).

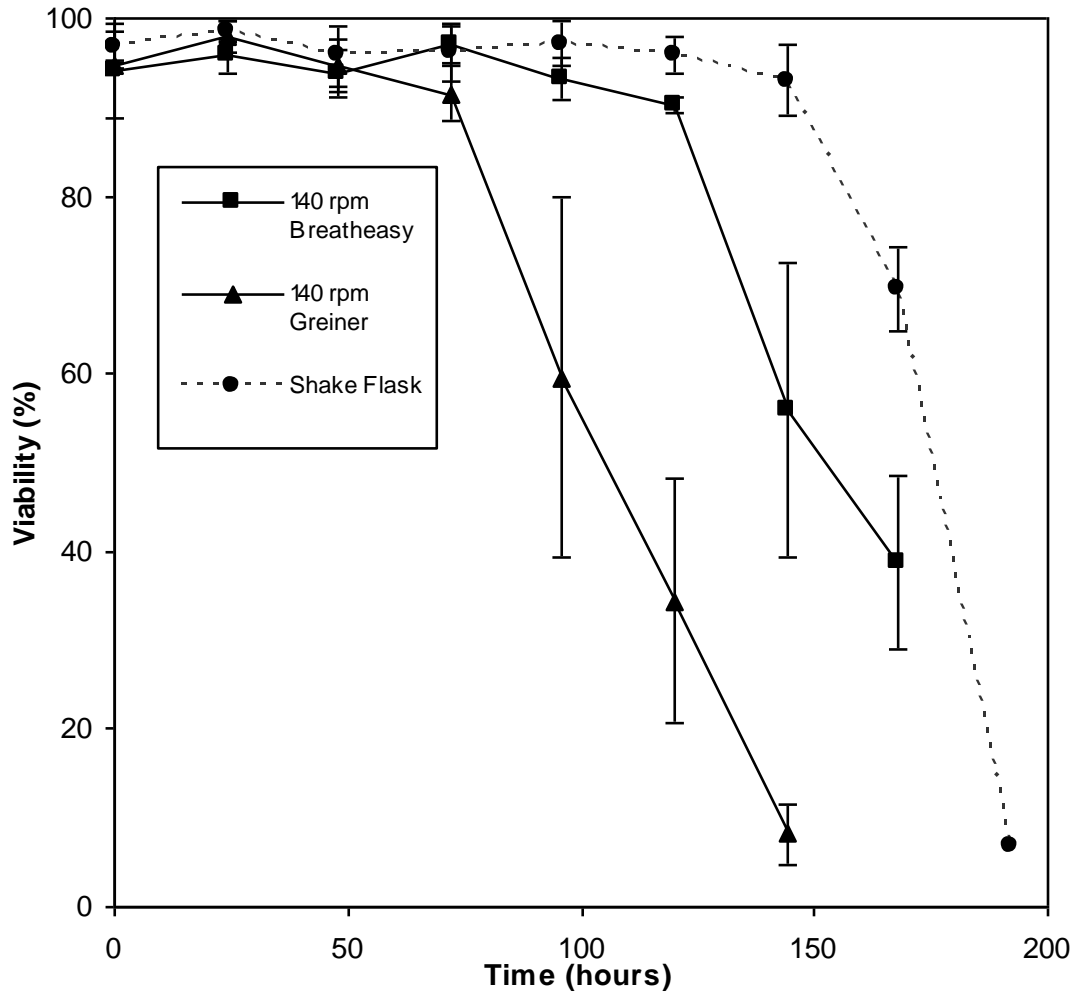


Figure 3.7: CHO-S viability measured for 24SRW plates sealed with different breathable membranes, and shake flask agitated at 120 rpm, in CD-CHO medium supplemented with 8 mM L-Glutamine. Viability was measured by trypan blue exclusion. Experiments were performed as described in Section 2.3.1. Error bars represent one standard deviation about the mean (n=3).

3.5 Batch CHO-S Cultivation in a 5 Litre Stirred Tank Reactor

The principle of matched mean energy dissipation was used by Barrett to achieve a fairly close match across shaken microwell, shake flask and stirred tank cultivations. Mean energy dissipation was therefore initially selected here as the rationale to define operating conditions for initial CHO-S cultivations in the 5 litre stirred tank reactor (as described in Section 2.4). An estimated power number of 1.5 was used for the impeller based on a geometrically equivalent system (a three bladed pitch-blade down-pumping impeller with a 45° blade angle). This together with Equation [5.6] was then used to determine an appropriate impeller speed. Aiming for a value of around 40 W m⁻³, an impeller speed of 260 rpm was used (full operating details in Section 2.4).

Initial CHO-S cultivation in the stirred tank yielded a maximum viable cell density of only 3.2 x 10⁶ mL⁻¹ compared to 4.5 x 10⁶ mL⁻¹ for the shake flask. In addition, viability dropped from 96.8% at time zero to 49.7% after 24 hours, only recovering to 67.5% after 168 hours.

The Kolmogorov microscale of turbulence under the conditions used was determined, and a value of 39.9 µm was calculated for the smallest turbulent eddies, based on a literature correlation for energy dissipation in the impeller zone (Chisti, 2001) (calculation of the microscale of turbulence is

given in Appendix II.1). As shown in Figure 3.8, the mean diameter of the CHO-S cells during the bioreactor run ranged from about 13.0 to 15.5 μm , and as such the cells are smaller than the predicted microscale eddies. In such circumstances shear damage to cells from energy dissipated at the microscale is not predicted.

It was subsequently found that exchanging the sintered sparger used for this first experiment with a nozzle sparger resulted in a substantial improvement in culture performance, with a peak viable cell density of approximately $1.2 \times 10^7 \text{ mL}^{-1}$ and viability maintained above 94% for the first 6 days (Figures 3.9 and 3.10). The key difference between these spargers is that the nozzle produces much larger bubbles, which has two main effects on the gas-liquid hydrodynamics. Firstly, the greater bubble diameter with the nozzle will decrease the interfacial area for gas-liquid mass transfer, thus reducing the k_{LA} (given a constant volumetric air flow rate of 100 mL min^{-1} in each case). Secondly, the damage caused to cells on bubble bursting at the liquid surface will be greatly reduced, as it is widely reported in the literature that smaller bubbles cause more damage (Chisti, 1993, Ma et al., 2004, Nienow, 2006).

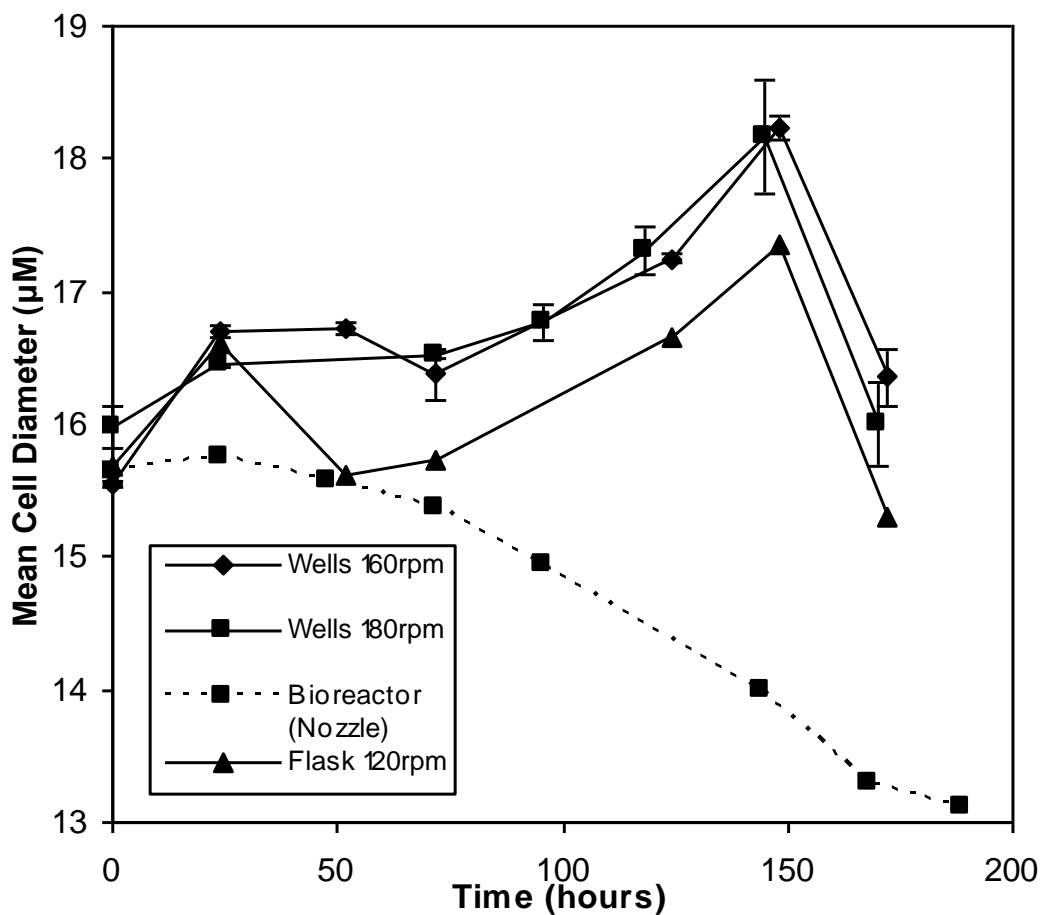


Figure 3.8: Mean cell diameter for CHO-S cultures measured using the CASY. Culture samples were diluted by a factor of 200 in CASYTON prior to measurement, as described in Section 2.7.6. Error bars represent one standard deviation about the mean (n=3).

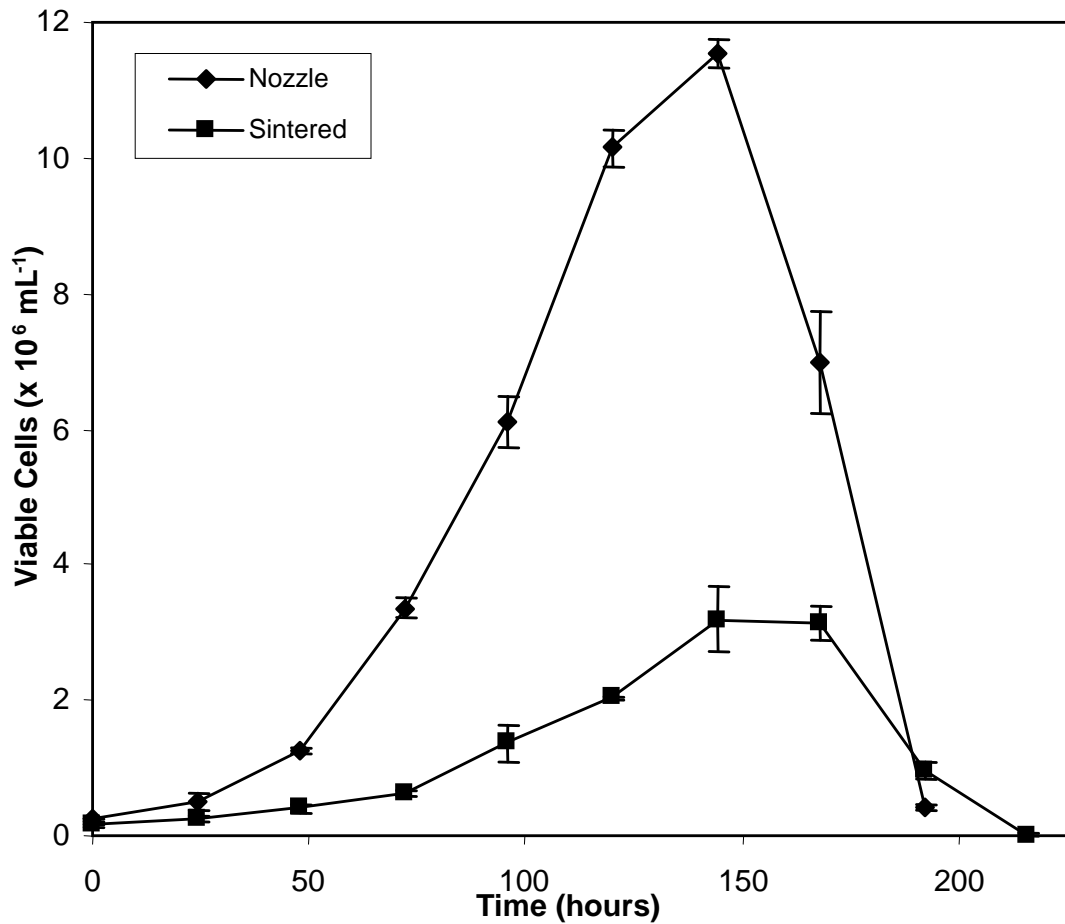


Figure 3.9: Growth profiles for CHO-S in 5 L Stirred Tank Bioreactor in CD-CHO medium supplemented with 8 mM L-Glutamine using Nozzle and Sintered spargers, with a working volume of 3.5 L, as described in Section 2.4. Cultures were agitated at 260 rpm and alternately sparged with air, oxygen, nitrogen and CO₂, temperature and pH controlled at 37°C and 7.10 respectively. Error bars represent one standard deviation about the mean (n=3).

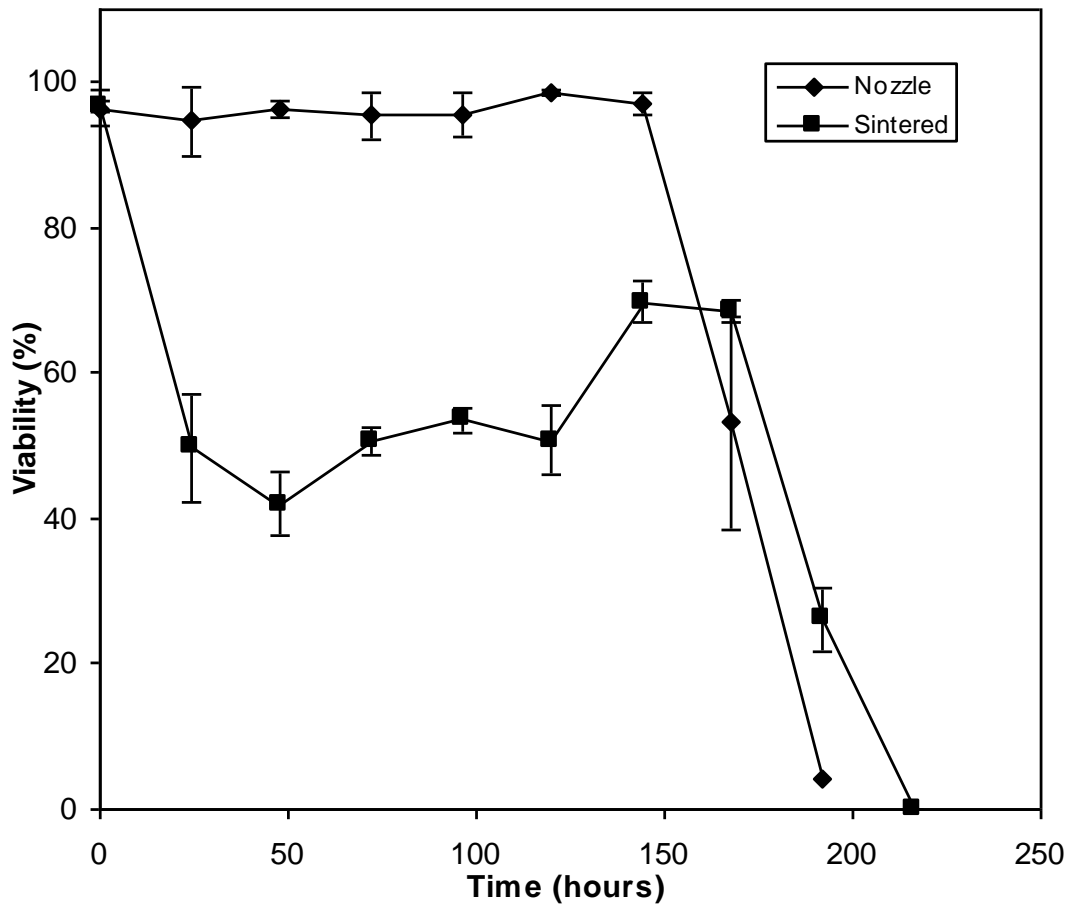


Figure 3.10: CHO-S viability in 5 L Stirred Tank Bioreactor in CD-CHO medium supplemented with 8 mM L-Glutamine using Nozzle and Sintered spargers, with a working volume of 3.5 L. Experiments were performed as described in Section 2.4. Error bars represent one standard deviation about the mean (n=3).

The damaging effect of small bubbles is more important than the reduction in k_{LA} in terms of selecting the appropriate sparger in this case. k_{LA} values for the two sparger types were measured by dynamic gassing out experiments (as described in Section 2.9.4) and found to be 24.7 and 3.6 h^{-1} for sintered and nozzle spargers respectively. The lower value for the nozzle unit is in the range of 1-15 h^{-1} quoted by Nienow (2006) as typical for the operation of animal cell culture bioreactors. Since it was shown that use of the nozzle sparger adequately satisfies the oxygen requirements of CHO-S cells, this unit was used in preference to the sintered model in all subsequent work.

It is initially surprising that hybridoma cells (described by Micheletti et al., 2006) were successfully cultured using the sintered sparger, given that these cells are generally more susceptible to hydrodynamic shear damage than CHO (Ma et al., 2002). However, the hybridoma cells were cultured in the presence of 10% Fetal Bovine Serum, which acts as a shear protectant in addition to its other benefits (Chattopadhyay et al., 1995). It is likely that it was the presence of serum that enabled growth of this cell line in the presence of small bubbles. Since CHO-S were cultured in chemically defined, serum-free media the damaging effect of the bubbles was not masked, resulting in the relatively poor growth and low viability observed.

3.5 Metabolite Profiles in Shaken CHO-S Batch Cultures

Utilization of the key carbon and nitrogen sources glucose and glutamine, and production of the corresponding waste metabolites lactate and ammonia were monitored for selected cultivations. Glucose, via glycolysis and the TCA cycle, is a key source of energy for growing cells, and glutamine is also a major source of carbon for the TCA cycle in suspension cultured mammalian cells (Neermann et al. 1996), and sometimes the principal source, as well as supplying nitrogen for biosynthetic pathways. Of the waste products lactate and ammonia, ammonia is the more toxic, and fed-batch and perfusion processes tend to be optimised with a view to minimising the accumulation of these compounds in the culture media (Xie & Wang, 1996).

Analysis of the metabolite profiles can suggest reasons for differences in growth kinetics and guide selection of conditions for improved performance (Xie et al., 1994). For example, the profiles for a shake flask with 100 mL of CD-CHO and 24SRW plate with 0.8 mL liquid fill volume, both at 120 rpm but with orbital shaking diameters of 10 and 20 mm respectively are shown in Figures 3.11 and 3.12.

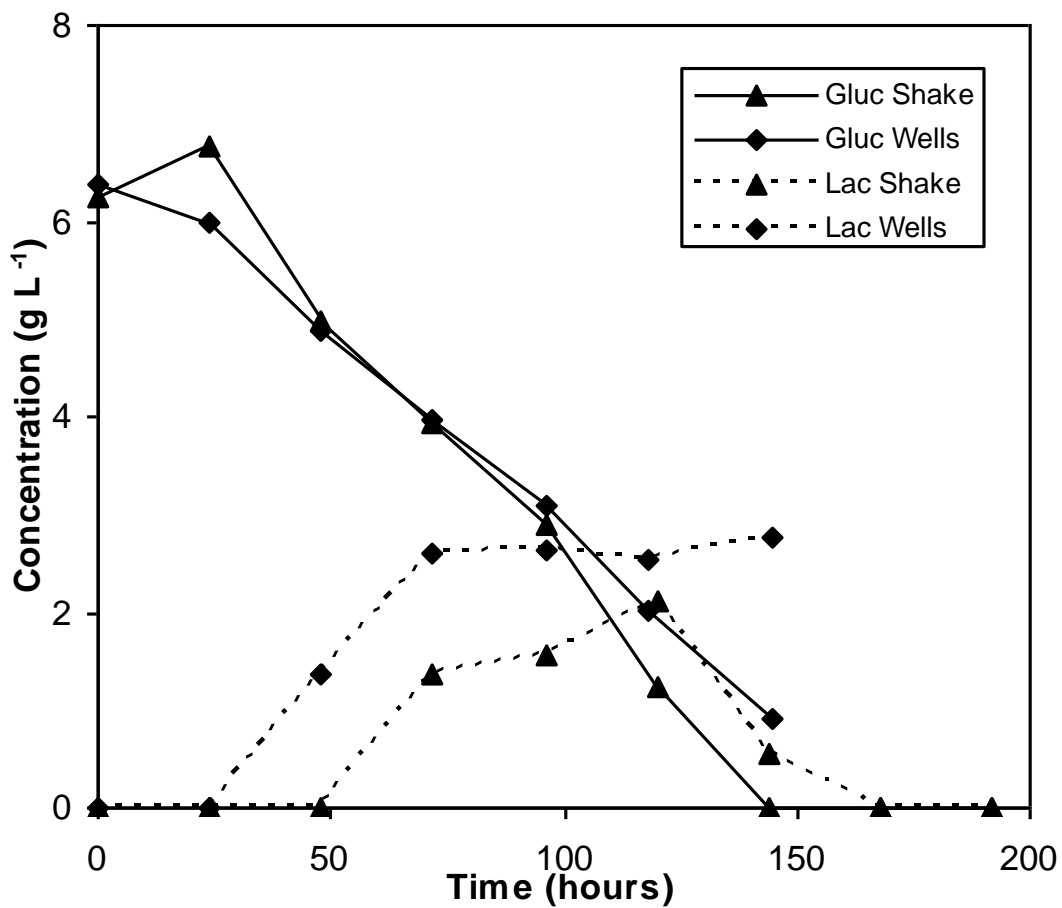


Figure 3.11: Glucose and Lactate profiles for CHO-S grown in CD-CHO medium supplemented with 8 mM L-Glutamine. Metabolite concentrations measured as described in Section 2.7.2. Experiments were performed as described in Section 2.3.1.

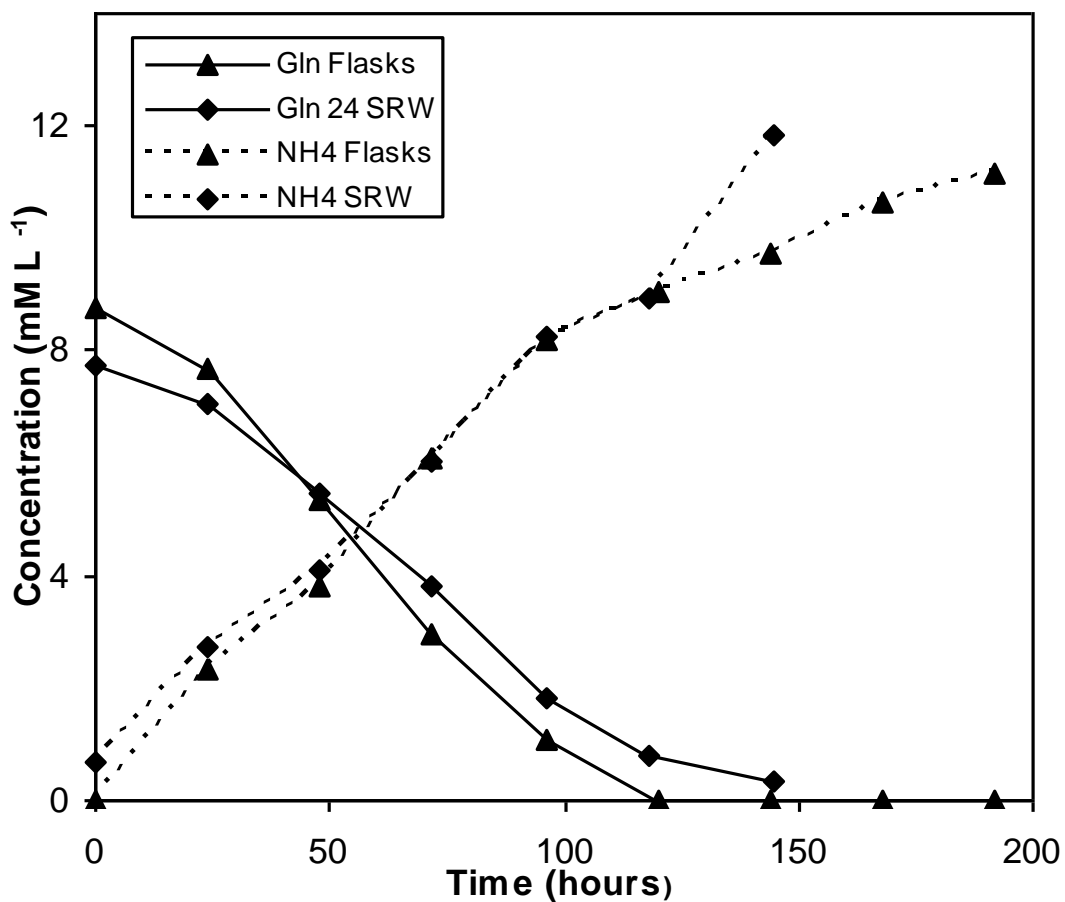


Figure 3.12: Glutamine and Ammonia profiles for CHO-S grown in CD-CHO medium supplemented with 8 mM L-Glutamine. Metabolite concentrations measured as described in Section 2.7.2. Experiments were performed as described in Section 2.3.1.

These data can also suggest which nutrient is limiting. For shake flask and microwell cultures, it appears that the initial decline in viable cell density seen in Figure 3.1 corresponds to the point at which glutamine first becomes depleted in the medium. However, for the bioreactor cultivation using the nozzle sparger, the onset of cell death appeared to occur as glucose levels approached zero (Figure 3.13). Since a comparison of the growth curves for these experiments indicate considerably inferior growth in the shaken systems, it is likely that the growth conditions for wells and flasks are limited by something other than nutrient levels (possibilities are discussed in Section 3.7). Consequently it may be concluded that it is glucose that is the limiting nutrient for the CHO-S cell line, and that the earlier cell death observed for shaken cultures is the result of another factor.

It should also be noted that despite the broadly similar utilization patterns for glucose and glutamine, the trends for lactate production differ significantly, with complete lactate re-utilization occurring for shake flask cultures while this product persists in the medium for the microwell cultures. This pattern of lactate formation was also seen for 24SRW cultivations at other shaking speeds (data not shown).

The persistence of lactate in the culture medium for the 24SRW system suggests that oxygen is limiting, whereas in the shake flask the lactate is re-utilised oxidatively by gluconeogenesis (Paoli et al., 2010). By contrast, CHO-S

cells cultured in the bioreactor with the nozzle sparger don't re-utilize all lactate but have a low yield of lactate on glucose (0.42), indicating that the majority of glucose is used oxidatively during growth, thus generating a greater amount of ATP per glucose molecule than for the shake flask and 24SRW plates (Figure 3.13). It is therefore useful to look not only at lactate patterns but also the relationship between glucose usage and lactate production.

Lactate is not simply an indicator of oxygen supply to a culture, its production is also linked to cell stress. The k_{La} for the sintered sparger is greater than that for the nozzle (24.7 and 3.6 h⁻¹), and so the availability of oxygen to the culture is correspondingly greater. Despite this there is still greater overall production of lactate, perhaps suggesting that cells are stressed due to the bursting of the smaller bubbles produced by the sinter.

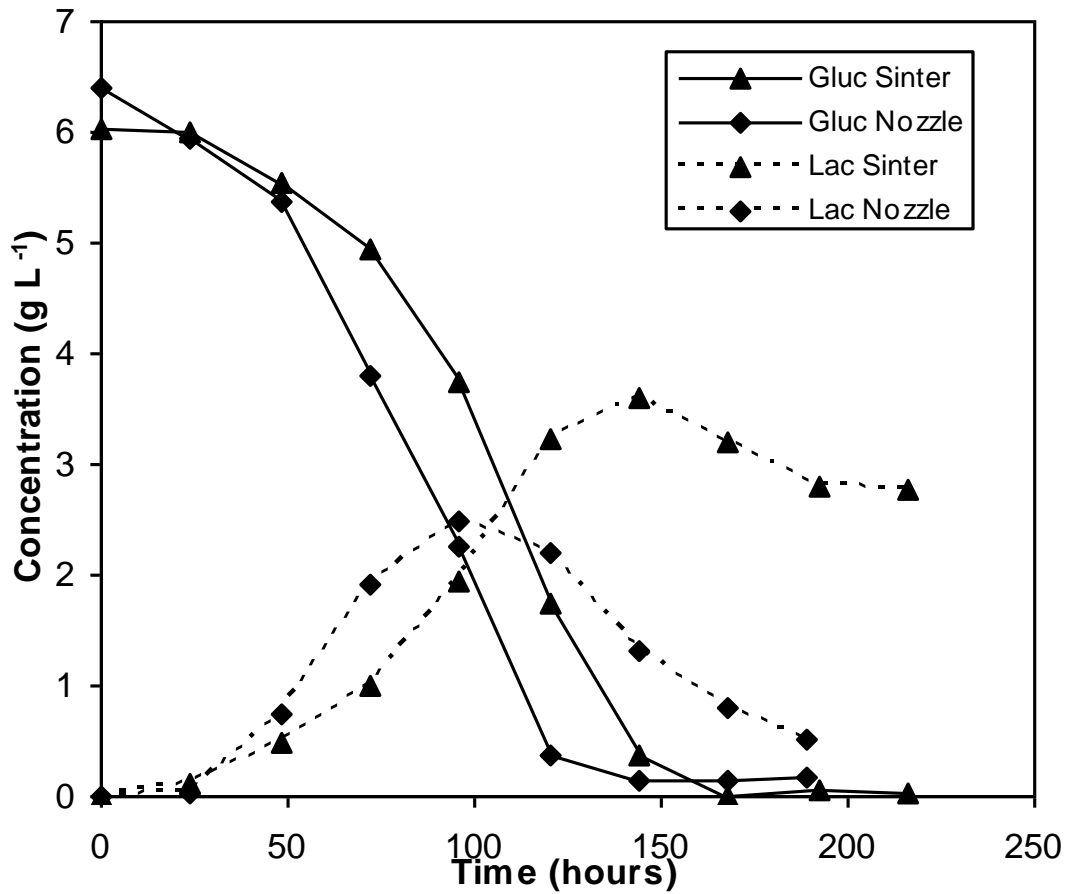


Figure 3.13: Glucose and Lactate profiles for CHO-S grown in a 5 L Stirred Tank Bioreactor in CD-CHO medium supplemented with 8 mM L-Glutamine, using either nozzle or sintered spargers. An impeller speed of 260 rpm was used for stirred tank cultures. Metabolite concentrations measured as described in Section 2.7.2. Experiments were performed as described in Section 2.4.

3.6 Comparison of CHO-S Batch Culture Kinetics and Metabolite Usage in Different Bioreactor Formats

Comparison of CHO-S culture performance in stirred tank, shake flask and shaken microwell bioreactors allows the feasibility of using shaken 24 SRW plates as a scale-down cell culture model to be assessed. Analysis of any differences in growth kinetics or metabolite profiles can then suggest potential changes to culture methods which could enhance cell culture performance in the shaken microwell format.

CHO-S attained a much higher viable cell density in the stirred tank bioreactor ($1.2 \times 10^7 \text{ mL}^{-1}$) than in either the shake flask or 24SRW formats ($4.5 \times 10^6 \text{ mL}^{-1}$ and $4.4 \times 10^6 \text{ mL}^{-1}$ respectively). There are a number of possible reasons for this. Firstly, the culture environment in the bioreactor is controlled such that the pH, temperature and dissolved oxygen all remain within narrow limits for the duration of the run. Such control is not possible in the flask or well formats unless additional systems are specifically introduced. Secondly, although the predicted k_{LA} for the 24SRW plate agitated at 160 rpm is 6.3 h^{-1} (from Equation [5.1], Doig et al., 2005), which compares favourably to the value of 3.6 h^{-1} experimentally determined for the nozzle sparger, oxygen enrichment is not available for the headspace of the microwells, while for the bioreactor oxygen is introduced into the system from around 63 hours onwards, which approximately corresponds to the point at which the growth

rate for the bioreactor first exceeds that for the microwells. The presence of oxygen in the sparged air increases the driving force for oxygen mass transfer in to the liquid, since:

$$\text{OTR} = k_{LA} (C_L^* - C_L) \quad [3.1]$$

Where OTR is the oxygen transfer rate from gas to liquid phase, C_L^* is the saturation concentration of oxygen in the liquid and C_L is the concentration of oxygen dissolved in the liquid. Using oxygen in the inlet air raises the saturation concentration of oxygen in the medium (C_L^*). While gas blending enhances oxygen transfer in the bioreactor, accumulation of condensed water vapour on the underside of the sealing membrane for the 24SRW plates introduces an additional mass transfer barrier which may further reduce the k_{LA} for this system. After around 72 hours, the membrane appears to be drawn downwards into the wells, suggesting that the cells are using oxygen from the headspace more rapidly than it can be replaced through the membrane. It is possible that this phenomenon also hinders oxygen transfer through the vent cap of the shake flask, but the opacity of the covering prevents confirmation of this. In addition, the conical shape of the flask allows water vapour to condense on the flask walls, perhaps minimising the accumulation of moisture at the sterile closure.

A third possibility is that the mixing in the microwells is insufficient to support higher cell densities, perhaps resulting in inhomogeneities and

nutrient gradients that are harmful to the cells. This would agree with the findings of Tim Barrett with hybridoma (Micheletti et al., 2006).

An issue of limitation for the 24SRW format is also implied by the observation that increasing the shaking speed for this system from 160 to 180 rpm fails to improve culture performance, despite the prediction from computational fluid dynamics (Barrett et al., 2010) that power input to the system increases with this change in conditions.

A summary of the microwell, shake flask and bioreactor metabolite utilization and growth kinetic data are given in Table 3.1 below.

There are a number of potential modifications to the microwell cell culture process which could address the issues described above:

- (i) Use of a sterile seal that reduces the rate at which liquid is lost from the wells by evaporation.
- (ii) Use of a fed-batch methodology to provide optimal nutrient concentrations, and potentially to replace water losses and thus mitigate increases in medium osmolality.
- (iii) Implementation of enhanced pH control through periodic addition of an alkaline solution to the microwells (such as bicarbonate).

While initial attempts at exploring a fed-batch microwell culture process are made in Section 3.9, all three options are considered in Chapter 4.

Table 3.1: Summary of CHO-S batch growth kinetics and metabolite utilization data in different Bioreactor formats. Metabolite concentrations determined as described in Section 2.7.2. Experimental data taken from Figures 3.1 to 3.13.

Format	Media	Fill Volume (mL)	Shaking Speed (rpm)	Orbital Shaking Diameter (mm)	μ_{max} (h ⁻¹)	Q _{gln} (mg 10 ⁶ cells h ⁻¹)	Q _{gluc} (mg 10 ⁶ cells h ⁻¹)	Q _{NH4+} (mg 10 ⁶ cells h ⁻¹)	Q _{lac} (mg 10 ⁶ cells h ⁻¹)	Y _{lac/gluc} (t0 – Peak VCN)	Y _{NH4+/gln} (t0 – Peak VCN)	CCH from t0 – t168 (cells mL ⁻¹ h)	Peak VCN (x mL ⁻¹)
24SRW	CD-CHO	0.8	120	20	0.037	5.8 x 10 ⁻³	3.1 x 10 ⁻²	1.0 x 10 ⁻³	1.6 x 10 ⁻²	1.68	0.87	2.01 x 10 ⁸	2.37 x 10 ⁶
24SRW	CD-CHO	0.8	160	20	0.042	3.2 x 10 ⁻³	1.4 x 10 ⁻²	5.1 x 10 ⁻⁴	7.1 x 10 ⁻³	1.24	0.81	4.44 x 10 ⁸	4.30 x 10 ⁶
24SRW	CD-CHO	0.8	180	20	0.038	2.9 x 10 ⁻³	1.5 x 10 ⁻²	5.4 x 10 ⁻⁴	7.5 x 10 ⁻³	1.59	1.28	4.51 x 10 ⁸	4.35 x 10 ⁶
24SRW Fed	CD-CHO	0.8	120	20	0.042	/	/	/	/	/	/	1.82 x 10 ⁸	2.62 x 10 ⁶
24DSW	CD-CHO	2.0	180	20	0.049	/	/	/	/	/	/	/	/
250mL Erlenmeyer	CD-CHO	100	120	10	0.043	4.5 x 10 ⁻³	1.7 x 10 ⁻²	3.9 x 10 ⁻⁴	7.5 x 10 ⁻³	0.93	0.95	4.57 x 10 ⁸	4.48 x 10 ⁶
125mL Erlenmeyer	CD-CHO	25	120	10	0.045	/	/	/	/	/	/	4.43 x 10 ⁸	5.21 x 10 ⁶
Bioreactor Sintered	CD-CHO	3500	225	/	0.033	6.0 x 10 ⁻³	2.6 x 10 ⁻²	9.1 x 10 ⁻⁴	2.4 x 10 ⁻²	1.27	0.75	2.28 x 10 ⁸	3.19 x 10 ⁶
Bioreactor Nozzle	CD-CHO	3500	260	/	0.041	3.8 x 10 ⁻³	9.5 x 10 ⁻³	1.8 x 10 ⁻⁴	1.3 x 10 ⁻²	0.42	0.78	8.77 x 10 ⁸	1.15 x 10 ⁷

3.8 Investigation of CHO-S Cultivation in Alternative Microwell Geometries

3.8.1. 96 DSW Plates

The possibility of performing cell culture in a 96 well format is attractive due to the four-fold greater throughput potentially offered when compared to use of 24 SRW plates. Use of square rather than standard round wells is thought to improve mixing and oxygen transfer due to the 'baffling' effect of the square geometry (Hermann et al., 2003). In addition, deep wells have a maximum fill volume of 2.2 mL compared to around 200 μ L for standard 96 round well plates. These advantages make investigation of this format for cell culture worthwhile, but present a challenge in terms of selection of shaking conditions suitable for mammalian cell culture.

The smaller surface area to volume ratio for this well geometry also reduces the evaporation rate in comparison to the 24SRW format (Figures 3.14 and 3.15). This is advantageous as there is will be correspondingly less of a change in medium osmolality and fluid hydrodynamics resulting from fluid losses over the course of the culture.

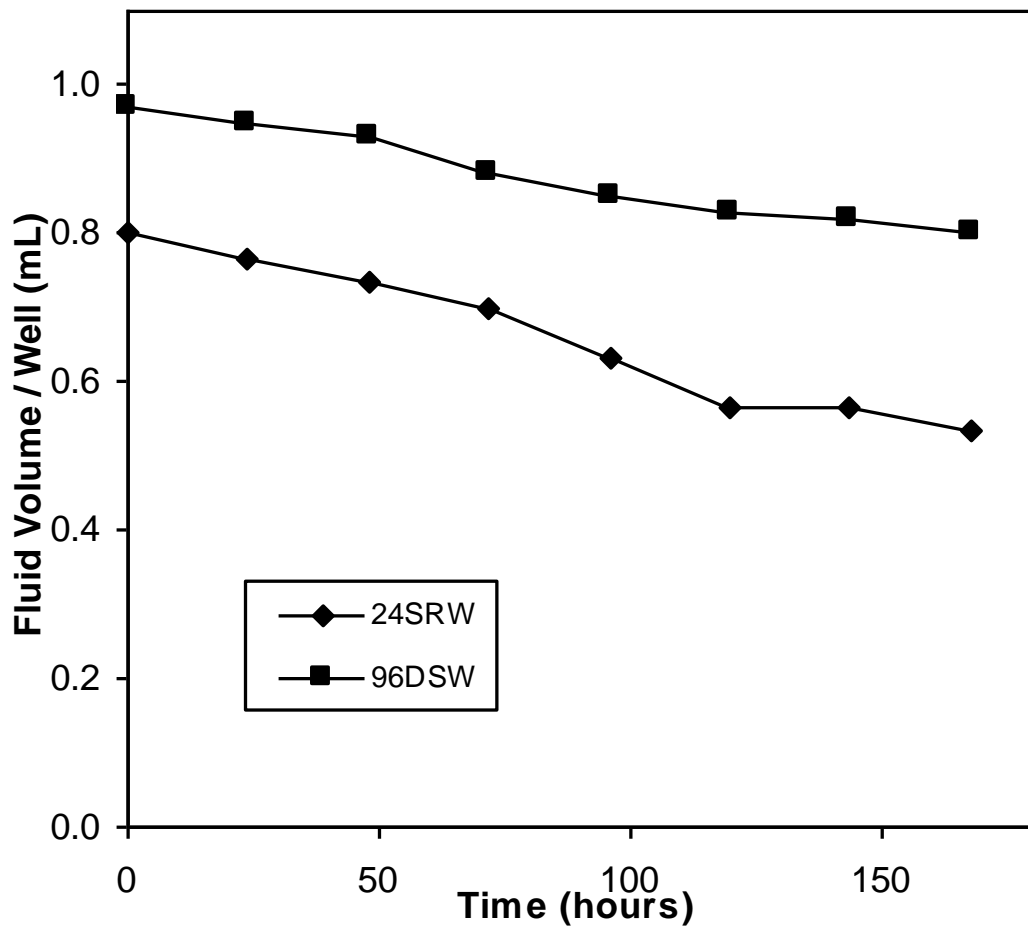


Figure 3.14: Change in well volume over time as a result of evaporation. Initial liquid fill volumes for 96-DSW and 24SRW formats were 1.0 and 0.8 mL respectively.

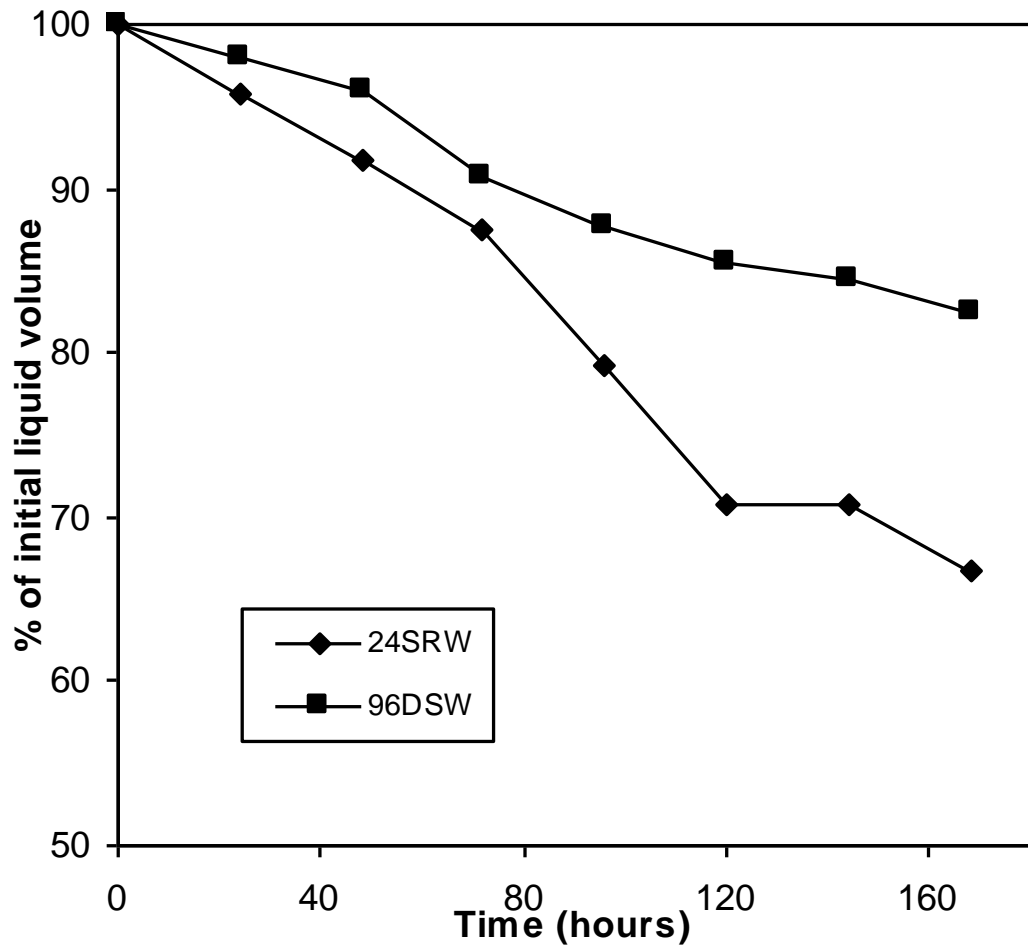


Figure 3.15: Percentage change in fluid volume for 96DSW and 24SRW well formats during culture. Initial liquid fill volumes for 96DSW and 24SRW formats were 1.0 and 0.8 mL respectively, and shaker speeds were approximately 580 rpm with a 4.5mm orbital shaking diameter and 120 rpm at 20 mm.

The initial approach for 96DSW cultivations was to use an orbital shaking diameter of 20 mm as used for 24SRW cultures, which is approximately equivalent to the shaker successfully used by Eli Lilly for CHO-S culture in this microwell format (Strobel et al., 2001). Initial data were not encouraging, and it appeared difficult to achieve any disruption of the liquid surface with speeds of up to 300 rpm (the maximum attainable speed

for the shaker). However, there was an appreciable difference in culture performance between static and shaken plates (Figure 3.16). This is likely to be a result of periodic renewal of the headspace air which occurs more readily in the shaken as opposed to the static system.

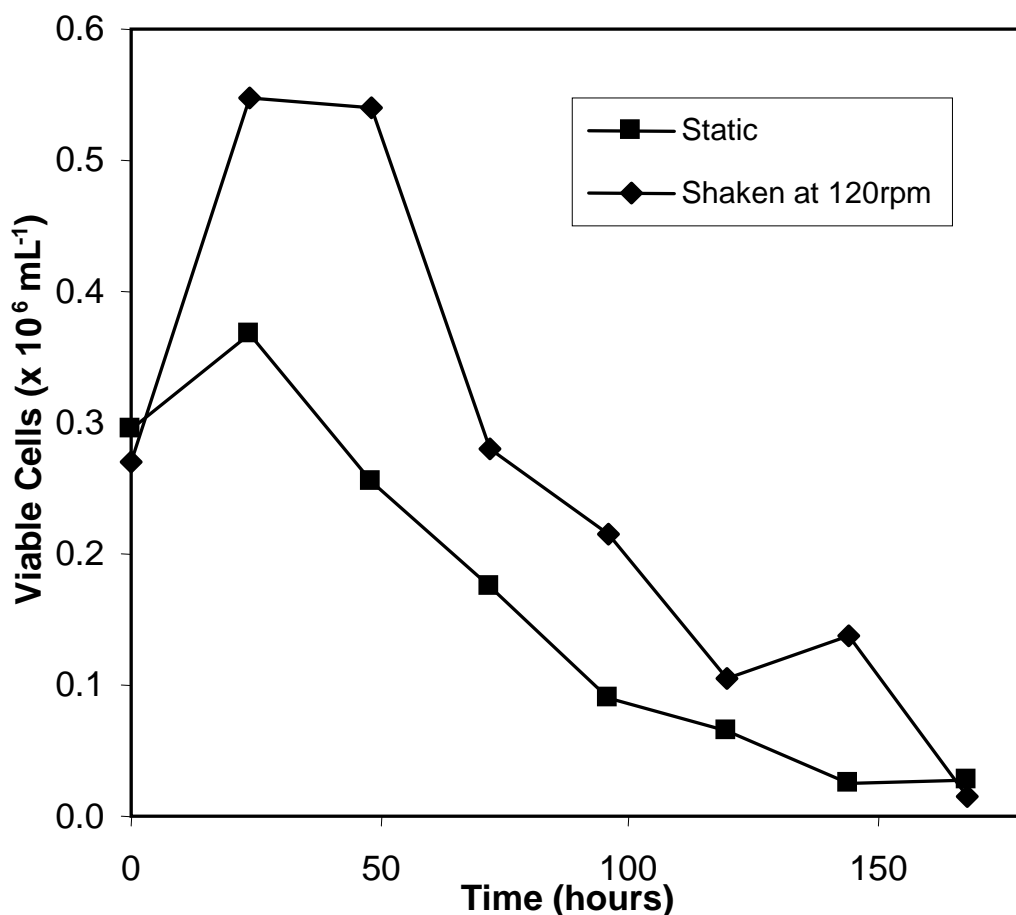


Figure 3.16: CHO-S growth for a 1 mL fill volume in 96DSW plates in CHO-S-SFM-II medium. Experiments were performed in a humidified incubator at 37°C with 5% ambient CO₂. Microwells and flasks were agitated at 120 rpm on shakers with shaking diameters of 20 mm and 10 mm respectively as described in Sections 2.2 and 2.3.3.

Use of an orbital shaking diameter of 4.5 mm at approximately 580 rpm gave more encouraging results but consistent growth could not be obtained

(Figure 3.17). Use of a smaller orbital shaking diameter to achieve adequate gas-liquid mass transfer and mixing runs contrary to the majority of literature observations in which larger orbital shaking diameter is positively correlated with enhanced oxygen transfer (Duetz & Witholt, 2004).

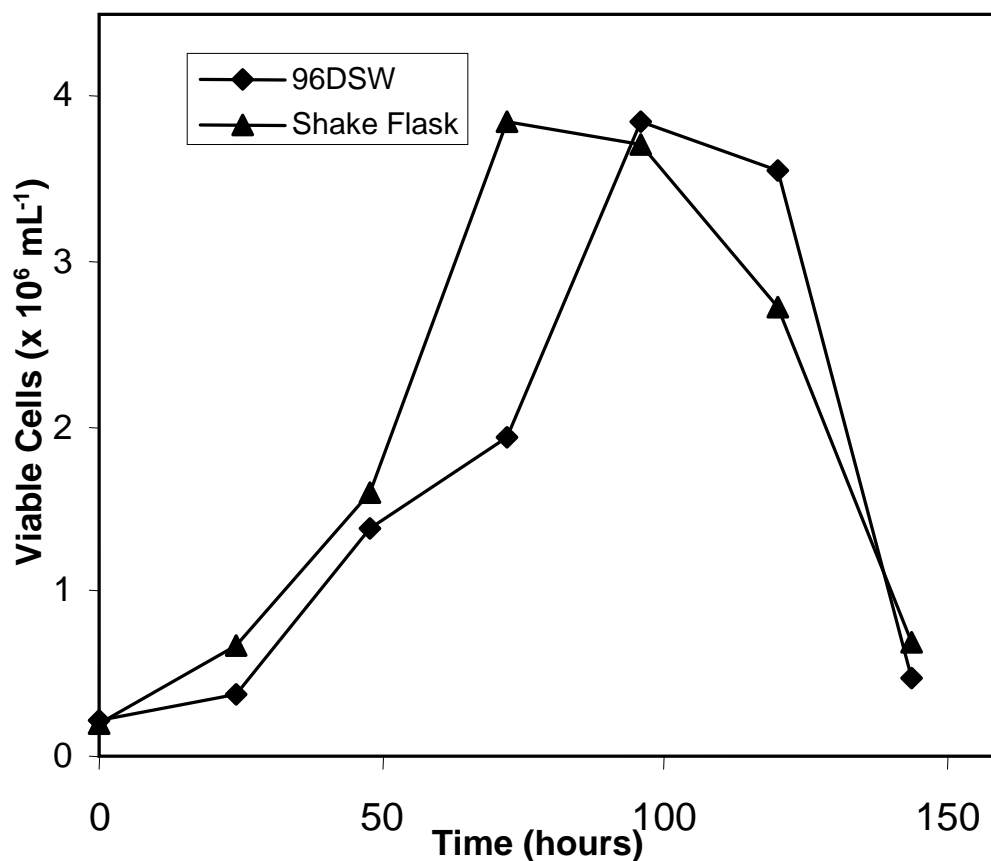


Figure 3.17: Comparison of CHO-S growth for 96DSW plate with a 1 mL fill and 25 mL shake flask using CHO-S-SFM-II medium. Experiments were performed in a humidified incubator at 37°C with 5% ambient CO₂. The microplate was agitated at approximately 580 rpm with an orbital shaking diameter of 4.5 mm while the flask was shaken at 120 rpm with an orbital shaking diameter of 10 mm as described in Sections 2.2 and 2.3.3.

3.8.2. 24 DSW Plates

Experiments with the 24DSW format were performed as a direct comparison with 24SRW cultivations (Figures 3.18 & 3.19). As highlighted for

the 96DSW plates, the square geometry is expected to have a 'baffling' effect, improving mixing and oxygen mass transfer into the culture media. The shape of the well is such that the bottom is pyramidal, which means that for culture volumes of less than approximately 1 mL the liquid will not be in contact with the square portion of the well and therefore not benefit from this effect. This means that the culture volume of 0.8 mL used in the 24SRW is not suitable for the DSW format, which prevents a direct comparison.

The results shown in Figures 3.18 and 3.19 are for 24 DSW and 24 SRW wells with liquid fill volumes of 2.0 and 0.8 mL respectively. Growth kinetics for the shake flask and both microwell cultivations are indistinguishable for the first 72 hours, following which the 24 DSW culture reaches a lower peak viable cell density of $3.58 \times 10^6 \text{ mL}^{-1}$ compared to $4.35 \times 10^6 \text{ mL}^{-1}$ and $4.48 \times 10^6 \text{ mL}^{-1}$ for the 24 SRW and shake flask systems. Differences in the viability profiles between the three bioreactor systems are minor. Although further work to optimise the cell culture process for 24 DSW plates was not performed, these data illustrate the potential of this bioreactor system for CHO-S cultivation, and presents an option for development through future work.

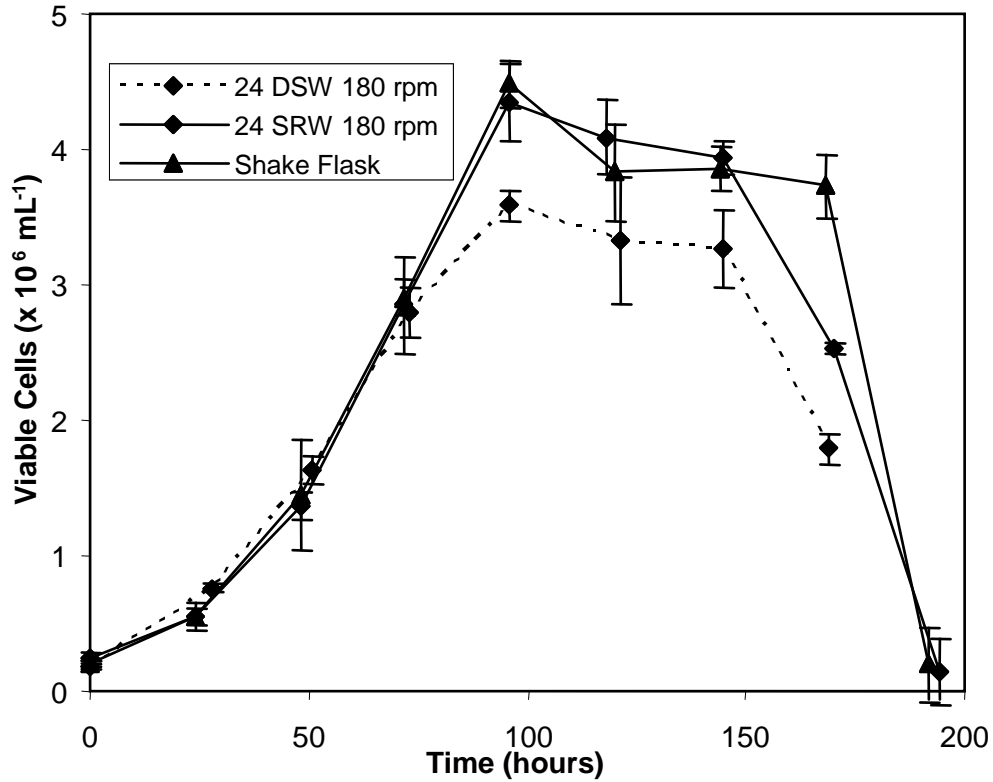


Figure 3.18: Comparison of CHO-S growth in 24 SRW, 24 DSW and Shake Flask formats. Experiments performed in a humidified incubator at 37°C with 5% ambient CO₂. Microwells and flasks were agitated on orbital shakers with orbital shaking diameters of 20 mm and 10 mm respectively as described in Sections 2.2 and 2.3.2. Error bars represent one standard deviation about the mean (n=3).

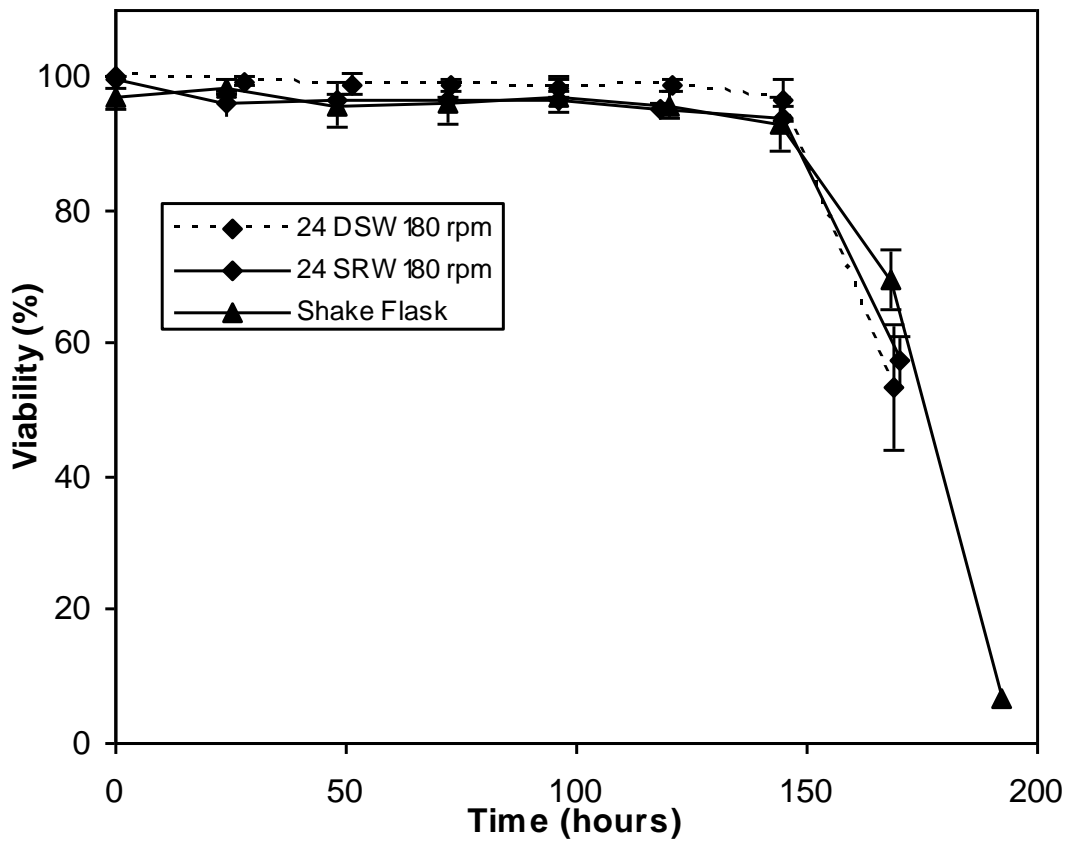


Figure 3.19: CHO-S viability profiles for cultivation in 24 SRW, 24 DSW and Shake Flask formats. Experiments performed in a humidified incubator at 37°C with 5% ambient CO₂. Microwells and flasks were shaken on orbital shakers with shaking diameters of 20 mm and 10 mm respectively as described in Sections 2.2 and 2.3.2. Error bars represent one standard deviation about the mean (n=3).

3.9 Preliminary Fed-Batch Microwell Experiments

Since the majority of cell culture production processes are operated as fed batch or perfusion methods (Hu & Aunins, 1997), the feasibility of performing feeding in microwell formats was investigated. The initial data for daily bolus feeding of wells demonstrate that this can be performed without contamination of the culture and that feeding results in a slightly increased

peak viable cell density ($2.62 \times 10^6 \text{ mL}^{-1}$ fed compared to $2.37 \times 10^6 \text{ mL}^{-1}$ unfed) but a decrease in cumulative cell hours (1.82×10^8 fed compared to 2.01×10^8 unfed) (Figure 3.20). After commencement of feeding there is an initial increase in viable cell density but then a drop in performance relative to the batch wells, which may be due to the increase in the concentration of the waste products lactate and or ammonia in the medium (Figure 3.22), or to a general increase in osmolality.

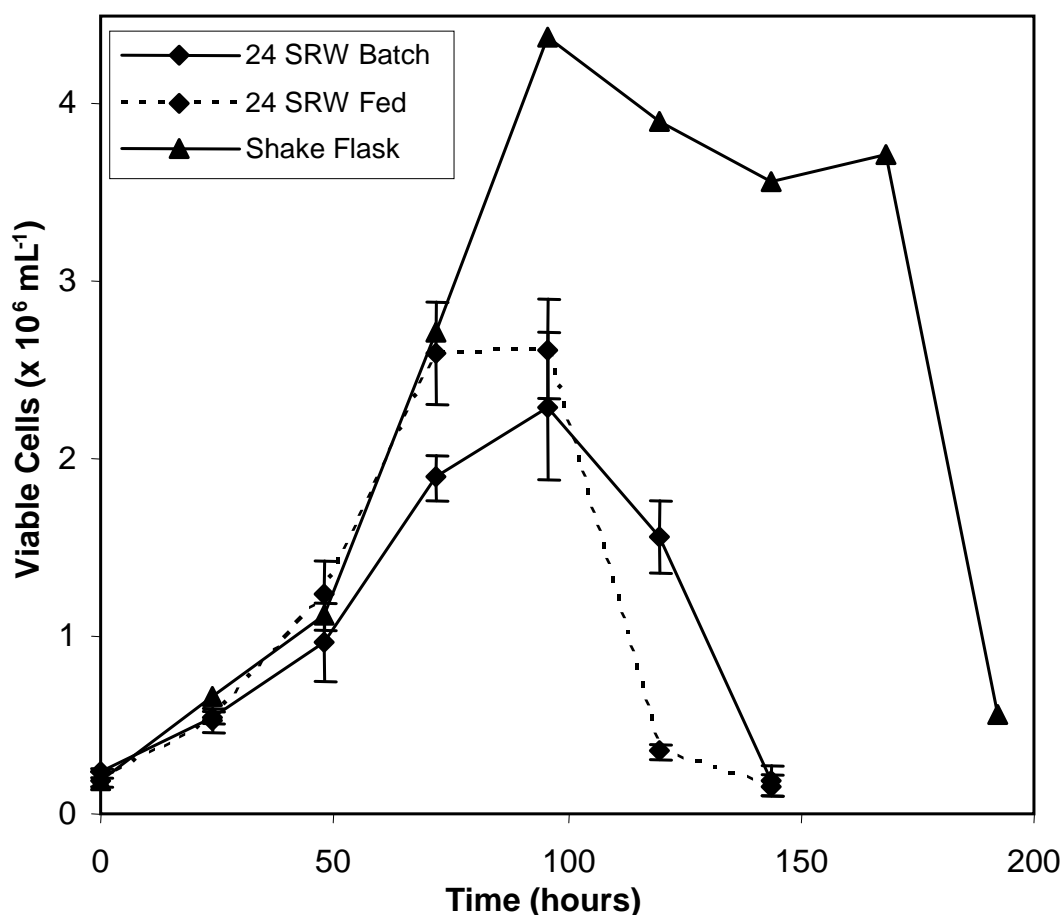


Figure 3.20: Growth profiles for CHO-S in a shake flask and in fed and batch 24SRW plates in CD-CHO medium supplemented with 8 mM L-Glutamine. Experiments performed as described in Section 2.3.1 using the Feeding method outlined in Section 2.5.1. Error bars represent one standard deviation about the mean (n=3).

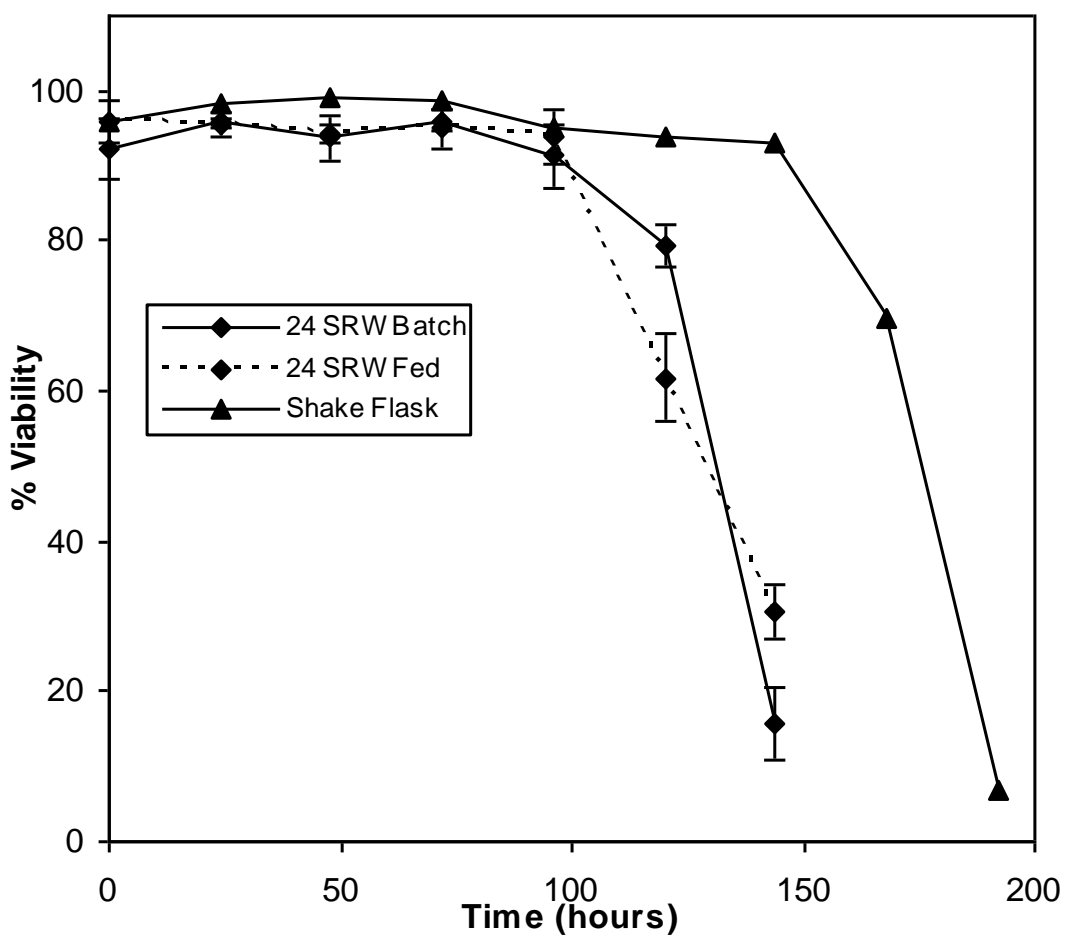


Figure 3.21: CHO-S viability measured for shake flask, fed and batch 24SRW plates in CD-CHO medium supplemented with 8 mM L-Glutamine. Viability was measured by trypan blue exclusion. Experiments performed as described in Section 2.3.1 using the Feeding method outlined in Section 2.5.1. Error bars represent one standard deviation about the mean (n=3).

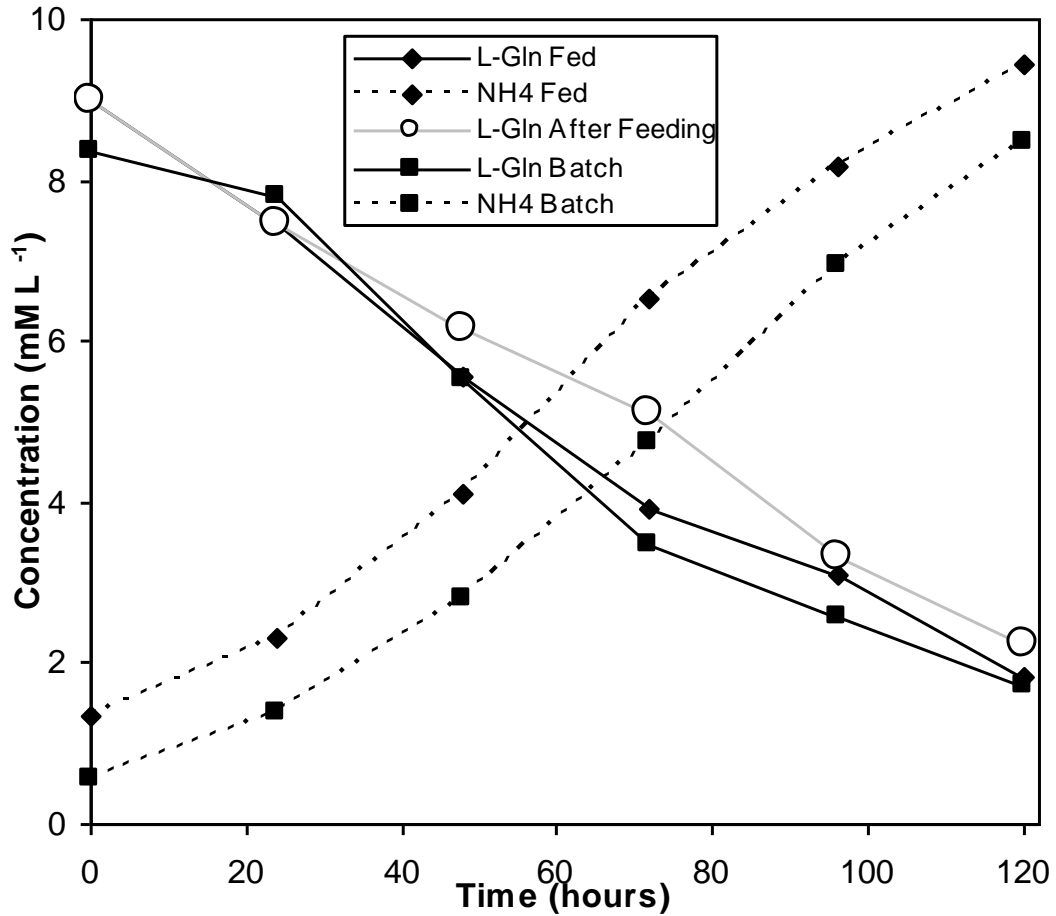


Figure 3.22: Glutamine utilization and ammonia production profiles for fed and batch 24SRW plate CHO-S cultures in CD-CHO medium supplemented with 8 mM L-Glutamine. Lime green points indicate L-Gln concentration immediately after bolus feeding. Experiments performed as described in Section 2.3.1 using the Feeding method outline in Section 2.5.1.

The adapted feed forward algorithm described in Section 2.5.1, which assumes that the specific L-glutamine utilization rate of the cells for the following 24 hours could be assumed to be the same as from the preceding 24 hour period, was only partially successful in predicting the growth kinetics and metabolite utilization of the cells. As such, the L-glutamine concentration strayed from the intended control point of 2mM. A further issue is that feeding was performed under conditions of limitation for the microwells,

before it was found that increasing the shaking speed allowed attainment of growth kinetics that more closely matched the shake flask. As such the main value of these data is as proof of principle that feeding is technically feasible.

It should be noted that feeding to microwells carries the risk of altering the fluid hydrodynamics (in a way that is insignificant for larger scale systems). As is apparent from the results shown above, an increase in the fill volume for 24SRW plates above 0.8 mL may result in cell sedimentation. As such, the liquid feed volumes should be minimised to prevent this. Use of concentrated feeds would minimise the addition volumes, but the concentration could be limited by (i) the accuracy of pipetting small volumes, especially if the solution is highly viscous and (ii) the solubility of the feed components. It is possible that in the case of the 24SRW format the high rate of evaporation could be an advantage for feeding, as the initial inoculum volume could be maintained by careful selection of the feed concentration such that the volume lost by evaporation is replaced each day. These considerations are less significant for shake flask and bioreactor feeding, where the fed volume is often negligible in comparison with the initial volume.

It is clear that there is a strong case for automation of the microwell feeding procedure, as the manual process is both time consuming and carries a contamination risk, as well as exposing cells to a period in which they are unshaken and hence liable to suffer oxygen limitation and medium

inhomogeneity. Whilst truly continuous feeding will remain difficult to achieve, automation would allow bolus feeds to be performed more frequently than once per day, thus reducing the chance of 'metabolic overflow' and the associated increase in waste metabolite concentration.

3.10 Summary

It has been demonstrated that batch cultivation of both hybridoma and CHO-S cells can be performed successfully in shaken 24 SRW microwell plates. However, rather than using a generic set of process conditions, it is clear that experimental parameters such as liquid fill volume and shaking speed and diameter must be optimised for each cell line.

Of the microwell formats assessed, the 24 SRW plate appears the best. However, evaporation remains a significant problem that must be solved.

The potential for implementation of a fed-batch methodology looks promising and this will be explored further with an industrial GS-CHO cell line in the next Chapter.

Chapter 4: Development of a Fed-Batch Cell Culture Methodology in Shaken 24 Well Bioreactors

4.1 Introduction and Aim

In the previous chapter the utility of shaken 24 SRW plates for batch cultivation of a commercially available CHO-S cell line was demonstrated. The technical feasibility of fed-batch operation was also tested (see Section 3.9) and it was found that liquid additions could be made manually without contamination of the well contents. However, the feed recipe and methodology employed were not appropriate for establishing high cell density, high productivity cell cultures.

Since the majority of industrial cell culture processes are operated in fed-batch or perfusion modes (Chu et al., 2001), it would clearly be of great benefit to have a small scale model of such culture conditions.

The availability of an industrially relevant GS-CHO cell line producing an IgG product, together with a pre-existing proprietary feeding methodology used for shake flasks (Section 2.5.2), presented an opportunity to further explore the implementation of a fed-batch methodology in shaken microwell bioreactors. Challenges with this approach included high relative levels of evaporation over the culture period (See Sections 3.4 and 3.9) and the

necessity of manual liquid additions without contamination of the well contents.

The aim of this chapter was demonstration of parallel fed-batch experiments in 24 SRW plates and shake flasks with similar cell growth and antibody production kinetics.

The specific objectives were as follows:

- Selection of an appropriate sterile closure for microwells to reduce the impact of water loss over the extended fed-batch cultivation period.
- Demonstration of parallel fed-batch experiments in 24 SRW plates and shake flasks with similar cell growth and antibody formation kinetics.
- Comparison of pH and DO profiles from microwell cultivations to those in shake flasks.

4.2 Selection of a Sterile Closure

Two sterile closures for 24-SRW plates were initially evaluated for their ability to support batch growth of a GS-CHO cell line, while simultaneously minimising evaporation but allowing adequate gas mass transfer. One was a standard Breatheasy membrane and the other a 'sandwich lid' system (as described in Section 2.3.1). The latter consists of a stainless steel microplate cover containing 24 holes, below which a further three layers including a

microfibre filter combine to minimise the rate of water loss from the wells while allowing adequate gas exchange between the microwell headspace and the air.

In terms of GS-CHO growth in batch cultures, use of the 'sandwich lid' resulted in a significantly higher viable cell density than the Breatheasy membrane (Figure 4.1), comparable to that seen in a conventional shake flask. This is attributed to the lower liquid evaporation rate measured through the 'sandwich lid' of $24 \mu\text{L well}^{-1} \text{ day}^{-1}$ compared to $50 \mu\text{L well}^{-1} \text{ day}^{-1}$ for the Breatheasy membrane. In the latter case this could lead to a doubling in the medium osmolality due to liquid losses over the course of the batch culture duration.

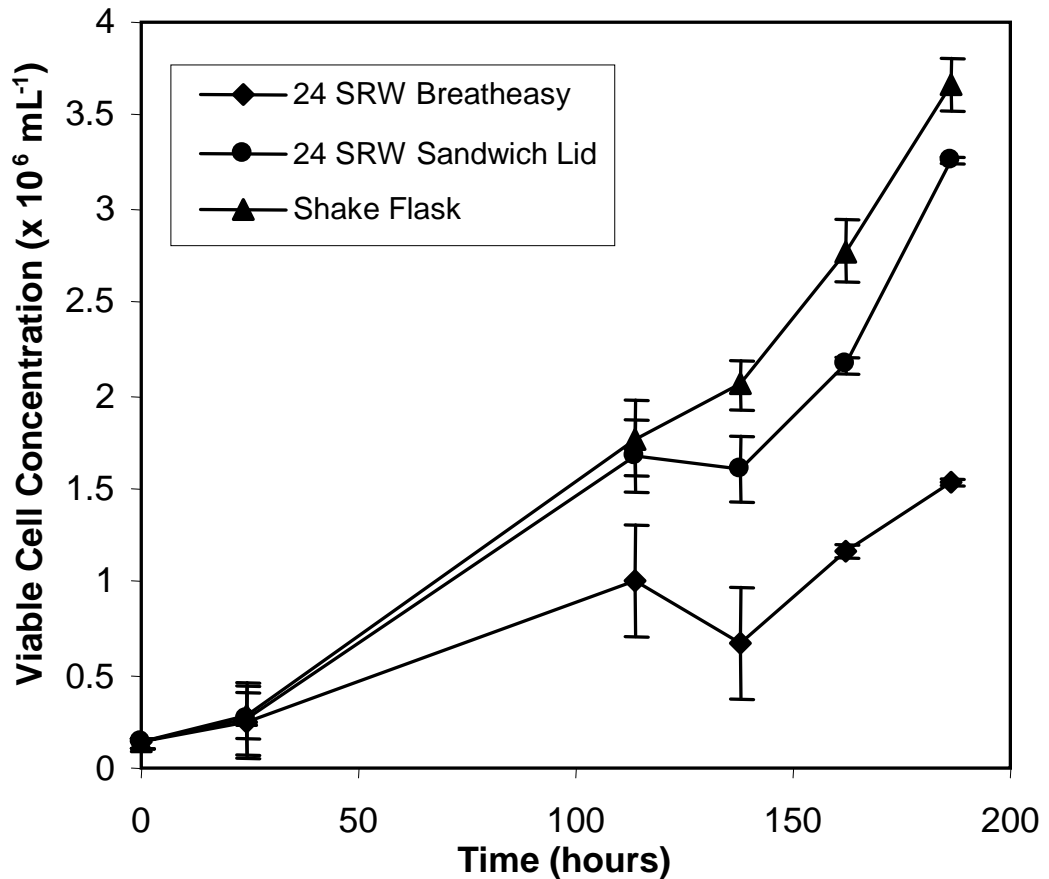


Figure 4.1. Typical GS-CHO batch culture kinetics: (◆) 24-SRW plate with a Breatheasy membrane; (●) 24-SRW plate with ‘sandwich lid’; (▲) 250 mL shake flasks with vent seal. Experiments performed at 36.5 °C with 5% CO₂ at 70% relative humidity and shaken with a 25 mm orbital diameter, as described in Section 2.3.1. Error bars represent one standard deviation about the mean (n=3).

Measured evaporation rates from the shake flask and microwell systems, expressed both in absolute terms and as a proportion of the initial liquid volume, are shown in Table 4.1. In the case of simple batch cultures it can be seen that while the absolute liquid evaporation rate from the shake flask is considerably higher than from the microwells, this is actually around five times lower when expressed as a proportion of the initial liquid volume. Consequently in the microwells the medium osmolarity is increased which

results in the lower GS-CHO growth rate and viable cell concentration seen in Figure 4.1.

Table 4.1: Absolute and Relative Rates of Evaporation from Shake Flasks and 24 Well Bioreactors.

Culture Vessel	Sterile Seal	Evaporation Rates			
		Batch Cultures		Fed-Batch Cultures	
		$\mu\text{L day}^{-1}$	% (v/v) day^{-1}	$\mu\text{L day}^{-1}$	% (v/v) day^{-1}
24-SRW Plate	Breatheasy Membrane	50	-6.3	30	-3.9
24-SRW Plate	Sandwich Lid	24	-3.0	5	-0.7
250 mL Shake Flask	Corning Vent Seal	310	-0.6	90	+0.2

4.3 Initial Parallel Fed Batch Experiments in Shaken Bioreactors

Microwell feeding was initially performed using an already established bolus feeding method for shake flasks, as described in Section 2.5.2. This involved five bolus feeds on consecutive days. Each feed comprised addition of nutrient medium followed by a shot of bicarbonate solution for pH control. Culture performance is shown in Figure 4.2, with respective peak viable cell densities for shake flask and microwell systems reaching 6.0×10^6 and 3.1×10^6 viable cells mL^{-1} respectively, with the viability of the cells in the microwell culture seen to fall rapidly after 140 hours (Figure 4.3). The resultant final antibody titre in the microwell system was also measured and found to be lower at 0.73 g L^{-1} compared to 1.3 g L^{-1} in the shake flask.

Since the evaporation rates from the flasks and wells were approximately 0.6% and 3% (v/v) of the initial liquid volume per day respectively (Table 4.1), it was found that this water loss combined with addition of concentrated feeds led to an average final osmolality of 746 mOsm Kg⁻¹ in the 24-SRW plates compared to 464 mOsm Kg⁻¹ in the shake flasks (Figure 4.4). This had a detrimental impact on microwell culture performance in terms of both cell growth and productivity. Takagi et al. (2000) found that productivity of suspended CHO cells was adversely affected at osmolalities in excess of 450 mOsm Kg⁻¹, a value that was exceeded by a considerable margin in these initial microwell fed-batch cultures.

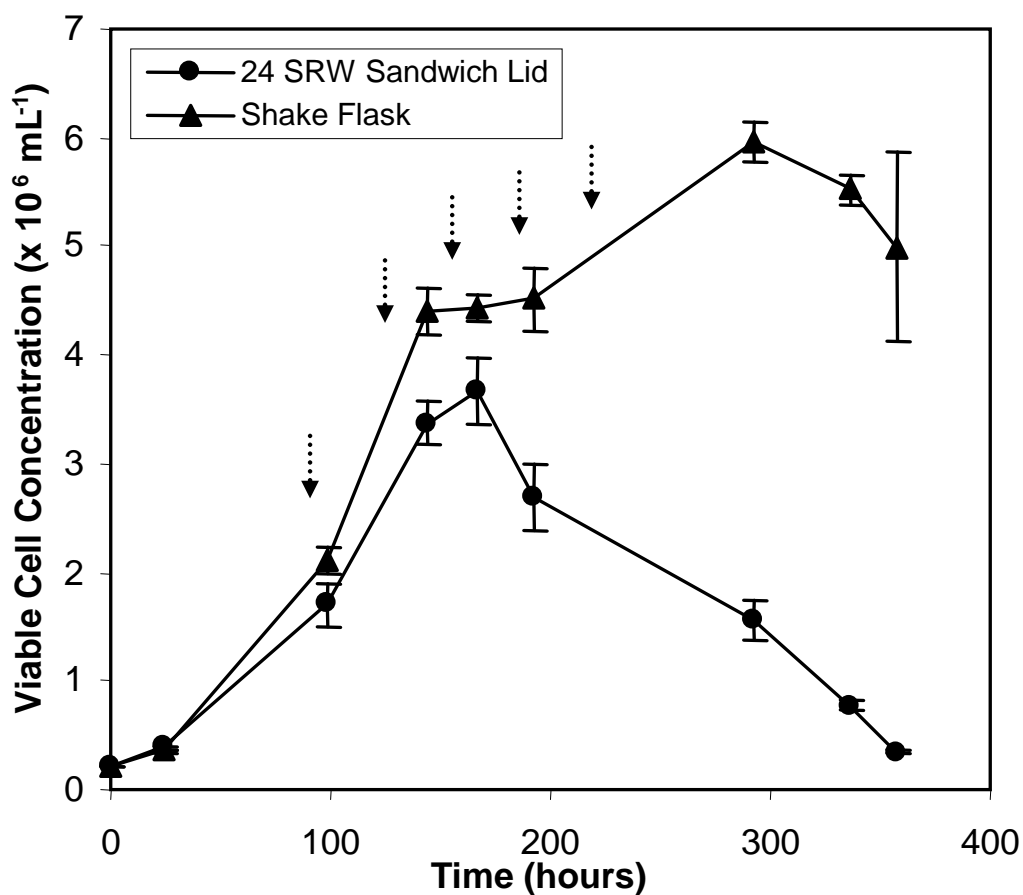


Figure 4.2: Growth profiles for fed-batch cultivation of a GS-CHO cell line in a 24 SRW plate and shake flask in CD-CHO medium. Experiments performed in a humidified incubator at 36.5°C with 5% ambient CO₂ as described in Section 2.3.1. Arrows represent points at which feed additions were made. Microwells and flasks were agitated at 140 rpm on an orbital shaker with a 25 mm shaking diameter. Error bars represent one standard deviation about the mean (n=3).

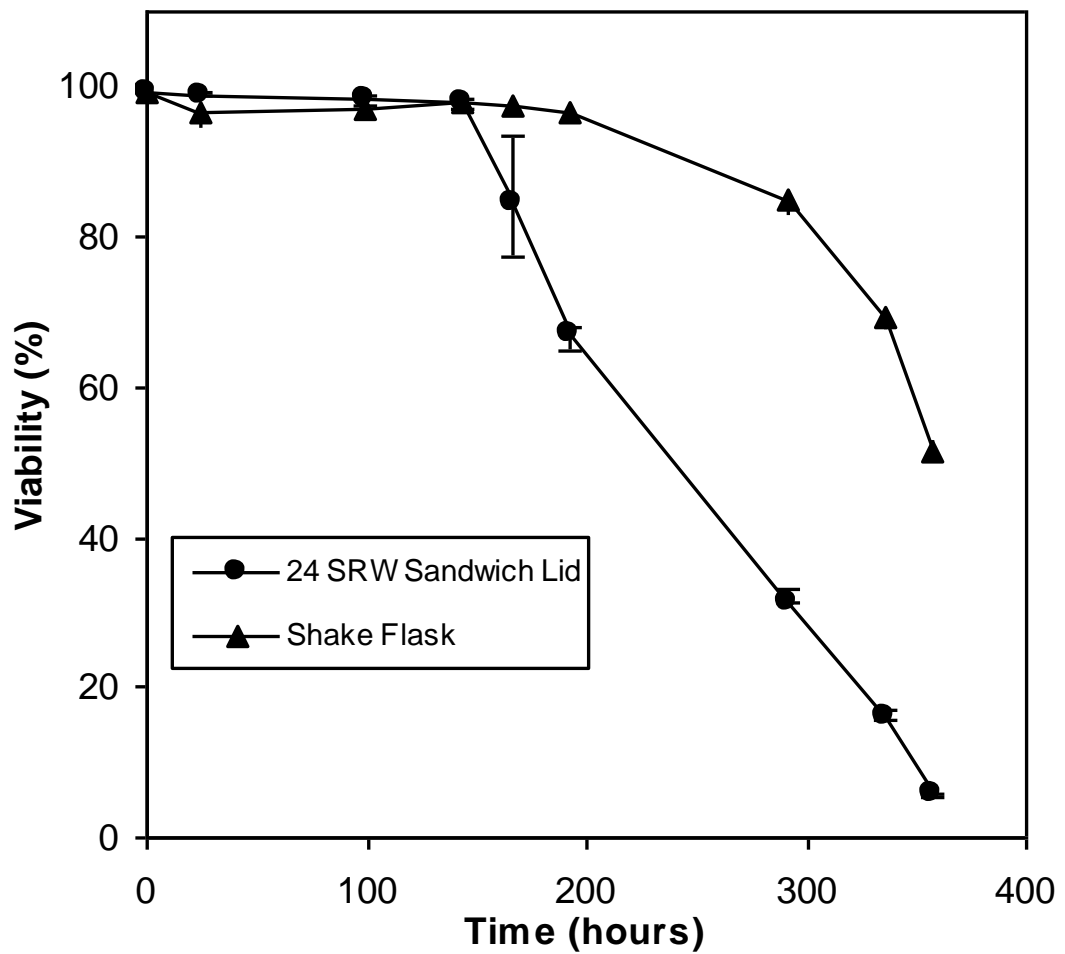


Figure 4.3: Viability profiles for fed-batch cultivation of a GS-CHO cell line in a 24 SRW plate and shake flask in CD-CHO medium. Experiments performed as described in Section 2.3.1. Error bars represent one standard deviation about the mean (n=3).

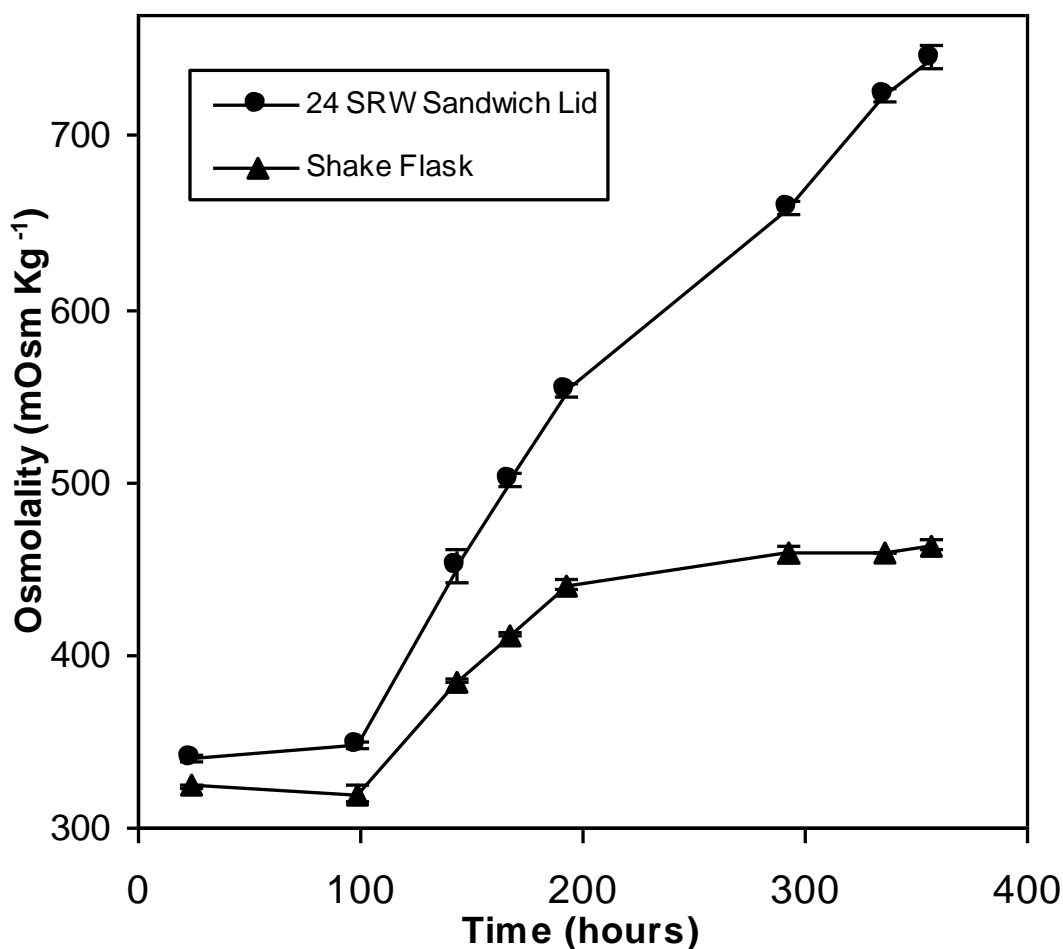


Figure 4.4: Osmolality profiles for fed-batch cultivation of a GS-CHO cell line in a 24 SRW plate and shake flask in CD-CHO medium. Culture method is as described in Section 2.3.1, with osmolality measured as described in Section 2.7.4. Error bars represent one standard deviation about the mean (n=3).

4.4 Fed Batch GS-CHO Culture Using Diluted Bolus Feeds

To further minimise evaporation and the measured increases in medium osmolality (Figure 4.4) the microwell feed and base additions were diluted by a factor of 2 and 10 respectively. The quantity of nutrients and base in the bolus shots were unchanged but the total liquid volume added per well per day was raised from 18 to 52 μL . Figures 4.5-4.8 show growth, viability,

product and osmolality data respectively for use of this diluted feed in shake flask and 24-SRW culture systems.

The cell growth rates and peak viable cell levels achieved are very similar in both cases while the cell viabilities remain high at around 90% after 300 hours of culture. However, cumulative cell hours (CCH) for the microwell cultivation are 17% lower than in the shake flasks. The kinetics of antibody formation are also very similar with final IgG titres for both shaken systems being around 1.5 g L^{-1} . The slightly higher IgG titre measured in the microwells is thought to be a consequence of the slightly raised final culture osmolality of 506 mOsm Kg^{-1} compared to 438 mOsm Kg^{-1} for the shake flasks. Increased specific antibody productivity at higher culture osmolalities is well documented for both CHO and Hybridoma cell cultures (Takagi et al., 2000, Yang et al., 1996), and this is demonstrated in Figure 4.9 (specific antibody production calculated using Equation 2.10). However, the additional water in the diluted feed prevents the osmolality reaching levels that significantly compromise cell culture performance.

Average specific antibody productivities for the fed cultivations were 17.9 and $23.0 \text{ mg } 10^9 \text{ cells}^{-1} \text{ day}^{-1}$ for shaken flasks and 24 SRW plates respectively. These values are similar to those obtained for a fed-batch GS-CHO process operated in the SimCell system (Amanullah et al., 2010, and described in Section 1.5.2), which was $22.1 \text{ mg } (10^9 \text{ cells.day})^{-1}$.

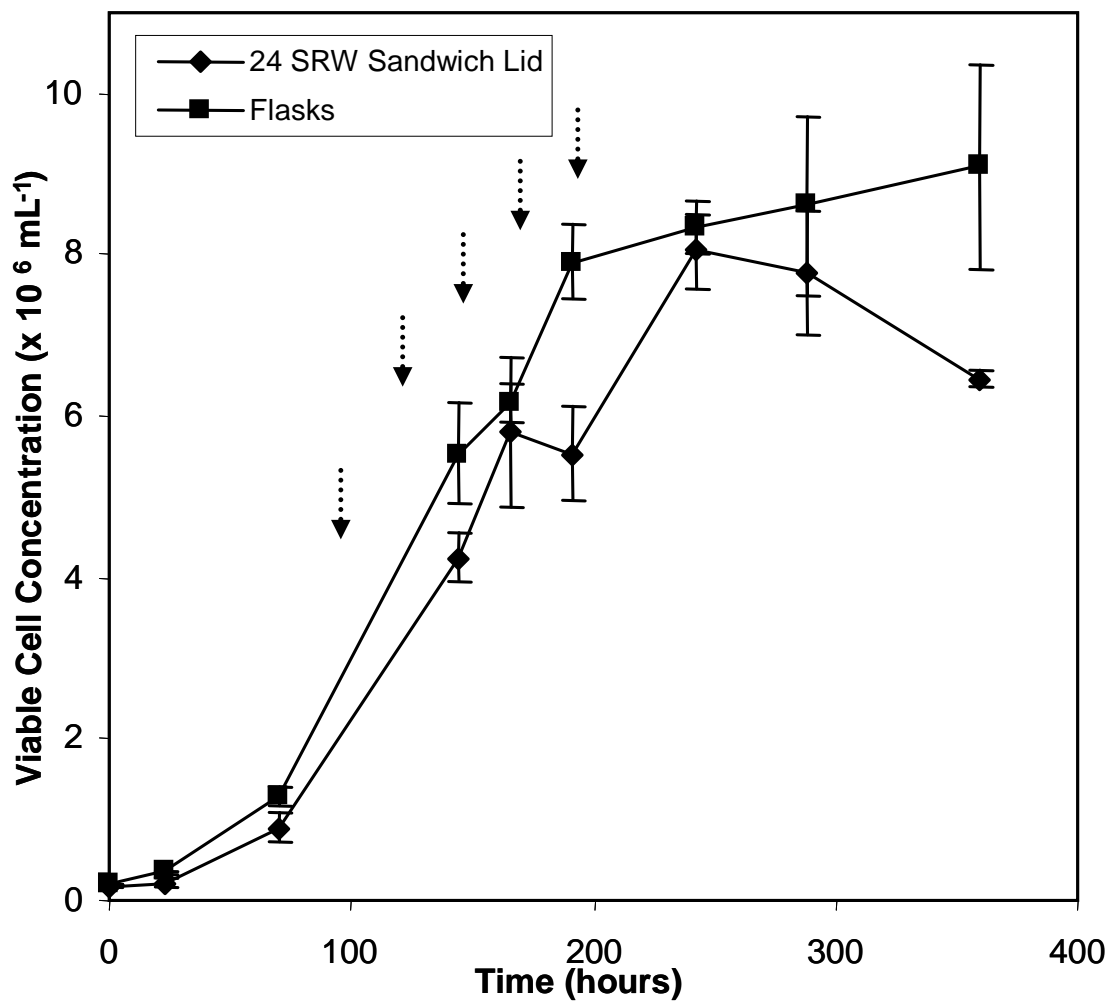


Figure 4.5: Growth profiles for fed-batch cultivation (diluted feeds) of a GS-CHO cell line in a 24 SRW plate and shake flask in CD-CHO medium. Experiments performed as described in Section 2.3.1. Arrows represent points at which feed additions were made. Error bars represent one standard deviation about the mean (n=3).

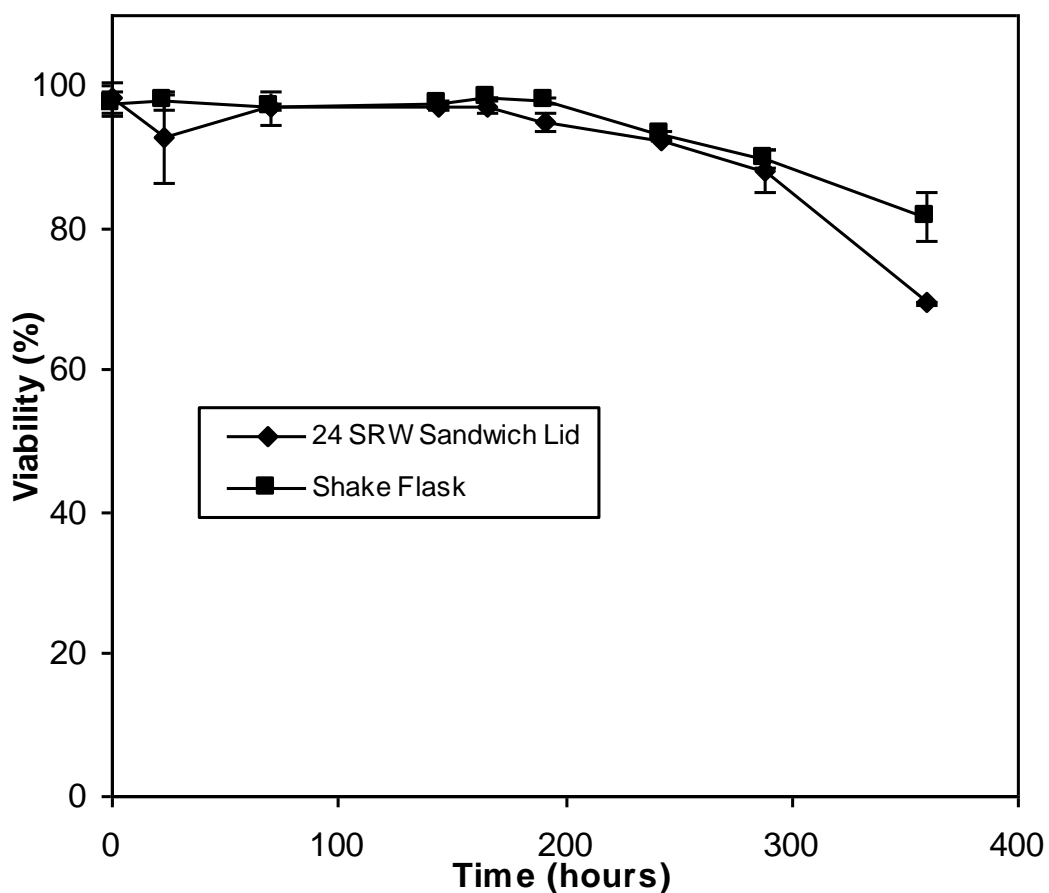


Figure 4.6: Viability profiles for fed-batch cultivation (diluted feeds) of a GS-CHO cell line in a 24 SRW plate and shake flask in CD-CHO medium. Experiments performed as described in Section 2.3.1. Error bars represent one standard deviation about the mean (n=3).

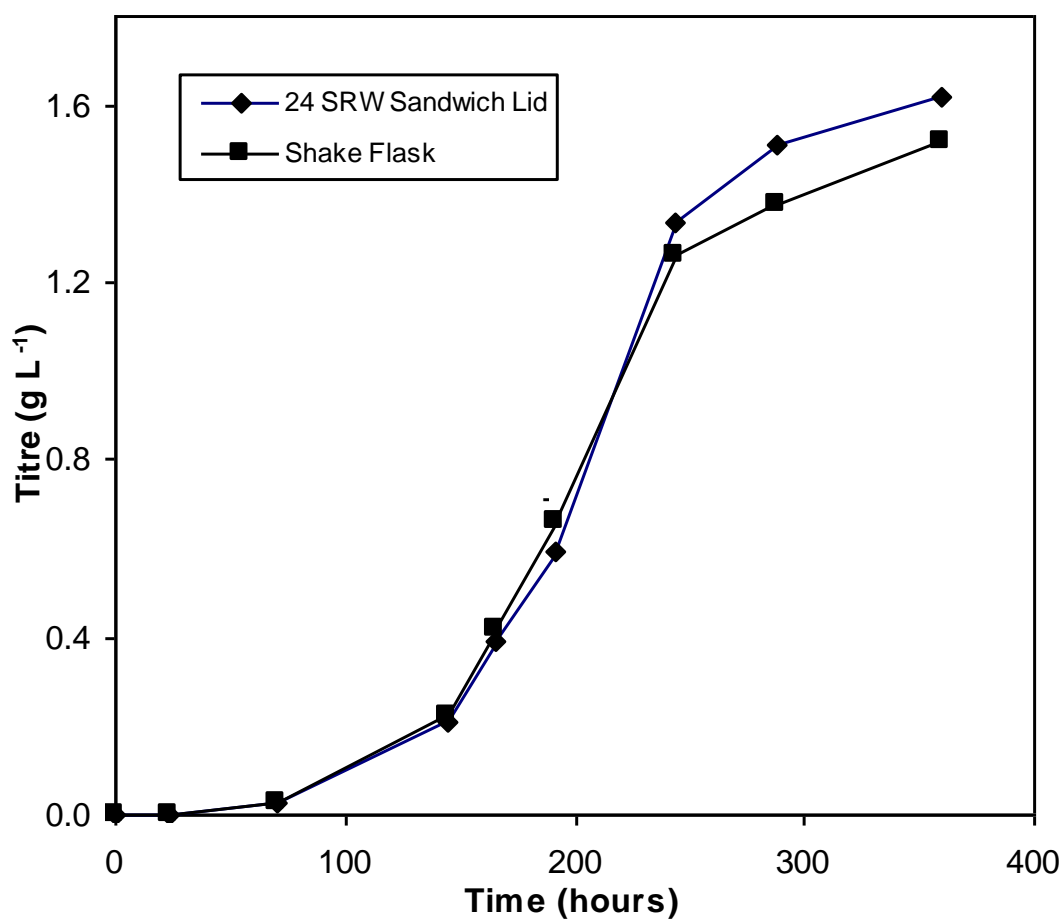


Figure 4.7: IgG production profiles for fed-batch cultivation (diluted feeds) of a GS-CHO cell line in a 24 SRW plate and shake flask in CD-CHO medium. Experiments performed as described in Section 2.3.1. IgG quantitation performed by Protein A HPLC, as described in Section 2.7.3.

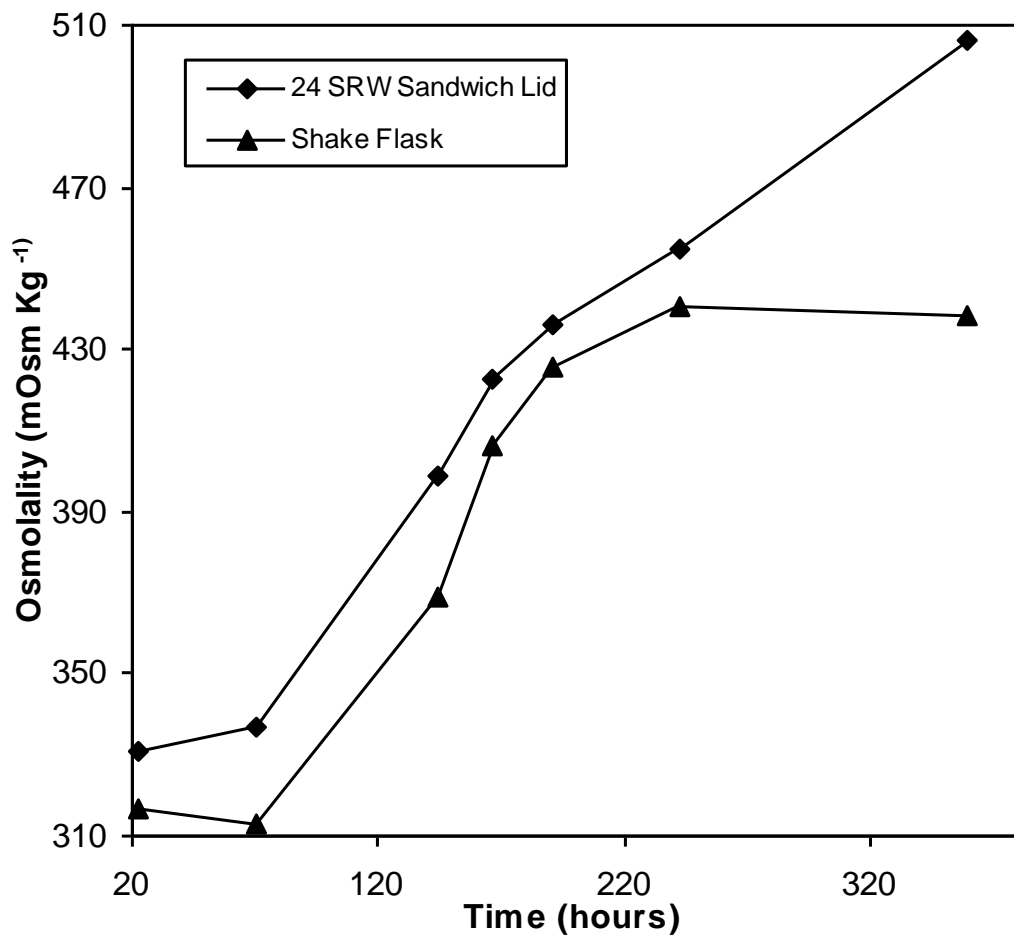


Figure 4.8: Osmolality profiles for fed-batch cultivation (diluted feeds) of a GS-CHO cell line in a 24 SRW plate and shake flask in CD-CHO medium. Experiments performed as described above in Section 2.3.1, and osmolality was measured as described in Section 2.7.4.

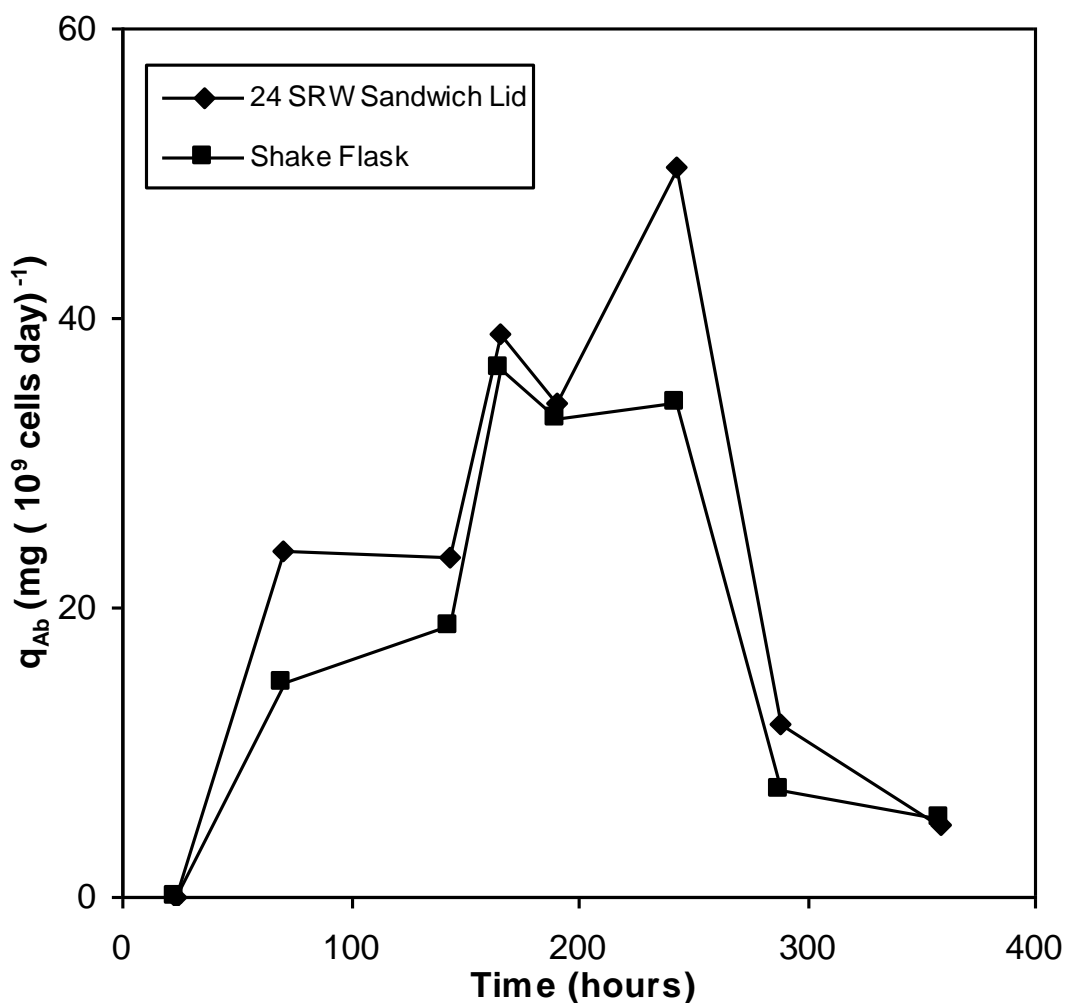


Figure 4.9: Profiles for specific MAb productivity for fed-batch cultivation (diluted feeds) of a GS-CHO cell line in a 24 SRW plate and shake flask in CD-CHO medium. Experiments performed as described in Section 2.3.1. q_{Ab} was calculated using Equation 2.10 as shown in Section 2.13.2.

4.5 Variation of Culture Environment During Shaken 24-SRW Cultures

Having shown that the use of diluted bolus feeds during fed-batch cultures allows comparable cell growth and antibody formation kinetics in shaken 24-SRW plates and shake flasks, it was important to check that all associated environmental parameters are also comparable. Therefore at-line analysis of culture samples was performed to assess dissolved oxygen, carbon

dioxide and pH as well as the concentrations of key metabolic indicators glucose, lactate, glutamine and ammonia (as described in Sections 2.7.2 and 2.7.5).

The measured pH profiles in both the microwell and shake flask experiments were found to be identical, with final values of pH 6.7 (Figure 4.10), which suggested that cell metabolism and the formation of acidic metabolites was the same in both formats. In addition, dissolved oxygen levels remain above 60% of air saturation in both flasks and microwells throughout the culture. The consistently higher dissolved oxygen levels measured for the microwells suggest that the oxygen transfer rate in this format is higher than for shake flasks.

The partial pressure of carbon dioxide is not significantly outside of the physiological range of 31-54 mmHg (Sharfstein, 2008) for either of the culture formats (Figures 4.11 and 4.12), suggesting that the rate at which it is stripped from the medium following evolution from the cells is adequate, although consistently lower levels in the microwells again indicate a higher rate of gas-liquid mass transfer in this format.

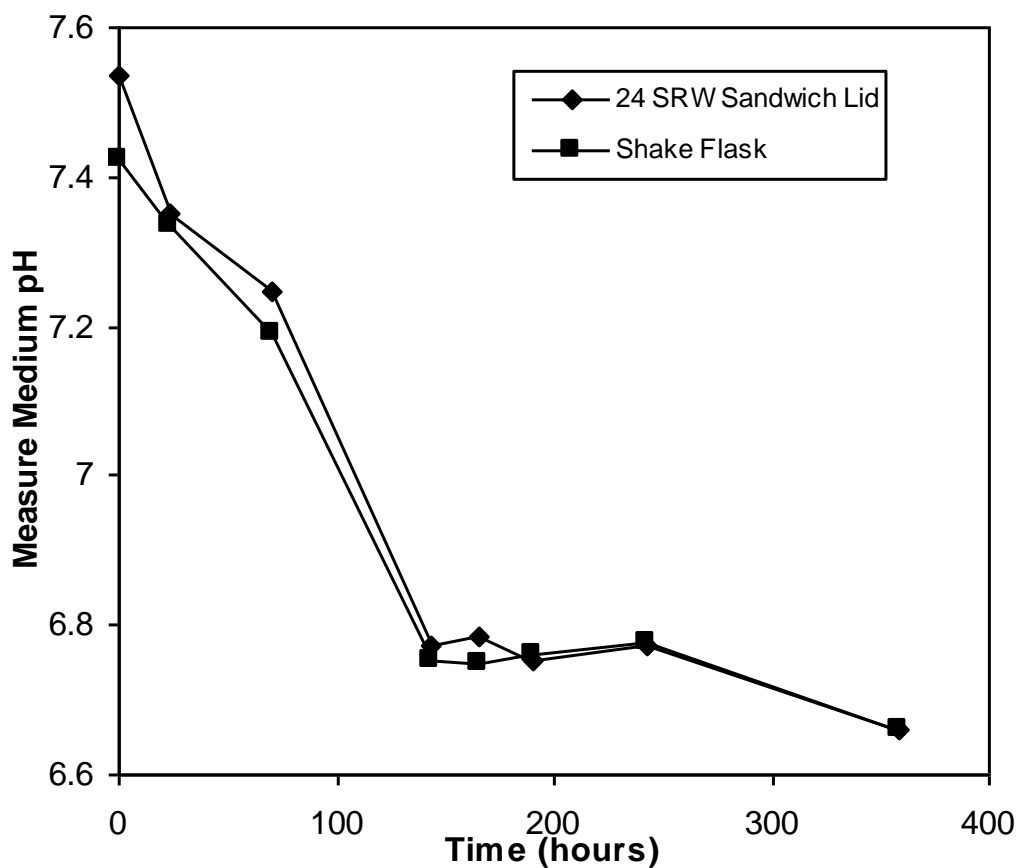


Figure 4.10: At-line pH profiles for fed-batch cultivation (diluted feeds) of a GS-CHO cell line in a 24 SRW plate and shake flask in CD-CHO medium. Experiments performed as described above in Section 2.3.1., with pH measured as described in Section 2.7.5.

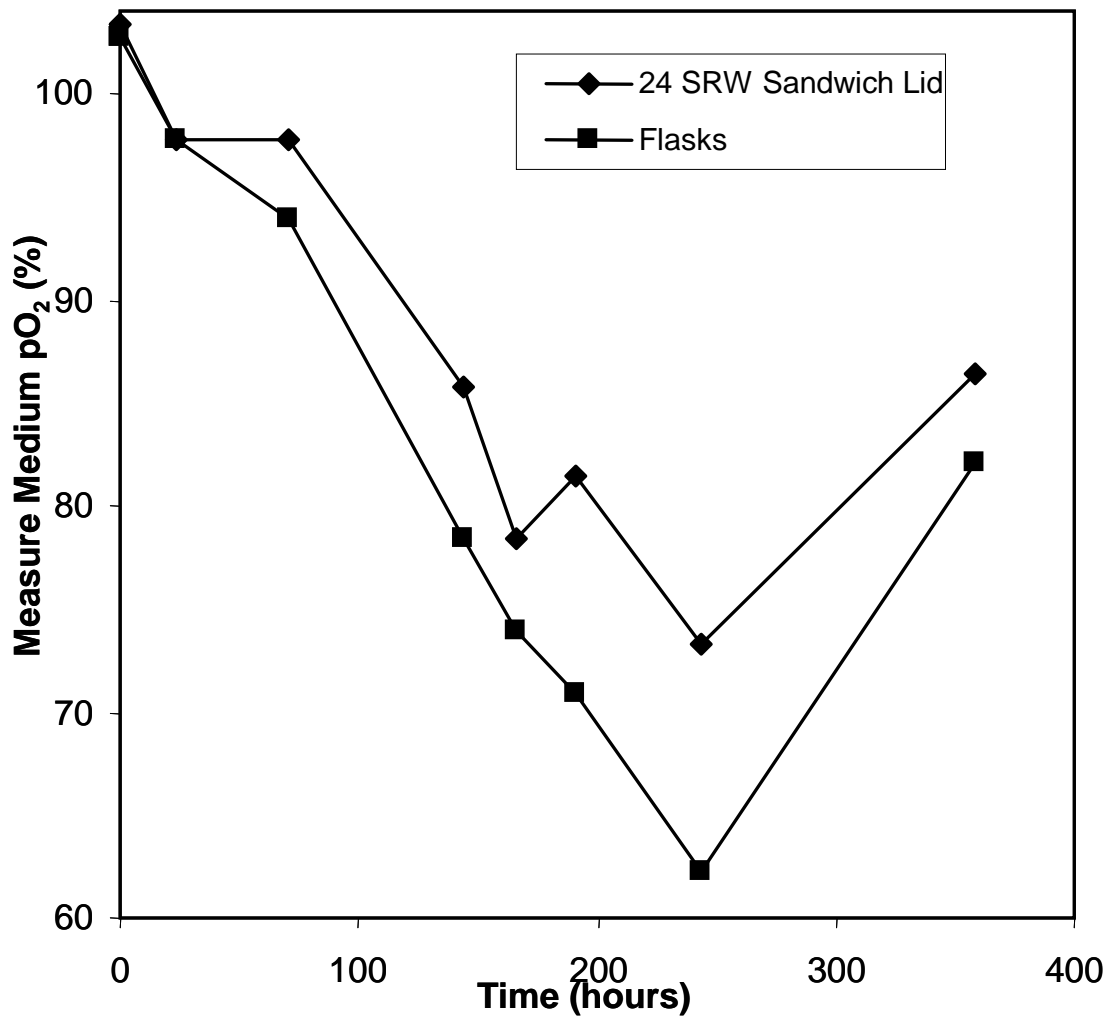


Figure 4.11: At-line dissolved oxygen profiles for fed-batch cultivation (diluted feeds) of a GS-CHO cell line in a 24 SRW plate and shake flask in CD-CHO medium. Experiments performed as described above in Section 2.3.1, with pO₂ measured as described in Section 2.7.5.

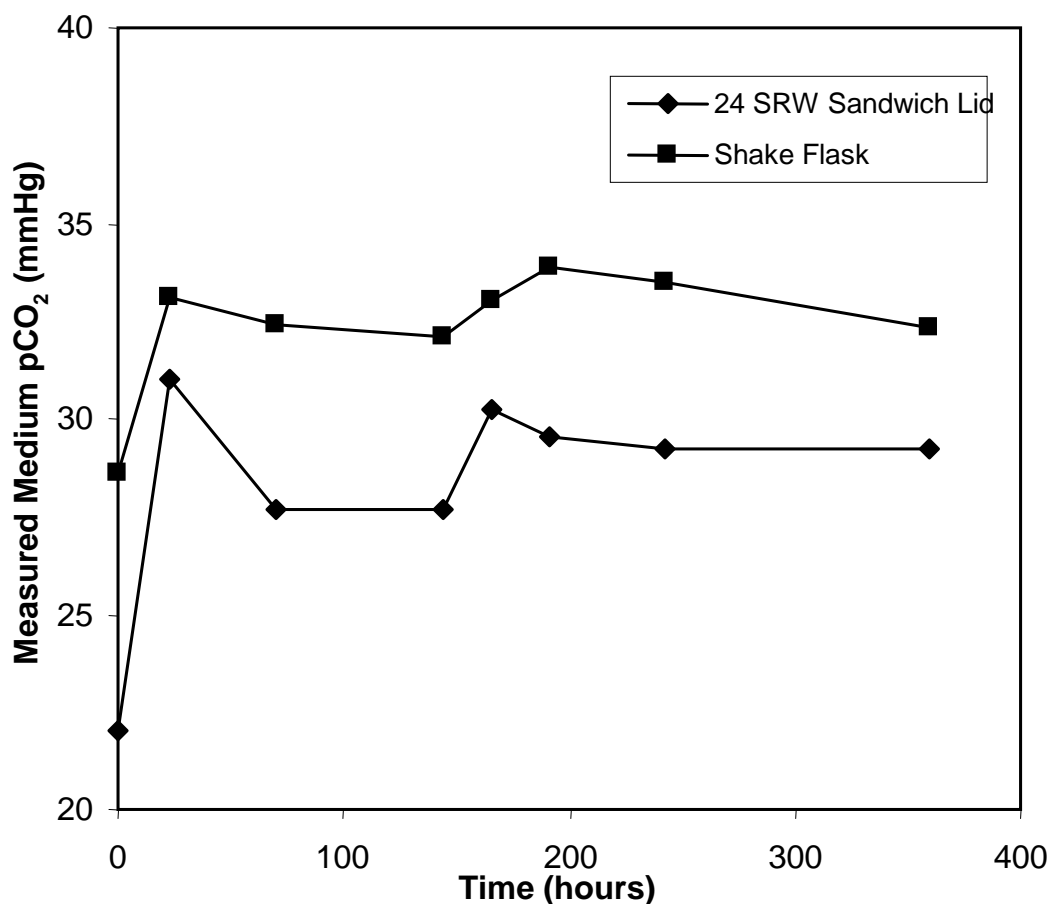


Figure 4.12: At-line dissolved carbon dioxide profiles for fed-batch cultivation (diluted feeds) of a GS-CHO cell line in a 24 SRW plate and shake flask in CD-CHO medium. Experiments performed as described in Section 2.3.1, with pCO₂ measured as described in Section 2.7.5.

It was also found that metabolite profiles for glucose, lactate, glutamine and ammonia were highly comparable (Figures 4.13 – 4.14). The key cell culture parameters are presented in Table 4.2.

Table 4.2: Comparison of fed-batch GS-CHO culture kinetics (diluted feeds) between microwell (24-SRW) and shake flask bioreactor geometries. Experiments performed as described above in Figure 4.2 and Section 2.3.1 and culture data as shown in Figures 4.5-4.12.

Parameter	24-SRW Plate	Shake Flask
Final antibody concentration [g L ⁻¹]	1.62	1.52
Integral viable cell concentration [10 ⁹ cells.day ⁻¹ .L ⁻¹]	70.3	84.8
Peak viable cell concentration [cells mL ⁻¹]	8.04	9.09
Maximum specific growth rate [h ⁻¹]	0.031	0.027
q _{Ab} [mg (10 ⁹ cells.day) ⁻¹]	23.0	17.9
q _{gluc} [g (10 ⁹ cells.day) ⁻¹]	0.15	0.14
q _{lac} [g (10 ⁹ cells.day) ⁻¹]	0.13	0.18
Lactate produced / glucose consumed [g.g ⁻¹]	0.46	0.56

In summary, the fed 24 SRW and shake flask cultivations with diluted feeds perform very similarly, with the main disparity being slightly reduced cell growth in the microwells which is compensated for by raised specific productivity resulting from raised osmolality. Ideally these differences would be removed such that a closer equivalence between the shaken formats is obtained.

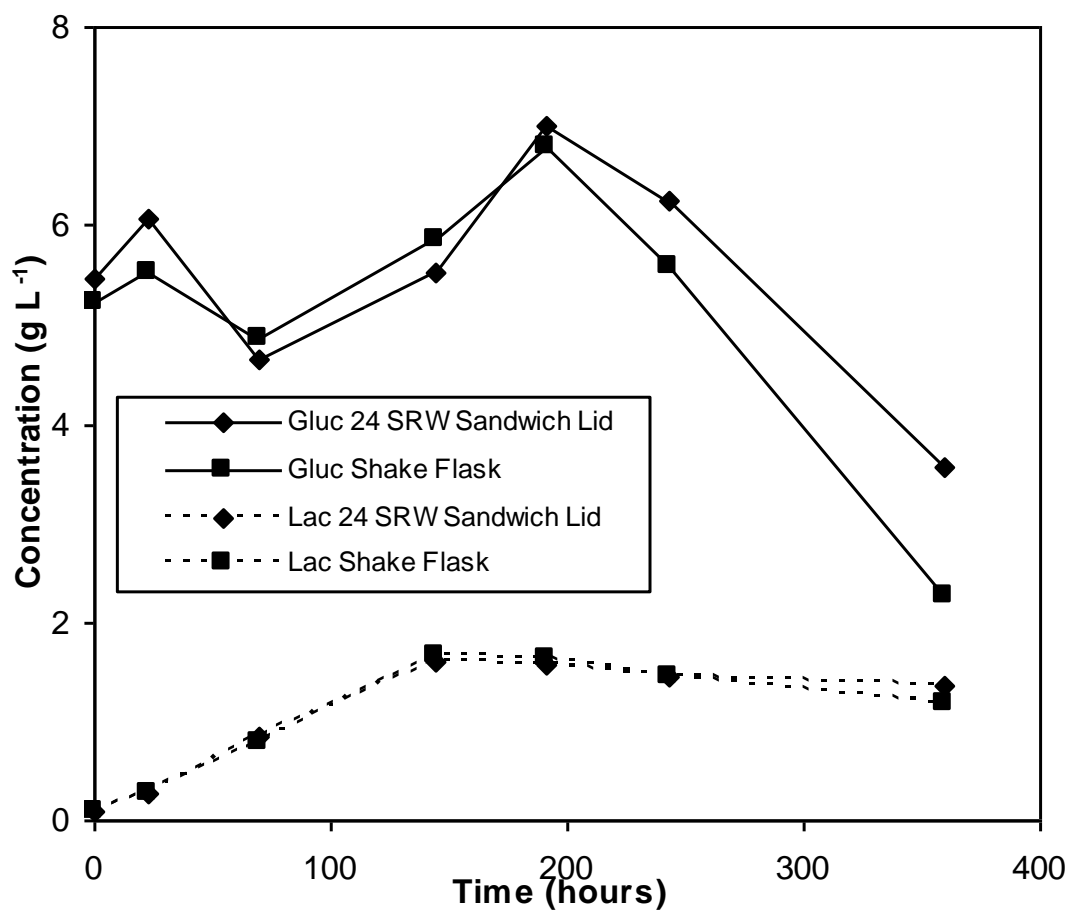


Figure 4.13: Glucose (Gluc) and lactate (Lac) profiles for fed-batch cultivation (diluted feeds) of a GS-CHO cell line in a 24 SRW plate and shake flask in CD-CHO medium. Experiments performed as described above in Section 2.3.1, and metabolite levels were measured as described in Section 2.7.2.

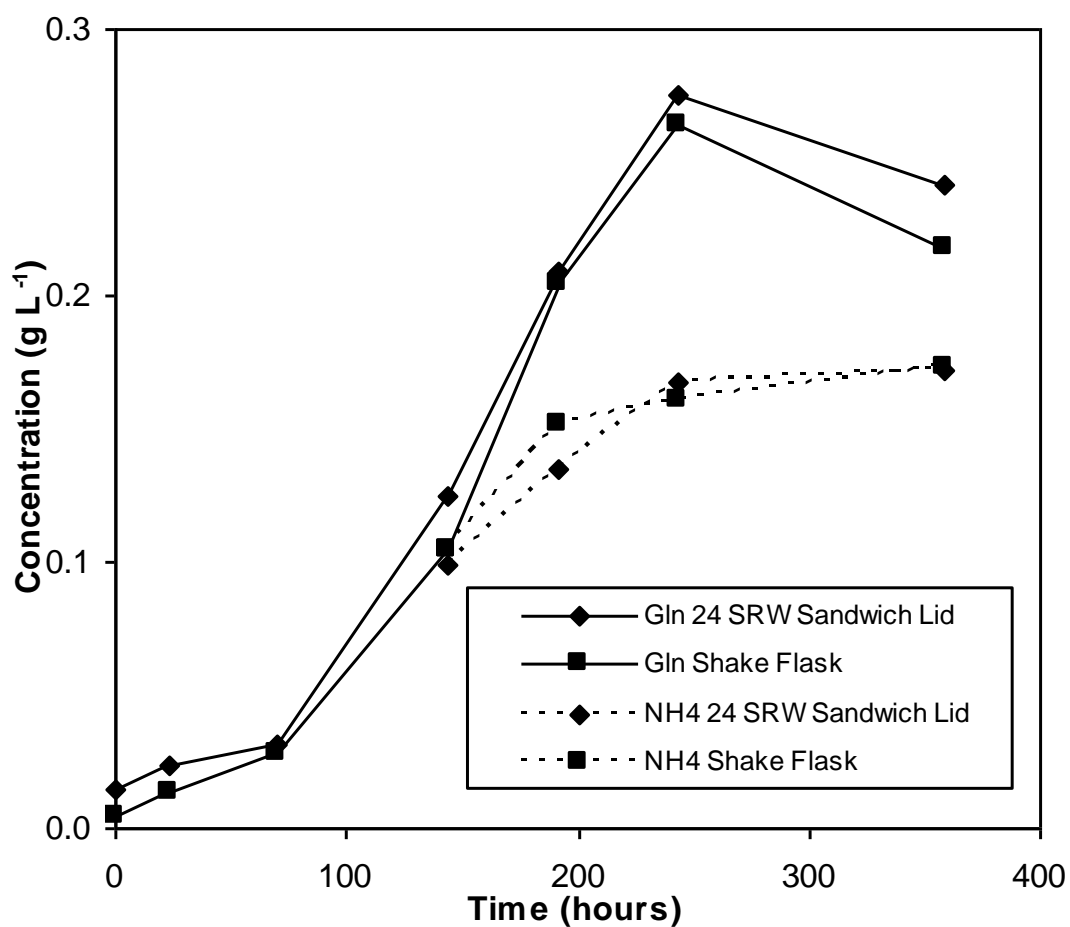


Figure 4.14: Glutamine (Gln) and ammonia (NH₄) profiles for fed-batch cultivation (diluted feeds) of a GS-CHO cell line in a 24 SRW plate and shake flask in CD-CHO medium. Experiments performed as described above in Section 2.3.1, and metabolite levels were measured as described in Section 2.7.2.

4.6 Assessment of well to well reproducibility in parallel 24 SRW cell cultures

Use of a microwell cell culture system requires that reproducible performance is obtained in each well, especially as sacrificial sampling is needed as a result of the small culture volumes used. In order to evaluate this three 24 SRW plates were inoculated and cultivated following the standard fed batch protocol described in Section 2.5.2 and using the 'sandwich lid' as the sterile seal. One entire plate was then harvested after 6, 10 and 15 days respectively. The liquid volume, viable cell density and product titre for each well were then measured, allowing any performance variations to be identified.

It was found that differences in volume, which would correspond to differential evaporation rates across the plate, were minor while viable cell density and titre were similar at days 6 and 10 with more substantial differences at day 15. These differences could be correlated with the position of the well on the plate, classified as either corner, edge or internal.

Use of microwell systems is based on the assumption that each well provides an identical environment for the cells. Even minor differences in temperature or evaporation rate, for example, will have an effect on culture performance, particularly for fed batch animal cell cultures lasting for up to 15 days. Positional effects have been noted in the literature, for example the

observation that the rate of evaporation from wells at the plate edge exceeds that for those located internally (Girard et al., 2001).

To assess the influence of well position on culture performance, the wells in the 24 SRW plate were sub-divided into three categories as shown in Figure 4.15:

A1	A2	A3	A4	A5	A6
B1	B2	B3	B4	B5	B6
C1	C2	C3	C4	C5	C6
D1	D2	D3	D4	D5	D6

Figure 4.15: Classification of wells on a 24 SRW plate by position. Red indicates a 'corner' well, orange an 'edge' well and green an 'internal' well.

The results for viable cell density, viability, fluid volume per well and product titre are shown for days 6, 10 and 15 of culture in Figures 4.16 to 4.19:

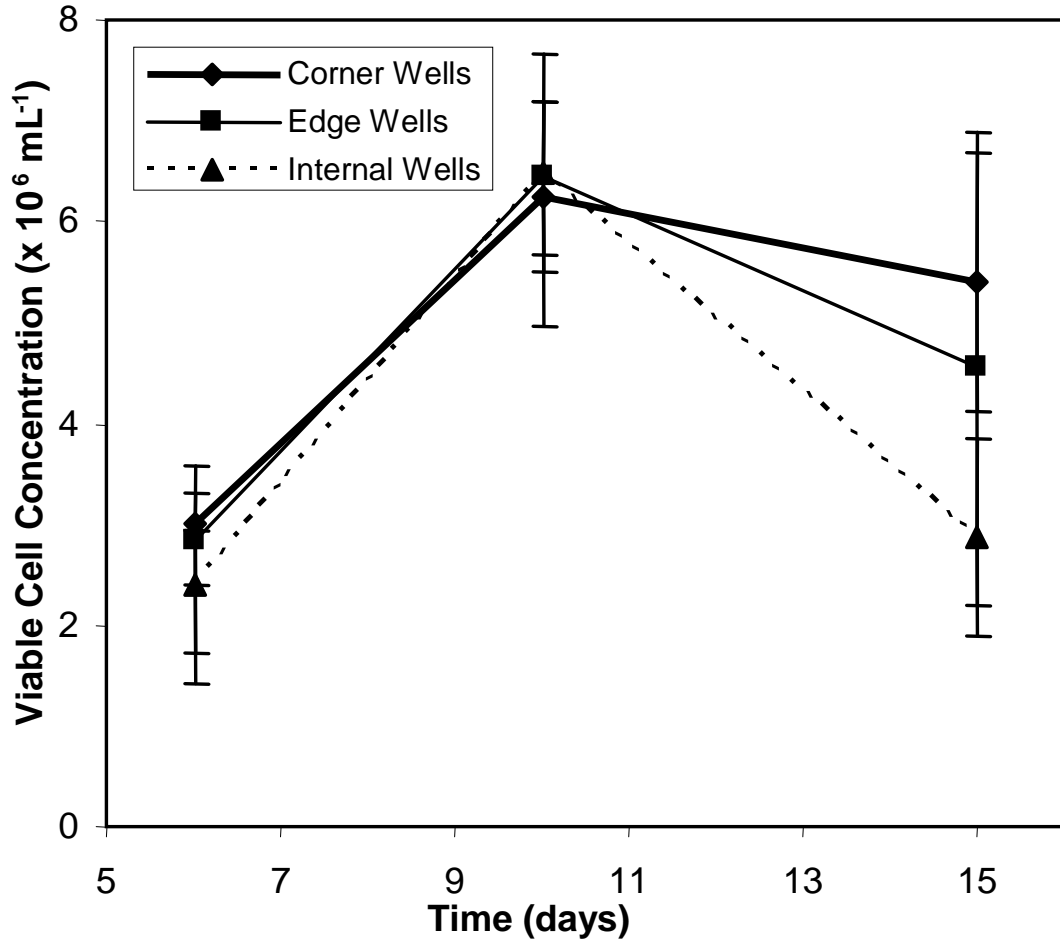


Figure 4.16: Viable cell density of a GS-CHO cell line 6, 10 and 15 days after inoculation, shown for corner, edge and internal wells (as defined in Figure 4.15). Cells were cultivated in 24 SRW plates in CD-CHO medium using a sandwich lid as the sterile seal, as described in Section 2.3.1. Experiments performed in a humidified incubator at 36.5°C with 5% ambient CO₂. Microwells were agitated at 140 rpm on an orbital shaker with a 25 mm orbital shaking diameter. Error bars represent one standard deviation about the mean (n=4 for corner wells, n=12 for edge wells, n=8 for internal wells).

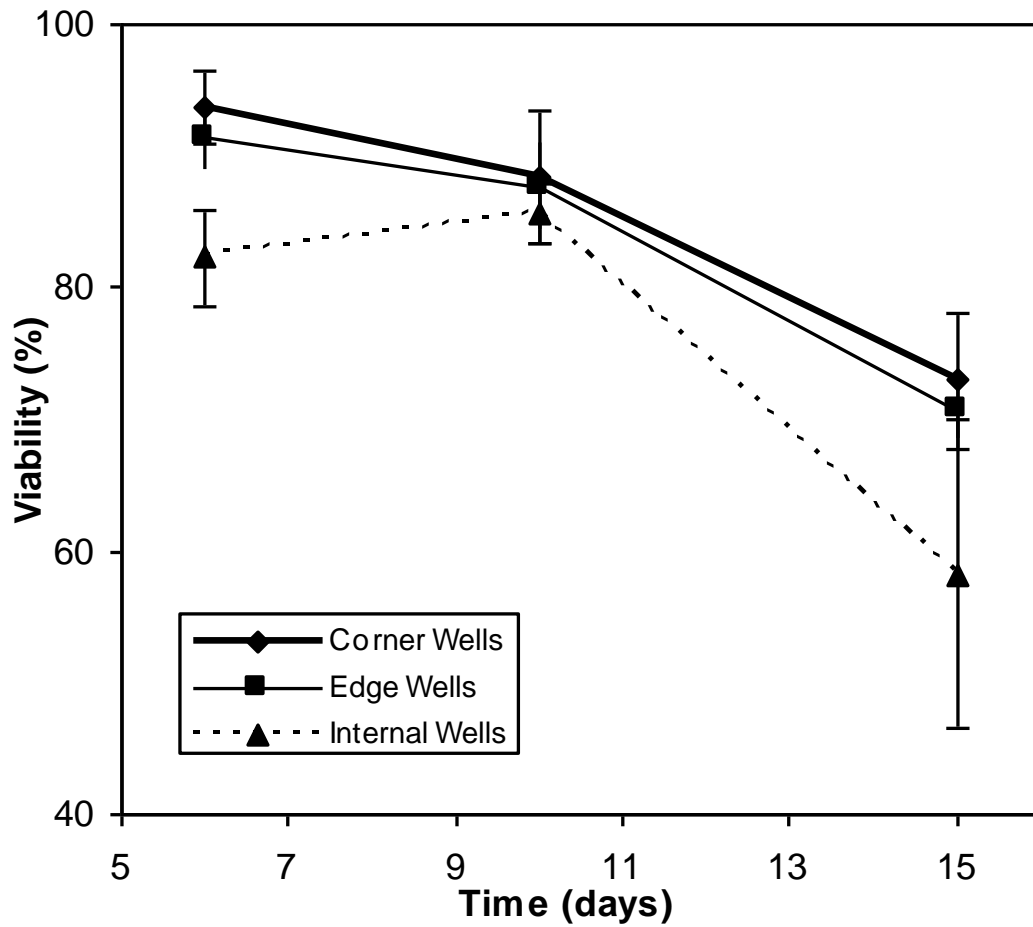


Figure 4.17: Viability of a GS-CHO cell line 6, 10 and 15 days after inoculation, shown for corner, edge and internal wells (as defined in Figure 4.15). Cells were cultivated as described in Section 2.3.1. Error bars represent one standard deviation about the mean (n=4 for corner wells, n=12 for edge wells, n=8 for internal wells).

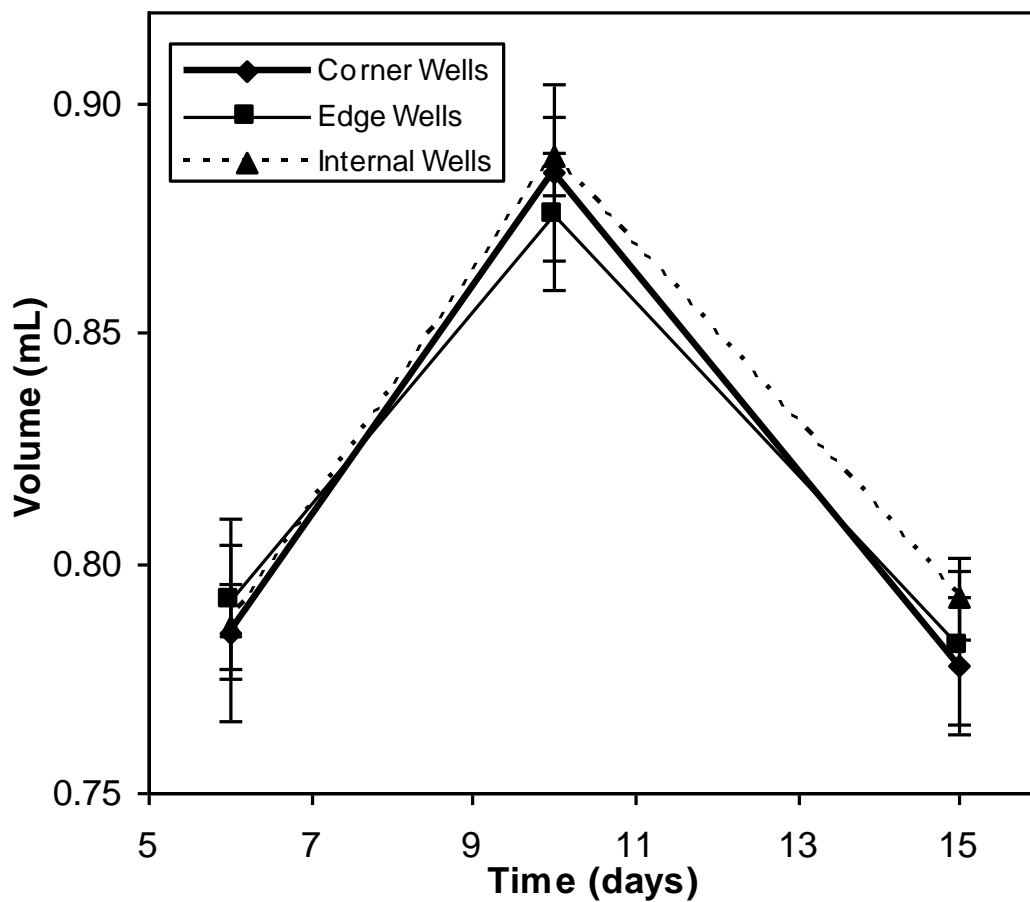


Figure 4.18: Fluid volume per well for a GS-CHO cell line 6, 10 and 15 days after inoculation, shown for corner, edge and internal wells (as defined in Figure 4.15). Cells were cultivated as described in Section 2.3.1. Error bars represent one standard deviation about the mean. (n=4 for corner wells, n=12 for edge wells, n=8 for internal wells)

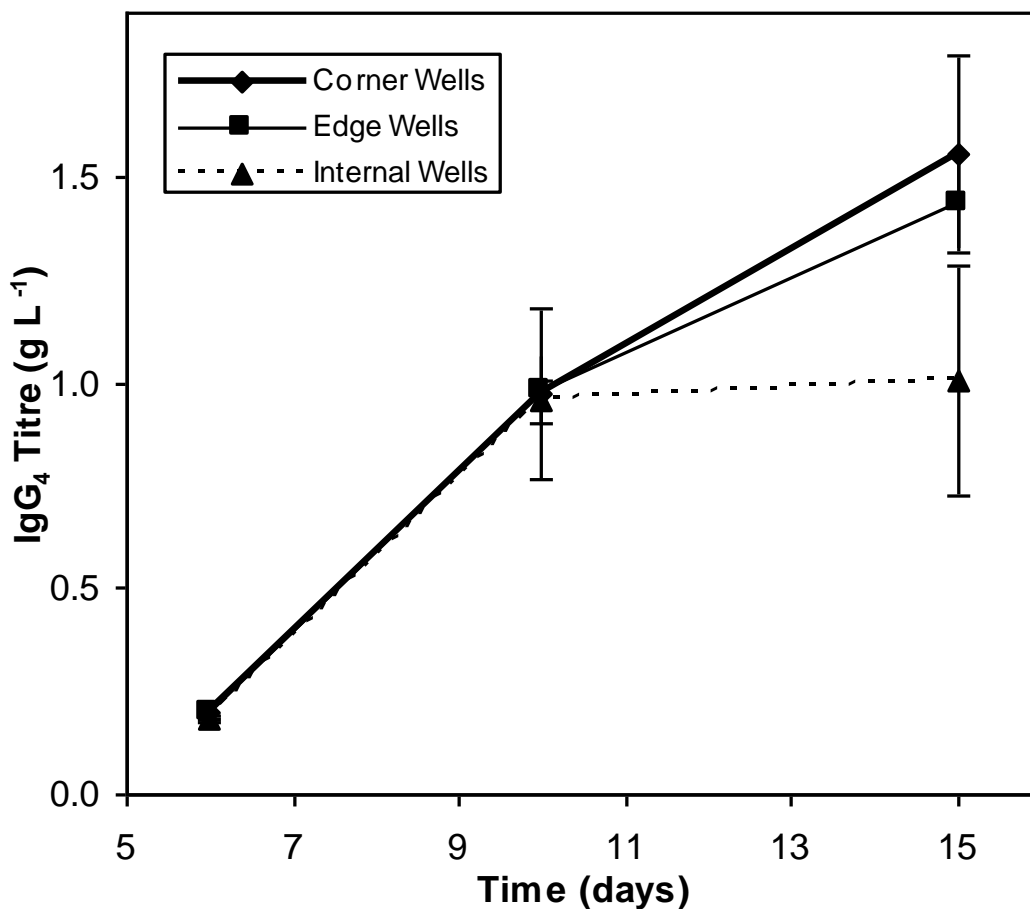


Figure 4.19: IgG product titre for a GS-CHO cell line 6, 10 and 15 days after inoculation, shown for corner, edge and internal wells (as defined in Figure 4.15). Cells were cultivated as described in Section 2.3.1. Error bars represent one standard deviation about the mean. (n=4 for corner wells, n=12 for edge wells, n=8 for internal wells)

It can be seen from these data that differences in evaporation rate are minor throughout the culture period, and that product titre, viability and viable cell density are also closely matched for the first ten days of the cultivation. However, greater differences are seen for the cells harvested on day 15, with titre, viability and viable cell density highest for corner wells, followed by edge and then internal wells respectively.

In the light of the data presented earlier in this chapter, it might have been predicted that the slightly lower volumes present in the corner wells after 15 days of cultivation (Figure 4.18) would result in lower viable cell density and product titre relative to the wells at edge and internal positions, perhaps through a slight effect on osmolality. As such it is perhaps surprising that the opposite pattern was observed, with the highest Day 15 product titre and viable cell density observed in the corner wells. One hypothesis is that the this result is a consequence of a slightly higher temperature for the internal wells, possibly due to heat dissipating into the surroundings from these internal positions less readily than for the edge and corner wells. This temperature increase might then have adversely impacted growth and productivity in the later stages of the cultivation. A temperature mapping experiment to assess each well would be required to verify this.

Perhaps one outcome of this experiment would be to harvest fed cultivations at day 10, since at this point the apparent disparities between well positions are negligible. This would thus ensure that the position of the well would not be a consideration when putting candidate cell lines in rank order, in the event that each well was being used to cultivate a different cell line as part of early stage screening.

4.7 Investigating the impact of a further reduction in microwell evaporation on culture performance

As discussed in Section 4.4, improvements to both cell growth and productivity were achieved through dilution of feed additions to microwells. This approach counteracted the high rate of evaporation from the wells and prevented detrimental increases in the osmolality of the culture media (Figure 4.8). However, it would be of benefit if the rate of evaporation from each well could be decreased still further, preferably matching the rate from the flasks as a proportion of the inoculated volume.

This would be desirable for a number of reasons. Firstly, although feed dilution counteracts osmolality increases in the wells over the five days for which the bolus feeds are added, the total cultivation time is fifteen days such that during the initial four and final six days no water is put back into the system. It is possible that this unchecked evaporation causes the decline of viable cell density in the wells relative to the flasks over the last few days of culture. An additional benefit to matching the proportional evaporation rates in wells and flasks is that it should allow undiluted feeds to be added to the microwells, and would remove the need for weighing of well plates after each sample time. This is currently necessary so that evaporation can be corrected for in viable cell counts and product titre, but would be unnecessary if both water loss (from evaporation) and water additions (from bolus feeding) were proportionally identical for shaken plates and flasks. Removal of a

requirement for weighing plates after sampling would also make automation of the microwell culture process more straightforward.

There are two further approaches that could thus be considered for reduction of the evaporation rate. The first is to increase the relative humidity in the shaken incubator used for cultures, thus decreasing the driving force for diffusion of water from the microwell headspace. The second is to increase the mass transfer resistance of the sterile closure used to seal the plates (Zimmerman et al., 2003). The first option has the disadvantage that raising the humidity level will increase the likelihood that microorganisms will grow on the walls of the incubator, therefore introducing a significant contamination risk. The second option is therefore preferable and was followed in this case.

A modified version of the 'sandwich lid' was thus manufactured by EnzyScreen, featuring an additional layer of metal in which small perforations are made. This metal sheet reduces the rate of gas exchange between the well headspace and the surroundings, and hence also the rate of water loss. This modification was made with an awareness that it limits the rate of oxygen mass transfer into the culture media, but the pO_2 measurements shown in Figure 4.11 suggest that this is unlikely to result in oxygen limitation.

A preliminary evaluation of the impact of the modified lids on evaporation rates (data not shown) found that the rate of water loss was reduced from approximately 24 to 9 $\mu\text{L well}^{-1} \text{ day}^{-1}$, which translates to a

change from 3.0 to 1.1 % (v/v) of the inoculated volume per day using a well fill volume of 800 μL . This is still greater than the 0.6 % (v/v) observed for shake flask cultivations (50 mL inoculum volume) but nevertheless represents a considerable reduction.

The relative performance of cultivations performed with the standard and modified sandwich lids was then evaluated more fully, with both standard and dilute feeds used for both lids, and a fed shake flask for control. The growth and viability profiles measured are shown below in Figures 4.20 and 4.21:

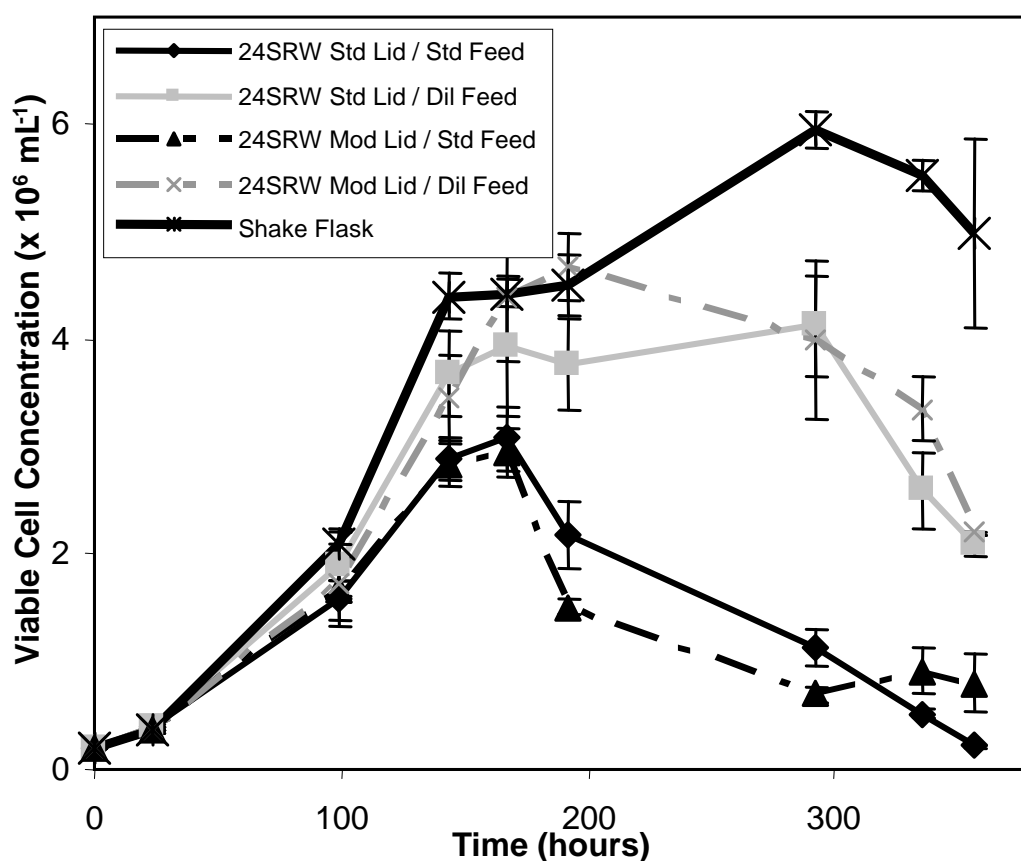


Figure 4.20: Comparison of growth profiles for GS-CHO cells cultivated using standard and modified sandwich lids and standard and diluted bolus

feeds. Cells were cultivated in 24 SRW plates in CD-CHO medium. Experiments performed in a humidified incubator at 36.5°C with 5% ambient CO₂, as described in Section 2.3.1. Microwells were agitated at 140 rpm on an orbital shaker with a 25 mm orbital diameter. Error bars represent one standard deviation about the mean (n=3).

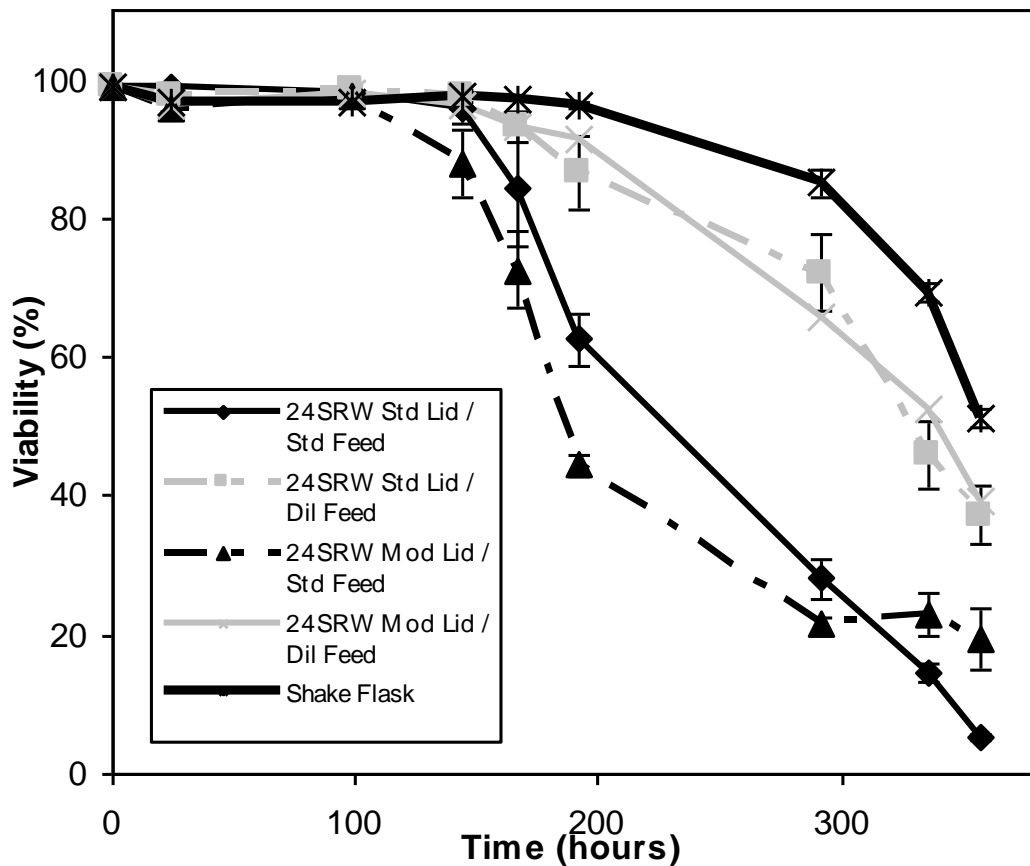


Figure 4.21: Viability profiles for GS-CHO cells cultivated using standard and modified sandwich lids and standard and diluted bolus feeds. Cells were cultivated as described in Section 2.3.1. Error bars represent one standard deviation about the mean (n=3).

Use of the modified sandwich lids does not appear to enhance culture performance. This is particularly surprising for the plates to which standard (non-diluted) feeds were added, as it was expected that the reduced water loss through the new lids would counteract excessive osmolality increases. It

was this increase in osmolality which was thought to have hampered cell growth in the cultivations initially performed for plates sealed with the unmodified lids.

It can be seen from Figure 4.22 that that the osmolality for microwells sealed with modified lids and using standard feeds after 15 days of cultivation is significantly lower than for those sealed with the standard lids (545 mOsm Kg⁻¹ compared to 746). It would thus be expected that the modified lid cultures would perform better than those using the standard lids.

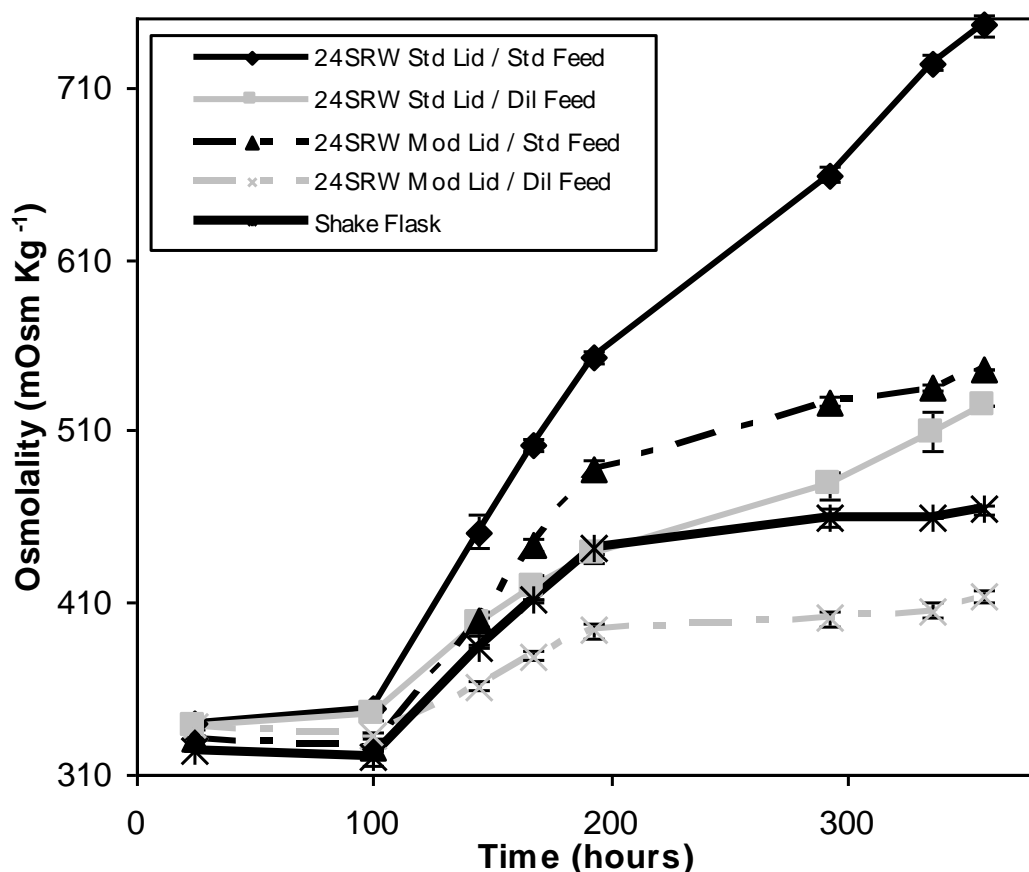


Figure 4.22: Osmolality profiles for GS-CHO cells cultivated using standard and modified sandwich lids and standard and diluted bolus feeds. Cells were cultivated as described in Section 2.3.1. Error bars represent one standard deviation about the mean (n=3).

There are a number of possible reasons as to why the expected performance gains are not observed. Firstly, it is possible that the reduced oxygen mass transfer efficiency that results from a decreased headspace refreshment rate has a negative impact on cell growth. Dissolved oxygen concentrations for selected cultivations measured at-line are shown below in Figure 4.23:

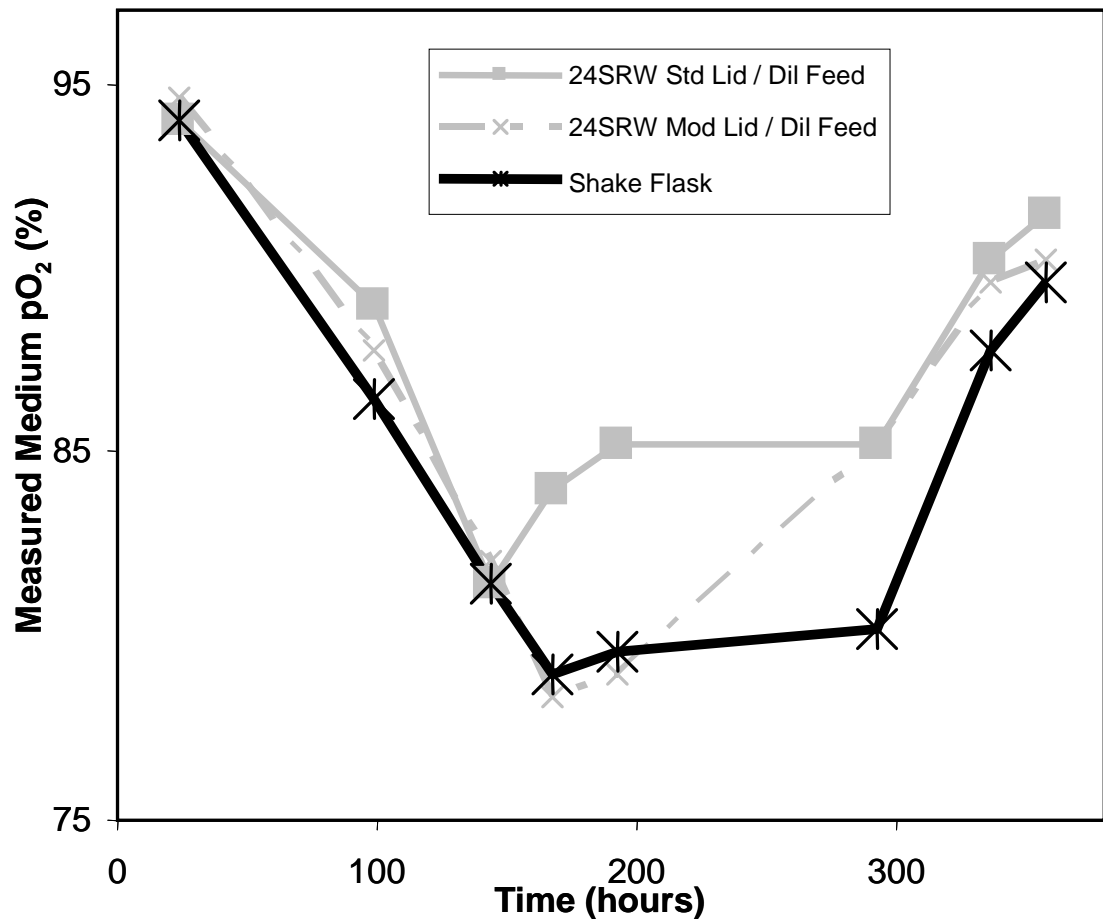


Figure 4.23: Dissolved oxygen profiles for GS-CHO cells cultivated using standard and modified sandwich lids and standard and diluted bolus feeds. Cells were cultivated as described in Figure 2.3.1, with pO_2 measured as described in Section 2.7.5.

It can be seen that the dissolved oxygen concentration does not fall below 75% of its saturation value for any of the cultures shown, such that oxygen limitation is unlikely to be an issue.

Another possibility is that it is the addition of concentrated feeds that is limiting performance. The feed formulation is highly acidic, hence the requirement for addition of bicarbonate to balance this out, and there is an inevitable delay between the addition of feed and base. Flasks are agitated by hand immediately after feed addition to remove any inhomogeneity and prevent a local area of very low pH from forming. However, for the microwell plates this is not feasible, as the narrow diameter of the well renders manual agitation ineffective in promoting the desired homogeneity. As a result, a region of very low pH will be formed, and this will not be alleviated by addition of bicarbonate, as this will also fail to be mixed fully until the plate is returned to the shaker. Consequently the standard sandwich lids were used for the remainder of the microwell cultivations performed.

4.8 Summary

This chapter has demonstrated that similar cell growth and antibody production kinetics can be obtained in parallel fed-batch experiments in 24 SRW plates and shake flasks.

A suitable sterile closure, the 'sandwich lid', was identified that limits evaporation from microwell plates to acceptable levels (Table 4.1), and a feeding strategy established (Figure 4.5) which provided the same antibody titre as in shake flasks (Figure 4.7), with osmolality profiles in the two formats also similar (Figure 4.8).

All other culture parameters monitored in the two formats also remained at similar levels (Figures 4.10 – 4.14 show pH, pO₂, pCO₂ levels and metabolite concentrations, with key culture parameters shown in Table 5.2). As such the aims set for this chapter have been met.

Chapter 5: Bioreactor Engineering Characterisation and Scale Translation

5.1 Introduction and Aim

Until recently there was a fairly limited understanding of the engineering environment in shaken flasks and microwell plates. This hampered their use in optimisation of culture processes and prevented the implementation of rational scale-up to stirred tank bioreactors (Barrett et al., 2010). However, a number of studies (including the work of Doig et al. (2005) and a number of publications from the group of Jochen Büchs) have enhanced our understanding of these small scale systems. It is envisaged that application of these advances to shaken cultures will make them more representative of manufacturing scale conditions and thus far more useful in early stage process development.

The aim of this Chapter is to conduct a thorough engineering characterisation of microwells and other bioreactors under conditions suitable for mammalian cell culture. The objectives were:

- To use appropriate methods to measure the mixing time, k_{LA} and power consumption in shake flasks, shaken microwell plates and stirred tank bioreactor.

- To define a suitable engineering basis for scale translation.

5.2 Oxygen mass transfer coefficient (k_{La})

5.2.1 k_{La} determination in microwells

A number of methodologies have been applied to the measurement of oxygen mass transfer rates in microwells, and calculation of k_{La} values. These include monitoring the growth rate of an obligate aerobe (Duetz et al. (2000)), measurement of sodium sulphite oxidation (Hermann et al. (2003)), catechol oxidation (Ortiz-Ochoa et al. (2005)) as well as the standard dynamic gassing out method (Doig et al. (2005)). Experimental data for a number of round-well geometries shaken at a range of speeds and orbital diameters were correlated by Doig et al. (2005) to enable prediction of k_{La} values. Predicted k_{La} values were found to agree with experimentally determined values to within $\pm 30\%$ over a wide range of conditions (Equation 5.1).

$$k_{La} = 31.35 Da_i Re^{0.68} Sc^{0.36} Fr^x Bo^y \quad [5.1]$$

In the majority of the microwell literature, however, the range of operating conditions over which oxygen transfer was studied were for cultivation of micro-organisms rather than mammalian cells. For example, the

minimum shaking speed used in the development of Equation 5.1 was 200 rpm, while the speeds used for cultivation of CHO-S (Chapter 3) and GS-CHO (Chapter 4) cell lines here were typically 180 and 140 rpm respectively. Predictions made by this correlation for mammalian cell culture thus need to be refined experimentally. The reasons for using slower shaking speeds for mammalian cells are: (i) perceived shear sensitivity of cells at higher agitation and energy dissipation rates (Yang et al. 2007), and (ii) lower oxygen uptake requirements of mammalian cells (Nienow, 2006).

Consequently k_{LA} values were measured in this work under relevant cell culture conditions. These were determined by a variety of methods including catechol oxidation (Section 2.9.1) and dynamic gassing out (Section 2.9.2).

Data obtained are summarized in Table 5.1 and Figure 5.1:

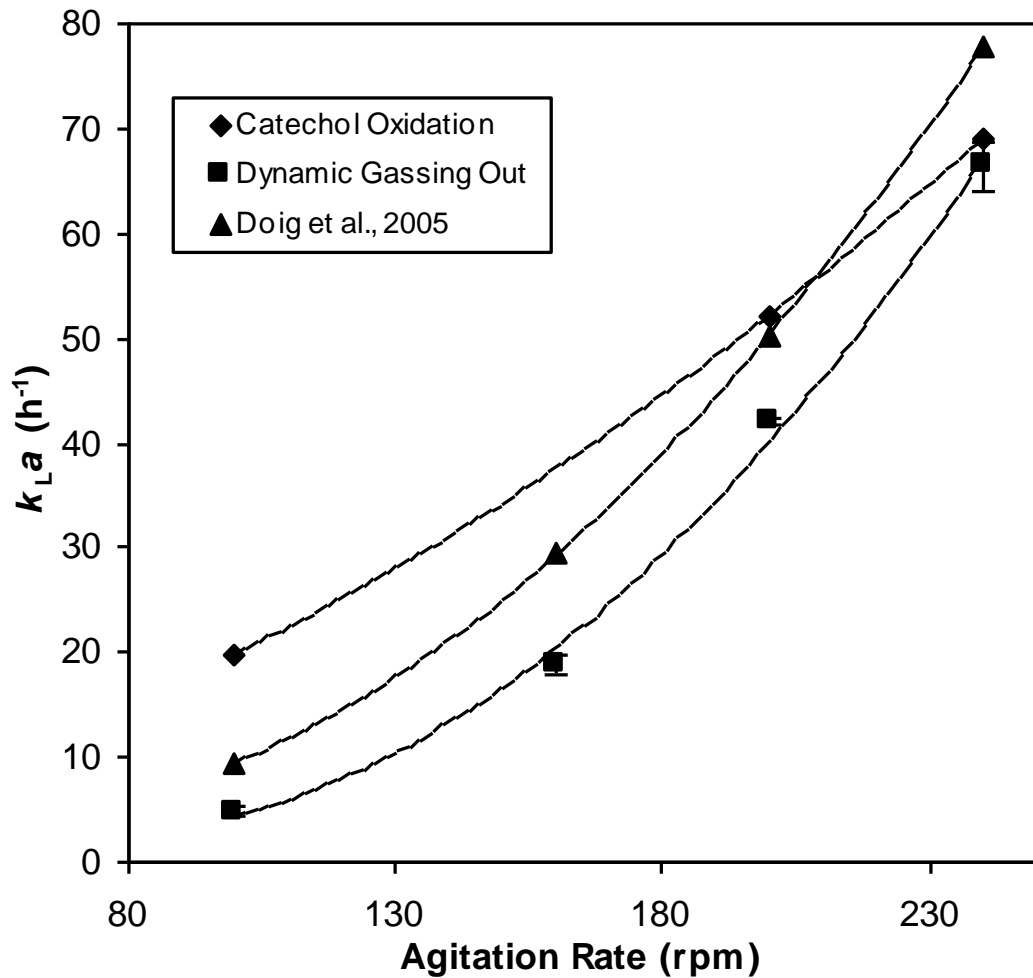


Figure 5.1: Experimental and predicted microwell k_{La} values under mammalian cell culture conditions. Values obtained for a 24SRW, $V_L = 0.8$ mL, $D_O = 20$ mM at a range of shaking frequencies. k_{La} values measured by catechol oxidation or dynamic gassing out as described in Sections 2.9.1 and 2.9.2 respectively. Predicted values were obtained using Equation 3.1. Error bars for dynamic gassing out data represent one standard deviation about the mean ($n=3$).

Table 5.1: Summary of measured and predicted k_{La} values over a range of culture conditions. Values determined as described in Figure 5.1.

Method	Well Geometry	Covered Well	Shaking Frequency (rpm)	Fill Volume (mL)	Measured k_{La} Value (h^{-1})	Doig Correlation k_{La} (h^{-1})	Variation of Predicted & Experimental Values
Gassing Out	24 SRW	N	100	0.8	4.8 ± 0.41	/	/
Gassing Out	24 SRW	Yes	100	0.8	6.2 ± 0.42	/	/
Gassing Out	24 SRW	N	100	1.5	2.8 ± 0.20	/	/
Gassing Out	24 SRW	N	160	0.5	36.4 ± 1.15	/	/
Gassing Out	24 SRW	N	160	0.8	18.8 ± 0.92	/	/
Gassing Out	24 SRW	N	200	0.8	42.0 ± 0.38	50.2	+19%
Gassing Out	24 SRW	Yes	200	0.8	44.5	50.2	+13%
Gassing Out	24 SRW	N	200	1.5	18.6 ± 1.00	26.8	+44%
Gassing Out	24 SRW	N	240	0.8	66.4 ± 2.37	77.8	+17%
Catechol	24 SRW	N	100	0.8	19.8	/	/
Catechol	24 SRW	N	100	1.5	14.4	/	/
Catechol	24 SRW	N	180	2.0	18.7	15.6	-17%
Catechol	24 DSW	N	180	2.0	25.2	/	/
Catechol	24 SRW	N	200	1.5	30.6	26.8	-12%
Catechol	24 SRW	N	200	0.8	52.2	50.2	-4%
Catechol	24 DSW	N	240	0.8	66.2	/	/
Catechol	24 SRW	N	240	0.8	69.1	77.8	+13%

In terms of the measured and predicted values, reasonable agreement was observed between k_{LA} values predicted using Equation 5.1 and those experimentally determined by catechol oxidation, for shaker speeds of 180 rpm or greater. The average difference was only $\pm 11.2\%$, well within the error quoted by Doig et al. (2005). For lower speeds the correlation appears to underestimate k_{LA} , probably because it was derived from data for which the minimum shaker speed used was 200 rpm. These data therefore appear to confirm the applicability of catechol oxidation to determining k_{LA} in small scale systems (Ortiz-Ochoa et al.). All results obtained are well in excess of 1h^{-1} , the value quoted in the literature as sufficient to support cell densities of $1 \times 10^7 \text{ mL}^{-1}$ (Nienow et al., 2006).

These k_{LA} data are directly related to the culture data obtained in Chapter 3 using CHO-S cells, as the shaker used had the same D_o (20 mM) as used for k_{LA} determination. For the fed batch GS-CHO cultures described in Chapter 4 a different shaker was used ($D_o = 25 \text{ mM}$) in order to align with conditions routinely used at MedImmune. The higher D_o is likely to lead to improved mixing and oxygen transfer (Duetz, 2007). However, since it appears that k_{LA} values are sufficient that oxygen transfer will not be rate limiting it was decided not to repeat k_{LA} measurements at a D_o of 25 mM.

k_{LA} values determined by dynamic gassing out are consistently lower than those from catechol oxidation (Figure 5.1). This is most likely a consequence of the position of the oxygen sensing patch at the base of the

microwell, as indicated in Figure 5.2, which was positioned to provide the worst case scenario for oxygen transfer. If the system is well mixed the time taken for oxygen to reach the sensor following entry at the gas-liquid interface should be negligible. However, as shown in Section 5.4.2, mixing times for the 24 SRW system are relatively high under the conditions tested. For $V_L = 0.8$ mL in a 24 SRW microwell, shaken at 140 rpm with an orbital diameter of 20 mm, mixing time is approximately 1,559s, falling to around 105s and 36s at 200 and 220 rpm respectively. The influence of such mixing effects on oxygen transfer measurements have previously been noted by Doig et al. (2005). As a result of these effects it would seem that the catechol oxidation method is best suited for quantification of the average k_{LA} values in microwells.

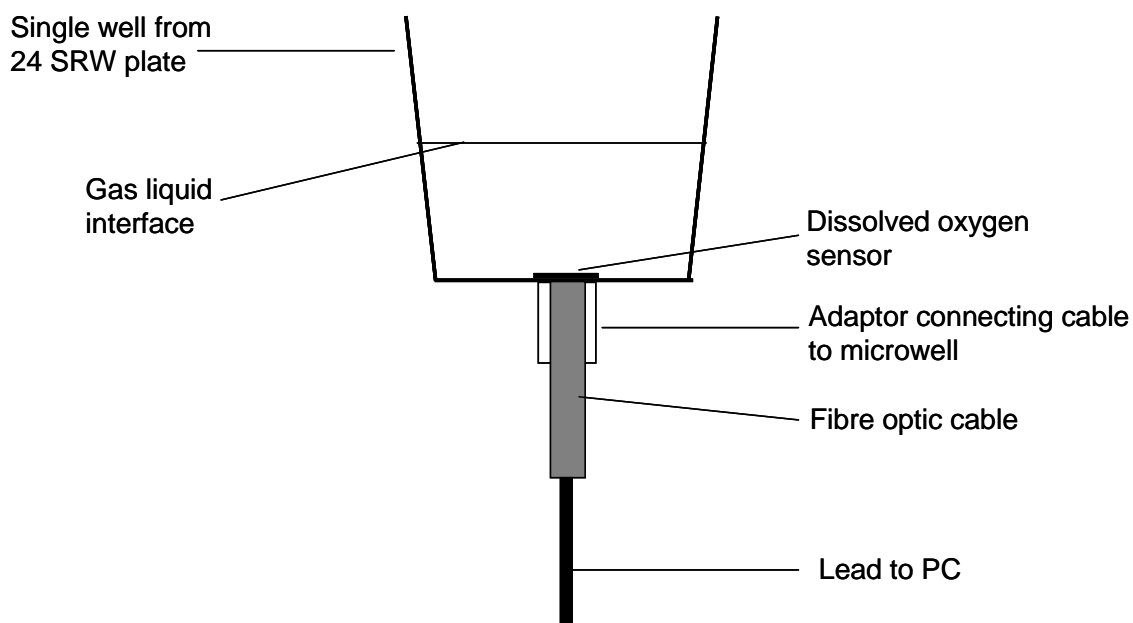


Figure 5.2: Experimental set-up for determination of microwell k_{LA} by dynamic gassing out using the PreSens system. Experiments performed as described in Section 2.9.2.

Further k_{LA} measurements were performed using the dynamic gassing out method to determine the additional resistance to oxygen transfer provided by the Breatheasy membrane (Zimmerman et al., 2003). As shown in Table 5.1 the membrane did not significantly alter the measured k_{LA} value for either 100 or 200 rpm shaker speeds.

k_{LA} measurements were also performed for 24 SRW and 24 DSW formats with matched fill volumes and under identical shaking conditions, using the catechol oxidation method. For $V_L = 2.0$ mL fill volume at 180 rpm, the k_{LA} was found to be 35% higher in the square geometry, while for $V_L = 0.8$ mL at 240 rpm there was only a 4% difference between the two k_{LA} values. The benefits of square wells in terms of mixing and oxygen mass transfer have been commented on by Hermann et al., 2003 and by Barrett et al., 2010. The absence of a significant effect for a 0.8 mL volume can be explained by examining the well geometry, which has a square upper section but a pyramidal base. For a 2.0 mL volume at least half of the liquid is within the square portion, and thus benefits from the 'baffling' effect noted by Hermann, whereas the majority of a 0.8 mL liquid sample is within the pyramidal section (as described for cell culture in 24 DSW plates in Section 3.8.2. Microwell geometries are shown in Figure 2.1).

5.2.2 k_{La} determination in stirred tank bioreactors

As a basis for later scale translation studies (Chapter 6) k_{La} values were also determined for a 5L stirred tank over a range of airflow rates and specific power inputs. These were performed using the dynamic gassing out method as described in Section 2.9.4 and the values calculated are shown in Table 5.1.

These data were compared to the van't Riet correlation (van't Riet, 1979):

$$k_{La} = K \left(\frac{P_g}{V} \right)^\alpha V_s^\beta \quad [5.2]$$

Table 5.2: Measured and predicted k_{La} values for a 5L stirred tank bioreactor. Dynamic gassing out experiments were performed in triplicate using 3.5L of CD-CHO culture medium as described in Section 2.9.4.

Stirrer Speed (rpm)	Airflow Rate (mL min ⁻¹)	k_{La} (h ⁻¹) Measured	k_{La} (h ⁻¹) Predicted
150	100	2.3 ± 0.17	2.1
	200	2.8 ± 0.02	2.7
	300	3.5 ± 0.17	3.1
250	100	4.2 ± 0.15	5.2
	200	5.5 ± 0.16	6.8
	300	6.5 ± 0.14	7.9
350	100	12.0 ± 0.48	9.7
	200	13.3 ± 0.40	12.5
	300	17.7 ± 1.24	14.5

As for the microwell k_{LAS} all values are greater than the benchmark of $1h^{-1}$, claimed to be sufficient to support a viable cell density of 1×10^7 cells mL^{-1} , and it should also be noted that the k_{LA} values determined for stirred tanks are significantly lower than those for the 24 SRW system in general.

The data obtained were fitted to the Van't Riet correlation using the data shown in Figures 5.3 and 5.4 (Van't Riet, 1979):

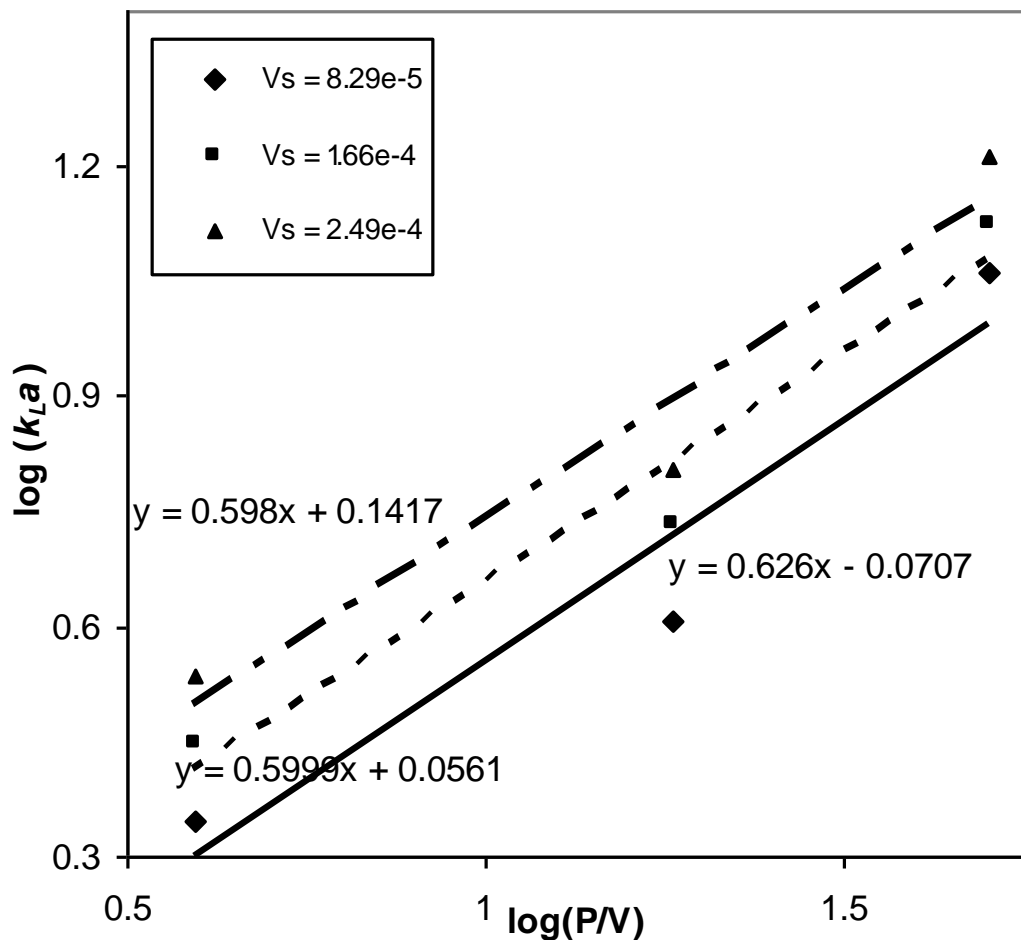


Figure 5.3: Plot of Log (P/V) against Log (k_{La}), where P/V and k_{La} are mean energy dissipation and the oxygen mass transfer coefficient respectively, at three difference values of superficial gas velocity (V_s). Experiments performed by dynamic gassing out as described in Section 2.9.4.

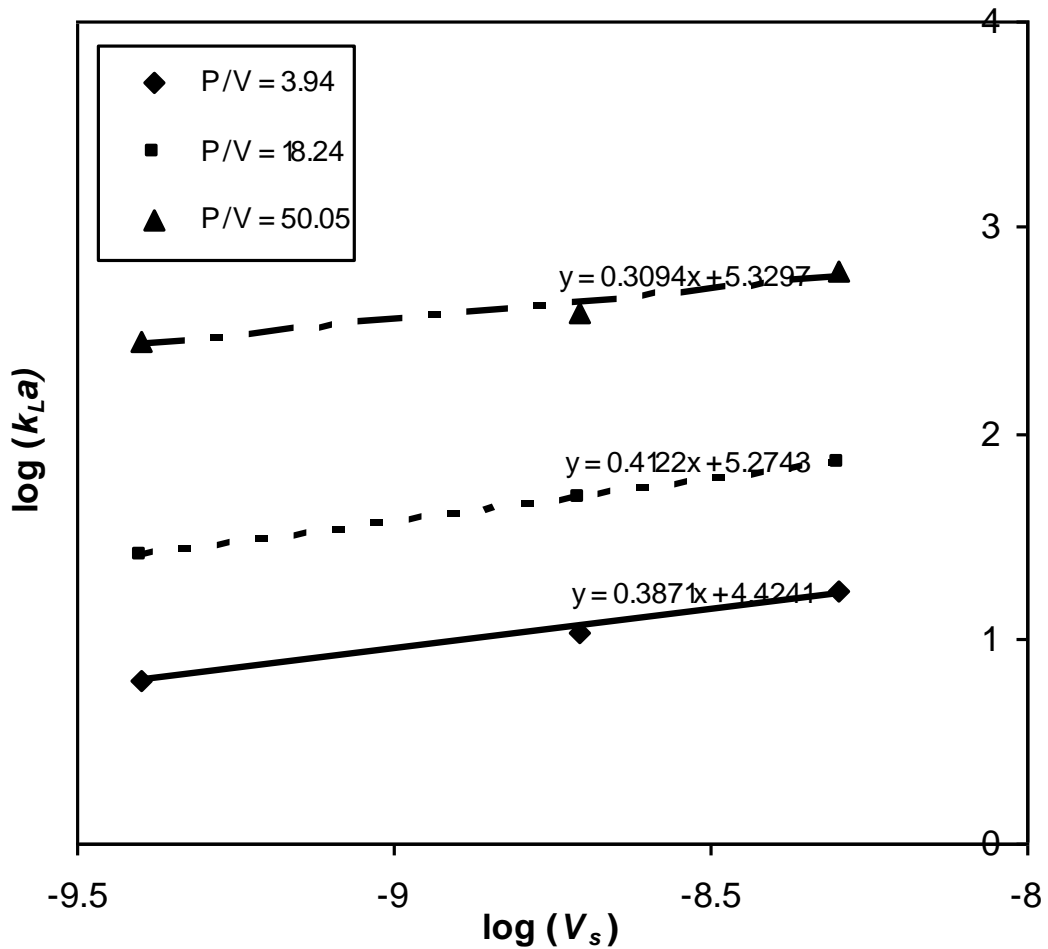


Figure 5.4: Plot of $\log(V_s)$ against $\log(k_{La})$, where V_s and k_{La} are superficial gas velocity and the oxygen mass transfer coefficient respectively, at three different values of mean energy dissipation (P/V). Experiments performed by dynamic gassing out as described in Section 2.9.4.

The exponents α and β in Equation 5.2 were calculated by taking the mean values of the gradients of the plots in Figures 5.3 and 5.4 respectively, and the value of K was calculated as described in Van't Riet, 1979, giving Equation 5.3 below:

$$k_L a = 28.8 \left(\frac{P_g}{V} \right)^{0.61} V_s^{0.37} \quad [5.3]$$

Where power dissipation was determined using the impeller number as experimentally determined using an air bearing (see Section 2.10.2), and superficial gas velocity (V_s) was calculated by division of the volumetric air flow rate by the cross-sectional area of the stirred tank.

5.2.3 Determination of Cell Specific Oxygen Uptake Rate (OUR)

The PreSens oxygen system was used to determine the oxygen uptake rate of the CHO-S cell line as described in Section 2.11. In summary, 1 mL of CHO-S culture was pipetted into a single well of a 24 SRW plate in which a dissolved oxygen (DO) sensing patch had been fixed to the base. The well was immediately sealed with gas impermeable tape and the rate at which the DO declined over time was measured, as shown in Figure 5.5:

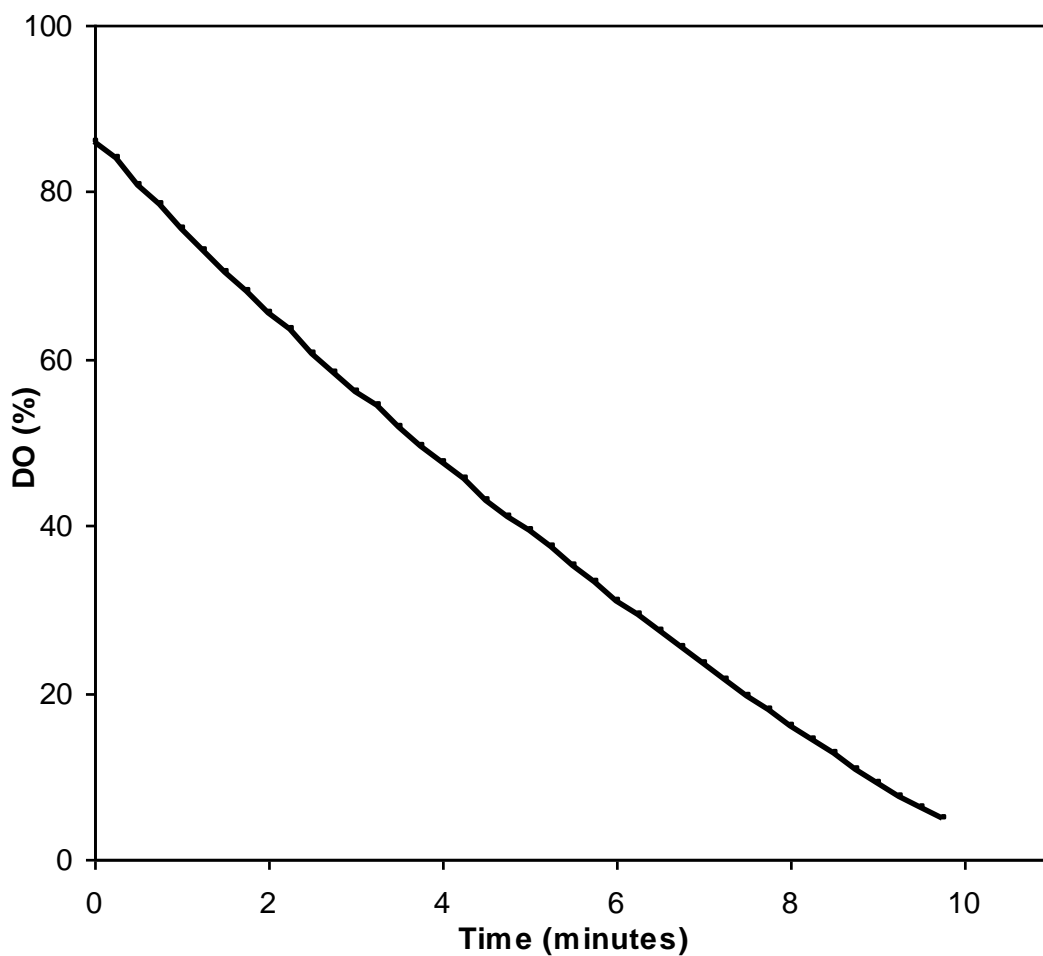


Figure 5.5: Change in dissolved oxygen tension over time in a sealed microwell containing 1 mL of CHO-S culture in CD-CHO medium. PreSens system used for oxygen measurement as described in Section 2.9.2.

The viable cell density in the culture medium was 2.76×10^6 cells mL⁻¹, allowing the oxygen uptake rate to be determined as described in Appendix II.3.

The mean OUR for two microwells was calculated as 4.07×10^{-13} mol O₂ cell⁻¹ h⁻¹. This is slightly outside the range of 1.8 and 3.2×10^{-13} mol O₂ cell⁻¹ h⁻¹ found by Deshpande et al. (2004) and greater than the maximum value reported by Nienow et al. (1996) of 3.6×10^{-13} mol O₂ cell⁻¹ h⁻¹.

5.2.4 Comparison of OUR with OTR in Shaken Microwells

Determination of the cell specific OUR described in Section 5.2.3 enables comparison with the oxygen mass transfer rate in microwells based on the k_{La} values measured in Section 5.2.1.

For the data described in Chapter 4, a sandwich lid system was used to seal the microwell plates. According to the manufacturer's website, a bacterial culture with an oxygen uptake rate of $40 \text{ mmol O}_2 \text{ L}^{-1} \text{ h}^{-1}$ will result in a reduction of the headspace mole fraction of oxygen to a minimum of 18% (v/v), from a saturation value of 21%.

The OUR for the CHO-S culture was found here to be $4.07 \times 10^{-13} \text{ mol O}_2 \text{ cell}^{-1} \text{ h}^{-1}$, which corresponds to $4.07 \text{ mmol O}_2 \text{ L}^{-1} \text{ h}^{-1}$. Clearly this is ten-fold lower than the value for a microbial cultivation, and so it is unlikely that the headspace mole fraction of oxygen would fall significantly below the saturation level. For the CO₂ incubators used in this study the mole fraction of O₂ would be:

$$0.95 * 0.21 = 0.20$$

due to the use of 5% CO₂ in the incubator.

The equation for oxygen transfer rate is given below:

$$\text{OTR} = k_{La} (C^* - C_L) \quad [5.4]$$

Therefore use of corrected k_{La} values to account for additional mass transfer resistance imposed by the sterile enclosure appears to be unnecessary, as the rate at which oxygen is supplied (OTR) greatly exceeds the oxygen requirements of the cells (OUR) such that the headspace mole fraction of oxygen will not fall significantly below the saturation value of 0.20. The lack of a requirement for a correction factor in determining microwell k_{La} values supports the conclusions drawn in Section 5.2.1 above.

Since the measured evaporation rate through the Breatheasy membrane used to seal the CHO-S cultivations (described in Section 3.3) is approximately double that which occurs through the sandwich lids (Section 4.2), and since there is generally a strong positive correlation between permeability of such membranes to water vapour and oxygen (Zimmerman et al. 2003), the assumption can be made that the Breatheasy membrane will also support an adequate refreshment rate of air into the microwell headspace.

It therefore appears that any constraints in oxygen supply to the cells will not be a result of mass transfer limitations imposed by either (i) the sterile closure or (ii) transfer of oxygen into the liquid at the gas-liquid interface (as supported by the k_{La} values described above), but instead may result from poor mixing reducing the rate at which dissolved oxygen can be dispersed throughout the well, and in particular to the base (as indicated by the PreSens

experiments at low shaking speeds). Further investigation of this effect can be found in Section 6.5.

5.3 Mean energy dissipation rate

5.3.1 Determination of mean energy dissipation

Matched mean energy dissipation (P/V , $W m^{-3}$) is commonly used when scaling up microbial fermentations, as maintenance of this parameter at the same point helps to ensure that efficient mixing and mass transfer are obtained (Geisler et al., 1993). However, as a result of concerns regarding the impact of shear forces on mammalian cells (Van der Pol et al., 1998), a limit is sometimes imposed on impeller tip speed in cell culture (Aloi et al., 1996) although more recently a consensus appears to have been reached that fears regarding shear sensitivity were greatly over-stated (Nienow, 2006).

For microwell systems under cell culture conditions, Zhang et al. (2008) have already described the use of computational fluid dynamics for estimation of mean energy dissipation rates in shaken 24 well plates. For shaken flasks Büchs et al. (2000) have developed a correlation to allow these values to be determined as a function of fluid properties and shaking conditions:

$$\frac{P}{V_L} = Ne' \rho \frac{n^3 d^4}{V_L^{2/3}} \quad [5.5]$$

For the stirred tank system mean energy dissipation was determined using Equation 5.6:

$$P = N_p \rho N^3 d_i^5 \quad [5.6]$$

Use of Equation 5.6 required empirical determination of the impeller power number as described in Section 5.3.2.

5.3.2 Experimental Results for Determination of Stirred Tank Power Number Using an Air Bearing

The power number results obtained using the air bearing (Section 2.10.3) are shown in Table 5.3:

Table 5.3: Values of the impeller power number N_p calculated at various impeller rotational speeds as described in Section 2.10.3.

N_i (s ⁻¹)	Re	N_p
2.5	9,738	0.88
3.4	13,070	1.08
4.1	15,889	1.03
5.1	19,476	0.99
5.9	22,744	0.85

The mean power number obtained was 0.97 with a relative standard deviation of 0.9%. The method used is described in Section 2.10.3.

5.3.3 Shake Flask Predictions

The correlation developed by Büchs et al. (2000) can be used to estimate the mean energy dissipation into the fluid within a shaken flask. Table 5.4 below gives some relevant values derived using equation [5.5] above for 250 mL Erlenmeyer flasks:

Table 5.4: Mean energy dissipation for a 250 mL Erlenmeyer flask estimated using Equation [5.5].

Fill Volume (mL)	Shaker Speed (rpm)	Mean Energy Dissipation ($W m^{-3}$)
100	120	39
50	140	96
50	220	341
50	300	812

Use of a 100 mL fluid volume at 120 rpm and 50 mL at 140 rpm correspond to the shake flask experiments performed in Chapters 3 and 4, with CHO-S and GS-CHO cell lines respectively.

5.4 Liquid Phase Mixing Time, t_m

5.4.1 Visualisation of Bioreactor Fluid Flow and Mixing

Use of a high speed video camera allowed visualisation of the fluid flow in shaken 24 SRW plates, as described in Section 2.8.1. Similar work was carried out by Barrett et al. (Barrett et al., 2009) However, since the orbital shaking diameter used for cultivation of GS-CHO in this study was higher

than that used for hybridoma cultivation (at 25 and 20 mm respectively), it was useful to repeat the work for the new shaking conditions.

In all mixing studies the fill volume within the 24 SRW well was 0.8 mL corresponding to the volume used for culture (Section 2.3.1). Video footage of the fluid, to which a small quantity of green food colouring was added to aid observation, was analysed frame by frame to observe the maximum angle obtained from deformation of the liquid surface. In addition, the rate at which the dye was dispersed throughout the bulk liquid at each shaking speed gave an indication of the speeds at which the well contents could be said to be 'well mixed.' Broadly speaking, the system is well-mixed when the time taken for complete mixing is less than the time constants for key cellular processes.

Figure 5.6 shows the maximum angle obtained by 0.8 mL of water shaken with an orbital diameter of 25 mm at speeds of 140, 200, 250 and 300 rpm respectively (clockwise from top left).

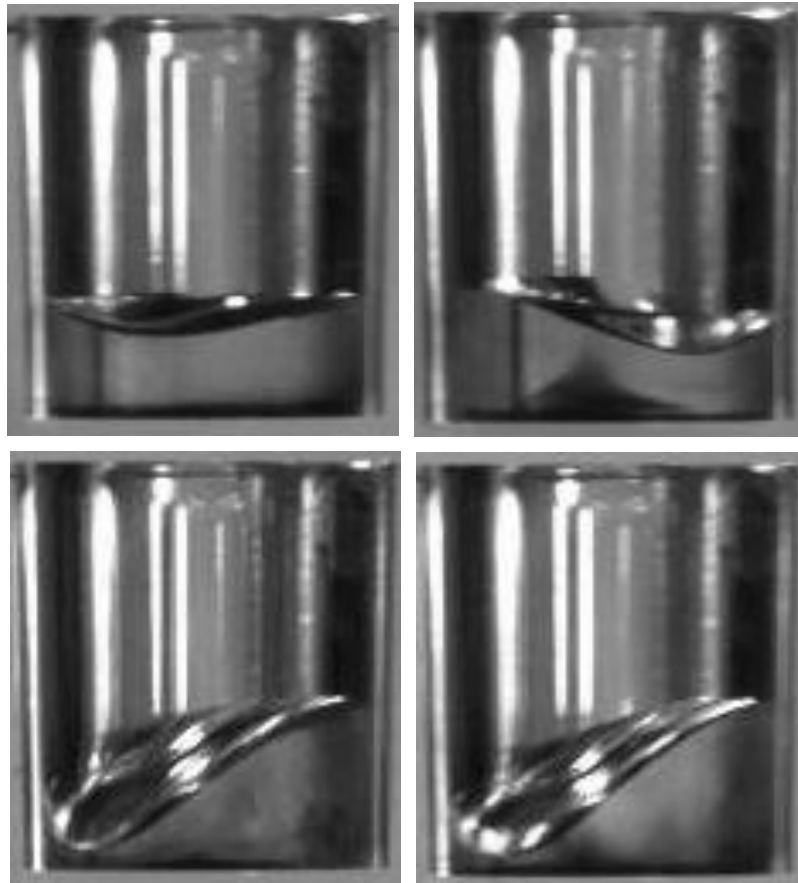


Figure 5.6 Fluid hydrodynamics in 24-SRW plates at shaking speeds of 140, 200, 250 and 300 rpm (clockwise from top left). Images selected to show surface deformation of the liquid within the microwell at each shaking speed. Experimental conditions: $V_L = 800 \mu\text{L}$, $d_s = 25\text{mm}$. Video camera operated as described in Section 2.8.1.

At 140 rpm it can be seen that the angle formed by the deformed liquid surface is very shallow, while there is a significant increase in the angle at 200 rpm. At 250 rpm the angle has reached its maximum such that the deformation now extends to the microwell base, and there is little discernible change at 300 rpm.

These qualitative data thus indicate that significant improvements to liquid mixing may be achieved by raising the shaking speed from the 140 rpm initially selected for fed-batch GS-CHO cultivation in 24 well plates. In order

to quantify this, the liquid mixing times for various conditions were determined.

5.4.2 Quantification of Liquid Phase Mixing Times

Adequate liquid mixing is essential for successful cell culture (Wayte et al., 1997). A minimum level of mixing is required simply to ensure complete suspension of cells in the medium, and beyond this to ensure homogeneous conditions are present to allow optimal growth, avoiding potentially harmful nutrient, pH, dissolved oxygen or carbon dioxide gradients (Hadjiev et al., 2005).

The iodine decolourisation method (Bujalski et al., 1999) was used to determine mixing times for 24 well, shaken flask and stirred tank bioreactors as described in Section 2.8.2. The results are summarized here in Figures 5.7 – 5.9:

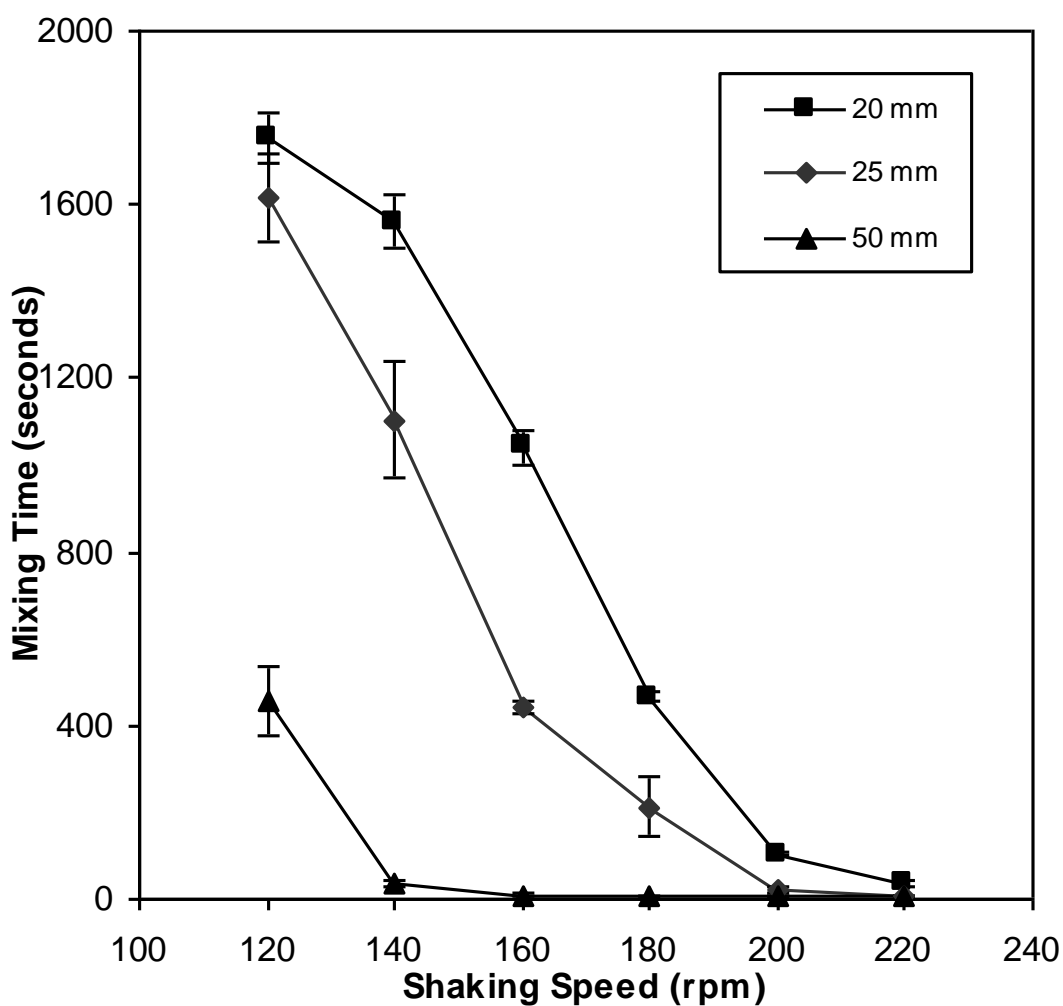


Figure 5.7: Measured liquid phase mixing times for an orbitally shaken 24 SRW plate based on iodine decolourisation measurements. Experiments performed as described in Section 2.8.2 with $V_L = 800 \mu\text{L}$, $d_s = 20 - 50 \text{ mm}$. Error bars represent one standard deviation about the mean ($n = 3$).

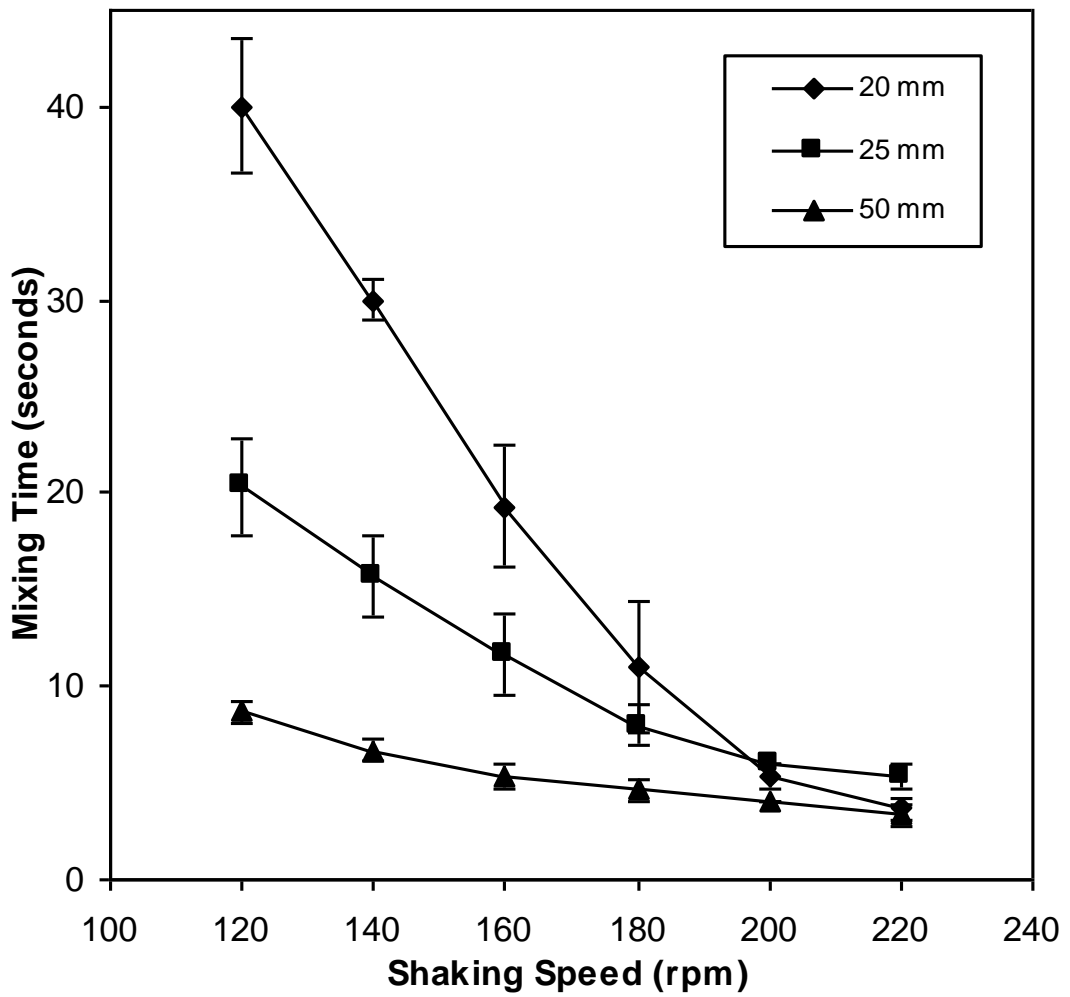


Figure 5.8: Measured liquid phase mixing times for an orbitally shaken 250 mL shake flask based on iodine decolourisation measurements. Experiments performed as described in Section 2.8.2 with $V_L = 50$ mL, $d_s = 20 - 50$ mm. Error bars represent one standard deviation about the mean ($n = 3$).

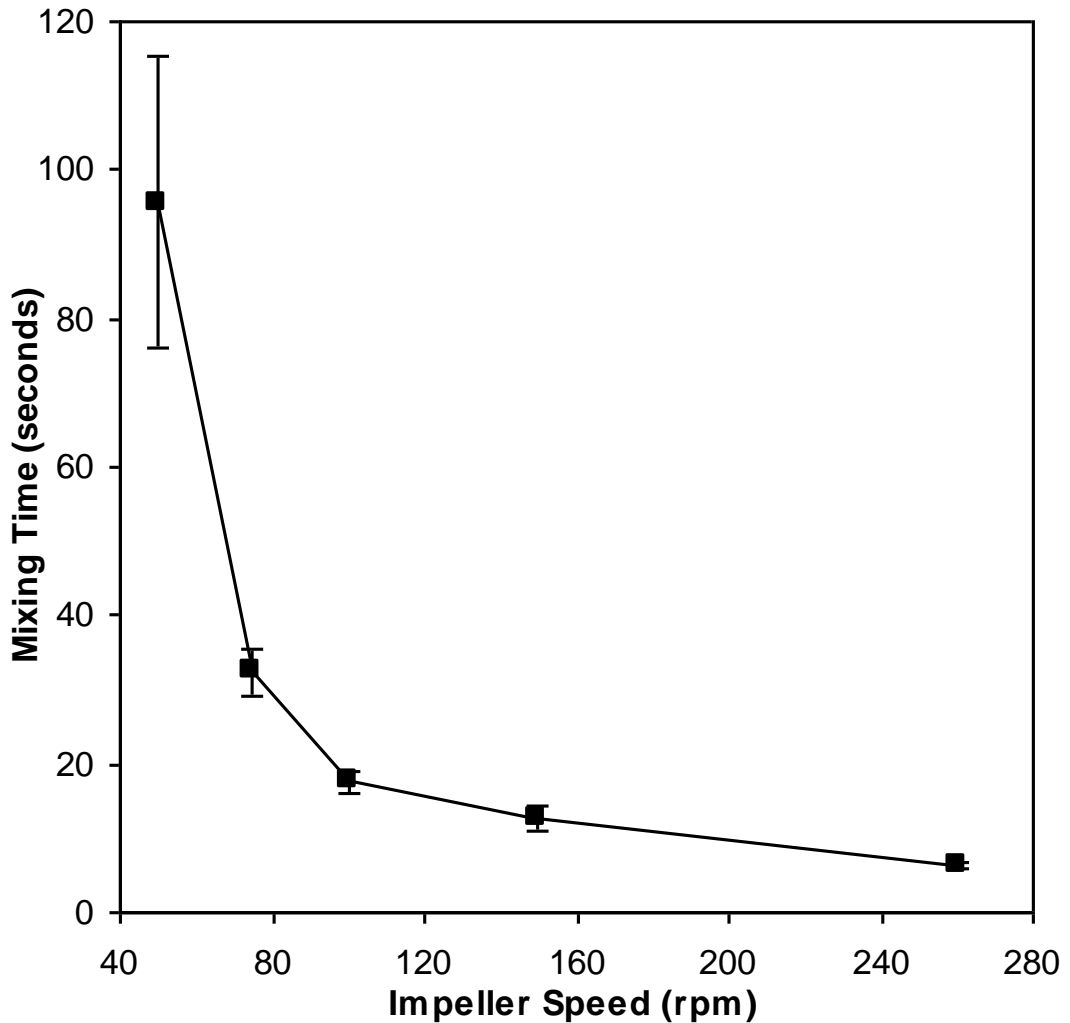


Figure 5.9: Measured liquid phase mixing times for a 5L stirred tank bioreactor based on iodine decolourisation measurements. Experiments performed as described in Section 2.8.2 with $V_L = 3.5$. Bioreactor geometry as described in Section 2.4. Error bars represent one standard deviation about the mean ($n = 3$).

It can be seen in Figure 5.7 that the greatest range of mixing times is observed for the shaken 24 SRW plate. For orbital shaking diameters of 20 or 25 mm, shaking speeds lower than 180 rpm result in mixing times in excess of 400 seconds, whilst the t_m values obtained for shake flask and stirred tank systems were less than 100 seconds for all conditions tested. Such poor mixing for shaken 24 SRW plates is not reported in the literature. For example the

work of Duetz (2007) suggests that surface tension effects should only impart a significant effect on liquid mixing for microwell geometries in which the well diameter is less than 8 mm, while a single well of a 24 SRW plate has a diameter of ≈ 15 mm. This work therefore highlights that, in order to obtain mixing times in 24 SRW plates that are comparable to those in shake flask and stirred tank systems, shaking speeds in excess of the 120 and 140 rpm used for the CHO-S and GS-CHO culture work respectively are required.

It can also be seen that the shaker speed for which mixing time in a 24 SRW plate agitated with a 20 mm orbital shaking diameter drops significantly is approximately 200 rpm, which corresponds to the speed above which k_{LA} values measured by the PreSens system and those empirically determined by catechol oxidation agree more closely (Section 5.2.1). This would support the hypothesis made above that the comparatively lower values measured by PreSens at slower speeds result from the necessity for oxygen to reach the sensing patch at the base of the well by diffusion in the event that the fluid is not well mixed.

It follows, therefore, that use of a higher shaking speed for cultivations would have the dual benefits of (i) increasing homogeneity and thus minimising the risk of nutrient gradients and (ii) reducing the likelihood of oxygen limitation at the base of the microwell.

5.5 Selection of a Scale Translation Parameter for Mammalian Cell Culture

Reproduction of cell culture performance between small scale shaken bioreactors and currently established STR scale-down models of production scale vessels requires identification of a suitable basis for scale translation (Li et al., 2006). This must apply across different scales, for different mechanisms of energy input, i.e. shaken or stirred, and for different mechanisms of oxygen transfer, i.e. surface aeration or a dispersed gas phase. Fundamental to culture performance is the engineering of a homogeneous and well controlled environment (Varley et al., 1999) to which the entire population of cells is exposed. At the bioreactor scales considered here this should enable optimal cell growth and antibody production irrespective of the exact mechanisms of agitation and gas-liquid mass transfer employed.

Table 5.5 compares the conditions used for the fed-batch GS-CHO cultures in microwell (Chapter 4), shake-flask and STR geometries. It can be seen that the shaking conditions used for the 24 SRW system result in significantly longer mixing times in the microwells than those measured in the shake flask and 5L STR. The magnitude of the microwell t_m value is such that culture performance could be adversely affected due to reduced oxygen transfer, heterogeneities introduced during the bolus additions of feed and bicarbonate for pH control (Wayte et al., 1997) and the possibility of cell settling (Duetz, 2007). Recent experiments have suggested that it is possible to

culture both CHO (Wu, 2008) and GS-CHO lines at higher shaking speeds than hybridoma cells.

Table 5.5: Comparison of previously used experimental conditions for fed-batch culture of an industrial GS-CHO cell line in microwell (24-SRW), shake flask and STR bioreactor geometries (Chapter 4). Engineering characteristics determined as described in Sections 2.8 – 2.10.

Bioreactor Geometry	Mixing Time (s)	Mean Energy Dissipation Rate (W m^{-3})	k_{La} (h^{-1})
24 SRW $N = 140$ rpm $V_L = 800$ μL $d_s = 25$ mm	1103 ± 134	40^{a}	>20
Shake Flask $N = 140$ rpm $V_L = 50$ mL $d_s = 25$ mm	16 ± 2.1	96^{b}	>10
5L STR $N = 260$ rpm $V_L = 3.5$ L 45° pitch blade	6 ± 0.6	21^{c}	4.1

- a. Estimated from CFD (Barrett et al, 2010).
- b. Calculated based on Equation [5.5].
- c. Measured experimentally in this work.

As now shown in Section 5.4.2 above, increases in microwell shaking speed lead to dramatic reductions in mixing times (Figure 5.6) and provide t_m values that can be readily matched to those in shaken-flasks (Figure 5.7) and a typical laboratory scale STR (Figure 5.8). In the absence of macroscopic instabilities and circulation time effects seen in much larger vessels (Marks, 2003) it is proposed that matched mixing times can be used for successful

scale translation between the small scale shaken and stirred bioreactor geometries examined in this work. Short mixing times ($t_m < 10\text{s}$) should provide the necessary homogeneous environment for comparable culture performance provided that other engineering factors do not become rate limiting.

Table 5.6 summarizes the engineering characteristics of the three bioreactor geometries for operation at a matched t_m of $\sim 5\text{s}$. The shaking conditions for the microwells and shaken-flasks were chosen so that they could be mounted on the same shaker in a single incubator thus minimising potential differences in temperature and humidity fluctuations during sampling of parallel cultures. Maintaining t_m constant necessarily means that there will be differences in power input and oxygen mass transfer and the likely impact of these differences on culture performance must be considered.

Table 5.6: Summary of experimental conditions and engineering characteristics for small scale bioreactor geometries operated at matched liquid phase mixing time, t_m . Engineering characteristics determined as described in Section 2.6.

Bioreactor Geometry	Mixing Time (s)	Mean Energy Dissipation Rate (W m^{-3})	k_{La} (h^{-1})
24 SRW $N = 220$ rpm $V_L = 800$ μL $d_s = 25$ mm	4 ± 1.7	$>40^{\text{d}}$	>20
Shake Flask $N = 220$ rpm $V_L = 50$ mL $d_s = 25$ mm	5 ± 0.6	341^{e}	>10
5L STR $N = 260$ rpm $V_L = 3.5$ L 45° pitch blade	6 ± 0.6	21^{f}	4.1

d. Estimated from CFD (Barrett et al, 2010).

e. Calculated based on Equation [5.5].

f. Measured experimentally in this work.

With regard to the mean energy dissipation rate, P_g/V_L , it can be seen that values range from 21 to 341 W m^{-3} with the lowest value being determined in the STR. The STR value is in agreement with typical values found in the literature at this scale (Ma et al., 2002) and while it might be matched with the 40 W m^{-3} predicted for the microwells this would require operation at a stirrer speed of 435 rpm. In practice it was found that this led to excessive foaming and a reduction in culture performance (data not shown). In more general terms mean energy dissipation rate is not commonly used for

cell culture scale translation and none of the values reported are close to the level at which mechanical damage to the cells would be expected (Mollet et al., 2007).

With regard to the oxygen mass transfer coefficient, k_{LA} , values range from 4 – 20 h^{-1} . It is generally considered that a k_{LA} of $> 1 \text{ h}^{-1}$ is sufficient to maintain adequate oxygen transfer to growing cultures with a peak viable cell density of around $1 \times 10^7 \text{ cells mL}^{-1}$ (Nienow, 2006). All the values reported in Table 5.6 are well above 1 h^{-1} and so considered acceptable.

5.6 Summary

In this chapter the engineering characteristics of two shaken bioreactor geometries have been determined and compared to those of a standard 5L STR.

In terms of oxygen transfer rates (Section 5.2) it was shown that k_{LA} values in shaken 24 SRW plates and shake flasks were considerably greater than for a 5L STR under conditions appropriate for mammalian cell culture. All values were found to be well in excess of 1 h^{-1} , which is sufficient to maintain adequate oxygen transfer to growing cultures with a peak viable cell density of around $1 \times 10^7 \text{ cells mL}^{-1}$ (Nienow, 2006).

With regard to mean energy dissipation rates (Section 5.3), it was found that high impeller speeds would be required to match stirred tank

values to those for shake flasks and 24 SRW plates. These would result in excessive foaming in the stirred tank and would approach levels that are predicted to result in shear damage to mammalian cells (Mollet et al., 2007).

Finally, measurement of liquid phase mixing times was performed (Section 5.4) and it was found that comparable mixing times could be obtained for all three bioreactor formats under appropriate conditions for mammalian cell culture.

In summary matched mixing time appears to provide a suitable criterion for scale translation between different small scale bioreactor geometries. Values of t_m can be matched while ensuring other parameters such as k_{LA} and P_g/V_L are maintained at adequate and realistic levels.

Experimental confirmation of scale translation is considered in the next chapter.

Chapter 6: Mixing Time as a Basis for Cell Culture Scale Translation

6.1 Introduction and Aim

Chapter 4 demonstrated the implementation of a fed-batch methodology for GS-CHO culture in shaken 24 SRW plates. However, the microwell system had a lower integral viable cell density over the culture period in comparison with the shake flask model (Table 4.2). While this was compensated for by higher specific antibody productivity in the microwells, thus leading to approximately matched IgG titre, it would be preferable for a match in both specific growth kinetics and specific IgG productivity to be achieved.

A variety of bases have been used for cell culture scale-up between lab scale (5L) stirred tanks and pilot / manufacturing scale vessels. The most common bases are matched k_{La} , matched energy dissipation per unit volume and matched mixing time (Yang et al., 2007, Li et al., 2006). For scale translation between smaller scale vessels and different geometries no such basis for scale translation has yet been established.

In the previous chapter, matched mixing time was suggested as a possible basis for scale translation between shaken microwell plates and a laboratory scale stirred tank bioreactor. Matched mixing times could be

achieved for each bioreactor configuration under appropriate cell culture conditions in each (Table 5.6). With this as a starting point, the aim of this chapter is to experimentally validate t_m as a suitable basis for scale translation in small scale fed batch GS-CHO cultures. Specific Objectives are:

- To perform cultivation of a GS-CHO cell line under conditions of matched mixing time in 24 SRW, shake flask and stirred tank bioreactors simultaneously.
- To assess the broader applicability of this approach through culture of an additional cell line.

6.2 Fed-Batch GS-CHO Cultivation at Matched Mixing Time

Table 5.6 in the previous chapter details the operating conditions required to achieve matched mixing times in each of the three culture formats. The mixing time obtained in the stirred tank under standard cultivation conditions was used as the benchmark.

For fed-batch cultures at laboratory scale and above there are two options for implementing feeding regimes. One option is to use a continuous feed for the stirred tank cultivation – this allows the quantity of feed to be tailored to cellular demand (as determined through offline cell count and metabolite data). The second option is a bolus feeding strategy employed for

the flask and microwell systems in Section 4.4. This uses a fixed volume feed at pre-determined times, and as such is not responsive to the metabolite levels in the media over the course of the cultivation. The disadvantage of this method is that there is the potential for 'over-feeding' of glucose and other nutrients, with potentially detrimental consequences for culture performance. However the advantage is the simplicity especially at manufacturing scale (Xing et al., 2010).

Since the aim of this work was to assess whether or not producing a quantitatively equivalent engineering environment, through matched mixing time, would lead to a corresponding match in culture performance, it was decided to use bolus feeds for the stirred tank.

Figures 6.1-6.4 show the viable cell density, viability, product titre and metabolite profiles for the GS-CHO cultivations performed in each bioreactor format.

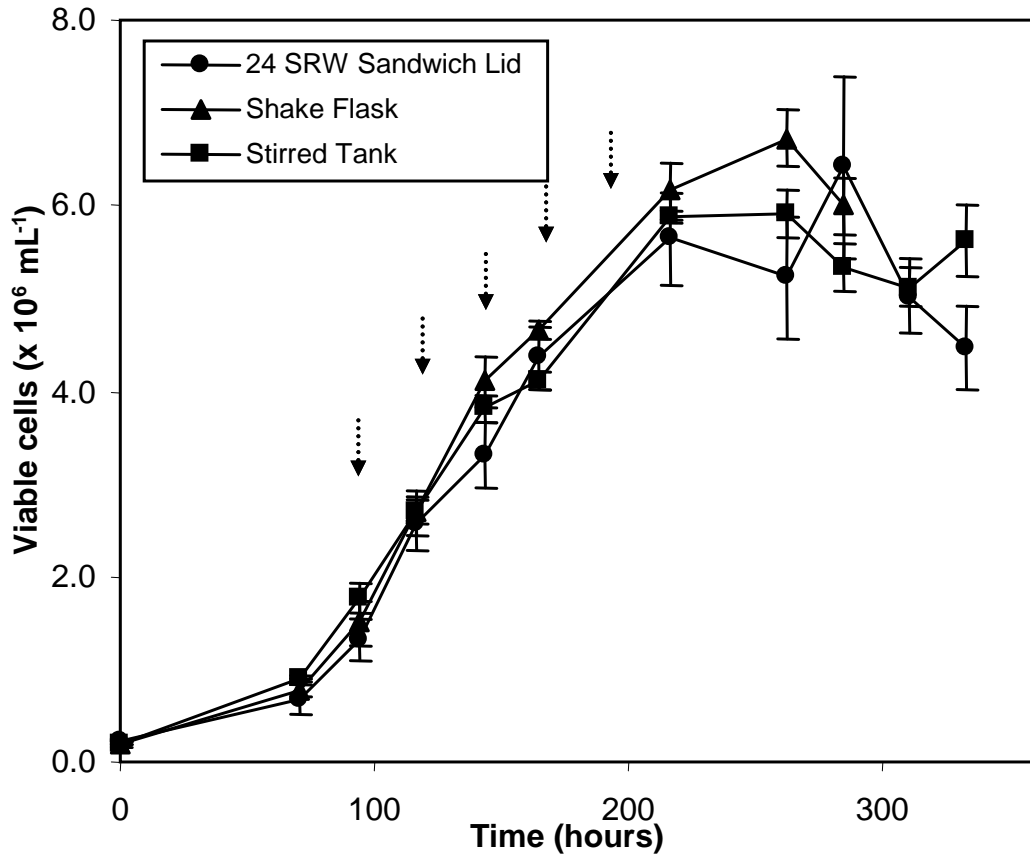


Figure 6.1: Viable cell density for fed-batch cultivation of a GS-CHO cell line in different small scale bioreactor geometries at a matched mixing time t_m of 5 s. Shaken cultures performed at 37 °C with 5% CO₂ at 70% relative humidity in a humidified incubator and shaken at $d_s = 25$ mm orbital diameter at 220 rpm, as described in Section 2.5.2, with feed addition points indicated by arrows. Stirred tank operated at 37°C at pH 7.10 and impeller speed of 260 rpm at a dissolved oxygen tension of 30% as described in Section 2.4. Error bars represent one standard deviation about the mean (n = 3).

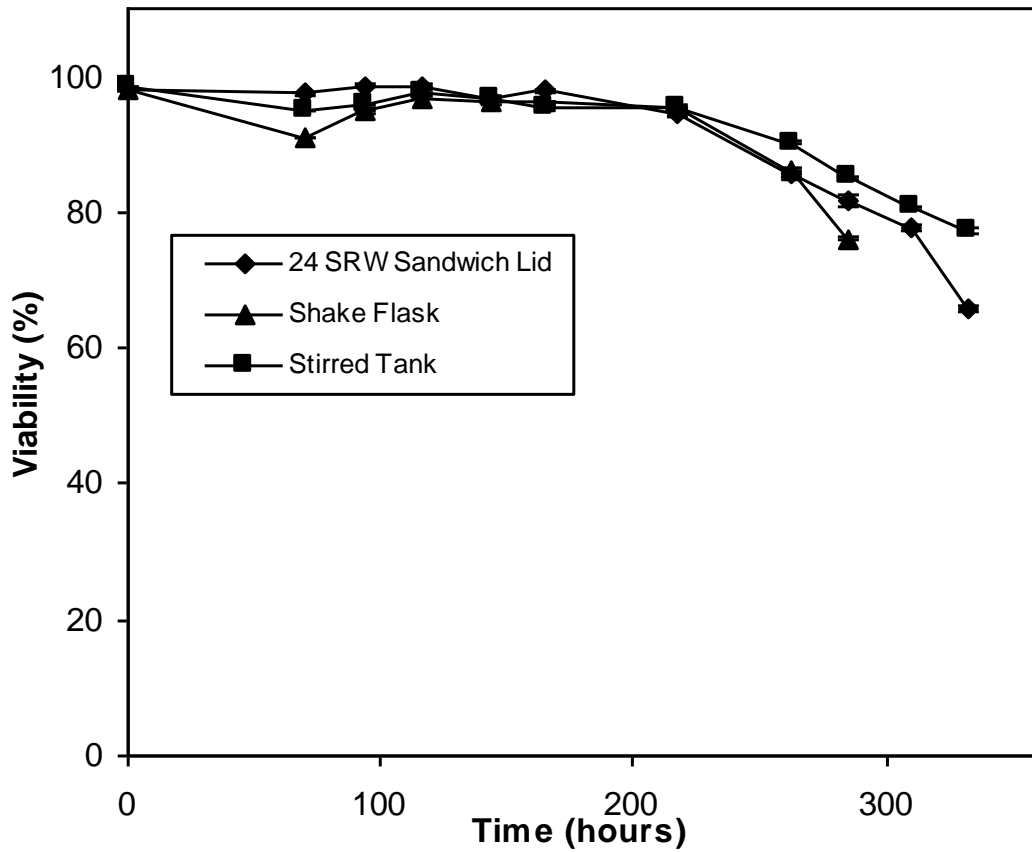


Figure 6.2: Viability for fed-batch cultivation of a GS-CHO cell line in different small scale bioreactor geometries at a matched mixing time $t_m = 5$ s. Culture method as described in Sections 2.4 and 2.5.2. Error bars represent one standard deviation about the mean ($n = 3$).

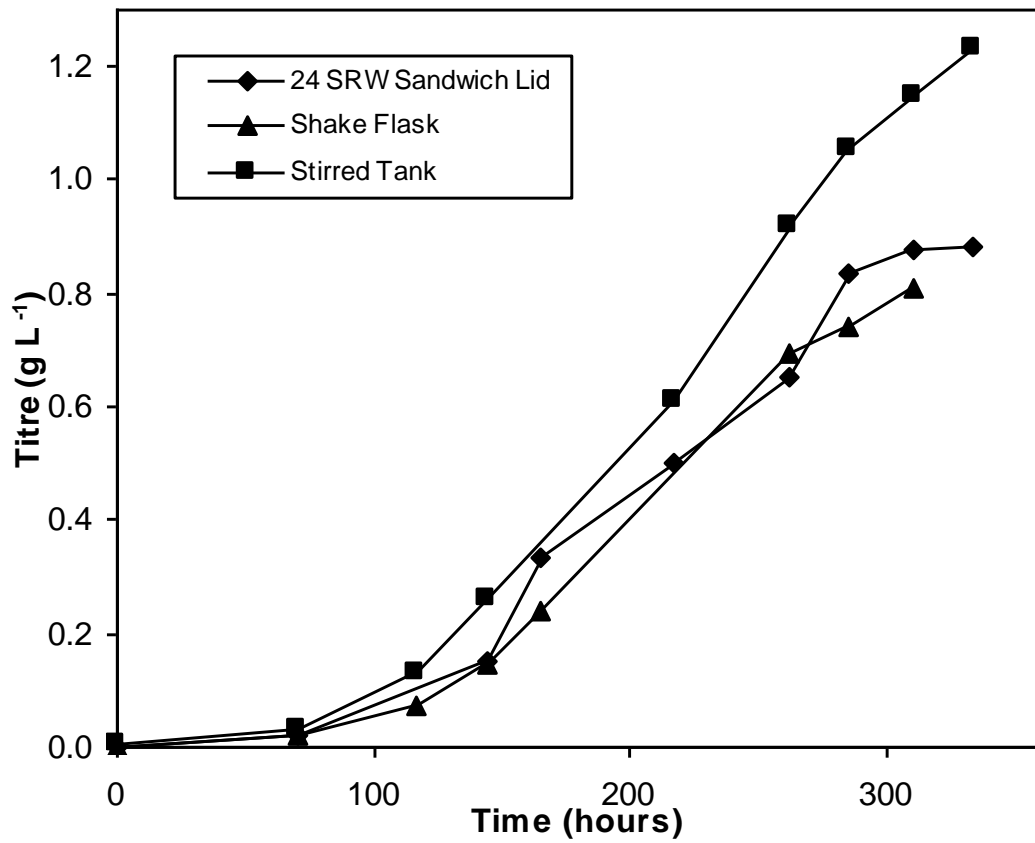


Figure 6.3: IgG titre for fed-batch cultivation of a GS-CHO cell line in different small scale bioreactor geometries at a matched mixing time $t_m = 5$ s. Culture method as described in Sections 2.4 and 2.5.2.

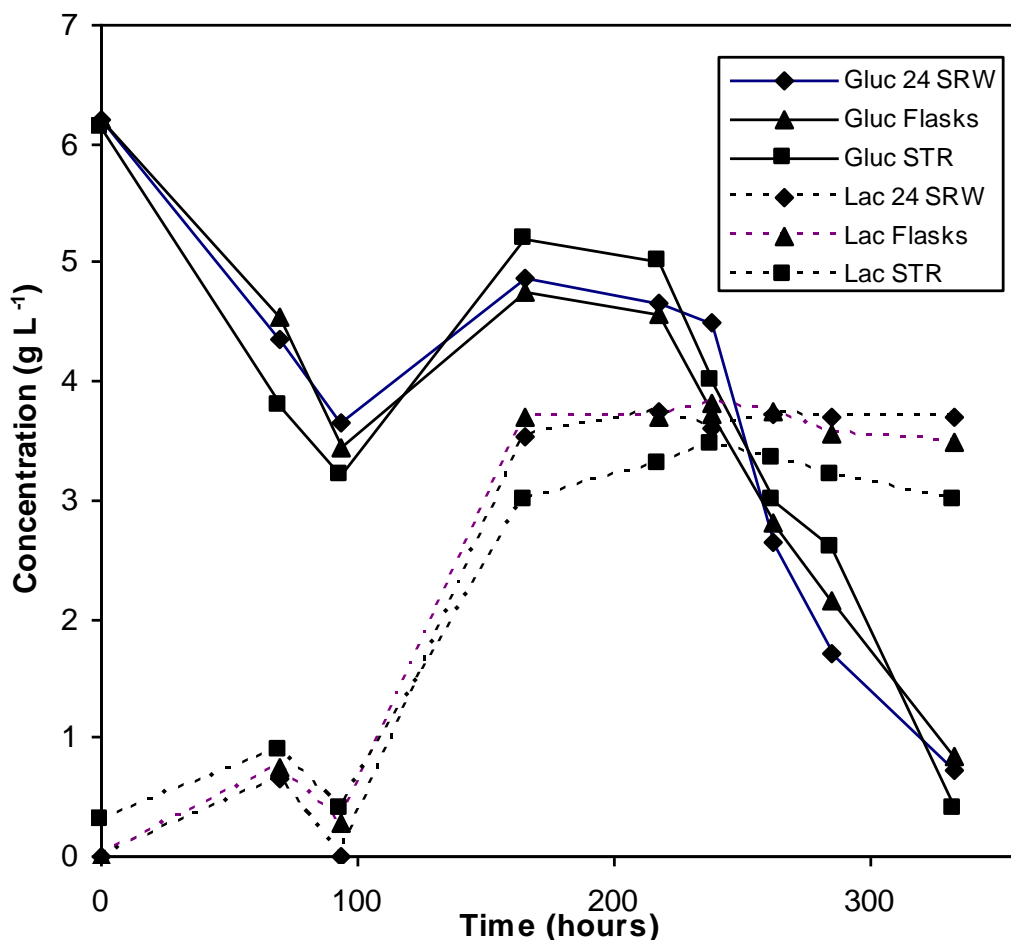


Figure 6.4: Glucose and lactate profiles for fed-batch cultivation of a GS-CHO cell line in different small scale bioreactor geometries at a matched mixing time $t_m = 5$ s. Culture method as described in Sections 2.4 and 2.5.2 and metabolite concentrations measured as described in Section 2.7.2.

It can be seen that comparable cell growth kinetics were obtained in all three bioreactor geometries reaching peak viable cell densities between $5.9 - 6.7 \times 10^6$ cells mL⁻¹ after around 285 hours. High cell viabilities (>90%) were also maintained up to 238 hours at which point viability began to decrease simultaneously in all bioreactors reaching final values between 70-80%. Both of the shaken bioreactor geometries attained peak IgG titres of between 0.81 and 0.88 g L⁻¹. Antibody formation in the STR, although initially following

similar formation kinetics, reached a 30% higher value toward the end of the culture. This is attributed to the better pH control in the STR (Wayte et al., 1997) due to direct addition of bicarbonate in the later stages of the culture compared to the reliance on head space CO₂ exchange in the two shaken bioreactors. Finally the metabolite data in Figure 6.4 indicates very similar kinetics for both carbon source utilisation and lactate formation in each bioreactor geometry.

Table 6.1 Comparison of fed-batch GS-CHO culture kinetics between microwell (24-SRW), shake-flask and stirred tank bioreactor geometries operated at matched mixing time, t_m of = 5s. Experimental conditions as described in Sections 2.4 and 2.5.2 and culture data as shown in Figures 6.1-6.4.

Parameter	24-SRW Plate	Shake Flask	5L STR
Final antibody concentration [g L ⁻¹]	0.88	0.81	1.23
Integral viable cell concentration [10 ⁹ cells.day ⁻¹ .L ⁻¹]	48.0	48.7	49.8
Peak viable cell concentration [cells mL ⁻¹]	6.41	6.73	5.92
Maximum specific growth rate [h ⁻¹]	0.029	0.028	0.028
q _{Ab} [mg (10 ⁹ cells.day) ⁻¹]	18.4	16.6	24.8
q _{gluc} [g (10 ⁹ cells.day) ⁻¹]	0.30	0.30	0.29
q _{lac} [g (10 ⁹ cells.day) ⁻¹]	0.17	0.13	0.12
Lactate produced / glucose consumed [g.g ⁻¹]	0.39	0.36	0.34

The integral viable cell concentrations and specific metabolite production and consumption rates are very similar across all three bioreactor formats. While the specific antibody production rate is higher for the stirred tank this is likely to be a result of tighter pH control in this system compared to the microwell and shake flask formats. Overall therefore t_m looks to be a good basis for scale translation.

6.3 Evaluation of Scale Translation Basis with Different Cell Culture Processes

For any scale translation methodology to be of industrial use it should be as broadly applicable as possible. Having demonstrated that use of matched mixing time as the scale translation parameter is effective, several culture experiments were performed with a second cell culture process supplied by the IMRC (as described in Section 2.3.1). In addition to using a different GS-CHO cell line producing a different IgG, these experiments also employed an alternative feeding methodology (described in more detail in Section 2.5.3) which provides an additional test of how robust the 24 well shaken system is. As described in Section 2.5.3 this feeding method requires daily measurement of the medium glucose concentration following which feed is added at a level sufficient to restore [glucose] to 2 g L⁻¹. Figures 6.5 – 6.8 show viable cell density, viability, product titre and metabolite data respectively:

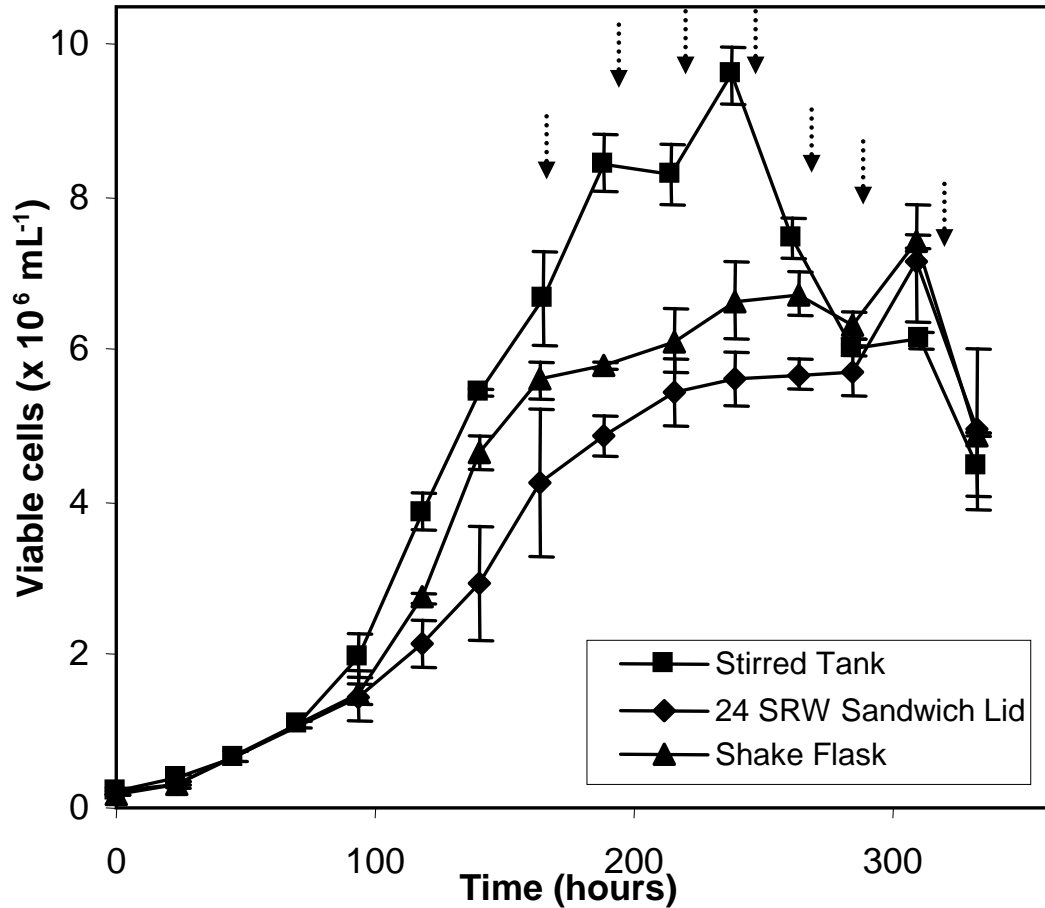


Figure 6.5: Viable cell density for fed-batch cultivation of a GS-CHO cell line in different small scale bioreactor geometries at a matched mixing time $t_m = 5$ s, with feed additions indicated by arrows. Shaken cultures performed at 37 °C with 5% CO₂ at 70% relative humidity in a humidified incubator and shaken at $d_s = 25$ mm orbital diameter at 220 rpm as described in Sections 2.3.1 and 2.5.3. Stirred tank operated at 37°C at pH 7.10 and impeller speed of 260 rpm at a dissolved oxygen tension of 30%. As described in Section 2.4. Error bars represent one standard deviation about the mean (n = 3).

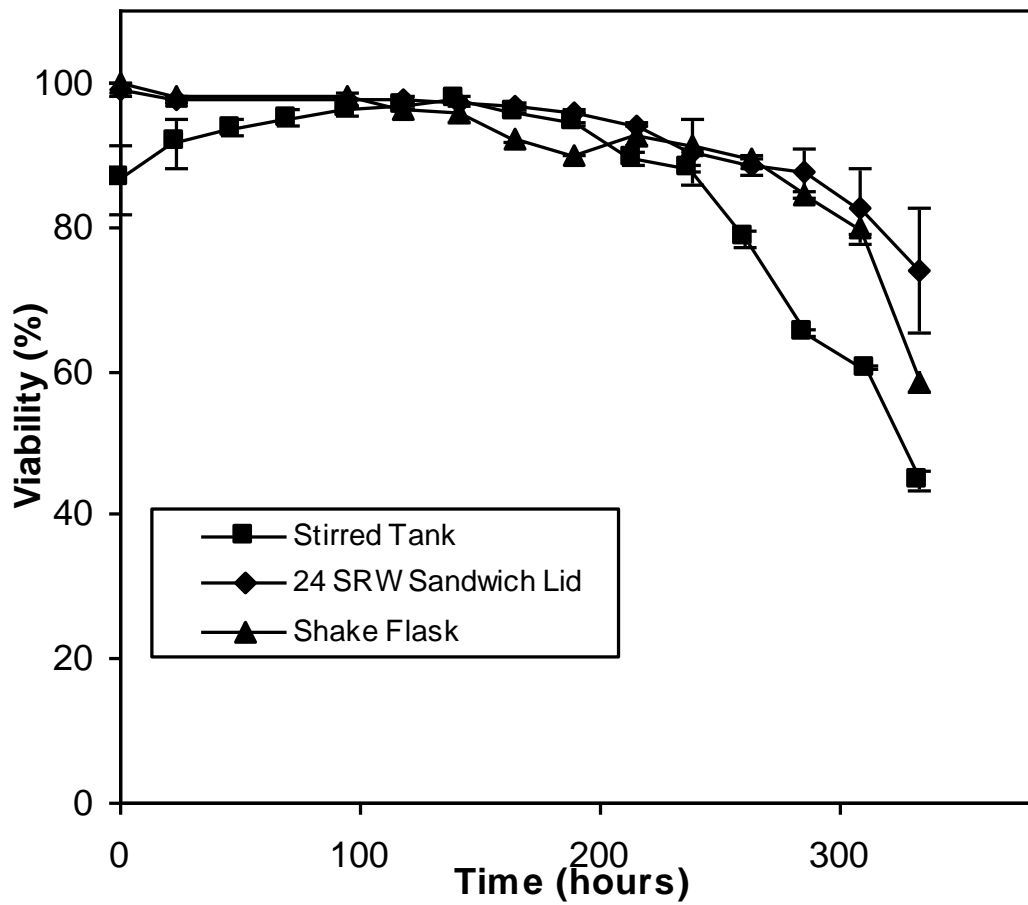


Figure 6.6: Viability for fed-batch cultivation of a GS-CHO cell line in different small scale bioreactor geometries at a matched mixing time $t_m = 5$ s. Culture method as described in Sections 2.3.1, 2.4 and 2.5.3. Error bars represent one standard deviation about the mean (n = 3).

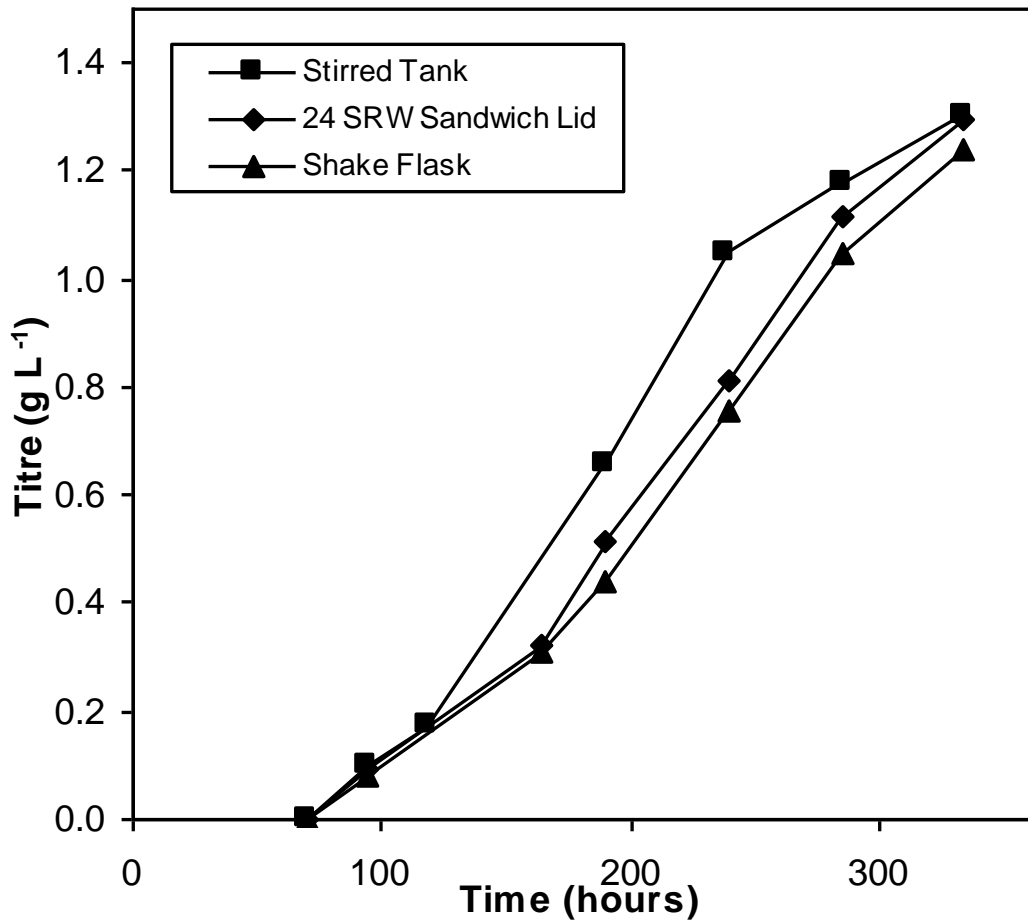


Figure 6.7 IgG titre for fed-batch cultivation of a GS-CHO cell line in different small scale bioreactor geometries at a matched mixing time $t_m = 5$ s. Culture method as described in Sections 2.3.1, 2.4 and 2.5.3.

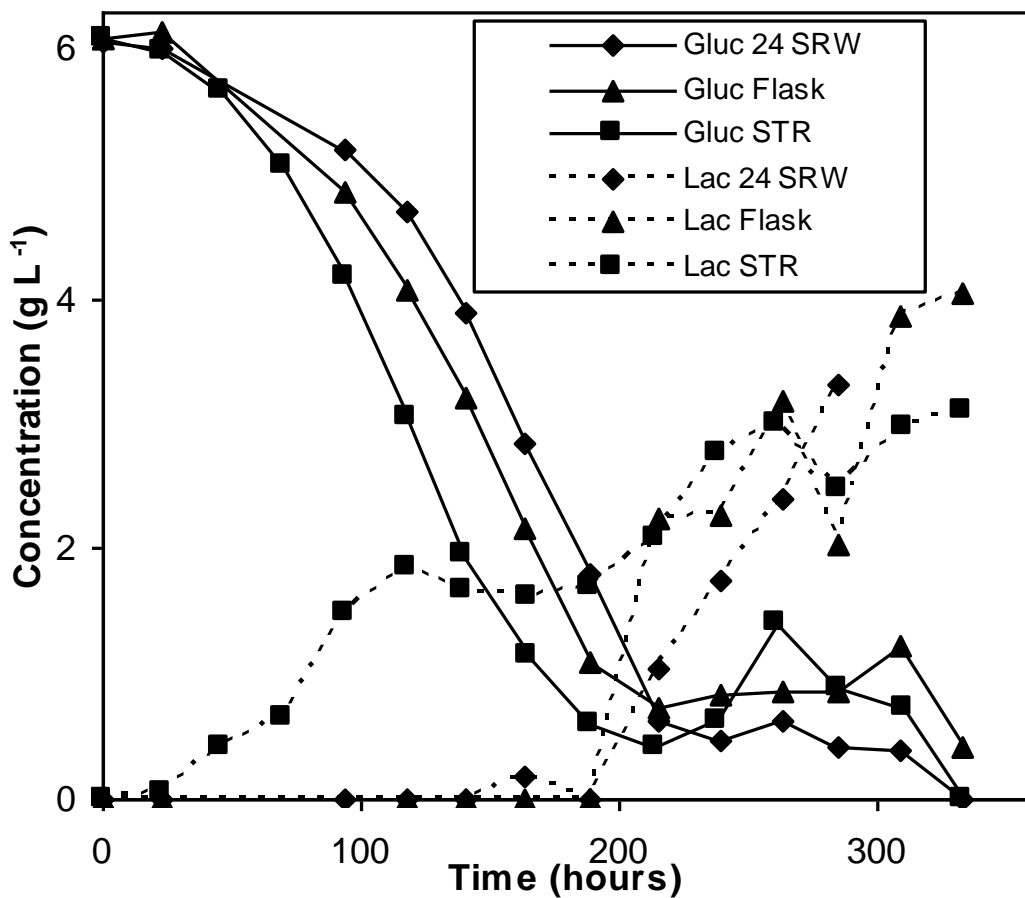


Figure 6.8: Glucose and lactate profiles for fed-batch cultivation of a GS-CHO cell line in different small scale bioreactor geometries at a matched mixing time $t_m = 5$ s. Culture method as described in Sections 2.3.1, 2.4 and 2.5.3 and metabolite concentrations measured as described in Section 2.7.2.

While the stirred tank culture reached a peak viable cell density of 9.6×10^6 cells mL⁻¹, the maximum densities obtained in the microwell and shake flask formats were 7.1 and 7.4×10^6 cells mL⁻¹ respectively. Cell viability in all bioreactors remained above 90% for the first 200 hours of culture. However, viability for the stirred tank declined steadily after 240 hours, falling to approximately 60% after 310 hours while the viability in microwell and shake flask was around 80% at this stage.

It can be seen that despite lower peak viable cell densities in the shaken flask and microwell cultivations, the final product titres are highly comparable for all three culture systems. This may be a result of higher medium osmolality in the microwells resulting from a higher relative rate of evaporation (as discussed in Chapter 4). Although the microwell feeds were diluted with water to correct this imbalance, the feeding method employed here (in which additions are only made once [glucose] falls below 2 g L⁻¹) resulted in the culture remaining un-fed until Day 9, in contrast to the situation for experiments performed in Section 6.2 for which feeding always commenced on Day 4. The result of this was that the opportunity to replace the water lost from the wells was delayed by 5 days, thus resulting in a likely osmolality increase over this period. Direct comparison with the shake flask culture supports this argument, as it is found that despite slightly lower cumulative cell hours for the microwells (13%), there was a compensating increase in specific productivity such that the final titre was 8% higher than in the flasks.

Table 6.2 Comparison of fed-batch GS-CHO culture kinetics between microwell (24-SRW), shake-flask and stirred tank bioreactor geometries operated at matched mixing time, $t_m = 5$ s. Experimental conditions as described in Figure 6.5 and culture data as shown in Figures 6.5-6.8.

Parameter	24-SRW Plate	Shake Flask	5L STR
Final antibody concentration [g L ⁻¹]	1.34	1.24	1.30
Integral viable cell concentration [10 ⁹ cells.day ⁻¹ .L ⁻¹]	49.9	58.0	68.4
Peak viable cell concentration [cells mL ⁻¹]	7.14	7.41	9.62
Maximum specific growth rate [h ⁻¹]	0.021	0.025	0.028
Q ^{Ab} [mg (10 ⁹ cells.day) ⁻¹]	26.8	21.4	18.0
Q ^{gluc} [g (10 ⁹ cells.day) ⁻¹]	0.28	0.22	0.21
Q ^{lac} [g (10 ⁹ cells.day) ⁻¹]	0.09	0.07	0.05
Lactate produced / glucose consumed [g.g ⁻¹]	0.33	0.34	0.22

Although the disparities in the onset of feeding make comparisons between culture systems more difficult, use of feeding strategies that aim to control [glucose] around a particular set-point are fairly common and as such this experiment represented an opportunity to test the flexibility of the 24 SRW system to alternative approaches.

6.4 Optimisation of the Method for Shaken 24 SRW Plates

The results in Section 6.3 confirmed the flexibility of the 24 SRW system with respect to (i) the cell line and (ii) the feeding method employed. However, it appears that the later onset of feeding when compared to the strategy used for the MedImmune cell line (9 days compared to 4 days after inoculation) may have impacted on the culture performance by resulting in a greater increase in the medium osmolality prior to initiation of feeding.

The reason for this osmolality shift is not the absolute rate of evaporation as such, but rather the relative evaporation rate from the microwells as a proportion of the inoculated volume (as discussed in Chapter 4). Therefore if the initial volume per well was increased, this would have the effect of reducing the relative rate of water loss and thus also the increase in osmolality.

Examining the mixing time data for 24 SRW plates in Figure 5.7, it is seen that increasing the fill volume from 0.8 to 1.6 mL resulted in an increase in t_m from 4 to 25 seconds. The latter time is still less than the majority of those quoted in the literature for stirred tank bioreactors, and as such the microwell contents could still be described as 'well-mixed' (Osman et al., 2001). The culture experiment described in Section 6.3 was therefore repeated using an initial microwell volume of 1.6 mL.

Figures 6.9-6.12 below show the viable cell density, viability, product titre and metabolite data obtained (note that no parallel stirred tank cultivation was performed for this experiment):

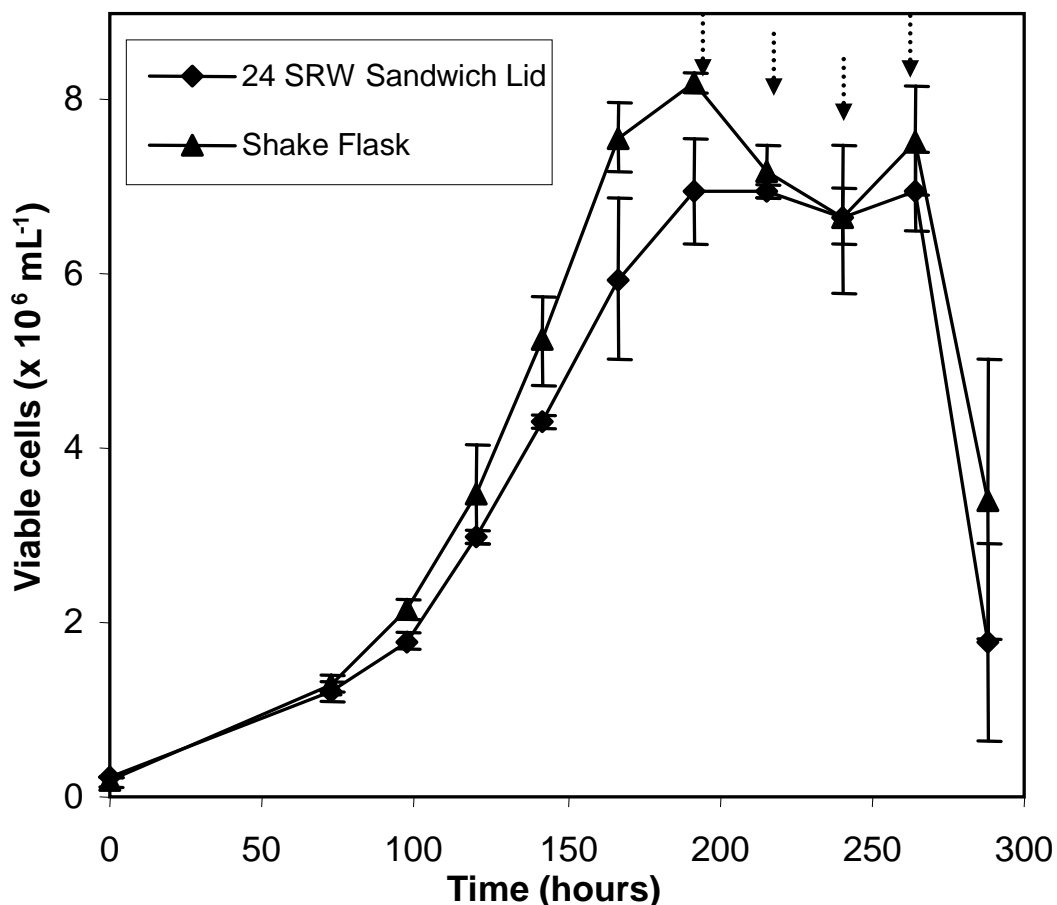


Figure 6.9 Viable cell density for fed-batch cultivation of a GS-CHO cell line in microwell (24-SRW) and shake-flask formats operated at mixing times, t_m of 25s and 5s respectively, with feed additions indicated by arrows. Shaken cultures performed at 37 °C with 5% CO₂ at 70% in a humidified incubator and shaken at $d_s = 25$ mm orbital diameter at 220 rpm as described in Sections 2.3.1 and 2.5.3. Error bars represent one standard deviation about the mean (n = 3).

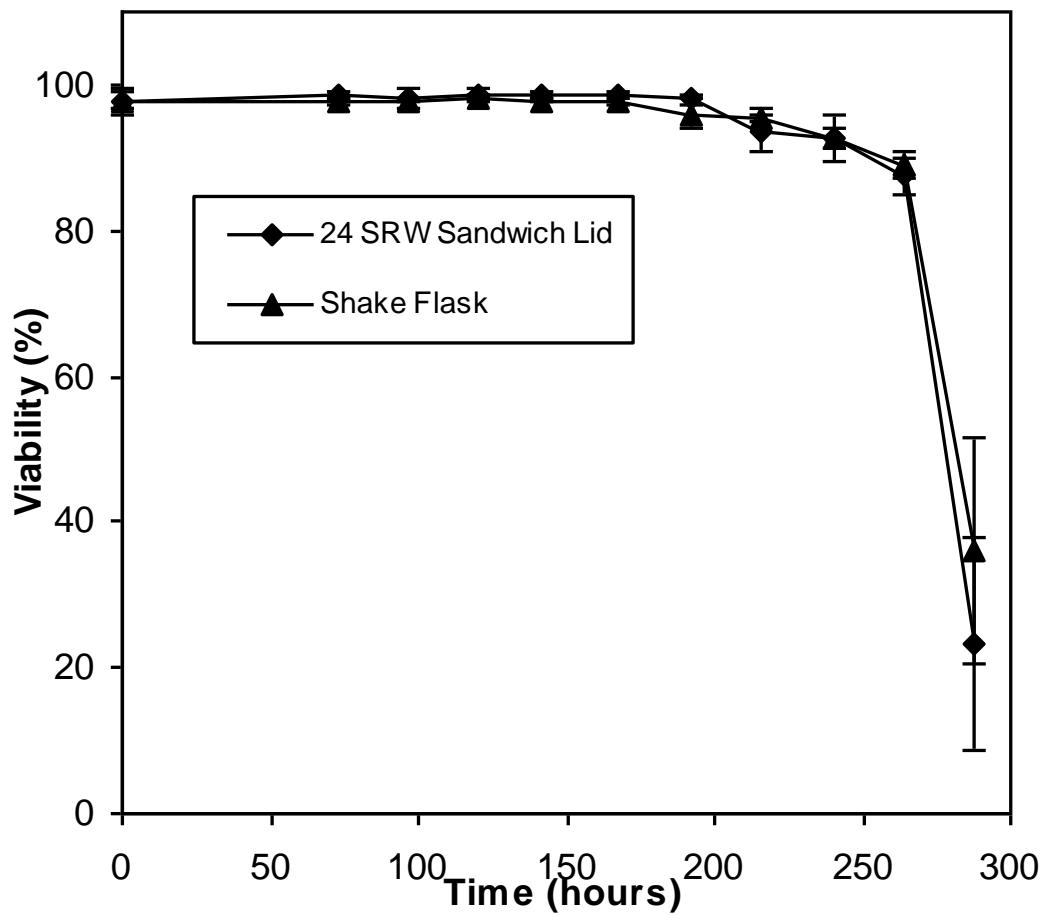


Figure 6.10 Viability for fed-batch cultivation of a GS-CHO cell line in microwell (24-SRW) and shake-flask formats operated at mixing times, t_m of 25s and 5s respectively. Culture method as described in Sections 2.3.1 and 2.5.3. Error bars represent one standard deviation about the mean (n = 3).

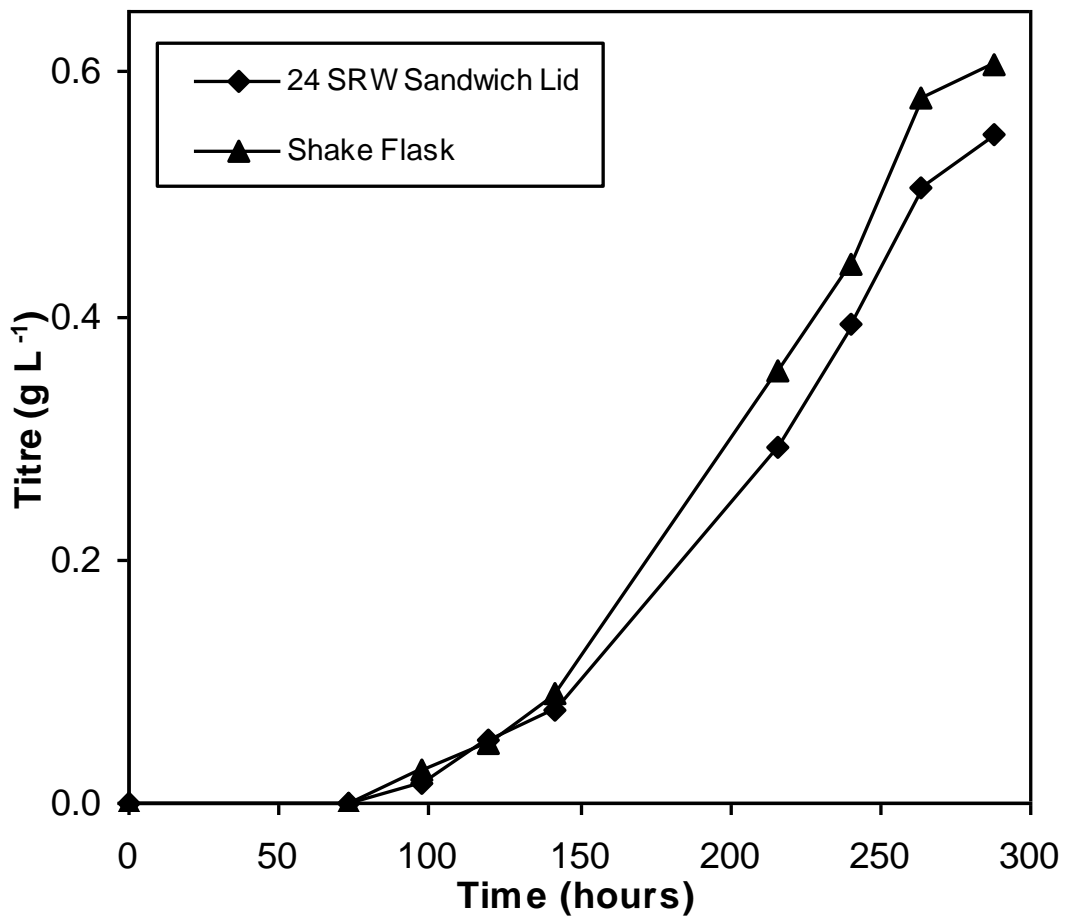


Figure 6.11: IgG titre for fed-batch cultivation of a GS-CHO cell line in microwell (24-SRW) and shake-flask formats operated at mixing times, t_m of 25s and 5s respectively. Culture method as described in Sections 2.3.1 and 2.5.3.

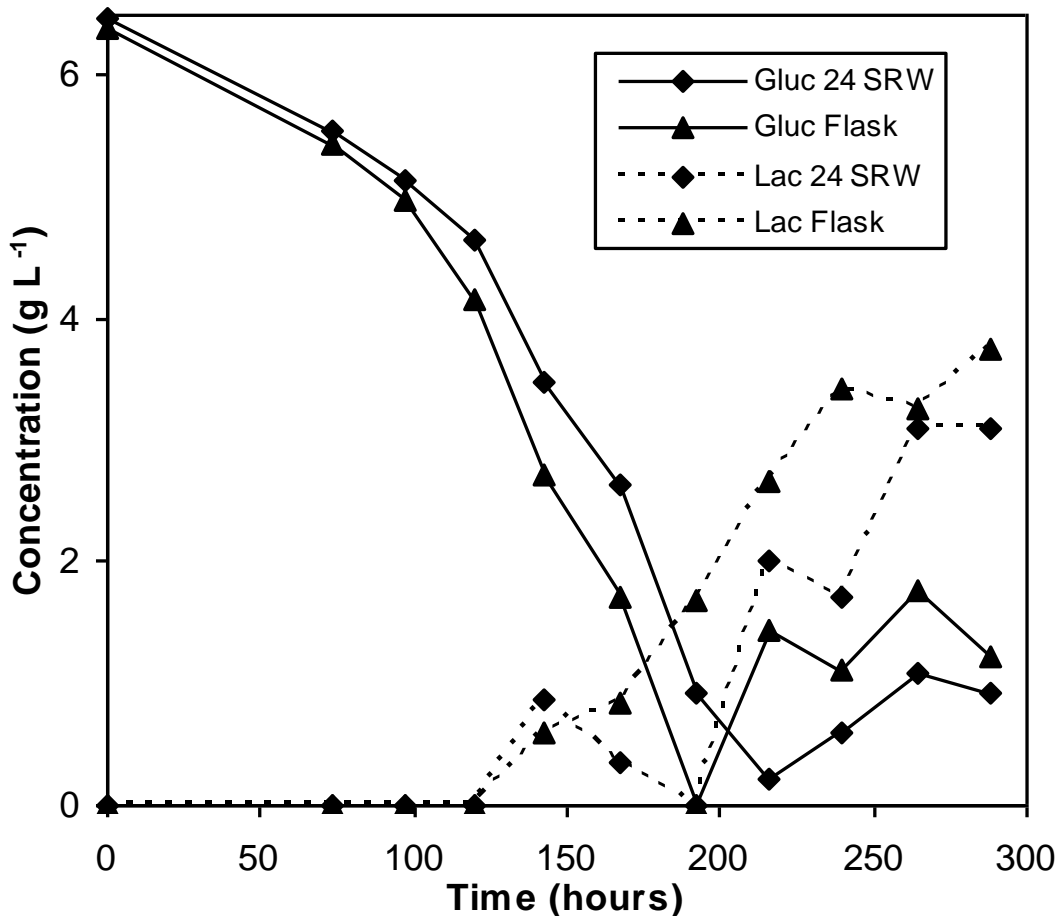


Figure 6.12: Glucose and lactate profiles for fed-batch cultivation of a GS-CHO cell line in microwell (24-SRW) and shake-flask formats operated at mixing times, t_m of 25s and 5s respectively. Culture method as described in Sections 2.3.1 and 2.5.3 and metabolite concentrations measured as described in Section 2.7.2.

For this experiment it was found that cumulative cell hours and product titre for the shake flask were 12% and 11 % greater than those for the 24 SRW system respectively. Therefore it appears that increasing the inoculated volume in the microwells from 0.8 to 1.6 mL had the intended effect of reducing the proportional rate of evaporation from the wells, and thus minimising any increase in osmolality. The direct consequence of this

was, as expected, a rate of specific productivity that more closely coincides with that observed for the shaken flask. This higher fill volume therefore allows the microwell to more closely mimic the shake flask performance.

Table 6.3 Comparison of fed-batch GS-CHO culture kinetics between microwell (24-SRW) and shake-flask operated at mixing times, t_m of 25s and 5s respectively. Experimental conditions as described in Figure 6.9 and culture data as shown in Figures 6.9-6.12.

Parameter	24-SRW Plate	Shake Flask
Final antibody concentration [g L ⁻¹]	0.55	0.60
Integral viable cell concentration [10 ⁹ cells.day ⁻¹ .L ⁻¹]	46.4	52.8
Peak viable cell concentration [cells mL ⁻¹]	7.65	8.21
Maximum specific growth rate [h ⁻¹]	0.023	0.027
q _{Ab} [mg (10 ⁹ cells.day) ⁻¹]	11.5	11.7
q _{gluc} [g (10 ⁹ cells.day) ⁻¹]	0.23	0.17
q _{lac} [g (10 ⁹ cells.day) ⁻¹]	0.07	0.07
Lactate produced / glucose consumed [g.g ⁻¹]	0.29	0.41

6.5 Confirmation of Adequate Oxygen Supply in Microwells During GS-CHO Cultivation

The above data indicate that culture performance in fed 24 SRW GS-CHO cultivations is significantly improved by increasing the shaking speed from 140 rpm (Chapter 4) to 220 rpm (Figures 6.1-6.12), which corresponds to

a decrease in the t_m from 1,103 to 4 seconds for a liquid fill volume of 0.8 mL. However, while this is likely to be due to enhanced mixing under the new conditions, it is also possible that improved oxygen transfer efficiency may be a factor.

While all measured k_{La} values for microwell plates are considerably in excess of the critical value of 1 h^{-1} (Nienow, 2006), the nature of liquid mixing in microwells may result in regions of low oxygen concentration. This is because, as described in Chapter 5, once oxygen has entered the fluid at the gas-liquid interface, it must then diffuse or be carried by convective motion to the base of the well. Therefore if mixing intensity is poor, as is the case for the 24 well system at 140 rpm, the rate at which oxygen is able to reach the lower regions of the microwell may be limited by mixing and therefore result in growth inhibition.

This possibility was investigated by performing a fed batch GS-CHO culture in microwell plates with fluorescence-based oxygen sensors immobilised at the base of each well (method as described in Section 2.12). As shown in Figure 6.13 for viable cell densities of around $8 \times 10^6 \text{ mL}^{-1}$ the measured dissolved oxygen tension (DOT) at the base of the well was 82 % when the culture was shaken at 220 rpm ($t_m = 4 \pm 1.7\text{s}$) and this only fell slightly to 73% when the shaking speed was dropped to 140 rpm ($t_m = 1103 \pm 134\text{s}$):

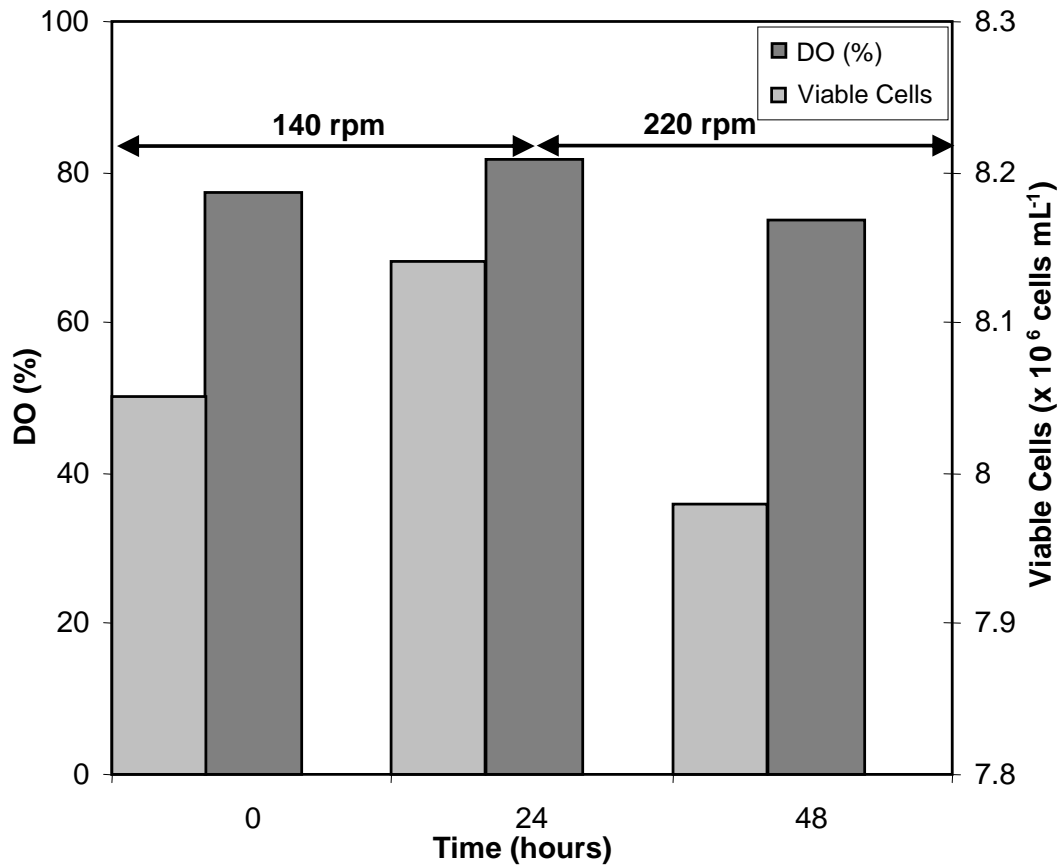


Figure 6.13: Measurement of dissolved oxygen (DO) at the base of the microwells during 24 SRW plate cultivations of GS-CHO cells at variable shaking speed. Experimental conditions: $V_L = 800 \mu\text{L}$ at $36.5 \text{ }^\circ\text{C}$ with 5% CO_2 , shaken with a 25 mm orbital diameter as described in Figure 6.1. Shaking speed used was 220 rpm between 0 and 24 hours and 140 rpm between 24 and 48 hours.

It can therefore be concluded that the enhanced culture performance observed for the microwells at 220 rpm is most probably the result of enhanced mixing rather than oxygen transfer.

6.6 Summary

This chapter supports the use of t_m as a suitable criterion for scale translation between different small scale bioreactor geometries. In addition to its applicability to the fed-batch cell culture process described in Chapter 4, close agreement between key cell culture parameters for 24 SRW, shake flask and stirred tank bioreactors was also obtained using an alternative culture process with a distinct cell line and feeding methodology. This suggests that use of matched t_m for scale translation may be broadly applied.

Investigation of oxygen transfer into the microwells under the experimental conditions used in Chapters 4 and 6 was also investigated. This demonstrated that the improved culture performance at the higher shaking speed used in Chapter 6 was likely to be a result of improved mixing rather than oxygen transfer.

Chapter 7: Conclusions and Future Work

7.1 Conclusions

The work presented in this thesis has demonstrated that shaken 24 SRW microwell plates are an effective scale down model for both shake flask and 5L stirred tank bioreactors. This was the main aim of the project as originally described in Section 1.7.

The initial feasibility studies showed that CHO-S cells could be successfully cultivated in 24 SRW plates, with batch growth kinetics and metabolite consumption rates achieved similar to those observed in shake flasks (Figures 3.1, 3.2, 3.11 and 3.12). This built on the work of Barrett et al. (2010) who initially showed that hybridoma cells could be cultured in shaken 24 SRW plates. Together with this work it is now clear that shaken 24 SRW plates can be used for the culture of a diverse range of mammalian cell lines provided that suitable culture conditions are identified for each (Section 3.10).

A key constraint identified was the rate of fluid evaporation from the microwell plates (Section 3.3). This had the potential to impact culture performance, as a result of raised medium osmolality, and quantification of key process indicators such as viable cell concentration and antibody titre. This would be a particular issue for fed cultures, as the concentrated feeds would raise solute concentrations in the medium yet further. To significantly

reduce water loss from the microwells, an alternative sterile seal was identified; the 'sandwich lid' (Figure 2.2). This was found to reduce the evaporation rate two-fold compared to the Breatheasy membrane used in previous work (Table 4.1). Use of this lid, combined with dilution of feeds to counteract increases in medium osmolality, led to a successful and easily implemented fed batch culture methodology for an industrial GS-CHO cell line in 24 SRW plates (Sections 4.3 and 4.4). Cell culture performance with regard to both viable cell density and IgG concentration were found to be comparable to those achieved in conventional shake flasks (Figures 4.5 and 4.7) currently used in early stage cell culture process development (Büchs et al., 2001).

Having developed successful batch and fed-batch culture processes in 24 SRW microwell plates, the next objective of the project was to understand how microwell culture performance could be related to that seen in a conventional 5L stirred tank bioreactor. This is important since such vessels currently represent established and validated scale-down models of pilot/commercial scale cell culture processes (Section 1.3). This required selection of an appropriate basis for scale translation, which was explored through engineering characterisation of all three bioreactor formats as described in Chapter 5. The oxygen mass transfer coefficient (k_{La}) (Tables 5.1 and 5.2), mean energy dissipation (Tables 5.4 and 5.4) and liquid phase mixing times (Figures 5.7 to 5.9) were determined over a range of operating

conditions. Mixing times in particular were shown to exhibit a wide variation over the range of process conditions tested. Based on analysis of factors limiting culture performance it was hypothesised that matched mixing time represented a suitable criterion for scale translation as discussed in Section 5.5.

In order to confirm this hypothesis, fed-batch cultivation of GS-CHO at a matched mixing time of 5 seconds was performed using the cell culture process from Chapter 4. The results showed comparable growth and antibody formation kinetics for 24 SRW plates, shake flask and stirred tank bioreactors (Figures 6.1 to 6.3). The slightly higher IgG titre achieved in the stirred tank is believed to be related to improved pH control in this system. Furthermore, use of matched mixing time was also successfully applied to an alternative fed-batch cell culture process using a different GS-CHO cell line (Section 6.3).

Since this work was conducted as part of an EngD project in collaboration with MedImmune, the final objective of the project was to demonstrate the industrial application of the fed-batch cell culture process in shaken 24 SRW plates in a commercial context. This work is described in detail in Appendix I. More than 50 cell lines were cultured simultaneously and measurements of both cell number and antibody titre obtained. It was found that the rank order of cell lines, in terms of both viable cell number and antibody production corresponded well with those obtained by currently used static plate and shake flask methods. This demonstrates that culture

kinetics for shaken 24 SRW plates correlate well with the shake flask and static plate systems across a wide range of cell lines, allowing broad application of the shaken microwell system. In addition, culture in shaken plates provides a far wider range of cell densities and antibody titres than the static microwell method, due to superior mixing and oxygen transfer in the former. This can assist cell line selection by increasing the distinction between high and low producing candidates.

Furthermore it was shown that the microwell approach could facilitate a greater than 30-fold increase in experimental throughput, and that suitable analytical devices are available to ensure that measurement of culture performance does not become rate limiting. Consequently, as a result of this project, the fed-batch 24-well cell culture methodology is now routinely used within MedImmune cell line selection and cell culture process development procedures.

7.2 Future Work

The use of a fed-batch 24 SRW process for early stage cell line selection at MedImmune demonstrates the industrial potential of this technology for biopharmaceutical product development. However, there remain a number of areas for further work.

There are a number of areas of this work that may have benefited from additional experiments or alternative approaches. For example, while three methods were used for determining the oxygen mass transfer coefficient in 24 SRW plates (Section 2.9), only a single method was used for measurement of liquid phase mixing time (Section 2.8.2). While the decolourisation method used is well established, it would have provided a useful validation to confirm that alternative methods (such as an amperometric approach (Mayr et al., 1992)) provided comparable results. It might also have been useful to use an automated method, for example using a fluorometer (Einsele et al., 1978) as this could reduce the error that is potentially introduced by monitoring the decolourisation by eye.

Use of additional analytical techniques may have shed light on the reasons for differences in culture performance between bioreactor formats. While metabolite concentrations (Section 3.6) and cell size (Section 3.5) provided insights, use of cell cycle analysis could potentially have been useful (Krampe et al., 2008), as arrest of the cell cycle in a particular phase can be associated with increased antibody productivity. For example, an extended period in G1 has been linked to increased productivity in hybridoma (Suzuki et al., 1989).

Further work could also be used to validate the selected scale translation parameter of matched mixing time. For example, while culture experiments have been performed under well-mixed conditions, performing

cell culture over a wider range of shaking speeds could establish process limits, and the point at which the liquid could be considered adequately mixed to support cell growth when speeds were reduced could be determined, for example. Conversely, higher speeds could be tested to establish the point at which excessive turbulence would result in cell damage. Establishing an appropriate range of operating parameters in this way could inform process scale-up by predicting whether particular stirred tank conditions would be suitable for cell culture.

No assessment has been performed on the impact of the microwell environment on product quality, which is a key factor in determining the feasibility of a cell culture process (Legmann et al., 2010). Common metrics include N-glycan sialylation, distribution of isomers and oligomeric structure of the antibody product (Meuwly et al., 2006). Potential methods range from gel electrophoresis for determination of oligomeric structure, and mass spectrometry for more detailed analysis of glycosylation and isoforms (Issaq et al., 2002). Comparison of product quality for IgG produced in the 24 SRW system compared to those achieved in the 5L bioreactor needs to be performed.

Despite the potential for improved throughput offered by the 24 SRW format, the requirement for manual liquid handling for both sampling and feed addition remains a bottleneck. Not only does this increase labour costs but it also raises the probability of contamination. Therefore it would be

useful if as many of the liquid handling stages as possible could be automated. This would have the potential to increase the precision and accuracy of the liquid handling as well as reducing the potential for contamination (Amanullah et al., 2010). A number of robotic platforms are available that could be modified to handle 24 SRW plates, although some logistical problems would have to be confronted, such as the difficulty of removing the sandwich lids from microwell plates automatically.

There is also a more fundamental question as to the ultimate use of this platform. While this thesis has provided data in support of use of a fed-batch 24 SRW system for initial screening of CHO-S cells, it has not conclusively demonstrated that culture performance is equivalent to that of a stirred tank system. As such it may be that comparative cultures of different cell lines would result in a different rank order when undertaken using the 24 SRW system as compared to use of a stirred tank, which could potentially prevent identification of the highest performing lines at the selection stage. This problem is discussed in two papers (Porter et al., 2010) which include a direct comparison of the rank order achieved in cell lines cultivated in static microwells, batch shake flask and fed batch cultivations respectively. It is found that, whilst all culture formats identify the highest performing cell lines, the rank order differs depending on the bioreactor used. This work highlights the importance of maintaining an awareness of the influence of different culture environments and operating conditions on performance. It

would be instructive to undertake additional comparison of culture performance in stirred tank and shaken microwell systems for a variety of cell lines.

In the event that the comparative rank order of cell lines in the shaken 24 SRW microwell system and a stirred tank bioreactor, as measured by product titre and other key performance metrics, fails to match there are then two options:

- (i) Further work could be undertaken in attempt to match the performance of the microwell system to the stirred tank, or:
- (ii) The disparity in performance could be accepted as an inevitable consequence of the inherent differences in geometry and engineering environment between the two systems.

Following the second option, the 24 SRW system could be used primarily as a convenient high throughput method for selecting high performing candidate cell lines. However, use in process development (for example, development and optimisation of feeding strategies) would be restricted as the shaken microwell culture performance could not be taken as wholly predictive of scale-up performance in a stirred tank.

There are a number of potential approaches for pursuing option (i), and attempting to produce a closer match with a stirred tank. For example,

EnzyScreen produce an air-tight box which would allow isolation of the shaken microwells within an incubator unit. If connected to a suitable gas supply and mass spectrometric detector, this could allow control of the headspace partial pressure of oxygen. In combination with the Pre-Sens system discussed in Chapters 5 and 6, this could allow dissolved oxygen control to be introduced to the microwell system. Given that lack of parameter control in the microwells is one potential reason for a disparity in performance with the stirred tank system, introduction of such control could be a means of redressing this.

However, there are two significant disadvantages of introducing such additional controls: a loss of simplicity and an increase in costs. Since these are primary selling points of using off the shelf microwells for high-throughput cultivations, thought should be given to the most effective and efficient application of additional work to this system, as there could be diminishing returns to further attempts at performance optimisation.

Appendix I: Industrial Application and Evaluation of a Microwell-Based Approach to Cell Culture Process Development*

I.1 Introduction and Aim

The work presented in Chapter 4 has been the first to show successful application of a fed-batch cell culture methodology for suspension culture of mammalian cells in microwells (Silk et al, 2010). Furthermore, it was shown in Chapter 6 that the culture process in shaken 24 SRW plates is an effective scale down model of both shake flask and stirred tank cultivations and that matched mixing times could be used as the basis for scale translation between the three bioreactor formats.

The aim of this Appendix is to demonstrate the applicability of this microwell process in a genuine industrial context to evaluate its integration within established company procedures. In particular the intention is to use the shaken microwell process to increase the throughput of the initial cell line characterisation stages following cell line transfection. The specific objectives of the evaluation are:

- To show the generic application of the microwell process for the parallel culture of a large number of cell lines in shaken 24 SRW plates.

*This Chapter is included as part of the UCL requirements for award of the EngD in Bioprocess Engineering Leadership

- To compare rank order of antibody production of the cell lines cultured in shaken plates to their performance when grown in static plates currently used by MedImmune (Cambridge, UK) for cell line selection.
- To assess the suitability of high throughput analytical techniques for determination of (i) cell number and (ii) IgG titre as alternatives to the methods previously used in Chapters 4 and 6.
- To evaluate the commercial potential of shaken microwell cultures in industrial cell line and cell culture process development.

I.2 Methodology for Cell Line Characterisation

Cell line characterisation following transfection is the first step in a lengthy process which could ultimately culminate in development of a manufacturing scale cell culture process to produce a biopharmaceutical product (Xing et al., 2009). As such, it is essential that the conditions under which initial cultures are conducted are appropriate to ensure that high performance at this initial stage will translate into high product titres once the manufacturing scale is reached later in process development (Barrett et al., 2010).

Both the original and microwell cell culture processes used at MedImmune for cell line characterisation are shown in Figure I.1. The current approach involves initial growth of cell lines in 96 SRW static plates, with

those producing the highest IgG titres selected for cultivation in static 24 SRW plates before transferring to shake flasks. Shake flask culture is initially under static conditions but shaking is subsequently begun to enhance mixing and mass transfer and result in greater cell growth and antibody production. Using the modified approach established in this thesis, cell cultivations for comparison of cell lines are performed in shaken 24 SRW plates (under similar conditions as those used in Chapter 6 and as described in Section 2.3.1) rather than in shake flasks.

Given that the cell lines taken forward for shaken culture are those that have performed well under static conditions, it is likely that some potentially high yielding cell lines, that would display improved growth and productivity under shaken conditions, are not selected. The improved throughput from use of shaken microwells provides an opportunity to characterise a greater number of candidates, and thus reduce the chance that such opportunities are missed.

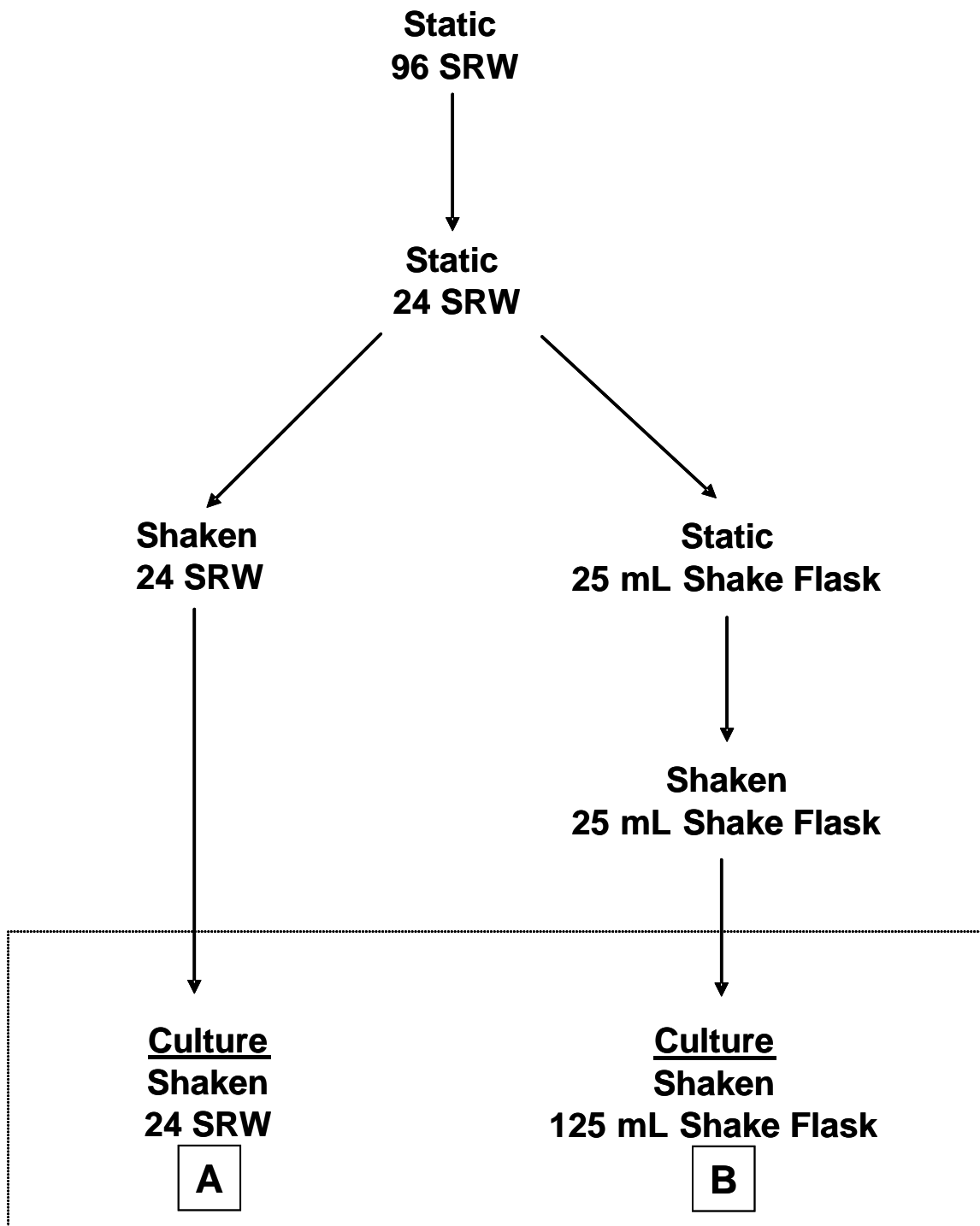


Figure I.1: Schematic flowsheet showing the current (B) and new (A) procedures for cell line characterisation. Microwell cell culture method as described in Section 2.3.1.

The two key markers of cell line performance are viable cell number and antibody titre. The Cellavista and Octet systems, used for determining cell number and antibody concentration respectively (as described in Sections 2.7.7 and 2.7.8), are compatible with this high throughput approach due to their ability to process large number of samples in a microwell format. For example, the Cellavista accepts 96 well plates and can process 96 samples in 30 minutes, while a representative time for analysis of an equivalent number of samples on the Vi-Cell (used to determine cell count results throughout Chapters 4 and 6) is more than three hours (assuming two minutes per sample as per the manufacturer's instructions). Similarly, the Octet can obtain IgG titre data of 96 samples in 20 minutes, while only a single sample can be analysed in 20 minutes when using Protein G HPLC (as described in Section 2.7.3).

I.3 Parallel Cell Culture and Cell Line Selection

In order to evaluate the generic nature and parallel operation of the microwell approach a total of 54 unique GS-CHO cell lines (newly transfected and expressing IgG product) were cultivated in three shaken 24 SRW plates, with feeding at days 3, 5 and 7. Figures I.2 and I.3 show the cell counts and IgG titre for these cultivations at seven and ten days after inoculation respectively. Those shaded gold were the highest performing cell lines in

static 96 SRW plates, and were thus taken forward for shake flask cultivations, while those in green and red would not have been selected on the basis of their performance under static conditions.

Successful cell growth was observed in 52 of the 54 cell lines cultured (96%). The top three ranking cell lines in the microwell cultivations (Figure I.1, route A) coincided exactly with the three lines that had been selected by shake flask cultivation (Figure I.1, route B) on the basis of their performance in static 96 SRW cultures. The three top performing lines were consistently the same for culture samples analysed on both days 7 and 10. Figure I.4 shows the distribution of cell counts and IgG titres obtained for all 54 cell lines.

In addition to these three candidates, a number of other cell lines were found to produce detectable IgG concentrations, for example those in wells B3 and B4 of the CCM2 plate and well C6 of the CCM3 plate.

I.4 Evaluation of Commercial Potential

The data in Figures I.2 and I.3 demonstrate that use of shaken 24 SRW plates in early stage cell line selection gives a comparable rank order for performance when compared to use of static 96 SRW plates. In addition, these results support the use of the high throughput Cellavista and Octet systems.

Use of this system results in a large increase in the potential throughput for cell line characterisation, and can thus allow a greater number

of cell lines to be taken forward for analysis than if shake flasks were used. Using the sandwich lid described in Section 2.3.1 together with a clamp system, up to three plates can be stacked, giving the potential for 72 cell culture experiments (or 60 if corner wells are not used) compared to the single shake flask that would occupy the same footprint in an incubator.

As such, use of this fed-batch shaken microwell system can offer potential commercial advantages through decreasing costs and increasing efficiency in early stage cell culture process development. The ability to characterise a larger number of cell lines also means that high performing candidates are less likely to be overlooked at this stage.

DAY 7

CCM 2	1	2	3	4	5	6	1	2	3	4	5	6	CCM 3
A	X	7.2	4.5	3.4	4.1	X	X	6.2	7.7	5.0	5.9	X	A
B	5.3	8.4	4.9	13.7	3.6	4.2		5.2	4.3	3.3	4.0	5.9	B
C		6.9	7.2	5.5	3.8	6.1	4.4		3.5	4.6		6.1	C
D	X	10.1	0.3	7.3	5.9	X	X	4.7	5.9	3.8	3.3	X	D
A	X	6.4	5.6	5.3	6.5	X							
B	5.1		3.4		5.2	5.3							
C	5.1	5.9	4.4	4.8	4.2	4.5							
D	X	5.7	3.0	5.7	2.6	X							
CCM 4	1	2	3	4	5	6							

DAY 10

CCM 2	1	2	3	4	5	6	1	2	3	4	5	6	CCM 3
A	X	9.5	7.0	4.0	6.8	X	X	5.6	6.3	7.4	6.2	X	A
B	12.0	11.2	6.7	16.1	5.0	4.9	0.4	5.0	4.3	5.4	5.4	8.9	B
C	0.2	8.4	9.0	6.6	6.7	8.5	5.6	0.4	5.0	4.7	0.4	8.3	C
D	X	11.6	0.3	8.6	6.4	X	X	4.3	7.1	5.4	3.9	X	D
A	X	9.7	5.7	5.7	7.9	X							
B	5.4	0.4	3.9	0.3	6.3	6.0							
C	5.6	8.0	5.0	5.9	4.7	4.6							
D	X	7.0	3.3	5.8	2.8	X							
CCM 4	1	2	3	4	5	6							

	Seeded well with density exceeding that at inoculation
	Seeded well with density lower than that at inoculation
	Well not seeded
X	Corner well not seeded
	Cell line also taken through for shake flask screening

Figure I.2: Summary of viable cell count data for 54 transformed CHO cell lines cultured in three shaken 24 SRW microwell plates. Measurements made seven and ten days after inoculation as described in Section 2.7.7. The cell culture process is described in Section 2.3.1. CCM refers to the proprietary medium formulation used by MedImmune.

DAY 7

CCM 2	1	2	3	4	5	6	1	2	3	4	5	6	CCM 3
A	X	0	0	44.5	0	X	X	0	0	0	0	X	A
B	26.3	0	0	0	0	0	0	0	0	0	0	0	B
C	0	0	0	0	0	0	0	0	0	0	0	31.3	C
D	X	0	0	0	0	X	X	0	0	0	0	X	D
A	X	0	0	0	0	X							
B	0		0		0	58.6							
C	0	0	0	0	0	0							
D	X	38.3	0	0	0	X							
CCM 4	1	2	3	4	5	6							

DAY 10

CCM 2	1	2	3	4	5	6	1	2	3	4	5	6	CCM 3
A	X	0	30.1	82.4	0	X	X	0	26.4	0	0	X	A
B	56	0	42.2	43	0	0	0	0	0	0	21.9	0	B
C	0	0	0	0	0	0	0	0	0	0	0	40.5	C
D	X	0	0	0	0	X	X	0	0	0	0	X	D
A	X	0	0	0	0	X							
B	0		0		0	111.9							
C	0	0	0	20.3	0	21.1							
D	X	70.3	0	0	0	X							
CCM 4	1	2	3	4	5	6							

	Well in which IgG was detected
	Well in which no IgG detected
	Well not seeded
X	Corner well not seeded
	Cell line also taken through for shake flask screening

Figure I.3: Summary of IgG titre data for 54 transformed CHO cell lines cultured in three shaken 24 SRW microwell plates. Measurements made seven and ten days after inoculation as described in Section 2.7.8. The cell culture process is described in Section 2.3.1. CCM refers to the proprietary medium formulation used by MedImmune.

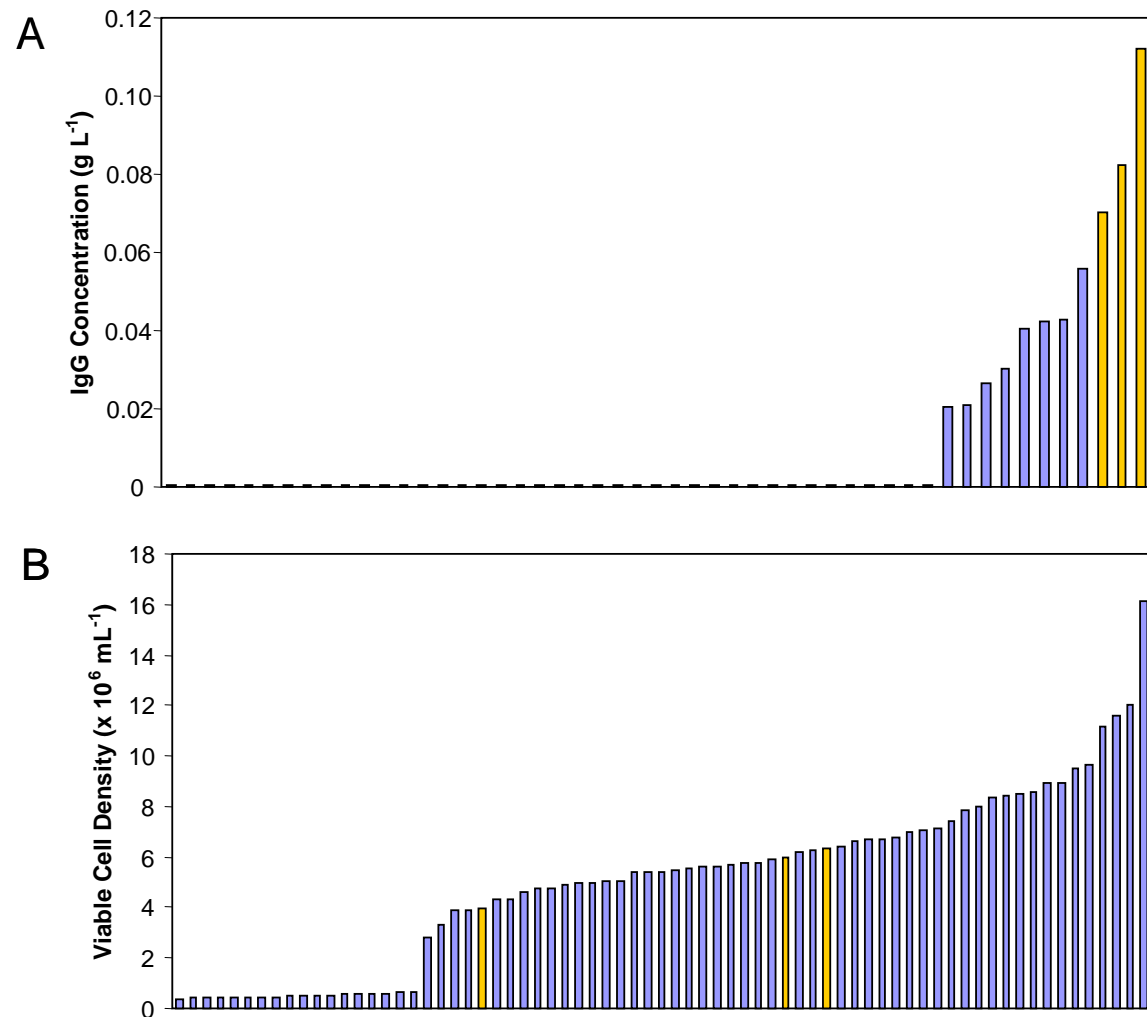


Figure I.4: Range of IgG concentrations (A) and viable cell densities (B) obtained for fed batch cultivation of 54 transformed GS-CHO cell lines in 24 SRW plates ten days after inoculation. Results for cell lines also taken through for shake flask screening shaded gold. Experiments performed as described in Section 2.7.7

Appendix II: Supplementary Calculations

II.1 Microscale of Turbulence

Rotation of impeller blades in the culture medium gives rise to currents, which in turn give rise to progressively smaller eddies. The energy of the smallest turbulent eddies is dissipated into the fluid as heat, and the size of these is termed the 'microscale of turbulence', denoted by the Greek letter lambda (λ):

$$\lambda = \left(\frac{\varepsilon}{\nu^3} \right)^{-1/4}$$

ε = energy dissipation per unit mass (W kg^{-1})*¹

ν = kinematic viscosity*² ($\text{m}^2 \text{s}^{-1}$)

*¹This can be calculated from the fluid density and the power dissipation. Since Power has units of W m^{-3} and Density of Kg m^{-3} , division of power by density gives units of W kg^{-1} and hence the value of ε .

*Kinematic viscosity = μ / ρ where μ is viscosity ($\text{kg m}^{-1} \text{s}^{-1}$) and ρ is fluid density. For a Newtonian fluid at 37°C these can be assumed to have values of $0.000692 \text{ kg m}^{-1} \text{ s}^{-1}$ and 993 kg m^{-3} respectively.

II.2: Evaporation Correction for Fed-Batch Cultures in 24 SRW Plates

Viable cell number and IgG titre data for Shake Flask and Stirred tank cultivations were not corrected for evaporation. However, the rate of water loss from the 24 SRW plates used for fed cultivations was considerably greater than for these systems, as shown in Table 4.1. As such a correction factor should be applied to microwell raw data to allow a meaningful comparison of results across the three culture formats.

As a consequence of the higher rate of evaporation from 24 SRW plates, diluted feeds were used to replace lost water while undiluted feed was used for shake flask and stirred tank cultures, as described in Section 4.4.

There are therefore two key differences that must be considered:

- (i) Higher rate of water loss from 24 SRW cultures due to evaporation.
- (ii) Replacement of the water lost through the use of diluted feeds.

Both of these differences were considered when determining viable cell number and IgG titre in the 24 SRW system.

In order to calculate an appropriate correction factor to apply to the 24 SRW data, the shake flask was used as a reference point. As an example, a cell count from day 6 of a fed batch cultivation will be used (method as described in Section 2.5.2). After six days, water will have been gained or lost from the shake flask for two reasons, and the contribution of each can be determined:

- (i) Evaporation, which occurs at a rate of 0.6% (v/v) day from the flask for a 50 mL inoculum volume (Table 4.1), will have caused a total loss of $6 \times 0.6 = 3.6\%$ of the total fluid volume.
- (ii) Feeding, which commenced on day 4 and involves addition of 2.25% (v/v) will have been performed twice, on days four and five, leading to an increase in volume of $2 \times 2.25 = 4.5\%$.

The combined impact of these effects will be that the volume of fluid in the shake flask will have increased by $4.5 - 3.6 = 0.9\%$ on day six. This figure is then used as a benchmark for the microwells as follows.

Sacrificial sampling of three microwells will be performed on day six, with the plate being weighed before and after. Assuming a culture fluid density of 1 g L^{-1} , this weight can be used to determine the average fluid volume in each microwell, V_{actual} .

A reference volume is then calculated based on the percentage volume change in the shake flask at the same time point, which was determined

above as an increase of 0.9%. The purpose of this is to calculate the volume that would be present in the microwells if the proportional changes to volume that resulted from evaporation and feeding were identical in the two systems. The reference volume, $V_{reference}$, is therefore:

$$\text{Reference Volume} = \text{Microwell inoculum volume} \times 1.009$$

$$V_{reference} = 0.8 \text{ mL} \times 1.009 = 0.807 \text{ mL}$$

The correction factor is then determined as:

$$\text{Correction Factor} = V_{actual} / V_{reference}$$

Multiplication of the raw cell number and IgG titre microwell data by this factor will therefore adjust the figures to correct for disparities between the shake flask and 24 SRW systems in terms of both water loss from evaporation and water gained from feeding.

If this were not done, it could result on either an over or under representation of the viable cell density in the 24 SRW plates. For example, the higher rate of water loss in the wells will reduce volume in the wells, which will cause an increase in viable cell density without an increase in cell number (eg an apparent increase can occur in the absence of cell growth). Conversely,

use of diluted feeds could result in under representation of cell growth in comparison to the flasks, as, for example, in increase in fluid volume without cell growth can lead to a decline in cell density without a decrease in cell number. Use of the correction factor shown above accounts for both feeding and evaporation aspects.

Appendix II.3: Determination of Cell Specific Oxygen Uptake Rate (OUR)

This was performed experimentally as described in Section 5.2.3. Given that the viable cell density was measured as 2.76×10^6 cells mL⁻¹, the rate of change of dissolved oxygen tension of the culture medium in the microwell was used to determine the oxygen uptake rate:

Henry's Constant (atm kg m ⁻³)	28.6
100% DO in bar:	0.21
100% DO in kg m ⁻³ :	7.34×10^{-3}
100% DO in mol mL ⁻¹ :	2.29×10^{-7}
% DO change per hour	500
Time for 100% DO drop (hours)	0.2
DO drop (mol ml ⁻¹ h ⁻¹)	1.15×10^{-6}
OUR (mol O₂ cell⁻¹ h⁻¹):	4.16×10^{-13}

Appendix II.4: Paired *t*-test for Peak CHO-S Viable Cell Densities Obtained in Shaken 24 SRW Microwells and Shake Flasks

A paired *t*-test was used to test the null hypothesis for the data shown below:

	Viable Cell Density ($\times 10^6 \text{ mL}^{-1}$)						Mean	Standard Deviation
24 SRW	3.84	4.49	4.56	4.22	4.67	4.14	4.32	0.31
Shake Flask	4.71	4.39	4.30	4.53	4.46	4.44	4.47	0.14

The paired *t* statistic was calculated as shown:

$$t = \frac{\bar{x}_1 - \bar{x}_2}{S_{x_1 x_2} \cdot \sqrt{\frac{2}{n}}}$$

where:

$$S_{x_1 x_2} = \sqrt{\frac{1}{2}(S_{x_1}^2 + S_{x_2}^2)}$$

Where \bar{x} = mean viable cell density, S_x = standard deviation and n = sample number.

t was calculated as 1.09, with four degrees of freedom. This is less than the critical value of 2.78 for a *p* value of 0.05, and as such the null hypothesis (that the difference between the mean value of viable cell density in shake flask and 24 SRW systems is zero) is confirmed at the 95% confidence level.

References

Aggarwal S. (2009) What's Fuelling the Biotech Engine – 2008. *Nature Biotechnology* 27(11): 987-993

Aloi, L.E. and Cherry, R.S. (1996) Cellular Response to Agitation Characterized by Energy Dissipation at the Impeller Tip. *Chem. Eng. Sci.* 51(9): 1523-1529

Amanullah, A., Otero, J.M., Mikola, M., Hsu, A., Zhang, J., Aunins, J., Schreyer, H.B., Hope, J.A. and Russo, A.P. (2010) Novel micro-bioreactor high throughput technology for cell culture process development: reproducibility and scalability assessment of fed-batch CHO cultures. *Biotech. Bioeng.* 106(1): 57-67/

Bareither, R. and Pollard, D. (2011) A Review of Advanced Small-Scale Parallel Bioreactor Technology for Accelerated Process Development: Current State and Future Need. *Biotechnology Progress*, 27(1): 2-14.

Barrett TA, Wu A, Zhang H, Levy MS, Lye GJ. (2010). Microwell engineering characterization for mammalian cell culture process development. *Biotech. Bioeng.* 105(2): 260-275

Betts, J.I. and Baganz, F. (2006) Miniature Bioreactors: current practices and future opportunities. *Microbial Cell Factories*, 5:21

Büchs, J. Maier, U., Milbradt, C. and Zoels, B. (2000). Power Consumption in Shaking Flasks in Rotary Shaking Machines: I. Power Consumption Measurement in Unbaffled Flasks at Low Liquid Viscosity. *Biotech. Bioeng.* 68(6): 589-593

Büchs, J., Lotter, S. and Milbradt, C. (2001) Out-of-phase operating conditions, a hitherto unknown phenomenon in shaking bioreactors. *Biochem. Eng. J.*, 7: 135-141

Büchs J (2001) Introduction to Advantages and Problems of Shaken Cultures. *Biochem. Eng. J.* 7, 99-108

Bujalski W., Takenaka K., Paolini S., Jahoda M., Paglianti A., Takahashi K., Nienow A.W. and Etchells A.W. (1999) Suspension and liquid

homogenization in high solids concentration stirred chemical reactors. *Chem. Eng. Res. Des.* 77: 241-247

Chattopadhyay, D., Rathman, J.F. and Chalmers, J.J. (1995) The Protective Effect of Specific Medium Additives with Respect to Bubble Rupture. *Biotech. Bioeng.* 45: 473-480

Chen, A., Chitta, R., Chang, D. and Amanullah, A. (2008) Twenty-four well plate miniature bioreactor system as a scale-down model for cell culture process development. *Biotech. Bioeng.*, 102(1): 148-160

Chisti, Y. (1993) Animal cell culture in stirred bioreactors: Observations on scale-up. *Bioprocess Engineering*, 9: 191-196.

Chisti, Y (2001) Hydrodynamic Damage to Animal Cells. *Critical Reviews in Biotechnology*, 21(2), 67-110

Chu L., Robinson DK. (2001) Industrial Choices for Protein Production by Large-Scale Cell Culture, *Current Opinion in Biotechnology*, 12, 180-187

Deshpande, R. and Heinzle, E. (2004) On-line oxygen uptake rate and culture viability measurement of animal cell culture using microplates with integrated oxygen sensors. *Biotechnology Letters*, 26: 763-767.

Doig, S.D., Pickering, S.C.R., Lye, G.J. and Baganz, F. (2005) Modelling the surface aeration rate in shaken microtitre plates using dimensionless groups. *Chem. Eng. Sci.*, 60: 2741-2750

Duetz, W.A., Rüedi, L., Hermann, R., O'Connor, K., Büchs, J. and Witholt, B. (2000) Methods for Intense Aeration, Growth, Storage, and Replication of Bacterial Strains in Microtitre Plates. *Applied and Environmental Microbiology*, 66: 2641-2646

Duetz, W.A. and Witholt, B. (2004) Oxygen Transfer by Orbital Shaking of Square Vessels and Deepwell Microtiter Plates of Various Dimensions. *Biochem. Eng. J.*, 17: 181-185.

Duetz W.A. (2007) Microtiter plates as mini-bioreactors: miniaturization of fermentation methods. *Trends in Microbiology* 15(10): 469-475

Eibl, R., Werner, S. and Eibl, D. (2010) Bag Bioreactor Base on Wave-Induced Motion: Characteristics and Applications. *Advances in Biochemical Engineering/Biotechnology*, 115: 55-87.

Einsele, A., Ristroph, D.L. and Humphrey, A.E. (1978) Mixing Times and Glucose Uptake Measured with a Fluorometer. *Biotechnology and Bioengineering*, 20(9): 1487-1492

Geisler, R.K., Buurman, C. and Mersmann, A.B. (1993) Scale-up of the necessary power input in stirred vessels with suspensions. *Chemical Engineering Journal*, 51:29-39

Gennari, J.F. 1984. Serum Osmolality – Uses and Limitations. (1984) *N Engl J Med* 310: 102-105

Gernot, T.J., Klimant, I., Wittman, C. and Heinzle, E. (2003) Integrated optical sensing of dissolved oxygen in microtiter plates: a novel tool for microbial cultivation, *Biotechnol. Bioeng.*, 81(7): 829-836.

Girard, P., Jordan, M., Tsao, M. and Wurm, F.M. (2001) Small-scale bioreactor system for process development and optimization. *Biochem. Eng. J.*, 7: 117-119.

Gupta A. and Rao G. (2003) A study of oxygen transfer in shake flasks using a non-invasive oxygen sensor. *Biotech. Bioeng.* 84(3): 351-358

Hadjiev, D., Sabiri, N.E. and Zanati, A. (2005) Mixing time in bioreactors under aerated conditions. *Biochem. Eng. J.* 27(3): 323-330

Hahn, C.E.W. (1987) A novel method for the measurement of oxygen mass transfer rates in small-scale vessels. *Biochem. Eng. J.* 25: 63-68

Heath, C. and Kiss, R. (2007) Cell culture process development: advances in process engineering. *Biotechnology Progress*, 23(1): 46-51

Hermann R., Lehmann M. and Büchs J. (2003) Characterization of gas-liquid mass transfer phenomena in microtiter plates. *Biotech. Bioeng.* 81(2): 178-186

Hu, W. and Aunins, J.G. (1997) Large-scale mammalian cell culture, *Current Opinion in Biotechnology*, 8: 148-153

Huber, R., Ritter, D., Hering, T., Hillmer, A., Kensy, F., Müller, C., Wang, L. and Büchs, J. (2009) Robo-Lector – a novel platform for automated high-throughput cultivations in microtiter plates with high information content. *Microbial Cell Factories*, 8: 42

Issaq, H.J., Veenstra, T.D., Conrads, T.P. and Felschow, D. (2002) The SELDI-TOF MS approach to proteomics: protein profiling and biomarker identification. *Biochemical and Biophysical Research Communications*, 292(3): 587-592.

Jones PT, Dear PH, Foote J, Neuberger MS, Winter G. (1986) Replacing the Complementarity-Determining Regions in a Human Antibody with those from a Mouse. *Nature* 321, 522-525

Kimura, R. and Miller, W.M. (1996). Effects of Elevated pCO₂ and/or osmolality on the Growth and Recombinant tPA Production of CHO Cells. *Biotech. Bioeng.* 52(1): 152-160.

Kohler G, Milstein C. (1975) Continuous cultures of fused cells secreting antibody of predefined specificity. *Nature* 256, 495-497

Krampe, B., Swiderek, H, Al-Rubeai, M. (2008) Transcriptome and Proteome Analysis of Antibody-Producing Mouse Myeloma NS0 Cells Cultivated at Different Cell Densities in Perfusion Culture. *Biotechnology and Applied Biochemistry*, 50(3): 133-141.

Lamping S.R., Zhang H., Allen B. and Ayazi-Shamlou P. (2003) Design of a prototype miniature bioreactor for high throughput automated bioprocessing.

Chem. Eng. Sci. 58: 747-758

Legmann, R., Schreyer, H.B., Combs, R.G., McCormick, E.L., Russo, A.P. and Rodgers, S.T. (2009) A predictive high-throughput scale-down model of monoclonal antibody production in CHO cells. *Biotech. Bioeng.* 104(6): 1107-1120

Li F., Hashimura Y., Pendleton R., Harms J., Collins E. and Lee B. (2006) A systematic approach for scale-down model development and characterization of commercial cell culture processes. *Biotechnol. Prog.* 22: 696-703

Ma, N., Koelling, K.W. and Chalmers, J.J. (2002) Fabrication and Use of a Transient Contractual Flow Device to Quantify the Sensitivity of Mammalian and Insect Cells to Hydrodynamic Forces. *Biotech. Bioeng.* 80(4): 428-437

Ma, N., Chalmers, J.J., Aunins, J.G., Zhou, W. and Xie, L. (2004) Quantitative Studies of Cell-Bubble Interactions and Cell Damage at Different Pluronic F-68 and Cell Concentrations. *Biotechnol. Prog.* 20: 1183-1191.

Maggon, K. (2007) Monoclonal antibody “gold rush.” *Current Medicinal Chemistry*, 14: 1978-1987

Mayr, B., Horvat, P. and Moser A. (1992) Engineering Approach to Mixing Quantification in Bioreactors. *Bioprocess and Biosystems Engineering*, 8(3): 137-143.

Meuwly, F., Weber, U., Ziegler, T., Gervais, A., Mastrangeli, R., Crisci, C., Rossi, M., Bernard, A., von Stockar, U. and Kadouri, A. (2006) Conversion of a CHO cell culture process from perfusion to fed-batch technology without altering product quality. *Journal of Biotechnology*, 123(1): 106-116.

Micheletti, M. and Lye, G.J (2006) Microscale bioprocess optimisation. *Current Opinion in Biotechnology*, 17: 611-618.

Micheletti, M., Barrett, T., Doig, S.D., Baganz, F., Levy, M.S., Woodley, J.M. and Lye, G.J. (2006) Fluid mixing in shaken bioreactors: Implications for scale-up predictions from microlitre scale microbial and mammalian cell cultures. *Chem. Eng. Sci.*, 61: 2939-2949.

Mollet M, Godoy-Silva R, Berdugo C, Chalmers JJ (2007) Acute Hydrodynamic Forces and Apoptosis: a Complex Question. *Biotech. Bioeng.*,98(4), 772-788

Nealon, A.J., O'Kennedy, R.D., Titchener-Hooker, N.J. and Lye, G.J. (2006) Quantification and prediction of jet macro-mixing times in static microwell plates, *Chem. Eng. Sci.*, 61: 4860-4870

Neermann, J. and Wagner, R. (1996) Comparative Analysis of Glucose and Glutamine Metabolism in Transformed Mammalian Cell Lines, Insect and Primary Liver Cells. *Journal of Cellular Physiology*, 166(1): 152-169

Nienow A.W. and Miles D. (1969) A dynamometer for the accurate measurement of mixing torque. *J Phys E: Sci Instrum* 2:994.

Nienow, A.W., Langheinrich, C., Stevenson, N.C., Emery, A.N., Clayton, T.M., and Slater, N.K.H. (1996) Homogenisation and oxygen transfer rates in large agitated and sparged animal cell bioreactors: some implications for growth and production. *Cytotechnology*, 22:87-94

Nienow, A.W. (2006) Reactor engineering in large scale animal cell culture, *Cytotechnology* 50:9-33

Ortiz-Ochoa K., Doig S.D., Ward J.M. and Baganz F. (2005) A novel method for the measurement of oxygen mass transfer rates in small-scale vessels.

Biochem Eng J 25: 63-68

Osman, J.J., Birch, J. and Varley, J. (2001) The response of GS-NS0 myeloma cells to pH shifts and pH perturbations, *Biotech Bioeng*, 75(1): 63-73

Paoli, T., Faulkner, J., O'Kennedy, R., Keshavarz-Moore, E. (2010) A Study of D-lactate and Extracellular Methylglyoxal Production in Lactate Re-Utilizing CHO Cultures. *Biotech. Bioeng.*, 107(1): 182-189.

Pavlou A.K, Belsey M.J. (2005) The Therapeutic Antibodies Market to 2008. *European Journal of Pharmaceutics and Biopharmaceutics* 59, 389-396

Porter, A.J., Dickson, A.J., Barnes, L.M. and Racher A.J. (2010) Behaviour of GS-CHO Cell Lines in a Selection Strategy. *ESACT Proceedings 2010*, 4(3): 165-169.

Porter, A.J., Dickson, A.J. and Racher, A.J. (2010) Strategies for Selecting Recombinant CHO Cell Lines for cGMP Manufacturing: Realizing the Potential in Bioreactors. *Biotechnol Prog* 26: 1446-1454.

Porter, A.J., Racher, A.J., Preziosi, R. and Dickson, A.J. (2010) Strategies for Selecting Recombinant CHO Cell Lines for cGMP Manufacturing Improving the Efficiency of Cell Line Generation. *Biotechnol Prog* 26: 1455-1464.

Sharfstein, S. (2008) Advances in cell culture process development: tools and techniques for improving cell line development and process optimisation. *Biotechnology Progress*, 24(3): 727-734

Silk N.J., Denby S., Lewis G., Kuiper M., Hatton D., Field R., Baganz F. and Lye G.J. (2010) Fed-batch operation of an industrial cell culture process in shaken microwells. *Biotech Letters* 32: 73-78

Strobel, R., Bowden, D., Bracey, M, Sullivan, G., Hatfield, C., Jenkins, N and Vinci, V. (2001) High Throughput Cultivation of Animal Cells Using Shaken Microplate Techniques. *Animal Cell Technology: From Target to Market*, 307-311 (E. Lindner-Olsson et al. (eds.))

Suzuki, E. and Ollis, D.F. (1989) Cell Cycle Model for Antibody Production Kinetics. *Biotech. Bioeng.* 34(11): 1398-1402

Takagi, M., Hayashi, H. and Yoshida, T. (2000) The effect of osmolarity on metabolism and morphology in adhesion and suspension chinese hamster ovary cells producing tissue plasminogen activator. *Cytotechnology* 32: 171-179.

Van der Pol, L. and Tramper, J. (1998) Shear sensitivity of animal cells from a culture medium perspective. *Tibtech*, 16: 323-328

Van't Riet, K. (1979) Review of Measuring Methods and Results in Nonviscous Gas-Liquid Mass Transfer in Stirred Vessels. *Ind.Eng.Chem. Process Des. Dev.*, 18(3): 357-364

Varley J, Birch J. (1999) Reactor Design for Large Scale Suspension Animal Cell Culture, *Cytotechnology*, 29, 177-205

Warnock JN, Al-Rubeai M (2006) Bioreactor Systems for the Production of Biopharmaceuticals from Animal Cells. *Biotechnol. Appl. Biochem.* 45, 1-12

Wayte J., Boraston R., Bland H., Varley J. and Brown, M. (1997) pH: Effects on growth and productivity of cell lines producing monoclonal antibodies: control in large-scale fermenters. *The Genetic Engineer and Biotechnologist* 17: 125-132

Weiner, L.M., Surana, R. and Wang, S. (2010) Monoclonal antibodies: versatile platforms for cancer immunotherapy. *Nature Reviews: Immunology*, 10(5): 317-327

Wu A. (2008). Examination of transient transfection as a potential means of recombinant protein production. PhD thesis, University of London, UK

Wurm F. (2004) Production of recombinant protein therapeutics in cultivated mammalian cells. *Nature Biotechnology* 22, 1393-1398

Xie, L. and Wang, D.I.C (1994) Fed-Batch Cultivation of Animal Cells Using Different Medium Design Concepts and Feeding Strategies. *Biotech. Bioeng.* 95(2): 270-284

Xie, L. and Wang, D.I. (1996) High Cell Density and High Monoclonal Antibody Production Through Medium Design and Rational Control in a Bioreactor. *Biotech. Bioeng.* 51: 725-729.

Xing Z., Kenty B.M., Zhenj J.L. and Lee S.S. (2009) Scale-up analysis for a CHO cell culture process in large-scale bioreactors. *Biotech. Bioeng.* 103(4): 733-746

Xing, Z., Bishop, N., Leister, K. and Zheng, J. (2010) Modelling kinetics of a large-scale fed-batch CHO cell culture by Markov chain Monte Carlo method. *Biotechnology Progress*, 26(1): 208-219

Yang, J., Lu, C., Stasny, B., Henley, J., Guinto, W., Gonzalez, C., Gleason, J., Fung, M., Collopy, B., Benjamino, M., Gangi, J., Hanson, M. and Ille, E. (2007) Fed-Batch Bioreactor Process Scale-Up from 3-L to 2,500-L Scale for Monoclonal Antibody Production From Cell Culture. *Biotech. Bioeng.*, 98(1): 141-154

Yang, X., Oehlert, G.W. and Flickinger, M.C. (1996) Specific protein secretion rate: application to monoclonal antibody secretion rate kinetics in response to osmotic stress. *Biotech. Bioeng.*, 50: 184-196.

Zhang H., Lamping S.R., Pickering S.C.R., Lye G.J. and Shamlou P.A. (2008) Engineering characterisation of a single well from 24-well and 96-well microtitre plates. *Biochem. Eng. J.* 40(1): 138-149

Zimmermann, H.F., John, G.T., Trauthwein, H., Dingerdissen, U. and Huthmacher, K. (2003) Rapid Evaluation of Oxygen and Water Permeation through Microplate Sealing Tapes. *Biotechnol. Prog.* 19: 1061-1063

